Immunofluorescent approaches to investigate the mammalian target of rapamycin (mTOR) complex in human skeletal muscle

Zhe Song

A thesis submitted to the

University of Birmingham

for the degree of

DOCTOR OF PHILOSOPHY

School of Sport, Exercise & Rehabilitation Sciences

College of Life and Environmental Sciences

University of Birmingham

November 2015

General Abstract

The mammalian target of rapamycin (mTOR) complex is a key regulator of protein synthesis, with resistance exercise and protein ingestion both shown to increase mTOR activity in human skeletal muscle. It has recently been proposed that mTOR activity is regulated via its intracellular localization and protein complex interaction, however no research to date has examined this process in human skeletal muscle. Accordingly, the aims of this thesis were to (1) develop immunofluorescent-based methodologies to study mTOR in human skeletal muscle, and (2) apply this approach to the study of mTOR in acute and chronic resistance exercise scenarios.

Chapter 3 describes the development of an immunofluorescence microscopy technique to observe mTOR and interacting proteins in human skeletal muscle *in vivo*. Antibodies applied to immunofluorescence staining were validated systemically to confirm specificity and sensitivity of fluorescence signals. In addition, quantification methods based on microscope images were established to measure mTOR content and colocalisation with interacting proteins/ organelles.

In Chapter 4, the immunofluorescent approached established in chapter 3 was applied to examine fibre-specific mTOR protein content and cellular distribution in skeletal muscle of young male individuals following 10- week resistance exercise training. Interestingly, though muscle strength increase was found in participants, mTOR content was not significantly increased post-training, either in total muscle or in relation to myosin heavy chain content. As such, chapter 4 demonstrates the value of our immunoflurescense approach for detailing skeletal muscle adaptation, and additionally suggests that fibre-specific increases in mTOR protein content do not correlate with muscle strength performance.

In Chapter 5, we moved into an acute model of resistance exercise to investigate the effect of resistance exercise on mTOR distribution and protein complex formation/regulation, in both fasted and fed conditions. In contrast to *in vitro* studies, we report that mTOR is highly localised to the lysosome in basal skeletal muscle, whilst resistance exercise results in mTOR-lysosome complex

translocation from the cytoplasm to the plasma membrane post exercise. Importantly, this translocation event appears to be functional, as mTOR was observed to interact with the vasculature, its positive regulator Rheb and the translation factor eIF3F. As such, our data indicate that translocation of mTOR to the cell periphery is critical in its activation following mechanical loading/contraction.

In summary, this thesis describes a novel approach to study mTOR regulation in human skeletal muscle *in vivo*. It is hoped that this approach will provide insight into the cellular regulation of skeletal muscle protein synthesis and by extension the control of skeletal muscle mass in humans during scenarios of health and chronic disease.

Acknowledgements

There are many people I should thank for their help and support during the course of my PhD study.

Firstly, I want to thank my supervisors, Dr Andy Philp and Dr Sarah Aldred, for their contribution, teaching and training on me. Andy gave me a day-to-day supervision and guidance on my PhD study, and always offered help when I encountered any problems. Sarah gave lots of valuable suggestions during the thesis writing. Undoubtedly their knowledge and encouragement shed light on my road to the success of the PhD study.

I would like to thank the collaborators involved in the studies within this thesis. Dr Daniel Moore, Dr Leigh Breen, Dr Gareth Wallis, Dan Craig, Baubak Shamim and Lloyd cheesman provided help on the muscle sample collection. I need to thank Dr Robert Shaw from medicine school for training me on confocal microscopy techniques. Also, I spent a lot of enjoyable time with other group members: Dr Jessica Dent, Dr Joaquin Perez-Schindler, Michael McLeod, Stephen Ashcroft, Ben Stocks, Alex Seabright, as well as the other laboratory members, Dr Jinglei Yu, Dr Adrian holiday, Dr Adrian Hodgson, Dr Rebecca Randell, Dr Alex Wadley, Benoit Smeuninx, James Mckendry, Dan Luo, Scott Robinson, Gareth Fletcher, Matthew Soden and Sahara Rai. I also want to thank the colleagues in my office, Johan, Fredrik, Saeng, Tania, Taweewat and everyone else.

I would like to thank the members of the Anton group who gave support on the immunofluorescence experiment and microscope image analysis, especially Dr Chris Shaw and Professor Anton Wagenmakers who provided me the opportunity to study in University of Birmingham. And it was happy to study with Dr Helen Bradly, Dr Oliver Wilson, Dr Sam Sherphed and Dr Matthew Cocks.

I would like to thank my housemates, especially the friends in the vale village. I would like to thank my girlfriend Xin. I can’t imagine achieving my goals without her accompanying and encouragement. Finally, I want to thank my parents and other family members for their love and support to my study and beyond.

Contents listings

List of Abstracts, conference communications and Publications

Conference communications

Resistance exercise results in mTOR cellular association with Rheb in human skeletal muscle. M5 biomedical imaging conference, University of Nottingham, Nottingham, 9th September 2014.

Resistance exercise results in mTOR cellular redistribution in human skeletal muscle. Physiology 2014, Queen Elizabeth II Conference Centre, London, 30th June- 2th July 2014.

Using Immunofluorescence approaches to study mTORC localisation in human skeletal muscle in response to exercise and nutrition. Postgraduate Research meeting, School of Sport, Exercise and Rehabilitation Sciences, University of Birmingham, Birmingham, 1st April 2014.

An evaluation of three neutral lipid dyes to visualise lipid droplets in human skeletal muscle.39th Adipose tissue discussion group meeting, University of Bath, Bath, 17th December 2012.

The potential lipids constitution variation in human skeletal muscle in response to endurance exercise training. Postgraduate Research meeting, School of Sport, Exercise and Rehabilitation Sciences, University of Birmingham, Birmingham, 13st Dec 2011.

Publications

Zhe Song, Daniel R. Moore, Lawrence L. Spriet et.al. Resistance exercise initiates mechanistic target of rapamycin (mTOR) translocation and protein complex interaction in human skeletal muscle. Scientific Reports (under review)

Zhe Song, Daniel R. Moore, Lawrence L. Spriet et.al. Resistance exercise results in mTOR cellular redistribution in human skeletal muscle. Proceeding of Physiology 2014 Conference, London

List of Abbreviations

AA Amino acid

BCAA Branch-chain amino acids

DAPI 4,6'-diamidino-2-phenylindole

EAA Essential amino acid

EIF3F Eukaryotic translation initiation factor 3 subunit F protein

FKBP12 FK506 Binding Protein-12

FKBP38 FK506-binding protein 38

GH Growth hormone

IGF Insulin-like growth Factor

Lamp2 Lysosomal-associated membrane protein 2

MHC I Myosin heavy chain I

MHC IIa Myosin heavy chain IIa

MHC IIx Myosin heavy chain IIx

mLST8 Mammalian lethal with SEC13 protein 8

mTORC Mammalian target of rapamycin complex

NEAA Non- essential amino acid

PA Phosphatidic acid

PI3K Phosphatidylinositol 3-kinase

PM Plasma membrane

PLD Phospholipase D

PRAS40 Proline-rich Akt substrate of 40 kDa

Rab7 Ras-associated binding protein 7

Rag RAS-related GTP-binding protein

Rheb Ras homologue enriched in brain

S6K1 Ribosomal protein S6 kinase 1

SLC Solute carrier

T2D Type 2 Diabetes

TA Tibialis anterior

TSC2 Tuberous Sclerosis Complex 2

UEA-I Ulex Europaeus Agglutinin I Lectin

Vps34 Vacuolar protein sorting 34

WGA	Wheat germ agglutinin
4E-BP1	EIF4E-binding protein 1

Author's declaration

I performed the development of the immunofluorescence histology technique and analysis method on all the antibodies detailed in chapter 3 and for the remainder of this thesis. I was taught the semi-quantification method by Dr Chris Shaw, Dr Helen Bradley and Dr Oliver Wilson.

The training study detailed in chapter 4 was run in collaboration with Dr Leigh Breen and Dan Craig. I was present during testing sessions to assist with muscle biopsy collection and storage, whilst Dan and his colleagues performed the training study.

The studies detailed in chapter 5 were run in collaboration with Dr Daniel R. Moore at the University of Toronto. Dan conducted all of the physiological experiment work and collected all muscle biopsy samples. I completed the sample sectioning, immunofluorescence histology staining, imaging capture, quantification and statistical analysis.

Table of Contents

List of Figures

List of Tables

Chapter 1

General Introduction

1.1 Skeletal muscle

1.1.1 Importance of skeletal muscle in health and wellbeing

Skeletal muscle is the most abundant and widely distributed organ in human body. There are more than 660 skeletal muscles, accounting for ~45% of total body weight [196]. Skeletal muscle plays an indispensible role in connecting the skeleton and supporting body movement, as well as contributing to immune system function [197]. As such, maintaining skeletal muscle functional capacity is a fundamental issue for human health and wellbeing.

In addition to maintaining posture, skeletal muscle represents the significant energy storage site, reserving the largest amount of peptides and free amino acid (AA) in body [1]. Muscle contraction is an ATP- driven mechanical event, requiring high-energy expenditure [198]. As such, improvement in skeletal muscle mass augments maximal workload and postpones muscle fatigue [199]. In contrast, a reduction in skeletal muscle mass, such as that induced by disuse, trauma, surgery, burn or sepsis can impair muscle strength and lead to muscle atrophy [197]. Ageing induced sarcopenia is the gradual loss of skeletal muscle mass resulting in deteriorated muscle strength and function [201, 202], affecting elderly people worldwide [203]. Collectively, it is therefore pivotal to maintain the skeletal muscle mass in human body in the context of health and wellbeing.

1.1.2 Maintenance of skeletal muscle mass

The maintenance of skeletal muscle mass is governed by net protein balance (i.e. the combined effect of daily fluctuations in rates of protein synthesis and degradation). Net protein balance can be directly influenced by physical activity, as resistance type exercise increases protein synthesis, thus increasing net protein balance, whereas inactivity/unloading reduces protein synthesis/increases degredation to ultimately reduced net protein balance [204-207]. In addition, provision of dietary protein can also maintain a positive net protein balance and when combined with resistance exercise lead to further enhancement of the stimulatory effects of resistance exercise in human skeletal muscle [221]. Given the fact that both resistance exercise and protein ingestion can increase net protein balance, considerable

research has been invested into understanding the regulation of skeletal muscle mass at the cellular level. Elegant studies in cell, rodent and human models collectively indicate that the mammalian target of rapamycin (mTOR) complex may be as a central signal protein regulating skeletal muscle protein synthesis [32, 58, 150, 151].

1.2 The mammalian target of rapamycin (mTOR)

The mammalian target of rapamycin (mTOR) is a serine/threonine kinase (molecular weight, MW= ~289kDa) with multi domains including a catalytic kinase domain, a FKBP12–rapamycin binding (FRB) domain, a putative auto-inhibitory domain ('repressor domain') near the C-terminus, ~20 tandem repeated HEAT (Huntingtin, EF3, A subunit of PP2A and TOR) motifs at the N-terminus, and FRAP–ATM–TRRAP (FAT) and FAT C-terminus domains. HEAT motifs facilitate the protein–protein interaction, whereas FAT and FAT C-terminus domains function in modulating the catalytic kinase activity of mTOR [19]. As it's name would suggest, mTOR is the central component constituting the mTOR complex (mTORC). However, the mTOR complex can be found in two structurally and functionally distinct complexes, mTORC1 and mTORC2 which differ in composition of mTOR interacting proteins. For example, the main composing subunits of mTORC1 include Raptor (regulatory-associated protein of mTOR) [20, 21], G-protein β subunit-like protein (GβL, also known as mLST8) [22], and PRAS40 (proline-rich Akt substrate 40 kDa) [23]. By contrast, mTORC2 contains Rictor (rapamycin-insensitive companion of mTOR) [24], mSin1 (yeast Avo1 homolog) [25], mLST8, and Protor (protein observed with ricTOR) [26]. A recent study has identified Deptor as a new protein interacting with both mTORC1 and mTORC2 [27]. Functionally, mTORC1 is sensitive to nutrition (principally the BCAA Leucine), inhibited by rapamycin and primarily functions to regulate protein translation and cell growth. In contrast, mTORC2 is sensitive to insulin, is rapamycin resistant and has been implicated in regulating cytoskeleton, cell survival and insulin sensitivity [14, 15].

1.3 mTORC1 regulation of protein synthesis in skeletal muscle

The functions of mTORC1 are greatly dependent on the substrates it regulates. When it comes to the regulation of protein synthesis, the best characterized substrates for mTORC1 are the ribosomal protein S6 kinase 1 (S6K1) and the eukaryote translation initiation factor 4E binding protein 1 (4E-BP1), two well-known protein translation regulators. S6K1 is a serine/threonine kinase, which, after being catalyzed at phosphorylation site (Threonine 389) by mTORC1, active S6K1 will phosphorylate its targets, S6 ribosomal protein and eukaryotic elongation factor 2 (eEF2) kinase [14, 15]. Subsequently, S6 and eEF2 kinase can enhance protein translation initiation and elongation, respectively. Ribosomal protein S6 is a component of the eukaryotic 40S ribosomal subunit [225]. eEF2 kinase is known to inhibit the phosphorylation of eEF2, mediating the GTP-dependent ribosome translocation on mRNA during the translation process [58, 226].

The interaction between mTORC1 and S6K1 is mediated by the eukaryotic translation initiation factor 3f (EIF3F) complex, a member of the Mov34 family [180, 183]. EIF3F complex provides a scaffold to allow interaction between mTORC1 and S6K1 to form the PIC complex [181, 182]. Overexpression of EIF3F in muscle cells and in adult skeletal muscle induced hypertrophy associated with an increase of sarcomeric proteins. In contrast, repression on EIF3F in differentiated skeletal muscle induced atrophy [183].

In contrast, following mTORC1 mediated phosphorylation at multiple residues (Thr37/46, Thr70, Ser65), 4E-BP1 no longer binds to eIF4E, allowing eIF4E binding with mRNA 7-methylguanosine cap structure, therefore allowing for recruitment of eIF4G, eIF4A, eIF3, 40S ribosomal subunits and the ternary complex (eIF2/Met-tRNA/GTP) to form the translation pre-initiation complex [15, 58].

1.4 Mechanisms of mTORC1 activation

1.4.1 Multi-site phosphorylation regulates mTORC1 function and activity

The catalytic/kinase activity of mTOR can be modulated by multi-site phosphorylation. Currently there are at least four phosphorylation sites characterized in mTOR, Ser2481, Ser2448, Thr2446 and Ser1261, respectively. Ser2481 is an autophosphorylation site, found to be closely related to the intrinsic catalytic activity of the mTOR [32]. As such, Ser2481 has been used as a biomarker to monitor the intrinsic catalytic activity of mTORC1. mTORC1 Ser2448 was reported to be a substrate for Akt *in vitro* and *in vivo* [35, 36, 37, 38], whereas a recent study identified S6K1 as a second Ser2448 kinase [39]. mTOR amino acids 2430–2450 sequence is thought to be a repressor region, deletion of which activated mTOR [39, 227]. Spatially, the Thr2446 site is adjacent to the Ser2448 site [32]. Although being in close proximity, it has been proposed that Thr2446/Ser2448 are phosphorylated by different kinases. For example, in direct evidence for this was provided by Cheng *et al* who found that Thr2446 phosphorylation status is inversely correlated with the Ser2448 phosphorylation level [40]. The significance of these two phosphorylation sites remains elusive, because substitution of Thr2446 and/or Ser2448 with alanine did not affect the mTOR activity [37]. In contrast, Ser1261 has been suggested to modulate mTOR catalytic activity [32]. Phosphorylated Ser1261 partially promotes mTORC1 catalytic activity as monitored by increased S6K1 and 4EBP1 phosphorylation and cell growth [41]. Though the work on identifying the Ser1261 kinase is still on going, it has been observed that insulin increases both mTORC1- and mTORC2 Ser1261 phosphorylation via PI3K kinase in cultured 3T3-L1 adipocytes [32].

1.4.2 mTORC1 interacting proteins

Raptor is a critical regulatory protein, directly associated with mTOR activity. Rapamycin and its associated protein FKBP12 can form complex and directly bind to the FRB domain of mTOR, blocking raptor access to mTOR, therefore uncoupling the mTOR from its substrates. Drummond *et al* found that taking 0.15 mg per kg of body weight rapamycin could effectively prohibit the protein

synthesis in skeletal muscle induced by acute bout of resistance exercise [42]. Nutritional status can also mediate mTOR activity through raptor. In the absence of nutrients, raptor interacts with mTOR via mLST8, which can block substrates accessing to the catalytic domain of the mTOR. In contrast, when nutritional supply is ample, the catalytic domain of mTOR will be accessible through disruption of Raptor/ mLST8 interaction, enabling accessibility of mTOR to its substrates (*e.g.*4E-BP1 or S6K1) [14].

Energy stress suppresses mTORC1 complex activity through AMPK mediated phosphorylation of raptor at Ser89 [43]. In addition, another interacting protein, PRAS40 (Proline-rich Akt substrate of 40 kDa), is thought to be a repressor of mTORC1 activity [45- 47]. Evidence demonstrates that PRAS40 binding to mTORC1 via raptor prevents substrates access to the catalytic domain of mTOR [46]. When PI3K/AKT signaling is activated by insulin, activated AKT phosphorylates PRAS40 at Thr246 and Ser183/Ser212/Ser221 to changes PRAS40 conformational structure, leading to detachment from the mTORC1 complex and allowing mTORC1 interaction with substrates [45]. As a newly characterised subunit, Deptor may play an inhibitory role in the mTORC1 activity in a manner similar to PRAS40, however understanding Deptor-mTORC1 interaction is still in its infancy [48, 49].

In addition to direct components of the mTOR complex, there are numerous associating proteins thought to be involved in mTOR activation. The two most chartacterised of these proteins are Ras homolog enriched in brain (Rheb) and the tuberous sclerosis complex proteins (TSC1 and TSC2). Rheb is a ~20kDa GTPase belonging to the Ras GTPase family. Like other small GTPases, Rheb is activated when loaded with GTP and become inactivated after hydrolysis of GTP into GDP [50]. Rheb is a direct upstream activator binding to mTOR complex. Bai *et al* found that Rheb prohibited FKBP38 (FK506-binding protein 38), an inhibitor of mTORC activity, from binding to mTOR complex as an antagonist [14,152,153]. However, the activity of the Rheb GTPase was also found to be inhibited by its upstream regulator TSC1/TSC2 complex [32, 50, 51]. The GTPase activating protein (GAP) domain in tuberous sclerosis complex 2 (TSC2 - Tuberin) can catalyze the hydrolysis of GTP to GDP, thus inactivating Rheb [50]. Mutations on genes encoding TSC1/TSC2 complex promote

mTOR complex activation and stimulate cell growth, which have been observed in several cancer cell lines with abnormal cell size expansion [14, 51].

1.4.3 Lipid molecules

Phosphatidic acid (PA) is a source of lipid widely distributed in cells, thought to act as a second messenger [228]. Importantly, mTORC1 and S6K1 are activated in response to increased PA [70] although the precise mechanism of this action is still under investigation. The PA synthase PLD2 (phospholipase D 2) has been reported to bind with mTORC1 subunit Raptor, linking PA generation with mTORC1 activation [191]. Alternatively, PA has been suggested to compete with Rapamycin/FKBP12 to bind on the FRB domain of mTOR, which blocks rapamycin/FKBP12 from inhibiting mTOR activity (Figure. 1.1). However, PA might also activate mTORC1 via alternative signalling pathways. Winter *et al* found that PA activites mTOR complex via upstream Raf-MAPK-ERK1/2 signalling mediated TSC1/TSC2 inhibition [53]. Rheb is believed to be the direct activator upstream PLD enzyme to facilitate mTOR translocation to lysosome membrane to be activated [208].

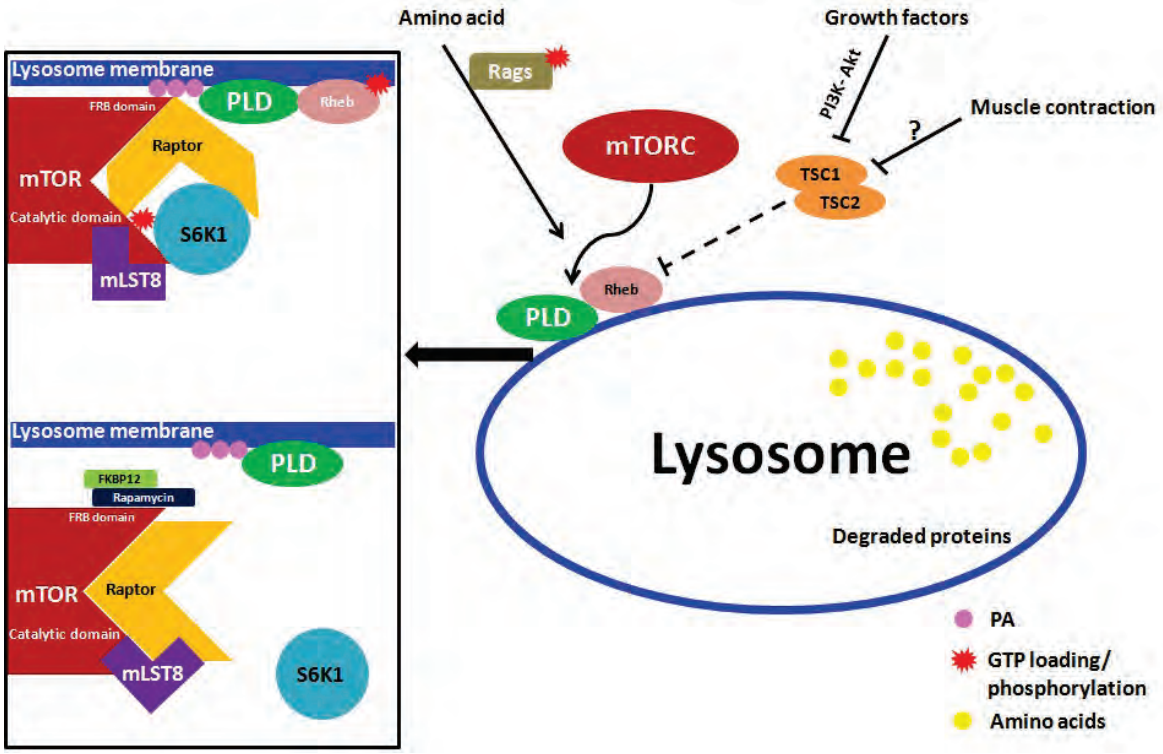

Figure 1.1 PLD2-generated PA activates mTORC1 through its FRB domain. PA (pink circles) and rapamycin/FKPB12 compete for the FRB domain on mTOR. In the presence of rapamycin (Rapa)/FKBP12complex, the FRB domain of mTOR is unable to bind PA, thus mTOR being unable to phosphorylate its substrates, such as S6K1 kinase. Excess supply of PA to the membrane would provide more sites for mTOR binding and compete with rapamycin/FKBP12 complex binding. The image was re- drawn based on Foster[70].

1.4.4 mTORC1 subcellular localization regulates intrinsic activity

The subcellular localisation of mTORC1 is key for its activation [154, 155,156]. Endosomal trafficking is thought to transport mTORC1 to specific cellular regions such as late endosome and lysosome (LEL), where mTORC1 is thought to undergo AA-induced mTORC1 activation [155, 156]. Furthermore, the membrane proteins on LEL are also found tightly associated with mTORC1 localization in response to stimulation. The Lysosome-associated membrane protein-2 (Lamp2) is regarded as one of the biomarkers on late lysosomes (Figure. 1.2), functioning to maintain the structural integrity of late lysosome membrane [157]. Importantly, mTORC1 has been reported to translocate to associate with Lamp2 protein-positive lysosome membrane regions after mechanical stimulation in mouse skeletal muscle [156].

Rab7 is an additional biomarker identified on LEL, inserted into the LEL membrane. When early endosome is matured during endosomal recycling, transition of Rab5 protein to Rab7 on the membrane, represents the formation of late endosome [156]. Many reports have pointed out the tight relationship between mTORC1 activity and Rab7, with mTORC1 observed to co-localise with Rab-7 positive regions during autophagosome maturation in cell model [195]. After AA stimulation, mTORC1 and Rheb were also observed to translocate to Rab7- positive vesicles in cultured HEK293T cells [99, 111]. As there is a high spatial association between mTORC1 and Rab7 during cellular events, Rab7 is thought be an important biomarker to indicate mTORC1 localization and biological activity.

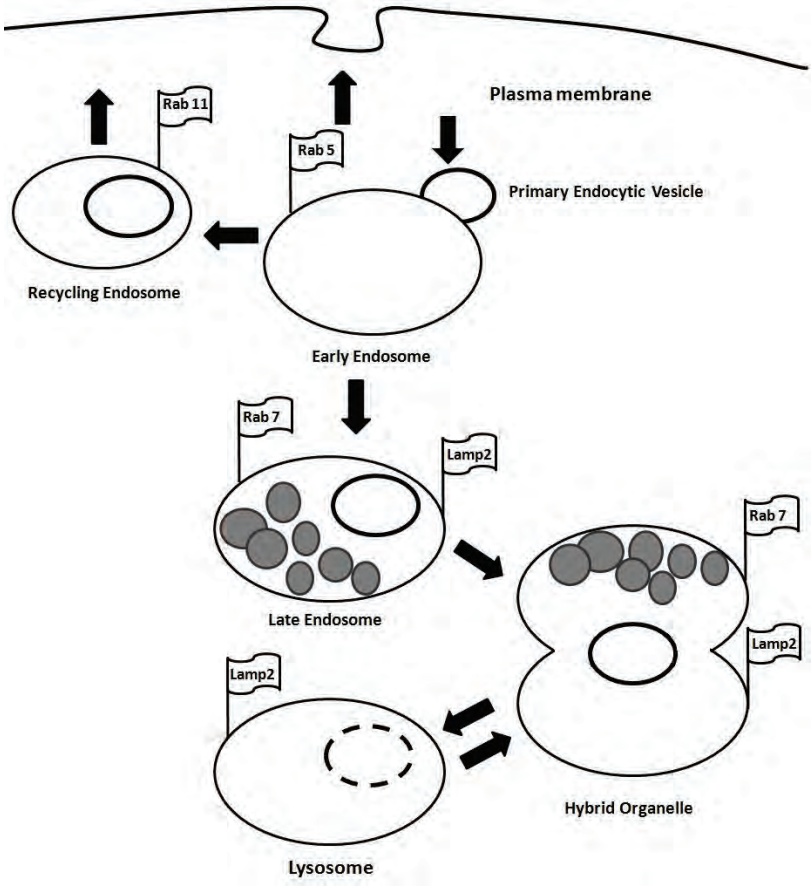

Figure 1.2 Endocytosis and the late endosome/lysosomal. Endocytosis starts from the uptake of plasma membrane into primary endocytic vesicles. The vesicles are transported to the early endosome characterized by the presence of Rab5 on its cytosolic membrane. The early endosome sorts the endocytosed material and returns the majority of endocytosed material to the plasma membrane either directly, or with the assistance of the recycling endosome which is characterized by the presence of Rab11. The remaining material for degradation is delivered by the early endosome to the late endosome compartment. The late endosome is characterized by the presence of Rab7 and multivesicular bodies. It also contains the lysosomal membrane protein Lamp2 which is delivered, along with endocytosed material, to the lysosome through the formation of a hybrid organelle. The hybrid organelle degrades the endocytosed material and the lysosome then recycles. The image is taken from Jacobs *et al* [156].

1.5 Effects of exercise on mTORC1 activation

Skeletal muscle mass is thought to be regulated *in vivo* by three physiological conditions; (1) growth factors, (2) mechanical loading/contraction and (3) nutrient provision. Each condition is thought to stimulate protein synthesis in skeletal muscle via distinct pathways, which ultimately converge on mTORC1 to regulate skeletal muscle mass [14].

1.5.1 Hormone and growth factor regulation of mTORC1 activity

Exercise induces the secretion of hormones such as growth hormone, insulin and insulin like growth factor (IGF) into the bloodstream. As shown in Figure 1.4, insulin/IGF trigger the PI3K-Akt axis through binding with their receptors in skeletal muscle [58]. Phosphoinositide 3-kinases (PI3Ks) phosphorylates membrane phosphatidylinositol 4, 5-bisphosphate (PIP2) to become phosphoinositide-3, 4, 5-trisphosphate (PIP3), a signal lipid acting as a docking site for protein kinase-1 (PDK1) and Akt [229]. Consequently, PDK1/Akt increase protein synthesis through direct phosphorylation of mTORC1, or removing the inhibitory factors (*e.g.* TSC1/TSC2 complex and PRAS40) binding to mTOR complex [15, 52]. Studies have suggested a key role for the Insulin/IGF-1/PI3K/Akt axis in regulating skeletal muscle mass, through increases in protein synthesis via mTORC1 activation [209], in addition to reducing protein degradation rate through reductions in FOXO signalling and associated atrogene expression (MuRF1, MaFbx) [210], all of which contribute to improved net protein balance and muscle hypertrophy [211].

1.5.2 Load-induced regulation of mTORC1 activity

In addition to hormone signalling, muscle contraction has been shown to regulate skeletal muscle protein synthesis. However, the mechano-sensor(s), transducing the effects of muscle contraction on mTORC1 activity, is still not fully understood. Based on current studies, muscle contraction is thought to active several signal pathways leading to mTORC regulation (Figure 1.4). The first evidence of load-specific induced mTORC1 activation was provided when it was demonstrated that the PI3- kinase inhibitor, wortmannin, did not prevent stretch- induced mTORC1 activity in isolated

extensor digitorum longus muscles [219]. Further research demonstrated that loading induced muscle contraction was found to promote mTORC1 activity independent of PI3K- Akt axis [220]. Currently the exact mechanism by which contraction increases mTORC1 activity is not known. It has been proposed that mTORC1 is mediated through stretch- activated calcium channels or through attachment complexes in the cell membrane (i.e. integrins) following contraction. However regulation and control of this process is currently unknown [220].

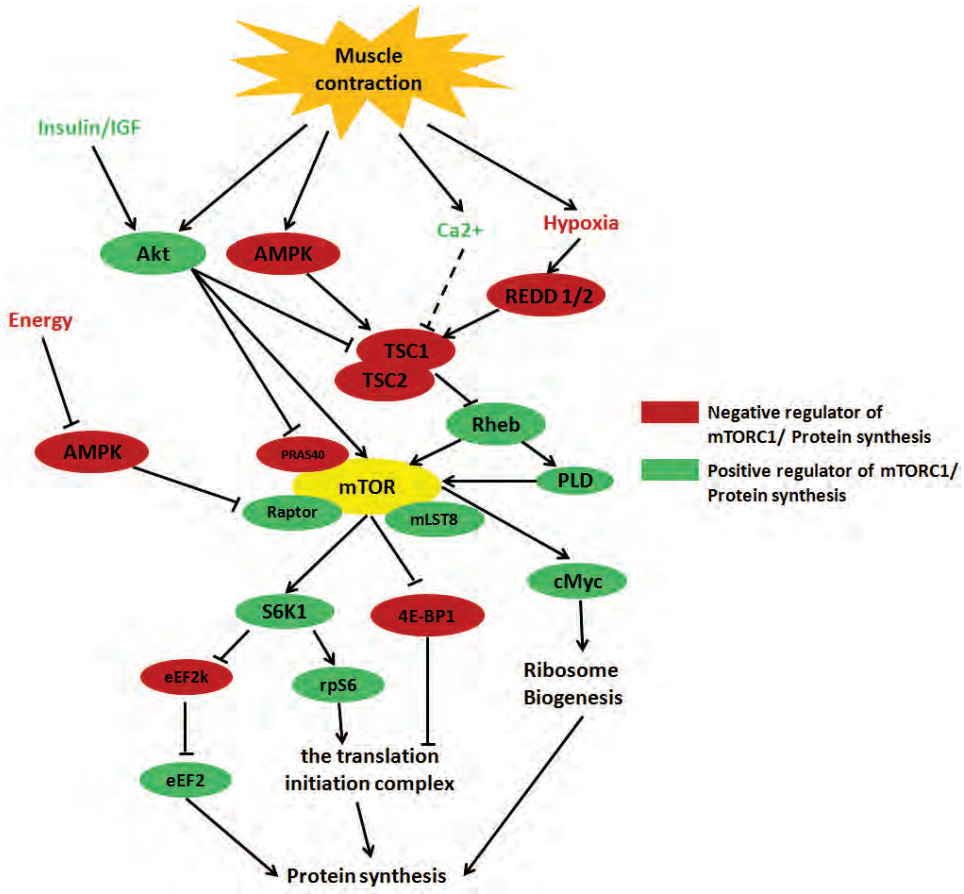

Figure 1.3 The diagram shows multiple signal pathways in skeletal muscle cross-talking on mTORC1, to influence protein synthesis as well as muscle cell growth. Insulin stimulates mTORC1 via PI3K-Akt axis while energy level modulates mTORC1 through influencing the AMPK signal pathway, which is in response to intracellular AMP/ATP ratio. Muscle contraction can induce multi-levels response of signaling transduction, which generates comprehensive effects on mTORC1 activity as well as the protein synthesis it conducts. The mechanical study of AA supplements on regulating mTORC1 activation and muscle protein

synthesis are just emerging, which is still poorly understood in many aspects. Image is taken from Drummond *et al*. [58].

1.5.3 Effects of different exercise modes on muscle protein synthesis

1.5.3.1 Resistance exercise

Early studies reported that the skeletal muscle protein turnover was depressed during the acute bout of resistance exercise [84, 85]. However, later studies demonstrate that the depression of muscle protein synthesis is quickly reversed during post-exercise recovery. Now it is commonly accepted that a single bout of resistance exercise can effectively stimulate net protein synthesis in human skeletal muscle, even in the fasted state [74- 77]. It should be emphasized that in addition, rates of muscle protein breakdown are also accelerated after resistance exercise [78, 79]. However, protein synthesis rates are increased to a greater extent than that of protein breakdown, thus stimulating the net increase of skeletal muscle protein balance post exercise [75, 76, 78].

At the molecular level, enhanced mRNA transcription has been observed after resistance exercise training, associating with increased muscle protein translation [224]. This can also be reflected by the activation of positive translation regulators. For example, S6K1 is reported to consistently be phosphorylated in the 1-6h after the bout of resistance exercise, together with increased protein synthesis [80, 81]. Meanwhile, another mTORC1 substrate 4E-BP1 is dephosphorylated to become inactivated post resistance exercise [80, 82] . Drummond *et al* found that the dephosphorylation of 4E-BP1 was only observed during resistance exercise, suggesting that 4E-BP1 might be independent of the regulating events in muscle protein anabolism post resistance exercise [58].

1.5.3.2 Endurance exercise

Besides resistance exercise, studies have also investigated the muscle protein synthesis response to different modes of muscle contraction, such as aerobic endurance exercise. Aerobic endurance

exercise is observed to stimulate muscle protein synthesis in both fasted [83-85] and fed conditions [84, 86, 87], with chronic aerobic exercise also leading to hypertrophy [88, 89]. However, compared with the obvious accumulation of myofibrillar proteins after acute bout of resistance exercise, the muscle protein turnover in acute aerobic endurance exercise is thought to be primarily caused by increase in mitochondrial expansion rather than by myofibrillar protein accretion based on various examinations on muscle protein in the fed states [90], except one study reporting the increase in myofibrillar protein synthesis after prolonged one-legged kicking exercise [91]. Currently, knowledge on the mechanisms of aerobic endurance exercise mediated increased muscle protein synthesis is still limited. There is some evidence that mTORC1 may be involved in this process given reports that mTORC1 Ser2448 phosphorylation is increased post acute aerobic exercise [92- 94], however this is still an area of intensive investigation.

1.6 Nutritional regulation of mTORC1 activity

AA supplementation is a potent activator of mTORC1 in skeletal muscle [98,160,177]. Of all the AA species, several are found to exhibit the significant stimulatory effects on mTORC1 activation, namely as the branch-chain amino acids (BCAA) [159]. Moreover, Leucine appears to be the most potent AA in stimulating mTORC1 activity [82,102].

1.6.1 Branch- chain amino acid

There are about three hundreds of AA species in nature, with twenty required for maintaining body functions [2]. Based on the needs for diet, nitrogen balance or cell growth, these twenty AAs can be generally classified as nutritionally essential (indispensable) or non-essential (dispensable) in human metabolism. The definition of essential AA (EAA) is those AAs whose carbon skeletons cannot be synthesized, or those that are inadequately synthesized *de novo* by the body. By contrast, non-essential AAs (NEAA) are AAs that can be synthesized *de novo* in adequate amounts by the body to meet optimal requirements [98].

Oral ingestion of EAAs stimulates muscle protein synthesis in rodents in addition to healthy young and old humans, either with or without exercise [96, 97, 99, 100, 150 [223]. Moreover, the stimulatory effect of complete mixture of EAAs on skeletal muscle protein turnover is mimicked by providing branched chain AA *in vitro* and *in vivo* rat experiments [103, 104]. On the contrary, feeding rat an AA mixture without the BCAAs showed no effert on muscle protein synthesis [105]. BCAAs belong to EAAs but are structurally different from other EAAs owing to their branch chain besides the main C-terminal chain, which includes valine, leucine and isoleucine. Of three BCAAs, leucine is found to have the most robust effects in stimulating protein synthesis in skeletal muscle [99,101,102,106]. Demonstrated by *in vitro* studies, the stimulating effect of leucine alone is nearly as equal as the mixture of three BCAAs together in both incubated diaphragm and perfused gastrocnemius [102, 104]. Moreover, oral ingestion of leucine is efficient to boost muscle protein synthesis whereas isoleucine or valine has no stimulatory effects [105].

1.6.2 Mechanistic regulation of mTORC1 by BCAA's.

Studies have identified that BCAAs, in particular leucine, are capable of activating mTORC1 and its downstream substrates directly, such as 4E-BP1 and p70S6K, to initiate protein synthesis [107, 108]. Direct microinjection of leucine into the cytoplasmic compartment of oocytes was effective to increase mTORC1 /p70S6K activity [119]. As to how leucine directly activiates mTORC1 is currently unclear, however, a number of mechanisms have recently been proposed. It has been suggested that BCAA may regulate mTORC1 activity via two proteins, raptor and/or Rheb. There is evidence supporting that leucine deprivation is counter-related to the interaction between mTOR and raptor, which can be restored by the re-addition of leucine into cell culture medium [105]. Conformational change is thought to be responsible for the mTOR- raptor interaction shift, and it is an interesting question to understand the roles leucine plays in this transformation [14]. On the other hand, overexpression of Rheb proteins can effectively stimulate the mTORC1 signaling in *Drosophila* S2 cells, even under the BCAA starvation [15]. By contrast, BCAA is insufficient to active mTORC1 in Rheb knock-down cells, suggesting the indispensible roles of Rheb in BCAA-stimulated mTORC1

signal transduction [110]. It is still not clear the molecular mechanism how BCAA mediate mTORC1 and Rheb interaction. It seems not to be through the inhibitory interaction between TSC1/TSC2 complex and Rheb, as the mTORC1 signaling was still prohibited after AA depletion in TSC2 knock-out mouse embryonic fibroblasts [109]. It is a question whether AA influence Rheb GTP/GDP exchange awaits further investigation [45]. Recent studies reported mTORC1 translocation to the Rheb-rich lysosomes after BCAA addition. Immunostaining analysis shows that mTOR is diffusely cytoplasmic under BCAA-starvation but aggregates onto a Rab7-rich membrane compartment, where Rheb is localized, upon re-addition of BCAA [99, 111]. A subfamily belonging to Ras GTPases family, named Rag, is identified to mediate BCAA- induced mTORC1 activation. Based on homological identity, Rag subfamily can be divided into two subgroups, RagA/B and RagC/D. Members in each subgroup are highly identical to each other, whereas the homology between subgroups is low (~20% identity between RagA/B and RagC/D) [15]. Functional Rag complexes are heterdimers composed of both subgroup members. There is direct evidence demonstrating the interaction of Rag GTPase with mTORC1 through association with raptor [111]. Depletion of either Rag complex or raptor by RNAi prevented the recruitment of mTOR to the Rab7-positive vesicles upon AA stimulation [99]. Like other GTPases, Rag function is controlled by its GTP load status. Binding of Rag to mTORC1 needs RagA/B charged GTP and is strengthened by RagC/D if GDP loaded. According to report by Sancak *et al.*, the supplementation of AA into culture medium was observed to promote GTP charging of endogenous Rag from 44% to 63%, as well as enhancing the association of Rag with mTORC1 [111]. So a model is proposed that AA could stimulate the recruitment of mTORC1 to Rheb-positive membrane area for activation by enhancing the GTP/GDP exchange of Rag complex. Nevertheless, because of lacking C-terminus membrane insertion sequences, it seems a problem for Rag complex *per se* to dock on the Rheb positive endosomal membranes, not to mention assisting mTORC1 translocation. Sabatini *et al.* identified additional new binding proteins based on biochemical experiments and demonstrated that Rag complex could reside on the Rheb positive membrane previously with the assistance of a “Ragulator” complex consisting of MP1, p14 and p18 [99]. However, they found AA addition only influenced the GTP loading form of Rag complex rather than

mediated the interaction of Rag complex with the regulator. In other words, AA supplements regulate the binding of mTORC1 on Rag complex. Intriguingly, the location of regulator complex on Rab7 positive microdomains is not clear, because there is little homology of the three new proteins with other known domains.

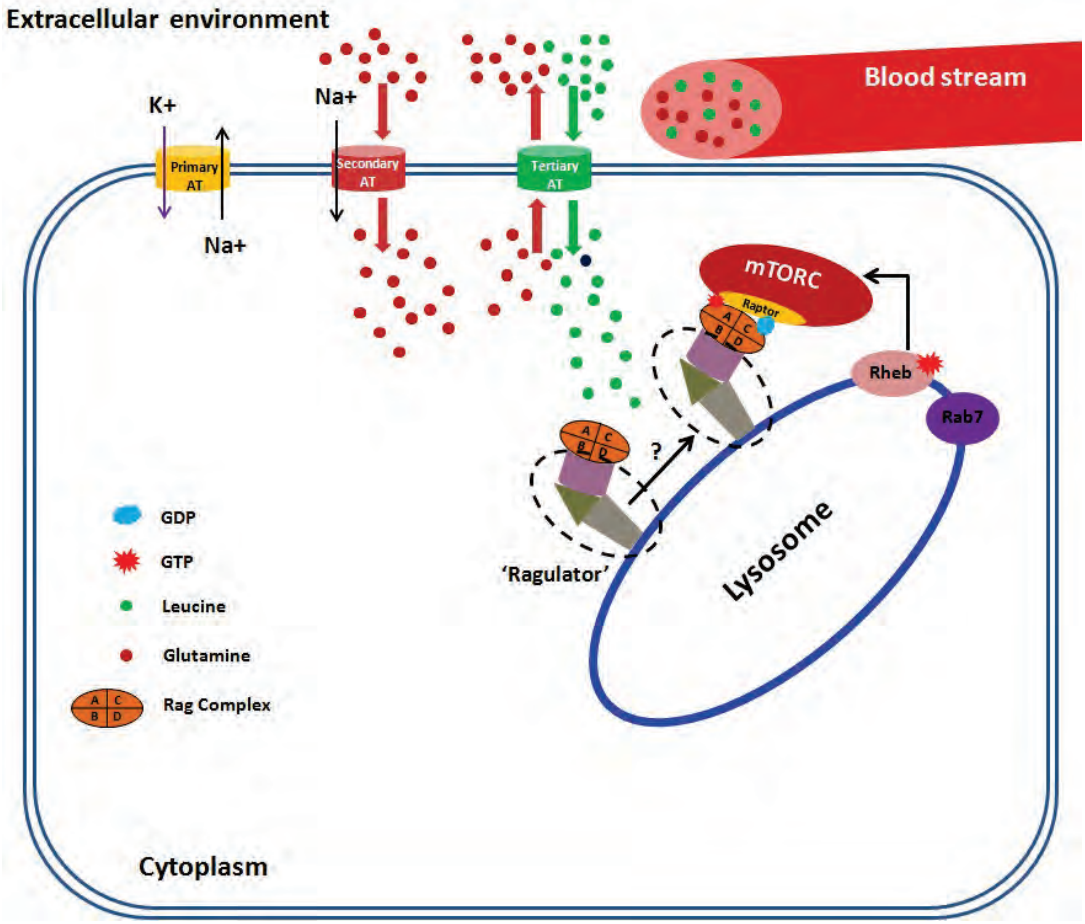

Figure 1.4 The diagram demonstrates the potential molecular mechanism of the Rag complex modulating mTORC1 activation when sensing nutrition avalibility. The Rag complex is heterodimer from two subgroups, RagA/B and Rag C/D. Special AA flux may be sensed by the Rag complex, which then assists mTORC1 translocating for activation. Specifically the Rag complex binds to Raptor in a GTP-RagA/B-dependent manner, which may be mediated by AA. "Ragulator" is consisted of MP1, p14 and p18, interacting with Rag proteins to target mTORC1 complex on the lysosome membrane, where Rheb and Rab7 is localized. In sum, it is proposed that mTORC1 is recruited by the Rag complex to the Rheb-positive compartment (possibly the

lysosome) in response to AA. The tertiary AA transporters (*e.g.* System L SLC7A5/SLC3A3) couple with secondary glutamine transport (*e.g.* System A SLC1A5) to efflux glutamine and to import leucine into muscle cells. This bidirectional transport enriches intracellular leucine pool to facilitate mTORC1 activation. However, it is not certain if the mammalian ortholog of Vps39 translocates toward the Rag complex owing to its GEF activity in response to AA. Image was adapted and re- drawn from Kim *et al* [15].

Another pertinent question is to how Rag complexes sense increased AA availability. It is reported that a PI kinase belonging to class III PI3K, named hVps34, may play the intermediate role between AA and mTORC1 [115, 116]. The catalyzed product of hVps34, PI(3)P, is often served as platforms on membrane to build trafficking complexes through the interaction of PI(3)P with other proteins owning special recognition domains. In these studies, AA was found to activate hVps34, hence inducing the accumulation of PI(3)P on endosomal membranes. And depletion of hVps34 could effectively suppress AA- stimulated mTORC1 signaling [115, 116]. Gulati *et al.* found AA addition could promote intracellular Ca^{2+} release and mTORC1 activity was inhibited after depleting the cellular Ca^{2+} [117]. They proposed that AA may activate hVps34 by enhancing interaction between hVps34 and Ca^{2+}/CaM if Ca^{2+} levels are increased. As a consequence, PI(3)P concentrations would be elevated on endosomal membranes, making it easier to recruit proteins forming functional complex, such as Rag and its regulators. In a report, *Yan et al.* showed that hVps34 bound to CaM. However, Ca^{2+} chelator treatment did not suppress its activity *in vivo*. In addition, there seemed no influence on hVps34 activity after removal of CaM by EDTA or EGTA washes in vitro [118]. Another possibility is that molecule conformational change is induced by increased cytoplasmic Ca^{2+} level. AA was previously reported to induce the conformational change of mTORC1 to access its substrates, though direct evidence is lacking in support of the regulation mediated by Ca^{2+}. So it is still questionable to the potential roles hVps34 plays in AA- induced mTORC1 activation. As parts of that, it is interesting to investigate the ‘platform’ components hVps34 recruits, especially whether including those reported involving in mTORC1 activation.

1.7 Immunofluorescence microscopy approaches to study mTORC *in vivo*

The intracellular localization of mTORC1 is tightly related with its activity. Advanced microscopy techniques have been applied to the molecule localization study, including mTORC1 research. For example, use of microscopy techniques have revealed mTORC1 to translocate to LEL compartment following the influx of AA into tumor cells [99].

In exercise physiology studies, the microscopy technique could therefore be a helpful experimental approach to study mTORC1 activation in response to muscle contraction. For example, immunofluorescence microscopy has been used as an effective way to investigate the spatial distribution and expression of mTORC proteins with LEL compartment in myosin heavy chain 2b muscle fibres in response to mechanical stimulation in mice skeletal muscle [156]. Moreover, immunofluorescence microscopy can be utilized to observe the redistribution of special signal molecules in response to stimuli such as nutrients and exercises in human skeletal muscle.

By virtue of the newly- developed computational semi-quantification techniques on microscope images, it is possible to not only visualize the molecule distribution and redistribution of proteins, but also to quantify the protein expression in local area, as well as the subcellular association between different proteins. The semi-quantification method based on microscopy images has been successfully utilized in various studies in skeletal muscle. For example, using semi-quantification method, Shepherd *et al* reported that the lipid droplet (LD)-associated proteins perilipin 2 is reduced in association with intramuscular lipid droplets after a single bout of endurance exercise, while the total perilipin 2 protein content is not changed in skeletal muscle [179].

As such, immunofluorescence microscopy is an effective research technique that can be used in combined with (semi)quantitative calculations, generating informative images demonstrating spatial distribution and local content of specific proteins. With regard to mTOR research, it will allow novel investigation into the role and regulation of mTOR biological activity in human skeletal muscle *in vivo*.

1.8 Overview of the thesis

Based on the aforementioned studies, the aim of this thesis is to develop analytical techniques to study mTOR cellular localization and protein complex regulation in human skeletal muscle.

In **Chapter 3**, we describe the development of new immunofluorescence microscopy methods to assess mTOR and its regulators in human skeletal muscle. To specify the immunofluorescence staining quality, a series of rigid testing methods were developed to qualify each antibody for experimental use. The results document that this novel experimental technique can reliably and reproducibly localize and measure skeletal muscle mTOR protein, two biomarkers of LEL membrane (Rab7, Lamp2) and its activity associated proteins (Rheb, EIF3F, TSC2), which will be applied in the further studies.

In **Chapter4,** we examined whether resistance exercise training would alter mTOR protein content and localisation in human skeletal muscle *in vivo*. To test this research question, we utilised the immunofluorescence microscopy approaches developed in **Chapter 3** to measure mTOR protein content in skeletal muscle cross sections obtained from young males in response to 10- week resistance exercise training. Further we then made use of the immunofluorescence approach to investigate the mTOR protein content relative to different myosin heavy chain subunits.

In **Chapter 5,** we changed our focus to investigate the spatial distribution and redistribution of mTOR in response to an acute bout of resistance exercise in combination with protein/carbohydrate ingestion. We observed high levels of association between mTOR and the lysosome in basal skeletal muscle, with a contraction-mediated translocation to the plasma membrane following exercise and nutrition. The functional relevance of this cellular redistribution appears to be to allow mTOR to interact with its positive regulator Rheb, in addition to the translation initiation factor eIF3f.

1.9 Reference

[1] Davis TA, Fiorotto ML (2009) Regulation of muscle growth in neonates. Curr Opin Clin Nutr Metab Care 12:78–85

[2] McArdle, William D. (2012). Exercise Physiology: Nutrition, Energy, and Human Performance Point (Lippincott Williams & Wilkins).

[3] Weiler, Tracey, Rumaisa Bashir, Louise VB Anderson, Keith Davison, Jennifer A. Moss, Stephen Britton, Edward Nylen et al. Identical mutation in patients with limb girdle muscular dystrophy type 2B or Miyoshi myopathy suggests a role for modifier gene (s). Human molecular genetics 8, no. 5 (1999): 871-877.

[4] England, S. B., L. V. B. Nicholson, M. A. Johnson, S. M. Forrest, D. R. Love, E. E. Zubrzycka-Gaarn, D. E. Bulman, J. B. Harris, and K. E. Davies. Very mild muscular dystrophy associated with the deletion of 46% of dystrophin. (1990): 180-182.

[5] Beggs, A. H., E. P. Hoffman, J. R. Snyder, Kiichi Arahata, Linda Specht, Frederic Shapiro, Corrado Angelini, Hideo Sugita, and L. M. Kunkel. Exploring the molecular basis for variability among patients with Becker muscular dystrophy: dystrophin gene and protein studies. American journal of human genetics 49, no. 1 (1991): 54.

[6] Hoffman, Eric P., Robert H. Brown, and Louis M. Kunkel. Dystrophin: the protein product of the Duchenne muscular dystrophy locus. Cell 51, no. 6 (1987): 919-928.

[7] Motlagh, Bahareh, Jay R. MacDonald, and Mark A. Tarnopolsky. Nutritional inadequacy in adults with muscular dystrophy. Muscle & nerve 31, no. 6 (2005): 713-718.

[8] Mok, Elise, Catherine Eléouet-Da Violante, Christel Daubrosse, Frédéric Gottrand, Odile Rigal, Jean-Eudes Fontan, Jean-Marie Cuisset, Joëlle Guilhot, and Régis Hankard. Oral glutamine and amino acid supplementation inhibit whole-body protein degradation in children with Duchenne muscular dystrophy. The American journal of clinical nutrition 83, no. 4 (2006): 823-828.

[9] MAKRIDES, SAVVAS C. Protein synthesis and degradation during aging and senescence. Biological Reviews 58, no. 3 (1983): 343-422.

[10] Fujita, Satoshi, and Elena Volpi. Amino acids and muscle loss with aging. The Journal of nutrition 136, no. 1 (2006): 277S-280S.

[11] Symons, T. Brock, Scott E. Schutzler, Tara L. Cocke, David L. Chinkes, Robert R. Wolfe, and Douglas Paddon-Jones. Aging does not impair the anabolic response to a protein-rich meal. The American Journal of Clinical Nutrition 86, no. 2 (2007): 451-456.

[12] Shakespeare, Valerie, and J. H. Buchanan. Increased degradation rates of protein in aging human fibroblasts and in cells treated with an amino acid analog. Experimental cell research 100, no. 1 (1976): 1-8.

[13] Vignos, Paul J., and Mary P. Watkins. The effect of exercise in muscular dystrophy. Jama 197, no. 11 (1966): 843-848.

[14] Hay, Nissim, and Nahum Sonenberg. Upstream and downstream of mTOR. Genes & development 18, no. 16 (2004): 1926-1945.

[15] Kim, Joungmok, and Kun-Liang Guan. Amino acid signaling in TOR activation. Annual review of biochemistry 80 (2011): 1001-1032.

[16] Hardie, D. Grahame, and Kei Sakamoto. AMPK: a key sensor of fuel and energy status in skeletal muscle. Physiology 21, no. 1 (2006): 48-60.

[17] Avruch, Joseph, Xiaomeng Long, Sara Ortiz-Vega, Joseph Rapley, Angela Papageorgiou, and Ning Dai. Amino acid regulation of TOR complex 1. American Journal of Physiology-Endocrinology and Metabolism 296, no. 4 (2009): E592-E602.

[18] Sehgal, S. N., H. Baker, and Claude Vézina. Rapamycin (AY-22,989), a new antifungal antibiotic. II. Fermentation, isolation and characterization. The Journal of antibiotics 28, no. 10 (1975): 727-732.

[19] Huang, Shile, and Peter J. Houghton. Targeting mTOR signaling for cancer therapy. Current opinion in pharmacology 3, no. 4 (2003): 371-377.

[20] Hara, Kenta, Yoshiko Maruki, Xiaomeng Long, Ken-ichi Yoshino, Noriko Oshiro, Sujuti Hidayat, Chiharu Tokunaga, Joseph Avruch, and Kazuyoshi Yonezawa. Raptor, a binding partner of target of rapamycin (TOR), mediates TOR action. Cell 110, no. 2 (2002): 177-189.

[21] Kim, Do-Hyung, Dos D. Sarbassov, Siraj M. Ali, Jessie E. King, Robert R. Latek, Hediye Erdjument-Bromage, Paul Tempst, and David M. Sabatini. mTOR interacts with raptor to form a nutrient-sensitive complex that signals to the cell growth machinery. Cell 110, no. 2 (2002): 163-175.

[22] Kim, Do-Hyung, Dos D. Sarbassov, Siraj M. Ali, Robert R. Latek, Kalyani VP Guntur, Hediye Erdjument-Bromage, Paul Tempst, and David M. Sabatini. GβL, a positive regulator of the rapamycin-sensitive pathway required for the nutrient-sensitive interaction between raptor and mTOR. Molecular cell 11, no. 4 (2003): 895-904.

[23] Fonseca, Bruno D., Ewan M. Smith, Vivian H-Y. Lee, Carol MacKintosh, and Christopher G. Proud. PRAS40 is a target for mammalian target of rapamycin complex 1 and is required for signaling downstream of this complex. Journal of Biological Chemistry 282, no. 34 (2007): 24514-24524.

[24] Sarbassov, Dos D., Siraj M. Ali, Do-Hyung Kim, David A. Guertin, Robert R. Latek, Hediye Erdjument-Bromage, Paul Tempst, and David M. Sabatini. Rictor, a novel binding partner of mTOR, defines a rapamycin-insensitive and raptor-independent pathway that regulates the cytoskeleton. Current biology 14, no. 14 (2004): 1296-1302.

[25] Yang, Qian, Ken Inoki, Tsuneo Ikenoue, and Kun-Liang Guan. Identification of Sin1 as an essential TORC2 component required for complex formation and kinase activity. Genes & development 20, no. 20 (2006): 2820-2832.

[26] Pearce, Laura, Xu Huang, Jérôme Boudeau, Rafal Pawlowski, Stephan Wullschleger, Maria Deak, Adel Ibrahim, Robert Gourlay, Mark Magnuson, and Dario Alessi. Identification of Protor as a novel Rictor-binding component of mTOR complex-2. Biochem. J 405 (2007): 513-522.

[27] Peterson, Timothy R., Mathieu Laplante, Carson C. Thoreen, Yasemin Sancak, Seong A. Kang, W. Michael Kuehl, Nathanael S. Gray, and David M. Sabatini. DEPTOR is an mTOR inhibitor frequently overexpressed in multiple myeloma cells and required for their survival. Cell 137, no. 5 (2009): 873-886.

[28] Chang, Yu-Yun, and Thomas P. Neufeld. An Atg1/Atg13 complex with multiple roles in TOR-mediated autophagy regulation. Molecular biology of the cell 20, no. 7 (2009): 2004-2014.

[29] Hosokawa, Nao, Taichi Hara, Takeshi Kaizuka, Chieko Kishi, Akito Takamura, Yutaka Miura, Shun-ichiro Iemura et al. Nutrient-dependent mTORC1 association with the ULK1–Atg13–FIP200 complex required for autophagy. Molecular biology of the cell 20, no. 7 (2009): 1981-1991.

[30] Jung, Chang Hwa, Chang Bong Jun, Seung-Hyun Ro, Young-Mi Kim, Neil Michael Otto, Jing Cao, Mondira Kundu, and Do-Hyung Kim. ULK-Atg13-FIP200 complexes mediate mTOR signaling to the autophagy machinery. Molecular biology of the cell 20, no. 7 (2009): 1992-2003.

[31] Kamada, Yoshiaki, Ken-ichi Yoshino, Chika Kondo, Tomoko Kawamata, Noriko Oshiro, Kazuyoshi Yonezawa, and Yoshinori Ohsumi. Tor directly controls the Atg1 kinase complex to regulate autophagy. Molecular and cellular biology 30, no. 4 (2010): 1049-1058.

[32] Foster, Kathryn G., and Diane C. Fingar. Mammalian target of rapamycin (mTOR): conducting the cellular signaling symphony. Journal of Biological Chemistry 285, no. 19 (2010): 14071-14077.

[33] Peterson, Randall T., Peter A. Beal, Michael J. Comb, and Stuart L. Schreiber. FKBP12-rapamycin-associated protein (FRAP) autophosphorylates at serine 2481 under translationally repressive conditions. Journal of Biological Chemistry 275, no. 10 (2000): 7416-7423.

[34] Soliman, Ghada A., Hugo A. Acosta-Jaquez, Elaine A. Dunlop, Bilgen Ekim, Nicole E. Maj, Andrew R. Tee, and Diane C. Fingar. mTOR Ser-2481 autophosphorylation monitors mTORC-specific catalytic activity and clarifies rapamycin mechanism of action. Journal of Biological Chemistry 285, no. 11 (2010): 7866-7879.

[35] Scott, Pamela H., Gregory J. Brunn, Aimee D. Kohn, Richard A. Roth, and John C. Lawrence. Evidence of insulin-stimulated phosphorylation and activation of the mammalian target of rapamycin mediated by a protein kinase B signaling pathway. Proceedings of the National Academy of Sciences 95, no. 13 (1998): 7772-7777.

[36] Nave, B., M. Ouwens, D. Withers, D. Alessi, and P. Shepherd. Mammalian target of rapamycin is a direct target for protein kinase B: identification of a convergence point for opposing effects of insulin and amino-acid deficiency on protein translation. Biochem. J 344 (1999): 427-431.

[37] Sekulić, Aleksandar, Christine C. Hudson, James L. Homme, Peng Yin, Diane M. Otterness, Larry M. Karnitz, and Robert T. Abraham. A direct linkage between the phosphoinositide 3-kinase-AKT signaling pathway and the mammalian target of rapamycin in mitogen-stimulated and transformed cells. Cancer research 60, no. 13 (2000): 3504-3513.

[38] Reynolds, Thomas H., Sue C. Bodine, and John C. Lawrence. Control of Ser2448 phosphorylation in the mammalian target of rapamycin by insulin and skeletal muscle load. Journal of Biological Chemistry 277, no. 20 (2002): 17657-17662.

[39] Chiang, Gary G., and Robert T. Abraham. Phosphorylation of mammalian target of rapamycin (mTOR) at Ser-2448 is mediated by p70S6 kinase. Journal of Biological Chemistry 280, no. 27 (2005): 25485-25490.

[40] Cheng, Susan WY, Lee GD Fryer, David Carling, and Peter R. Shepherd. Thr2446 is a novel mammalian target of rapamycin (mTOR) phosphorylation site regulated by nutrient status. Journal of Biological Chemistry 279, no. 16 (2004): 15719-15722.

[41] Acosta-Jaquez, Hugo A., Jennifer A. Keller, Kathryn G. Foster, Bilgen Ekim, Ghada A. Soliman, Edward P. Feener, Bryan A. Ballif, and Diane C. Fingar. Site-specific mTOR phosphorylation promotes mTORC1-mediated signaling and cell growth. Molecular and cellular biology 29, no. 15 (2009): 4308-4324.

[42] Drummond, Micah J., Christopher S. Fry, Erin L. Glynn, Hans C. Dreyer, Shaheen Dhanani, Kyle L. Timmerman, Elena Volpi, and Blake B. Rasmussen. Rapamycin administration in humans blocks the contraction‐induced increase in skeletal muscle protein synthesis. The Journal of physiology 587, no. 7 (2009): 1535-1546.

[43] Laplante, Mathieu, and David M. Sabatini. mTOR signaling at a glance. Journal of cell science 122, no. 20 (2009): 3589-3594.

[44] Wang, Lifu, John C. Lawrence, Thomas W. Sturgill, and Thurl E. Harris. Mammalian target of rapamycin complex 1 (mTORC1) activity is associated with phosphorylation of raptor by mTOR. Journal of Biological Chemistry 284, no. 22 (2009): 14693-14697.

[45] Sancak, Yasemin, Carson C. Thoreen, Timothy R. Peterson, Robert A. Lindquist, Seong A. Kang, Eric Spooner, Steven A. Carr, and David M. Sabatini. PRAS40 is an insulin-regulated inhibitor of the mTORC1 protein kinase. Molecular cell 25, no. 6 (2007): 903-915.

[46] Wang, Lifu, Thurl E. Harris, Richard A. Roth, and John C. Lawrence. PRAS40 regulates mTORC1 kinase activity by functioning as a direct inhibitor of substrate binding. Journal of Biological Chemistry 282, no. 27 (2007): 20036-20044.

[47] Vander Haar, Emilie, Seong-il Lee, Sricharan Bandhakavi, Timothy J. Griffin, and Do-Hyung Kim. Insulin signalling to mTOR mediated by the Akt/PKB substrate PRAS40. Nature cell biology 9, no. 3 (2007): 316-323.

[48] Adami, Alessandra, Begoña García-Álvarez, Ernesto Arias-Palomo, David Barford, and Oscar Llorca. Structure of TOR and its complex with KOG1. Molecular cell 27, no. 3 (2007): 509-516.

[49] Proud, Christopher G. Dynamic balancing: DEPTOR tips the scales. Journal of molecular cell biology 1, no. 2 (2009): 61-63.

[50] Inoki, Ken, Yong Li, Tian Xu, and Kun-Liang Guan. Rheb GTPase is a direct target of TSC2 GAP activity and regulates mTOR signaling. Genes & development 17, no. 15 (2003): 1829-1834.

[51] Huang, Jingxiang, and B. Manning. The TSC1-TSC2 complex: a molecular switchboard controlling cell growth. Biochem. J 412 (2008): 179-190.

[52] Avruch, J., K. Hara, Y. Lin, M. Liu, X. Long, S. Ortiz-Vega, and K. Yonezawa. Insulin and amino-acid regulation of mTOR signaling and kinase activity through the Rheb GTPase. Oncogene 25, no. 48 (2006): 6361-6372.

[53] Winter, Jeremiah N., Todd E. Fox, Mark Kester, Leonard S. Jefferson, and Scot R. Kimball. Phosphatidic acid mediates activation of mTORC1 through the ERK signaling pathway. American Journal of Physiology-Cell Physiology 299, no. 2 (2010): C335-C344.

[54] Wang, Lifu, Thurl E. Harris, and John C. Lawrence. Regulation of proline-rich Akt substrate of 40 kDa (PRAS40) function by mammalian target of rapamycin complex 1 (mTORC1)-mediated phosphorylation. Journal of Biological Chemistry 283, no. 23 (2008): 15619-15627.

[55] Oshiro, Noriko, Rinako Takahashi, Ken-ichi Yoshino, Keiko Tanimura, Akio Nakashima, Satoshi Eguchi, Takafumi Miyamoto et al. The proline-rich Akt substrate of 40 kDa (PRAS40) is a physiological substrate of mammalian target of rapamycin complex 1. Journal of Biological Chemistry 282, no. 28 (2007): 20329-20339.

[56] Walker, Dillon K., Jared M. Dickinson, Kyle L. Timmerman, Micah J. Drummond, Paul T. Reidy, Christopher S. Fry, David M. Gundermann, and Blake B. Rasmussen. Exercise, amino acids and aging in the control of human muscle protein synthesis. Medicine and science in sports and exercise 43, no. 12 (2011): 2249.

[57] Drummond, Micah J., Christopher S. Fry, Erin L. Glynn, Hans C. Dreyer, Shaheen Dhanani, Kyle L. Timmerman, Elena Volpi, and Blake B. Rasmussen. Rapamycin administration in humans blocks the contraction‐induced increase in skeletal muscle protein synthesis. The Journal of physiology 587, no. 7 (2009): 1535-1546.

[58] Drummond, Micah J., Hans C. Dreyer, Christopher S. Fry, Erin L. Glynn, and Blake B. Rasmussen. Nutritional and contractile regulation of human skeletal muscle protein synthesis and mTORC1 signaling. Journal of applied physiology 106, no. 4 (2009): 1374-1384..

[59] Rose, Adam J., Thomas J. Alsted, Thomas E. Jensen, J. Bjarke Kobberø, Stine J. Maarbjerg, Jørgen Jensen, and Erik A. Richter. A Ca2+–calmodulin–eEF2K–eEF2 signalling cascade, but not AMPK, contributes to the suppression of skeletal muscle protein synthesis during contractions. The Journal of physiology 587, no. 7 (2009): 1547-1563.

[60] Bolster, Douglas R., Stephen J. Crozier, Scot R. Kimball, and Leonard S. Jefferson. AMP-activated protein kinase suppresses protein synthesis in rat skeletal muscle through down-regulated mammalian target of rapamycin (mTOR) signaling. Journal of Biological Chemistry 277, no. 27 (2002): 23977-23980.

[61] Bylund-Fellenius, Ann-Christin, KAIE M. Ojamaa, KATHRYN E. Flaim, JEANNE B. Li, STEVEN J. Wassner, and LEONARD S. Jefferson. Protein synthesis versus energy state in contracting muscles of perfused rat hindlimb. American Journal of Physiology-Endocrinology and Metabolism 246, no. 4 (1984): E297-E305.

[62] Dreyer, Hans C., Satoshi Fujita, Jerson G. Cadenas, David L. Chinkes, Elena Volpi, and Blake B. Rasmussen. Resistance exercise increases AMPK activity and reduces 4E‐BP1 phosphorylation and protein synthesis in human skeletal muscle. The Journal of physiology 576, no. 2 (2006): 613-624.

[63] Corradetti, Michael N., Ken Inoki, and Kun-Liang Guan. The stress-inducted proteins RTP801 and RTP801L are negative regulators of the mammalian target of rapamycin pathway. Journal of Biological Chemistry 280, no. 11 (2005): 9769-9772.

[64] DeYoung, Maurice Phillip, Peter Horak, Avi Sofer, Dennis Sgroi, and Leif W. Ellisen. Hypoxia regulates TSC1/2–mTOR signaling and tumor suppression through REDD1-mediated 14–3–3 shuttling. Genes & development 22, no. 2 (2008): 239-251.

[65] Inoki, Ken, Tianqing Zhu, and Kun-Liang Guan. TSC2 mediates cellular energy response to control cell growth and survival. Cell 115, no. 5 (2003): 577-590.

[66] Murakami, Taro, Kazuya Hasegawa, and Mariko Yoshinaga. Rapid induction of REDD1 expression by endurance exercise in rat skeletal muscle. Biochemical and biophysical research communications 405, no. 4 (2011): 615-619.

[67] Chaillou, Thomas, Nathalie Koulmann, Nadine Simler, Adélie Meunier, Bernard Serrurier, Rachel Chapot, Andre Peinnequin, Michèle Beaudry, and Xavier Bigard. Hypoxia transiently affects skeletal muscle hypertrophy in a functional overload model. American Journal of Physiology-Regulatory, Integrative and Comparative Physiology 302, no. 5 (2012): R643-R654.

[68] D'Hulst, Gommaar, Cécile Jamart, R. Thienen, Peter Hespel, Marc Francaux, and Louise Deldicque. Effect of acute environmental hypoxia on protein metabolism in human skeletal muscle. Acta physiologica 208, no. 3 (2013): 251-264.

[69] Liu, Liping, Timothy P. Cash, Russell G. Jones, Brian Keith, Craig B. Thompson, and M. Celeste Simon. Hypoxia-induced energy stress regulates mRNA translation and cell growth. Molecular cell 21, no. 4 (2006): 521-531.

[70] Foster, David A. Regulation of mTOR by phosphatidic acid?. Cancer research 67, no. 1 (2007): 1-4.

[71] Sherwood, Daniel J., Scott D. Dufresne, Jeffrey F. Markuns, Bentley Cheatham, David E. Moller, Doron Aronson, and Laurie J. Goodyear. Differential regulation of MAP kinase, p70S6K, and Akt by contraction and insulin in rat skeletal muscle. American Journal of Physiology-Endocrinology And Metabolism 276, no. 5 (1999): E870-E878.

[72] Kramer, Henning F., Carol A. Witczak, Nobuharu Fujii, Niels Jessen, Eric B. Taylor, David E. Arnolds, Kei Sakamoto, Michael F. Hirshman, and Laurie J. Goodyear. Distinct signals regulate AS160 phosphorylation in response to insulin, AICAR, and contraction in mouse skeletal muscle. Diabetes 55, no. 7 (2006): 2067-2076.

[73] Whitehead, J., M. Soos, Rune Aslesen, Stephen Orahilly, and Jørgen Jensen. Contraction inhibits insulin-stimulated insulin receptor substrate-1/2-associated phosphoinositide 3-kinase activity, but not protein kinase B activation or glucose uptake, in rat muscle. Biochem. J 349 (2000): 775-781.

[74] Biolo, Gianni, Sergio P. Maggi, Bradley D. Williams, Kevin D. Tipton, and Robert R. Wolfe. Increased rates of muscle protein turnover and amino acid transport after resistance exercise in humans. American Journal of Physiology-Endocrinology And Metabolism 268, no. 3 (1995): E514-E520.

[75] Chesley, A., J. D. MacDougall, M. A. Tarnopolsky, S. A. Atkinson, and K. Smith. Changes in human muscle protein synthesis after resistance exercise. Journal of Applied Physiology 73, no. 4 (1992): 1383-1388.

[76] MacDougall, J. Duncan, Martin J. Gibala, Mark A. Tarnopolsky, Jay R. MacDonald, Stephen A. Interisano, and Kevin E. Yarasheski. The time course for elevated muscle protein synthesis following heavy resistance exercise. Canadian Journal of Applied Physiology 20, no. 4 (1995): 480-486.

[77] Yarasheski, Kevin E., Jeffrey J. Zachwieja, and Dennis M. Bier. Acute effects of resistance exercise on muscle protein synthesis rate in young and elderly men and women. American Journal of Physiology-Endocrinology And Metabolism 265, no. 2 (1993): E210-E214.

[78] Phillips, Stuart M., Kevin D. Tipton, Asle Aarsland, Steven E. Wolf, and Robert R. Wolfe. Mixed muscle protein synthesis and breakdown after resistance exercise in humans. American Journal of Physiology-Endocrinology And Metabolism 273, no. 1 (1997): E99-E107.

[79] Phillips, Stuart M., K. D. Tipton, Arny A. Ferrando, and Robert R. Wolfe. Resistance training reduces the acute exercise-induced increase in muscle protein turnover. American Journal of Physiology-Endocrinology And Metabolism 276, no. 1 (1999): E118-E124.

[80] Dreyer HC, Fujita S, Cadenas JG, Chinkes DL, Volpi E, Rasmussen BB. Resistance exercise increases AMPK activity and reduces 4E-BP1 phosphorylation and protein synthesis in human skeletal muscle. J Physiol 576 (2006): 613–624.

[81] Glover, Elisa I., Bryan R. Oates, Jason E. Tang, Daniel R. Moore, Mark A. Tarnopolsky, and Stuart M. Phillips. Resistance exercise decreases eIF2Bε phosphorylation and potentiates the feeding-induced stimulation of p70S6K1 and rpS6 in young men. American Journal of Physiology-Regulatory, Integrative and Comparative Physiology 295, no. 2 (2008): R604-R610.

[82] Dreyer, Hans C., Micah J. Drummond, Bart Pennings, Satoshi Fujita, Erin L. Glynn, David L. Chinkes, Shaheen Dhanani, Elena Volpi, and Blake B. Rasmussen. Leucine-enriched essential amino acid and carbohydrate ingestion following resistance exercise enhances mTOR signaling and protein synthesis in human muscle. American Journal of Physiology-Endocrinology And Metabolism 294, no. 2 (2008): E392-E400.

[83] Carraro, F. A. B. I. O., Charles A. Stuart, Wolfgang H. Hartl, Judah Rosenblatt, and Robert R. Wolfe. Effect of exercise and recovery on muscle protein synthesis in human subjects. American Journal of Physiology-Endocrinology And Metabolism 259, no. 4 (1990): E470-E476.

[84] Harber, Matthew P., Adam R. Konopka, Bozena Jemiolo, Scott W. Trappe, Todd A. Trappe, and Paul T. Reidy. Muscle protein synthesis and gene expression during recovery from aerobic exercise in the fasted and fed states. American Journal of Physiology-Regulatory, Integrative and Comparative Physiology 299, no. 5 (2010): R1254-R1262.

[85] Sheffield-Moore, M., C. W. Yeckel, E. Volpi, S. E. Wolf, B. Morio, D. L. Chinkes, D. Paddon-Jones, and R. R. Wolfe. Postexercise protein metabolism in older and younger men following moderate-intensity aerobic exercise. American Journal of Physiology-Endocrinology and Metabolism 287, no. 3 (2004): E513-E522.

[86] Harber, Matthew P., Justin D. Crane, Jared M. Dickinson, Bozena Jemiolo, Ulrika Raue, Todd A. Trappe, and Scott W. Trappe. Protein synthesis and the expression of growth-related genes are altered by running in human vastus lateralis and soleus muscles. American Journal of Physiology-Regulatory, Integrative and Comparative Physiology 296, no. 3 (2009): R708-R714.

[87] Howarth, Krista R., Natalie A. Moreau, Stuart M. Phillips, and Martin J. Gibala. Coingestion of protein with carbohydrate during recovery from endurance exercise stimulates skeletal muscle protein synthesis in humans. Journal of Applied Physiology 106, no. 4 (2009): 1394-1402.

[88] Pikosky, Matthew A., Patricia C. Gaine, William F. Martin, Kimberly C. Grabarz, Arny A. Ferrando, Robert R. Wolfe, and Nancy R. Rodriguez. Aerobic exercise training increases skeletal muscle protein turnover in healthy adults at rest. The Journal of nutrition 136, no. 2 (2006): 379-383.

[89] Short, Kevin R., Janet L. Vittone, Maureen L. Bigelow, David N. Proctor, and K. Sreekumaran Nair. Age and aerobic exercise training effects on whole body and muscle protein metabolism. American Journal of Physiology-Endocrinology and Metabolism 286, no. 1 (2004): E92-E101.

[90] Wilkinson, Sarah B., Stuart M. Phillips, Philip J. Atherton, Rekha Patel, Kevin E. Yarasheski, Mark A. Tarnopolsky, and Michael J. Rennie. Differential effects of resistance and endurance exercise in the fed state on signalling molecule phosphorylation and protein synthesis in human muscle. The journal of physiology 586, no. 15 (2008): 3701-3717.

[91] Miller, Benjamin F., Jens L. Olesen, Mette Hansen, Simon Døssing, Regina M. Crameri, Rasmus J. Welling, Henning Langberg et al. Coordinated collagen and muscle protein synthesis in human patella tendon and quadriceps muscle after exercise. The Journal of physiology 567, no. 3 (2005): 1021-1033.

[92] Benziane, Boubacar, Timothy J. Burton, Brendan Scanlan, Dana Galuska, Benedict J. Canny, Alexander V. Chibalin, Juleen R. Zierath, and Nigel K. Stepto. Divergent cell signaling after short-term intensified endurance training in human skeletal muscle. American Journal of Physiology-Endocrinology and Metabolism 295, no. 6 (2008): E1427-E1438.

[93] Camera, Donny M., Johann Edge, Michael J. Short, John A. Hawley, and Vernon G. Coffey. Early time course of Akt phosphorylation after endurance and resistance exercise. Medicine and science in sports and exercise 42, no. 10 (2010): 1843-1852.

[94] Mascher, Henrik, H. Andersson, P‐A. Nilsson, Björn Ekblom, and Eva Blomstrand. Changes in signalling pathways regulating protein synthesis in human muscle in the recovery period after endurance exercise. Acta Physiologica 191, no. 1 (2007): 67-75.

[95] Fujita, Satoshi, Takashi Abe, Micah J. Drummond, Jerson G. Cadenas, Hans C. Dreyer, Yoshiaki Sato, Elena Volpi, and Blake B. Rasmussen. Blood flow restriction during low-intensity resistance exercise increases S6K1 phosphorylation and muscle protein synthesis. Journal of Applied Physiology 103, no. 3 (2007): 903-910.

[96] Wolfe, Robert R. Regulation of muscle protein by amino acids. The Journal of nutrition 132, no. 10 (2002): 3219S-3224S.

[97] Paddon-Jones, Douglas, Melinda Sheffield-Moore, Xiao-Jun Zhang, Elena Volpi, Steven E. Wolf, Asle Aarsland, Arny A. Ferrando, and Robert R. Wolfe. Amino acid ingestion improves muscle protein synthesis in the young and elderly. American Journal of Physiology-Endocrinology and Metabolism 286, no. 3 (2004): E321-E328.

[98] Wu, Guoyao. Amino acids: metabolism, functions, and nutrition. Amino acids 37, no. 1 (2009): 1-17.

[99] Sancak, Yasemin, Liron Bar-Peled, Roberto Zoncu, Andrew L. Markhard, Shigeyuki Nada, and David M. Sabatini. Ragulator-Rag complex targets mTORC1 to the lysosomal surface and is necessary for its activation by amino acids. Cell 141, no. 2 (2010): 290-303.

[100] Fujita, Satoshi, Hans C. Dreyer, Micah J. Drummond, Erin L. Glynn, Jerson G. Cadenas, Fumiaki Yoshizawa, Elena Volpi, and Blake B. Rasmussen. Nutrient signalling in the regulation of human muscle protein synthesis. The Journal of physiology 582, no. 2 (2007): 813-823.

[101] Rennie, Michael J., Julien Bohé, Ken Smith, Henning Wackerhage, and Paul Greenhaff. Branched-chain amino acids as fuels and anabolic signals in human muscle. The Journal of nutrition 136, no. 1 (2006): 264S-268S.

[102] Buse, Maria G., and S. SANDRA Reid. Leucine. A possible regulator of protein turnover in muscle. Journal of Clinical Investigation 56, no. 5 (1975): 1250.

[103] Fulks, Richard M., Jeanne B. Li, and Alfred L. Goldberg. Effects of insulin, glucose, and amino acids on protein turnover in rat diaphragm. Journal of Biological Chemistry 250, no. 1 (1975): 290-298.

[104] Li, Jeanne B., and Leonard S. Jefferson. Influence of amino acid availability on protein turnover in perfused skeletal muscle. Biochimica et Biophysica Acta (BBA)-General Subjects 544, no. 2 (1978): 351-359.

[105] Kimball, Scot R., and Leonard S. Jefferson. Signaling pathways and molecular mechanisms through which branched-chain amino acids mediate translational control of protein synthesis. The Journal of nutrition 136, no. 1 (2006): 227S-231S.

[106] Smith K, Barua JM, Watt PW, Scrimgeour CM, Rennie MJ. Flooding with L-[1-13C] leucine stimulates human muscle protein incorporation of continuously infused L-[1-13C] valine. American Journal of Physiology-Endocrinology And Metabolism 262, no. 3 (1992): E372-E376.

[107] Karlsson, Håkan KR, Per-Anders Nilsson, Johnny Nilsson, Alexander V. Chibalin, Juleen R. Zierath, and Eva Blomstrand. Branched-chain amino acids increase p70S6k phosphorylation in human skeletal muscle after resistance exercise. American Journal of Physiology-Endocrinology and Metabolism 287, no. 1 (2004): E1-E7.

[108] Liu, Zhenqi, Linda A. Jahn, Wen Long, David A. Fryburg, Liping Wei, and Eugene J. Barrett. Branched Chain Amino Acids Activate Messenger Ribonucleic Acid Translation Regulatory Proteins in Human Skeletal Muscle, and Glucocorticoids Blunt This Action 1. The Journal of Clinical Endocrinology & Metabolism 86, no. 5 (2001): 2136-2143.

[109] Roccio, M., J. L. Bos, and F. J. T. Zwartkruis. Regulation of the small GTPase Rheb by amino acids. Oncogene 25, no. 5 (2006): 657-664.

[110] Avruch, J., K. Hara, Y. Lin, M. Liu, X. Long, S. Ortiz-Vega, and K. Yonezawa. Insulin and amino-acid regulation of mTOR signaling and kinase activity through the Rheb GTPase. Oncogene 25, no. 48 (2006): 6361-6372.

[111] Sancak, Yasemin, Timothy R. Peterson, Yoav D. Shaul, Robert A. Lindquist, Carson C. Thoreen, Liron Bar-Peled, and David M. Sabatini. The Rag GTPases bind raptor and mediate amino acid signaling to mTORC1. Science 320, no. 5882 (2008): 1496-1501.

[112] Sancak, Yasemin, Liron Bar-Peled, Roberto Zoncu, Andrew L. Markhard, Shigeyuki Nada, and David M. Sabatini. Ragulator-Rag complex targets mTORC1 to the lysosomal surface and is necessary for its activation by amino acids. Cell 141, no. 2 (2010): 290-303.

[113] Sancak, Yasemin, Carson C. Thoreen, Timothy R. Peterson, Robert A. Lindquist, Seong A. Kang, Eric Spooner, Steven A. Carr, and David M. Sabatini. PRAS40 is an insulin-regulated inhibitor of the mTORC1 protein kinase. Molecular cell 25, no. 6 (2007): 903-915.

[114] Kim, Eunjung, Pankuri Goraksha-Hicks, Li Li, Thomas P. Neufeld, and Kun-Liang Guan. Regulation of TORC1 by Rag GTPases in nutrient response. Nature cell biology 10, no. 8 (2008): 935-945.

[115] Nobukuni, Takahiro, Manel Joaquin, Marta Roccio, Stephen G. Dann, So Young Kim, Pawan Gulati, Maya P. Byfield et al. Amino acids mediate mTOR/raptor signaling through activation of class 3 phosphatidylinositol 3OH-kinase. Proceedings of the National Academy of Sciences of the United States of America 102, no. 40 (2005): 14238-14243.

[116] Byfield, Maya P., James T. Murray, and Jonathan M. Backer. hVps34 is a nutrient-regulated lipid kinase required for activation of p70 S6 kinase. Journal of Biological Chemistry 280, no. 38 (2005): 33076-33082.

[117] Gulati, Pawan, Lawrence D. Gaspers, Stephen G. Dann, Manel Joaquin, Takahiro Nobukuni, Francois Natt, Sara C. Kozma, Andrew P. Thomas, and George Thomas. Amino acids activate mTOR complex 1 via Ca 2+/CaM signaling to hVps34. Cell metabolism 7, no. 5 (2008): 456-465.

[118] Yan, Ying, Rory Flinn, Haiyan Wu, Rachel Schnur, and Jonathan Backer. hVps15, but not Ca2+/CaM, is required for the activity and regulation of hVps34 in mammalian cells. Biochem. J 417 (2009): 747-755.

[119] Hundal, Harinder S., and Peter M. Taylor. Amino acid transceptors: gate keepers of nutrient exchange and regulators of nutrient signaling. American Journal of Physiology-Endocrinology and Metabolism 296, no. 4 (2009): E603-E613.

[120] Shennan, David B., and Jean Thomson. Inhibition of system L (LAT1/CD98hc) reduces the growth of cultured human breast cancer cells. Oncology reports 20, no. 4 (2008): 885-889.

[121] Kim, Chang-Hyun, Kyung Jin Park, Jung Rim Park, Yoshikatsu Kanai, Hitoshi Endou, Joo-Cheol Park, and K. I. M. DO KYUNG. The RNA interference of amino acid transporter LAT1 inhibits the growth of KB human oral cancer cells. Anticancer research 26, no. 4B (2006): 2943-2948.

[122] Ohkame, Hirohisa, Hideki Masuda, Yukimoto Ishii, and Yoshikatsu Kanai. Expression of L‐type amino acid transporter 1 (LAT1) and 4F2 heavy chain (4F2hc) in liver tumor lesions of rat models. Journal of surgical oncology 78, no. 4 (2001): 265-272.

[123] Kanai, Yoshikatsu, and Matthias A. Hediger. The glutamate/neutral amino acid transporter family SLC1: molecular, physiological and pharmacological aspects. Pflügers Archiv 447, no. 5 (2004): 469-479.

[124] Alvestrand, A., P. Fürst, and J. Bergström. Plasma and muscle free amino acids in uremia: influence of nutrition with amino acids. Clinical nephrology 18, no. 6 (1982): 297-305.

[125] Vinnars E, Bergstro¨m J, Fürst P. Influence of the postoperative state on the intracellular free amino acids in human muscle tissue. Annals of surgery 182, no. 6 (1975): 665- 671.

[126] Evans, Kate, Zeerak Nasim, Jeremy Brown, Heather Butler, Samira Kauser, Hélène Varoqui, Jeffrey D. Erickson, Terence P. Herbert, and Alan Bevington. Acidosis-sensing glutamine pump SNAT2 determines amino acid levels and mammalian target of rapamycin signalling to protein

synthesis in L6 muscle cells. Journal of the American Society of Nephrology 18, no. 5 (2007): 1426-1436.

[127] Evans, Kate, Zeerak Nasim, Jeremy Brown, Emma Clapp, Amin Amin, Bin Yang, Terence P. Herbert, and Alan Bevington. Inhibition of SNAT2 by metabolic acidosis enhances proteolysis in skeletal muscle. Journal of the American Society of Nephrology 19, no. 11 (2008): 2119-2129.

[128] Verrey, François, Ellen I. Closs, Carsten A. Wagner, Manuel Palacin, Hitoshi Endou, and Yoshikatsu Kanai. CATs and HATs: the SLC7 family of amino acid transporters. Pflügers Archiv 447, no. 5 (2004): 532-542.

[129] Bevington, A., J. Brown, H. Butler, S. Govindji, K. Sheridan, and J. Walls. Impaired system A amino acid transport mimics the catabolic effects of acid in L6 cells. European journal of clinical investigation 32, no. 8 (2002): 590-602.

[130] Fumarola, Claudia, Silvia La Monica, and Guido G. Guidotti. Amino acid signaling through the mammalian target of rapamycin (mTOR) pathway: Role of glutamine and of cell shrinkage. Journal of cellular physiology 204, no. 1 (2005): 155-165.

[131] Christie, Graham R., Eric Hajduch, Harinder S. Hundal, Christopher G. Proud, and Peter M. Taylor. Intracellular sensing of amino acids in Xenopus laevis oocytes stimulates p70 S6 kinase in a target of rapamycin-dependent manner. Journal of Biological Chemistry 277, no. 12 (2002): 9952-9957.

[132] Low, Sylvia Y., Michael J. Rennie, and Peter M. Taylor. Involvement of integrins and the cytoskeleton in modulation of skeletal muscle glycogen synthesis by changes in cell volume. FEBS letters 417, no. 1 (1997): 101-103.

[133] Low, S. Y., M. J. Rennie, and P. M. Taylor. Signaling elements involved in amino acid transport responses to altered muscle cell volume. The FASEB journal 11, no. 13 (1997): 1111-1117.

[134] Berlanga, Juan J., Javier Santoyo, and César de Haro. Characterization of a mammalian homolog of the GCN2 eukaryotic initiation factor 2α kinase. European Journal of Biochemistry 265, no. 2 (1999): 754-762.

[135] Ameri, Kurosh, and Adrian L. Harris. Activating transcription factor 4. The international journal of biochemistry & cell biology 40, no. 1 (2008): 14-21.

[136] Kilberg, M. S., Y-X. Pan, H. Chen, and V. Leung-Pineda. Nutritional control of gene expression: how mammalian cells respond to amino acid limitation. Annual review of nutrition 25 (2005): 59–85.

[137] Novoa, Isabel, Huiqing Zeng, Heather P. Harding, and David Ron. Feedback inhibition of the unfolded protein response by GADD34-mediated dephosphorylation of eIF2α. The Journal of cell biology 153, no. 5 (2001): 1011-1022.

[138] Watanabe, Ryosuke, Yukihiro Tambe, Hirokazu Inoue, Takahiro Isono, Masataka Haneda, Ken-ichi Isobe, Toshiyuki Kobayashi, Okio Hino, Hidetoshi Okabe, and Tokuhiro Chano. GADD34 inhibits mammalian target of rapamycin signaling via tuberous sclerosis complex and controls cell survival under bioenergetic stress. International journal of molecular medicine 19, no. 3 (2007): 475-483.

[139] Guo, Feifan, and Douglas R. Cavener. The GCN2 eIF2α kinase regulates fatty-acid homeostasis in the liver during deprivation of an essential amino acid. Cell metabolism 5.2 (2007): 103-114.

[140] Xiao, Fei, Zhiying Huang, Houkai Li, Junjie Yu, Chunxia Wang, Shanghai Chen, Qingshu Meng et al. Leucine deprivation increases hepatic insulin sensitivity via GCN2/mTOR/S6K1 and AMPK pathways. Diabetes 60, no. 3 (2011): 746-756.

[141] Hyde, Russell, Emma L. Cwiklinski, Katrina MacAulay, Peter M. Taylor, and Harinder S. Hundal. Distinct sensor pathways in the hierarchical control of SNAT2, a putative amino acid transceptor, by amino acid availability. Journal of Biological Chemistry 282, no. 27 (2007): 19788-19798.

[142] Forsberg, Hanna, and Per O. Ljungdahl. Sensors of extracellular nutrients in Saccharomyces cerevisiae. Current genetics 40, no. 2 (2001): 91-109.

[143] Reynolds, Bruno, Robert Laynes, Margrét H. Ögmundsdóttir, CA Richard Boyd, and Deborah CI Goberdhan. Amino acid transporters and nutrient sensing mechanisms: new targets for treating insulin-linked disorders? Biochemical Society Transactions 35, no. Pt 5 (2007): 1215.

[144] Hyde, Russell, Karine Peyrollier, and Harinder S. Hundal. Insulin promotes the cell surface recruitment of the SAT2/ATA2 system A amino acid transporter from an endosomal compartment in skeletal muscle cells. Journal of Biological Chemistry 277, no. 16 (2002): 13628-13634.

[145] Usui, Takeo, Yoko Nagumo, Ai Watanabe, Takaaki Kubota, Kazusei Komatsu, Jun'ichi Kobayashi, and Hiroyuki Osada. Brasilicardin A, a natural immunosuppressant, targets amino acid transport system L. Chemistry & biology 13, no. 11 (2006): 1153-1160.

[146] NII, Tomoko, Hiroko Segawa, Yutaka Taketani, Yoshiko Tani, Makiko Ohkido, Sachie Kishida, Mikiko Ito et al. Molecular events involved in up-regulating human Na+-independent neutral amino acid transporter LAT1 during T-cell activation. Biochem. J 358 (2001): 693-704.

[147] Esmarck, B., J. L. Andersen, S. Olsen, Erik A. Richter, M. Mizuno, and Michael Kjær. Timing of postexercise protein intake is important for muscle hypertrophy with resistance training in elderly humans. The Journal of physiology 535, no. 1 (2001): 301-311.

[148] Tipton, Kevin D., Tabatha A. Elliott, Melanie G. Cree, Asle A. Aarsland, Arthur P. Sanford, and Robert R. Wolfe. Stimulation of net muscle protein synthesis by whey protein ingestion before and after exercise. American Journal of Physiology-Endocrinology and Metabolism 292, no. 1 (2007): E71-E76.

[149] Andersen, Lars L., Goran Tufekovic, Mette K. Zebis, Regina M. Crameri, George Verlaan, Michael Kjær, Charlotte Suetta, Peter Magnusson, and Per Aagaard. The effect of resistance training combined with timed ingestion of protein on muscle fiber size and muscle strength. Metabolism 54, no. 2 (2005): 151-156.

[150] Dickinson, Jared M., Christopher S. Fry, Micah J. Drummond, David M. Gundermann, Dillon K. Walker, Erin L. Glynn, Kyle L. Timmerman, Shaheen Dhanani, Elena Volpi, and Blake B. Rasmussen. Mammalian target of rapamycin complex 1 activation is required for the stimulation of human skeletal muscle protein synthesis by essential amino acids. The Journal of nutrition 141, no. 5 (2011): 856-862.

[151] Polak, Pazit, and Michael N. Hall. mTOR and the control of whole body metabolism. Current opinion in cell biology 21, no. 2 (2009): 209-218.

[152] Bai, Xiaochun, Dongzhu Ma, Anling Liu, Xiaoyun Shen, Qiming J. Wang, Yongjian Liu, and Yu Jiang. Rheb activates mTOR by antagonizing its endogenous inhibitor, FKBP38. Science 318, no. 5852 (2007): 977-980.

[153] Long, Xiaomeng, Sara Ortiz-Vega, Yenshou Lin, and Joseph Avruch. Rheb binding to mammalian target of rapamycin (mTOR) is regulated by amino acid sufficiency. Journal of Biological Chemistry 280, no. 25 (2005): 23433-23436.

[154] Narita, Masako, Andrew RJ Young, Satoko Arakawa, Shamith A. Samarajiwa, Takayuki Nakashima, Sei Yoshida, Sungki Hong et al. Spatial coupling of mTOR and autophagy augments secretory phenotypes. Science 332, no. 6032 (2011): 966-970.

[155] Flinn, Rory J., Ying Yan, Sumanta Goswami, Peter J. Parker, and Jonathan M. Backer. The late endosome is essential for mTORC1 signaling. Molecular biology of the cell 21, no. 5 (2010): 833-841.

[156] Jacobs, Brittany L., Craig A. Goodman, and Troy A. Hornberger. The mechanical activation of mTOR signaling: an emerging role for late endosome/lysosomal targeting. Journal of muscle research and cell motility 35, no. 1 (2014): 11-21.

[157] Eskelinen, Eeva-Liisa. Roles of LAMP-1 and LAMP-2 in lysosome biogenesis and autophagy. Molecular aspects of medicine 27.5 (2006): 495-502.

[158] Cheng, Susan WY, Lee GD Fryer, David Carling, and Peter R. Shepherd. Thr2446 is a novel mammalian target of rapamycin (mTOR) phosphorylation site regulated by nutrient status. Journal of Biological Chemistry 279, no. 16 (2004): 15719-15722.

[159] D'Antona, Giuseppe, Maurizio Ragni, Annalisa Cardile, Laura Tedesco, Marta Dossena, Flavia Bruttini, Francesca Caliaro et al. Branched-chain amino acid supplementation promotes survival and supports cardiac and skeletal muscle mitochondrial biogenesis in middle-aged mice. Cell metabolism 12, no. 4 (2010): 362-372.

[160] Paddon-Jones, Douglas, Melinda Sheffield-Moore, Xiao-Jun Zhang, Elena Volpi, Steven E. Wolf, Asle Aarsland, Arny A. Ferrando, and Robert R. Wolfe. Amino acid ingestion improves muscle protein synthesis in the young and elderly. American Journal of Physiology-Endocrinology and Metabolism 286, no. 3 (2004): E321-E328.

[161] Avruch, Joseph, Xiaomeng Long, Sara Ortiz-Vega, Joseph Rapley, Angela Papageorgiou, and Ning Dai. Amino acid regulation of TOR complex 1. American Journal of Physiology-Endocrinology and Metabolism 296, no. 4 (2009): E592-E602.

[162] Palacín, Manuel, Raúl Estévez, Joan Bertran, and Antonio Zorzano. Molecular biology of mammalian plasma membrane amino acid transporters. Physiological Reviews 78, no. 4 (1998): 969-1054.

[163] Nicklin, Paul, Philip Bergman, Bailin Zhang, Ellen Triantafellow, Henry Wang, Beat Nyfeler, Haidi Yang et al. Bidirectional transport of amino acid regulates mTOR and autophagy. Cell 136, no. 3 (2009): 521.

[164] Hyde, Russell, P. Taylor, and H. Hundal. Amino acid transporters: roles in amino acid sensing and signalling in animal cells. Biochem. J 373 (2003): 1-18.

[165] Drummond, Micah J., Christopher S. Fry, Erin L. Glynn, Kyle L. Timmerman, Jared M. Dickinson, Dillon K. Walker, David M. Gundermann, Elena Volpi, and Blake B. Rasmussen. Skeletal

muscle amino acid transporter expression is increased in young and older adults following resistance exercise. Journal of Applied Physiology 111, no. 1 (2011): 135-142.

[166] Drummond, Micah J., Erin L. Glynn, Christopher S. Fry, Kyle L. Timmerman, Elena Volpi, and Blake B. Rasmussen. An increase in essential amino acid availability upregulates amino acid transporter expression in human skeletal muscle. American Journal of Physiology-Endocrinology and Metabolism 298, no. 5 (2010): E1011-E1018.

[167] Reidy, Paul T., Dillon K. Walker, Jared M. Dickinson, David M. Gundermann, Micah J. Drummond, Kyle L. Timmerman, Mark B. Cope et al. Soy-dairy protein blend and whey protein ingestion after resistance exercise increases amino acid transport and transporter expression in human skeletal muscle. Journal of Applied Physiology 116, no. 11 (2014): 1353-1364.

[168] Dickinson, Jared M., David M. Gundermann, Dillon K. Walker, Paul T. Reidy, Michael S. Borack, Micah J. Drummond, Mohit Arora, Elena Volpi, and Blake B. Rasmussen. Leucine-Enriched Amino Acid Ingestion after Resistance Exercise Prolongs Myofibrillar Protein Synthesis and Amino Acid Transporter Expression in Older Men. The Journal of nutrition 144, no. 11 (2014): 1694-1702.

[169] Fujita, Satoshi, Hans C. Dreyer, Micah J. Drummond, Erin L. Glynn, Elena Volpi, and Blake B. Rasmussen. Essential amino acid and carbohydrate ingestion before resistance exercise does not enhance postexercise muscle protein synthesis. Journal of Applied Physiology 106, no. 5 (2009): 1730-1739.

[170] Hulmi, Juha J., Jörgen Tannerstedt, Harri Selänne, Heikki Kainulainen, Vuokko Kovanen, and Antti A. Mero. Resistance exercise with whey protein ingestion affects mTOR signaling pathway and myostatin in men. Journal of Applied Physiology 106, no. 5 (2009): 1720-1729.

[171] Moore, Daniel R., Meghann J. Robinson, Jessica L. Fry, Jason E. Tang, Elisa I. Glover, Sarah B. Wilkinson, Todd Prior, Mark A. Tarnopolsky, and Stuart M. Phillips. Ingested protein dose response of muscle and albumin protein synthesis after resistance exercise in young men. The American journal of clinical nutrition 89, no. 1 (2009): 161-168.

[172] Biolo, Gianni, Kevin D. Tipton, Samuel Klein, and Robert R. Wolfe. An abundant supply of amino acids enhances the metabolic effect of exercise on muscle protein. American Journal of Physiology-Endocrinology and Metabolism 273, no. 1 (1997): E122-E129.

[173] Børsheim, Elisabet, Kevin D. Tipton, Steven E. Wolf, and Robert R. Wolfe. Essential amino acid and muscle protein recovery from resistance exercise. American Journal of Physiology-Endocrinology and Metabolism 283, no. 4 (2002): E648-E657.

[174] Hartman, Joseph W., Jason E. Tang, Sarah B. Wilkinson, Mark A. Tarnopolsky, Randa L. Lawrence, Amy V. Fullerton, and Stuart M. Phillips. Consumption of fat-free fluid milk after resistance exercise promotes greater lean mass accretion than does consumption of soy or carbohydrate in young, novice, male weightlifters. The American journal of clinical nutrition 86, no. 2 (2007): 373-381.

[175] Tipton, Kevin D., Arny A. Ferrando, Stuart M. Phillips, David Doyle Jr, and Robert R. Wolfe. Postexercise net protein synthesis in human muscle from orally administered amino acid. American Journal of Physiology-Endocrinology and Metabolism 276, no. 4 (1999): E628-E634.

[176] Rasmussen, Blake B., Kevin D. Tipton, Sharon L. Miller, Steven E. Wolf, and Robert R. Wolfe. An oral essential amino acid-carbohydrate supplement enhances muscle protein anabolism after resistance exercise. Journal of Applied Physiology 88, no. 2 (2000): 386-392.

[177] Børsheim, Elisabet, Melanie G. Cree, Kevin D. Tipton, Tabatha A. Elliott, Asle Aarsland, and Robert R. Wolfe. Effect of carbohydrate intake on net muscle protein synthesis during recovery from resistance exercise. Journal of Applied Physiology 96, no. 2 (2004): 674-678.

[178] Bradley, Helen, Christopher S. Shaw, Philip L. Worthington, Sam O. Shepherd, Matthew Cocks, and Anton JM Wagenmakers. Quantitative immunofluorescence microscopy of subcellular GLUT4 distribution in human skeletal muscle: effects of endurance and sprint interval training. Physiological reports 2, no. 7 (2014): e12085.

[179] Shepherd, Sam O., Matthew Cocks, Kevin D. Tipton, Aaron M. Ranasinghe, Thomas A. Barker, Jatin G. Burniston, Anton JM Wagenmakers, and Christopher S. Shaw. Sprint interval and traditional endurance training increase net intramuscular triglyceride breakdown and expression of perilipin 2 and 5. The Journal of physiology 591, no. 3 (2013): 657-675.

[180] Hofmann, Kay, and Philipp Bucher. The PCI domain: a common theme in three multiprotein complexes. Trends in biochemical sciences 23, no. 6 (1998): 204-205.

[181] Holz, Marina K., Bryan A. Ballif, Steven P. Gygi, and John Blenis. mTOR and S6K1 mediate assembly of the translation preinitiation complex through dynamic protein interchange and ordered phosphorylation events. Cell 123, no. 4 (2005): 569-580.

[182] Harris, Thurl E., An Chi, Jeffrey Shabanowitz, Donald F. Hunt, Robert E. Rhoads, and John C. Lawrence. mTOR-dependent stimulation of the association of eIF4G and eIF3 by insulin. The EMBO journal 25, no. 8 (2006): 1659-1668.

[183] Lagirand-Cantaloube, Julie, Nicolas Offner, Alfredo Csibi, Marie P. Leibovitch, Sabrina Batonnet-Pichon, Lionel A. Tintignac, Carlos T. Segura, and Serge A. Leibovitch. The initiation factor eIF3-f is a major target for Atrogin1/MAFbx function in skeletal muscle atrophy. The EMBO journal 27, no. 8 (2008): 1266-1276.

[184] Rose, Adam J., Christa Broholm, Kristian Kiillerich, Stephen G. Finn, Christopher G. Proud, Mark H. Rider, Erik A. Richter, and Bente Kiens. Exercise rapidly increases eukaryotic elongation factor 2 phosphorylation in skeletal muscle of men. The Journal of physiology 569, no. 1 (2005): 223-228.

[185] Ryazanov, Alexey G. Ca< sup> 2+</sup>/calmodulin-dependent phosphorylation of elongation factor 2. FEBS letters 214, no. 2 (1987): 331-334.

[186] Deldicque, Louise, Daniel Theisen, and Marc Francaux. Regulation of mTOR by amino acid and resistance exercise in skeletal muscle. European journal of applied physiology 94, no. 1-2 (2005): 1-10.

[187] Glass, David J. Signalling pathways that mediate skeletal muscle hypertrophy and atrophy. Nature cell biology 5, no. 2 (2003): 87-90.

[188] Jackman, Robert W., and Susan C. Kandarian. The molecular basis of skeletal muscle atrophy. American Journal of Physiology-Cell Physiology 287, no. 4 (2004): C834-C843.

[189] Hunter, R. Bridge, Eric J. Stevenson, Alan Koncarevic, Heather Mitchell Felton, David A. Essig, and Susan C. Kandarian. Activation of an alternative NF-κB pathway in skeletal muscle during disuse atrophy. The FASEB Journal 16, no. 6 (2002): 529-538.

[190] Kandarian, Susan C., and Robert W. Jackman. Intracellular signaling during skeletal muscle atrophy. Muscle & nerve 33, no. 2 (2006): 155-165.

[191] Ha, Sang Hoon, Do-Hyung Kim, Il-Shin Kim, Jung Hwan Kim, Mi Nam Lee, Hyun Ju Lee, Jong Heon Kim, Sung Key Jang, Pann-Ghill Suh, and Sung Ho Ryu. PLD2 forms a functional complex with mTOR/raptor to transduce mitogenic signals. Cellular signalling 18, no. 12 (2006): 2283-2291.

[192] van IJzendoorn, Sven CD. Recycling endosomes. Journal of cell science 119, no. 9 (2006): 1679-1681.

[193] Huotari, Jatta, and Ari Helenius. Endosome maturation. The EMBO journal 30, no. 17 (2011): 3481-3500.

[194] Cai, Sheng-Li, Andrew R. Tee, John D. Short, Judith M. Bergeron, Jinhee Kim, Jianjun Shen, Ruifeng Guo, Charles L. Johnson, Kaoru Kiguchi, and Cheryl Lyn Walker. Activity of TSC2 is inhibited by AKT-mediated phosphorylation and membrane partitioning. The Journal of cell biology 173, no. 2 (2006): 279-289.

[195] Mavrakis, Manos, Jennifer Lippincott-Schwartz, Constantine A. Stratakis, and Ioannis Bossis. mTOR kinase and the regulatory subunit of protein kinase A (PRKAR1A) spatially and functionally interact during autophagosome maturation. Autophagy 3, no. 2 (2007): 151-153.

[196] Brooks GA, Fahey TD, Baldwin KM. Skeletal muscle structure and contractile properties. In: Exercise physiology - Human bioenergetics and its applications. 4th edn (2005). McGraw Hill Companies, New York, USA, pp 363-395

[197] Pedersen, Bente Klarlund, and Laurie Hoffman-Goetz. Exercise and the immune system: regulation, integration, and adaptation. Physiological reviews 80, no. 3 (2000): 1055-1081.

[198] Bárány, Michael. ATPase activity of myosin correlated with speed of muscle shortening. The Journal of General Physiology 50, no. 6 (1967): 197-218.

[199] Izquierdo, Mikel, Javier Ibáñez, Keijo Häkkinen, William J. Kraemer, Maite Ruesta, and Esteban M. Gorostiaga. Maximal strength and power, muscle mass, endurance and serum hormones in weightlifters and road cyclists. Journal of sports sciences 22, no. 5 (2004): 465-478.

[200] Rasmussen, Blake B., and Stuart M. Phillips. Contractile and nutritional regulation of human muscle growth. Exercise and sport sciences reviews 31, no. 3 (2003): 127-131.

[201] Waters, Debra L., Richard N. Baumgartner, and Philip J. Garry. Sarcopenia: current perspectives. The journal of nutrition, health & aging 4, no. 3 (1999): 133-139.

[202] Vandervoort, Anthony A., and T. Brock Symons. Functional and metabolic consequences of sarcopenia. Canadian Journal of Applied Physiology 26, no. 1 (2001): 90-101.

[203] Van Kan, G. Abellan. Epidemiology and consequences of sarcopenia. JNHA-The Journal of Nutrition, Health and Aging 13, no. 8 (2009): 708-712.

[204] Taaffe, Dennis R. Sarcopenia: exercise as a treatment strategy. Australian family physician 35, no. 3 (2006): 130.

[205] Song, Wook, Hyo-Bum Kwak, and John M. Lawler. Exercise training attenuates age-induced changes in apoptotic signaling in rat skeletal muscle. Antioxidants & redox signaling 8, no. 3-4 (2006): 517-528.

[206] Booth, F. W., and D. S. Criswell. Molecular events underlying skeletal muscle atrophy and the development of effective countermeasures. International journal of sports medicine 18, no. S 4 (1997): S265-S269.

[207] Linderman, J. K., KRISTIN L. Gosselink, FRANK W. Booth, VENKAT R. Mukku, and RICHARD E. Grindeland. Resistance exercise and growth hormone as countermeasures for skeletal muscle atrophy in hindlimb-suspended rats. American Journal of Physiology 267 (1994): R365-R365.

[208] Sun, Yan, Yimin Fang, M-S. Yoon, Chongben Zhang, Marta Roccio, F. J. Zwartkruis, Miles Armstrong, H. A. Brown, and Jie Chen. Phospholipase D1 is an effector of Rheb in the mTOR pathway. Proceedings of the National Academy of Sciences 105, no. 24 (2008): 8286-8291.

[209] Glass, David J. Signalling pathways that mediate skeletal muscle hypertrophy and atrophy. Nature cell biology 5, no. 2 (2003): 87-90.

[210] Stitt, Trevor N., Doreen Drujan, Brian A. Clarke, Frank Panaro, Yekatarina Timofeyva, William O. Kline, Michael Gonzalez, George D. Yancopoulos, and David J. Glass. The IGF-1/PI3K/Akt pathway prevents expression of muscle atrophy-induced ubiquitin ligases by inhibiting FOXO transcription factors. Molecular cell 14, no. 3 (2004): 395-403.

[211] Hitachi, Keisuke, and Kunihiro Tsuchida. Role of microRNAs in skeletal muscle hypertrophy. Frontiers in physiology 4 (2013).

[212] Mathews, Lawrence S., Gunnar Norstedt, and Richard D. Palmiter. Regulation of insulin-like growth factor I gene expression by growth hormone. Proceedings of the National Academy of Sciences 83, no. 24 (1986): 9343-9347.

[213] Yarasheski, Kevin E. Growth hormone effects on metabolism, body composition, muscle mass, and strength. Exercise and sport sciences reviews 22, no. 1 (1994): 285-312.

[214] Rooyackers, Olav E., and K. Sreekumaran Nair. Hormonal regulation of human muscle protein metabolism. Annual review of nutrition 17, no. 1 (1997): 457-485.

[215] Copeland, K. C., and K. S. Nair. Acute growth hormone effects on amino acid and lipid metabolism. The Journal of Clinical Endocrinology & Metabolism 78, no. 5 (1994): 1040-1047.

[216] Forbes, Gilbert B. The effect of anabolic steroids on lean body mass: the dose response curve. Metabolism 34, no. 6 (1985): 571-573.

[217] Bhasin, Shalender, Thomas W. Storer, Nancy Berman, Carlos Callegari, Brenda Clevenger, Jeffrey Phillips, Thomas J. Bunnell, Ray Tricker, Aida Shirazi, and Richard Casaburi. The effects of supraphysiologic doses of testosterone on muscle size and strength in normal men. New England Journal of Medicine 335, no. 1 (1996): 1-7.

[218] Urban, Randall J., Yvonne H. Bodenburg, Charles Gilkison, J. U. D. Y. Foxworth, Andrew R. Coggan, Robert R. Wolfe, and A. Ferrando. Testosterone administration to elderly men increases skeletal muscle strength and protein synthesis. American Journal of Physiology-Endocrinology And Metabolism 269, no. 5 (1995): E820-E826.

[219] Hornberger, Troy, Rudy Stuppard, Kevine Conley, Markj Fedele, Martal Fiorotto, Evar Chin, and Karyna Esser. Mechanical stimuli regulate rapamycin-sensitive signalling by a phosphoinositide 3-kinase-, protein kinase B-and growth factor-independent mechanism. Biochem. J 380 (2004): 795-804.

[220] Philp, Andrew, D. Lee Hamilton, and Keith Baar. Signals mediating skeletal muscle remodeling by resistance exercise: PI3-kinase independent activation of mTORC1. Journal of applied physiology 110, no. 2 (2011): 561-568.

[221] Cermak, Naomi M., Lisette CPGM de Groot, Wim HM Saris, and Luc JC van Loon. Protein supplementation augments the adaptive response of skeletal muscle to resistance-type exercise training: a meta-analysis. The American journal of clinical nutrition 96, no. 6 (2012): 1454-1464.

[222] Burd, Nicholas A., Daniel WD West, Daniel R. Moore, Philip J. Atherton, Aaron W. Staples, Todd Prior, Jason E. Tang, Michael J. Rennie, Steven K. Baker, and Stuart M. Phillips. Enhanced

amino acid sensitivity of myofibrillar protein synthesis persists for up to 24 h after resistance exercise in young men. The Journal of nutrition 141, no. 4 (2011): 568-573.

[223] Walker, Dillon K., Jared M. Dickinson, Kyle L. Timmerman, Micah J. Drummond, Paul T. Reidy, Christopher S. Fry, David M. Gundermann, and Blake B. Rasmussen. Exercise, amino acids and aging in the control of human muscle protein synthesis. Medicine and science in sports and exercise 43, no. 12 (2011): 2249.

[224] Pilegaard, Henriette, George A. Ordway, Bengt Saltin, and P. Darrell Neufer. Transcriptional regulation of gene expression in human skeletal muscle during recovery from exercise. American Journal of Physiology-Endocrinology And Metabolism 279, no. 4 (2000): E806-E814.

[225] Sturgill, Thomas W., L. Bryan Ray, Eleanor Erikson, and James L. Maller. Insulin-stimulated MAP-2 kinase phosphorylates and activates ribosomal protein S6 kinase II. Nature 334 (1988): 715-718.

[226] Browne, Gareth J., and Christopher G. Proud. Regulation of peptide‐chain elongation in mammalian cells. European Journal of Biochemistry 269, no. 22 (2002): 5360-5368.

[227] Sekulić, Aleksandar, Christine C. Hudson, James L. Homme, Peng Yin, Diane M. Otterness, Larry M. Karnitz, and Robert T. Abraham. A direct linkage between the phosphoinositide 3-kinase-AKT signaling pathway and the mammalian target of rapamycin in mitogen-stimulated and transformed cells. Cancer research 60, no. 13 (2000): 3504-3513.

[228] English, Denis. Phosphatidic acid: a lipid messenger involved in intracellular and extracellular signalling. Cellular signalling 8, no. 5 (1996): 341-347.

[229] Schiaffino, Stefano, and Cristina Mammucari. Regulation of skeletal muscle growth by the IGF1-Akt/PKB pathway: insights from genetic models. Skeletal Muscle 1, no. 1 (2011): 4-4.

Chapter 2

General Methods

2.1 Ethical approval

Human skeletal muscle samples used in chapter 4 were obtained from the School of Sports, Exercise and Rehabilitation sciences, University of Birmingham, which was approved by the west midlands NHS ethics committee (NHS REC Solihul West Midlands, 14/WM/0088). Human skeletal muscles samples used in study 5 and 6 were obtained from the University of Guelph and University of McMaster.

2.2 Human skeletal muscle sample analysis

2.2.1 Sample collection

Skeletal muscle samples used to develop the immunofluorescence histological microscopy methods were obtained from the *m. vastus lateralis* of one young healthy human volunteer (age, 20 years; body mass index (BMI) 25 $kg.m^{-2}$), using the percutaneous needle biopsy technique [1]. Samples were blotted to remove excess blood and dissected free of fat and collagen. Samples were then embedded in Tissue-Tek OCT compound (Sakura, 4583) and frozen in liquid nitrogen cooled isopentane solution (Sigma Aldrich, 270342). Sample preparation and embedding for immunofluorescence took ~1-2 min before samples were frozen in isopentane. After immediate freeznig, samples were stored in an aluminium cryotube (Caltag Medsystems, PA6003) and maintained at -80^{o}C until experimental analysis was performed.

2.2.2 Sample preparation for histology

Embedded muscle samples were fixed on solid ion cylinders by Tissue-Tek OCT under -25 °C temperature. Samples were then fixed in position in front of the microtome blade (Bright 5040, Bright Instrument Company limited, Huntingdon, England). The angle of the blade and samples were adjusted to guarantee that sections were cut in the proper direction (*e.g.* transverse or longitudinal sections), and an optical microscope (x10, Leica) was used for determining section orientation. Once the cutting angle was fixed, muscle sections were serially cut (5μm) under temperature maintained at -

25 °C and collected onto room temperature uncoated glass slides (VWR international). Sections were left to air dry at room temperature for at least 10min, to remove excess crystallized water of sections under storage. Each slide was then observed under the optical microscope before treatment, with only fresh sections used for histological experiments. Slides were kept under -20 °C freezer for short- term storage (≤ 3 months), or stored at -80 °C for longer- term storage (≥ 3 months).

2.3 Antibodies preparation

2.3.1 Primary antibody

When appropriate, monoclonal primary antibodies were applied for immunofluorescence histological staining due to their high sensitivity and specificity. If monoclonal antibodies were not available, polyclonal antibodies were applied to studies. For both classes of antibodies, a series of validation methods were developed to ascertain staining specificity and optimal conditions for application in human skeletal muscle.

2.3.2 Secondary antibody

Considering species cross- affinity, 5% normal goat serum was pre-incubated with tissue sections to reduce potential unspecific binding from secondary antibodies. All secondary antibodies were conjugated with Alexa$^{@}$ series fluorophores (invitrogen, Paisley, UK) unless stated elsewhere. In multiple costaining experiments, secondary antibodies targeting different proteins were visually distinguished by different Alexa dye fluorophores. For example, mTOR primary antibody was detected with secondary antibody conjugated with Alexa 594nm fluophores (red), Lamp2 primary antibody incubated with a secondary antibody tagged with Alexa 488nm fluophores (green). Validation methods were also developed to preclude potential cross- binding between two secondary antibodies during costaining experiments.

2.3.3 Other reagents

Phosphate buffered saline (PBS, 137 mM sodium chloride, 3 mM potassium chloride, 8 mM disodium hydrogen phosphate and 3 mM potassium dihydrogen phosphate, pH of 7.4. from Sigma Aldrich) was used for dilution of antibodies, goat serum, reagents and antibody washing steps.

Mowiel (6 g glycerol (Sigma Aldrich, G5150), 2.4 g mowiol 4-88 (Fluka, 81381) and 0.026 g 1,4-diazobicyclo-[2,2,2]-octane (DABCO) (Fluka, 33490) dissolved in 18 ml 0.2M Tris-buffer (pH 8.5) (Sigma Aldrich, T5030)) was used to mount all cover slips and slides.

2.4 Immunofluorescence histological staining method

2.4.1 Sample Fixation

Cryosections (5 μm) were fixed in both formaldehyde and acetone/ethanol fixation reagent (3:1) to determine the fixative that provided the highest quality images. Formaldehyde approaches can be problematic due to reaction with glycol bond to form the methylene (-CH2-) bridges among proteins of tissue, which further assembly into a molecular network to help stablise the structural integrity of tissue [2, 3]. However, the dense structure fixed over the tissue will also block the access of antibodies to their targeted proteins. So it may be necessary to permeate the tissue in the following steps to allow for the accessibility of antibodies. In contrast, the acetone/ethanol methods fix the muscle tissue through denaturing the biological structure of protein molecules rather than forming bonds. Coagulated proteins will lose their original shape, which might lead to the failure of some primary antibodies to recognize the specific site on targeted proteins. However, this reaction barely causes spatial blocking of antibodies to proteins, which facilitates the staining consistence throughout the whole section. In this study, based on the aforementioned justification, acetone/ethanol was selected as the universal fixation method unless stated.

2.4.2 Antibody incubation

The appropriate primary antibody dilution, incubation time and temperature were also studied and optimised. Initially, primary antibodies were tested at a series of dilutions ranging from 1:25 to 1:200 with incubation time of 2 hours at room temperature. For secondary antibodies, antibody dilution tests were performed at 1:100 and 1:200 and 1:300, with 30min incubation time under room temperature.

2.4.3 Staining protocols targeting one protein

Following air-drying for 10min, the prepared sections (5 μm) mounted on slides were fixed in acetone and ethanol (3:1) solution (Fisher technology) for 5 min. Sections were fully washed with 3x 5min in phosphate buffered saline (PBS) to remove fixation reagent. Sections were then pre-incubated with 5% normal goat serum for 30min. After another 3 x 5min PBS washing, primary antibody solution diluted with 5% normal goat serum (NGS, Invitrogen) was incubated with sections for 2 hours at room temperature. Sections were then washed 3x5min with PBS to remove unbound primary antibodies. Secondary antibody solution targeting specific primary antibodies were prepared in PBS with an incubation time of 30min at room temperature. Excess secondary antibodies were removed by 3x 5min PBS washing after incubation. Sections were finally incubated with wheat Germ Agglutinin conjugated with Alexa $^{@}$ 350(WGA-350) for 20min at room temperature to mark the sarcolemma membrane. Following a further 5min PBS wash to preserve the WGA fluorophores, slides were left to air dry for 1-2 min at room temperature until the visual water stains evaporated. Sections were then mounted with 20μL Mowiol and sealed by glass coverslips to protect the muscle sections and to preserve fluorescence signals. Slides were left fully dry overnight before observation under microscope.

2.4.4 Co-staining protocols targeting multiple proteins

Primary antibodies targeting different proteins were diluted into one mixed solution for simultaneous incubation to save time and fluorescences signals, previously described as the ‘cocktail’ method. To preclude the possibility of cross reactivity, we verified each antibody compared to negative controls.

2.4.5 Antibody validation

Rigid systemic testing protocols were established to test the specificity of images produced by each antibody cocktail. For every primary antibody applied in this thesis, we performed concentration optimization testing, double negative controls testing, signal channel specificity testing and reproducibility testing. For multiple protein staining experiments, cross-reaction negative control testing was applied on co-stained antibodies to establish the specificity of protein signals. More details on the staining performance of each antibody applied in the study can be found in the chapter 3.

2.5 Microscopy

2.5.1 Image capturing

Prepared slides were observed under a Nikon E600 microscope using a 40×0.75 numerical aperture objective. Images per area were captured under three colour filters achieved by a SPOT RT KE colour three shot CCD camera (Diagnostic Instruments Inc., MI, USA), illuminated by a 170 W Xenon light source. For images capture, DAPI UV (340–380 nm) filter was used to view WGA signals (blue) and mTOR stains tagged with Alexa 594 fluorophore (red) was visualised under the Texas red (540–580 nm) excitation filter. FITC (465–495nm) excitation filter was left to capture signals of mTOR-associated proteins, which were conjugated with Alexa Fluor 488 fluorophore unless stated elsewhere. DAPI UV (340-380 nm) was used to observe the DAPI stained nucleus. Switching among Filters was performed using a semi-automated filterwheel (10B 10 Position Filterwheel, Sutter, USA). All widefield images were obtained using a 40x objective (0.75 NA).

To provide enhanced clarity, higher resolution images were captured by an upright confocal microscope (Zeiss LSM 510 Meta, Carl Zeiss), using a 40× 1.4 NA water immersion objective. Fluorophores were visualised under three laser filters simultaneously. Alexa Fluor 488 fluorophore was excited by an argon laser and 498-571 nm emission, while a 594nm line of the helium–neon laser

with 601-713 nm emission was used to excite Alexa Fluor 594 fluorophore. WGA conjugated with Alexa 350 and DAPI was visualised under the excitation of the 405nm line from a Diode 405-30 filter.

The image capture setting was optimized following the indication of range indicators. Signal strength was controlled by the exposure time and photon sensitivity ("gain"). A range of image capture settings were tested to achieve optimal fluorescence signals. All the images in one experiment were taken under the same image settings.

2.5.2 Image analysis

All microscope images were processed under grey/white raw image format. The association between mTOR and cellular organelles, as well as between mTOR and regulating proteins was measured by colocalisation analysis. The subcellular distribution of mTOR was measured by quantification analysis.

2.5.2.1 Fluorescence colocalisation analysis

For colocalisation analysis, five to seven areas per section were randomly selected and imaged under the same capture settings. Images were processed and analysed under the Image-Pro Plus 5.1 software (Media Cybernetics, MD, USA). Image signals generated by WGA or dystrophin were used to estimate cell membrane borders, then merged with the corresponding target proteins images to identify the association between these proteins and plasma membrane. Pearson's correlation coefficient was used to measure colocalisation of two proteins in immunofluorescence images [4, 5, 6]. This method was also applied into the colocalisation analysis between mTOR and its associated proteins. All images analysis methods were kept consistent in the same study.

2.5.2.2 Fluorescence quantification analysis

Quantification of mTOR protein signal within nucleus area was achieved by analysing the fluorescence intensity of the signal within the dapi- positive area corresponding to the positive Alexa®594 staining. Firstly, threshold was optimized to extract the positive fluorescent signal for

creating a mask of the area stained positive for the nucleus (stained by Dapi) using routine parameter settings. Before quantification, fluorescence signals of proteins were filtered to exclude the background noise by setting the adjusted lower limit and upper limit in threshold settings. Then the extracted nucleus outline was overlaid onto the corresponding protein images and fluorescence intensity of the protein fluorescence was quantified within the outlined nucleus area. Mean fluorescent intensity of the signal was measured from five to seven images per section resulting from 70-100 muscle fibres. The final mean fluorescent intensity was considered from the average of duplicates.

2.6 Statistics

Reproducibility of antibodies was obtained from repeated colocalisation analysis or fluorescence quantification (three duplicate measures) from the same subject before formal studies. The reproducibility of duplicate measures for specific antibodies was assessed by the range and coefficient of variation (CV) between duplicates.

In each experimental chapter, all immunofluorescence image analysis was performed in duplicate (2 sections on 1 slide). The table data for each time point was the mean value of 2 duplicate sections on 1 slide from 7 persons in each group. For statistical analysis, Pearson's correlation coefficient values achieved from 5-7 areas captured in each section at each time point were successively input into statistical analysis software (SPSS for windows version (SPSS, Chicago, IL)), and a two- way ANOVA was applied to calculate significance of data among different time points between groups. For quantification analysis, mean value of data from protein fluorophore intensity was calculated and compared following the same statistic analysis strategy as that of colocalisation analysis in SPSS. Significance was set at $P < 0.05$. Data was presented as means ± S.E.M.

2.7 Acknowledgement

I would like to acknowledge the help and advice of Dr. Chris Shaw, Dr. Helen Bradley and Dr. Oliver Wilson on protein quantification methods and protein colocalisation analysis method development.

2.8 References

[1] Bergström, Jonas. Percutaneous needle biopsy of skeletal muscle in physiological and clinical research. Scandinavian Journal of Clinical & Laboratory Investigation 35.7 (1975): 609-616.

[2] Fox, Cecil H., et al. Formaldehyde fixation. J Histochem Cytochem 33.8 (1985): 845-853.

[3] Helander, Kerstin G. Kinetic studies of formaldehyde binding in tissue. Biotechnic & histochemistry 69.3 (1994): 177-179.

[4] Bolte, S., and Fabrice P. Cordelières. A guided tour into subcellular colocalization analysis in light microscopy. Journal of microscopy 224.3 (2006): 213-232.

[5] Landmann, Lukas, and Permsin Marbet. Colocalization analysis yields superior results after image restoration. Microscopy research and technique 64.2 (2004): 103-112.

[6] Lachmanovich, E., et al. Co-localization analysis of complex formation among membrane proteins by computerized fluorescence microscopy: application to immunofluorescence co-patching studies. Journal of microscopy 212.2 (2003): 122-131.

Chapter 3

Antibody Validation

3.1 Abstract

The aim of the chapter was to develop a series of immunofluorescence histology staining methods in human skeletal muscle to visualize the mTOR protein complex, as well as mTOR associated proteins. All immunofluorescence signals observed were validated through the double negative, signal channel specificity and cross binding control approaches to verify specificity of signal capture. For signal sensitivity, all immunofluorescence signals were optimized to capture the microscope images with strong fluorescence strength *versus* low background, ensuring accuracy of fluoresecence measured in the microscope images. Lastly, the primary antibodies applied in this chapter endured repeatability validation testing, which was designed to measure the reliability of experimental data. In conclusion, this chapter details a novel analysis method to study mTOR in human skeletal muscle. All antibodies applied into the studies in the thesis were validated under a series of methodologies to guarantee the specificity, sensitivity and repeatability of fluorescence signals achieved from the immunofluorescence microscopy technique.

3.2 Introduction

Immunocytochemistry was first reported in 1942 by Albert et al, who developed a fluorescent-labelled antibody to localize the pneumococcal antigen in liver sections [1]. The approach was a significant advance as it provided a powerful method utilising antibodies to localize subcellular structures in both cultured cells *in vitro* and tissue sections *in vivo*. Labelling methods used in immunocytochemistry can be divided into three types: fluorescence, enzymes and particulate [2]. As one of the derivative methods, immunofluorescence is a widely used immunocytochemistry technique that utilises fluorophores to visualize the localisation of proteins stained by antibodies [2, 3].

The recognition of a primary antibody to a specific antigen is important to guarantee specific staining in immunofluorescence experiments. The antibody structure is constituted by a variable region (Fab portion) that binds the epitope part of the antigen and the constant region (Fc portion) that is specific to the animal where the antibody was raised [4]. Antibody isotypes are categorized based on the differences in the AA sequence in the constant region (Fc) of the antibody heavy chains. There are five major antibody isotypes, and the immunoglobulin G (IgG) is the most common antibody type applied in the immunofluorescence experiment [2]. There are four IgG subclasses (designated 1- 4) present in human, mouse and rat [5, 6]. The subclasses differ in the number of disulfide bonds and the length and flexibility of the hinge region [6]. In addition to the heavy chain, sequence variations in the constant region of the antibody light chain are further subclassified as kappa (κ) and lambda (λ) [7]. The antibody that directly binds to the interested antigen through its variable region is referred to as the primary antibody. In contrast, the antibody that binds the constant region (Fc portion) of the primary antibody in animal specificity type is also known as a secondary antibody [2, 3, 4].

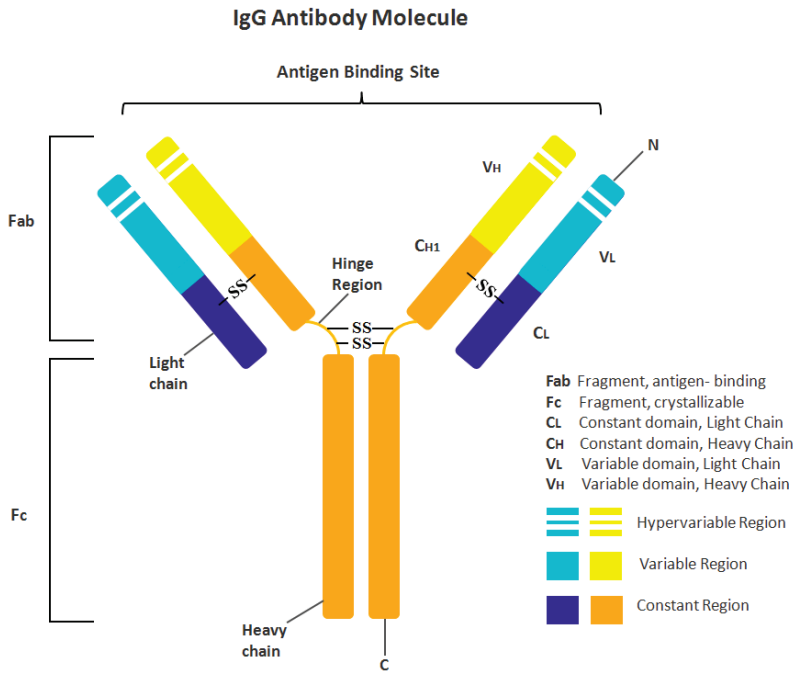

Figure 3.1 Diagram to demonstrate IgG antibody structure. Antibody is composed of two fragments, the Fab fragment and Fc fragment. Fc fragment is sequence reserved while Fab fragment is sequence variable. Antigen binds with the Fab fragment of antibody, while Fc fragment determines the isotype of antibody [12]. Image was re- drawn based on Wang *et al* [12] and Edelman [13].

There are three types of immunocytochemistry controls proposed, primary antibody controls, secondary antibody controls and label controls [2]. For direct immunocytochemistry, the primary antibody control is used to examine the binding between antibody and antigen. Most primary antibody controls are based on gene manipulation methods in transgenic animals. However, there are some key principles to follow. Normal serum is incubated on sample to fill the redundant space among cells, which reduce the unspecific binding of antibody [2]. And it is recommended that when obtaining the primary antibody, those antibodies validated under immunocytochemistry testing are primarily considered for experiments [2]. It is also suggested to compare the novelty of the antigen sequence on which monoclonal antibody is generated [8, 10]. The published immunocytochemisty data from the similar study model is referred to when distinguishing the signals [8].

For indirect immunocytochemistry with an unlabelled primary antibody, and a species- specific labelled secondary antibody, secondary antibody controls are needed to show that each secondary antibody binds to the correct primary antibody. The secondary antibody control should be applied without the primary antibody incubation, under which circumstances no labelled fluorescence should be visualized [2, 9]. Utilization of the label conjugated secondary antibody eliminates the unspecific binding of labels on antibodies. For multiple antibodies staining experiment, it is important to validate the signal emission specificity to guarantee no bleed- through of signals into other channels affecting the specificity of signals [8, 10]. For the 'cocktail' costaining method, rigid control experiment is indispensible to exclude the false signals from the cross-staining between primary antibodies and secondary antibodies.

As highlighted in chapter 2, there is a close relationship between mTOR activity and its intracellular distribution. Taking advantage of immunofluorescent approaches, studies have been made in cell and rodent models [14, 15]. However, microscopy data in human skeletal muscle is lacking. To develop the immmunofluorescence technique obtaining high quality mTOR microscope images from human skeletal muscle, all antibodies applied into studies need systemically validation here to guarantee their staining specificity and sensitivity. To address these issues, within this chapter we describe immunofluorescent approaches to study mTOR and associated proteins in human skeletal muscle.

3.3 Antibodies and dyes

3.3.1 Primary antibodies

The monoclonal antibody against mTOR was from Merck Millipore Corporation (Billerica, MA; Cat No. #05-1592); polyclonal antibody against Lamp2 was from Abgent Technology Company (Suzhou, China; Cat No. AP1824d); monoclonal antibody against Rab7 was from Abcam biotech company (Cambridge, ENG; Cat No. ab50533); monoclonal antibody against Rheb was from GenWay Biotech, Inc (San Diego, CA; Cat No. GWB-2AD39C); polyclonal antibody against EIF3F was from Abcam biotech company (Cambridge, ENG; Cat No. ab74568); monoclonal antibody against integrin ß-3 was from Cell signaling (USA; Cat No. #13166); Monoclonal antibody against Tuberin was from Abgent Technology Company (Suzhou, China; Cat No. S1798); Lectin from Ulex europaeus conjugated with FITC was from Sigma- Aldrich Company Ltd. (Gillingham, UK; Cat No. L9006 Sigma); Monoclonal antibody against myosin heavy chain I was from Developmental Studies Hybridoma Bank (Iowa, USA; Cat No. A4.840); Monoclonal antibody against myosin heavy chain IIx was from Developmental Studies Hybridoma Bank (Iowa, USA; Cat No. 6H1); Monoclonal antibody against myosin heavy chain I and IIa was from Developmental Studies Hybridoma Bank (Iowa, USA; Cat No. N2.261); Wheat Germ Agglutinin conjugated with Alexa Fluor® 350 was from Life Technologies Ltd. (Paisley, UK; Cat No. W11263); Monoclonal antibody against dystrophin was from Developmental Studies Hybridoma Bank (Iowa, USA; Cat No. MANDYS1(3B7)).

3.3.2 Secondary antibodies

If not otherwise stated, secondary antibodies were conjugated with Alexa$^{@}$ Series immunofluorescences dyes. For multiple proteins staining experiment, secondary antibodies with different isotypes were used to guarantee that specific fluorescence from each protein was observed under distinguished wavelength channel from the others. The following table describes the combination of primary antibodies with corresponding secondary antibodies applied in this chapter.

Primary Antibody	Secondary Antibody
Mouse monoclonal antibody anti-mTOR,isotype IgG γ1 kappa	Goat anti- mouse IgG γ1 Alexa®594
Rabbit polyclonal antibody anti-Lamp2,isotype IgG	Goat anti- rabbit IgG Alexa®488
Mouse monoclonal antibody anti- Rab7,isotype IgG 2β	Goat anti- mouse IgG 2β Alexa®488
Rabbit monoclonal antibody anti- Rheb,isotype IgG	Goat anti- rabbit IgG Alexa®488
Rabbit polyclonal antibody anti- EIF3F, isotype IgG	Goat anti- rabbit IgG Alexa®488
Mouse monoclonal antibody anti- Tuberin, isotype IgGγ1	Goat anti- mouse IgG γ1 Alexa®594
Lectin from *Ulex europaeus* Agglutinin conjugated with FITC fluorescences (UEA-I)	Alexa Fluor® 488 Conjugated
Mouse monoclonal antibody anti- myosin heavy chain I , isotype IgG M	Goat anti- mouse IgG M Alexa®488
Mouse monoclonal antibody anti- myosin heavy chain IIx , isotype IgG M	Goat anti- mouse IgG M Alexa®488
Mouse monoclonal antibody anti- myosin heavy chain I and IIa, isotype IgG G1	Goat anti- mouse IgG G1 Alexa®594
Wheat Germ Agglutinin	Alexa Fluor® 350 Conjugated
Mouse monoclonal antibody anti- dystrophin, isotype IgG 2α	Goat anti- mouse IgG 2α Alexa®488

Table 3.1 List of validated primary antibody combined with secondary antibody for study.

3.3.3 Additional antibodies and dyes

Cellular nuclei were stained by the 4', 6-diamidino-2-phenylindole (DAPI, 1:1000, Sigma D9542). Blood vessels were stained by Lectin from Ulex europaeus Agglutinin conjugated with FITC fluorescences (Sigma Aldrich, UK, L9006). The plasma membrane (PM) was either outlined by the monoclonal antibody against the membrane protein dystrophin (Glenn E. Morris, MANDYS1 clone 3B7) or stained by another membrane protein Wheat Germ Agglutinin conjugated with Alexa Fluor®350 (1:100, Invitrogen, UK), generally depending on the excitation filters of cell membrane

staining signals. To determine different muscle fiber types, the myosin heavy chain I and IIx proteins were stained by primary antibodiese purchased from Developmental Studies Hybridoma Bank (University of Iowa, USA; Cat No. A4. 840 for MHC I and Cat No. 6H1 for MHC IIx).

3.4 Antibody optimization

3.4.1 Primary antibody dilution

Each antibody was tested at a series of dilutions following the same staining procedures and same concentration of secondary antibody. The best dilution was selected based on the high signal strength as well as low background noise level. Also, the specificity of protein stains was validated by a series of negative control staining (in 3.3.3). Phosphate buffered saline was used for the dilution of antibodies, reagents and washing steps. The incubation time for primary antibody was 2 hour at room temperature if not mentioned elsewhere.

3.4.2 Secondary antibody dilution

For secondary antibody, the dilution test was performed at 1:100 and 1:200 with incubation time for 30min under room temperature. 1:100 and 1:200 dilution exhibited similar stain signal strength, while the background fluorescences noise for 1:200 dilution was lower than that of 1:100 dilution. So the dilution 1:200 was generally applied for all immunofluorescence staining experiments unless stated elsewhere.

3.4.3 Additional dyes/antibodies dilution

DAPI was used to stain the nucleus of muscle cells. The dye was optimized at 1:1000 dilution in human skeletal muscle, and the incubation time was optimized as long as 5min. Wheat Germ Agglutinin conjugated with Alexa Fluor®350 (1:100, W11263, Invitrogen, UK) was optimised to incubate with samples for 20min.

3.5 Antibody validation

Antibodies were validated through a series of control experiments, designed to assess signal specificity and signal stability for each antibody applied into studies.

3.5.1 Double negative control

Double negative control samples were tested for each antibody, in which the immunofluorescence staining was completed following the same procedure as positive experiments, with PBS solution used to instead of the primary antibody. This allowed for testing of any non-specific staining that may occur. For consistency, the secondary antibody was replaced by PBS solution to exclude the possibility that unspecific immunofluorescence would be stained by primary antibody itself as a negative control.

3.5.2 Signal channel specificity control

Signal channel specificity controls were also developed to exclude the chance of data being confounded by bleed of signal into different channels. For example, when using the DAPI filter to observe the Alexa-350 signals, these images were also acquired with the FITC filter and Texas red filter to guarantee that no signal was detected in the other two channels applied to visualise other protein signals. This procedure was also carried out for the other secondary antibodies used (Alexa Fluor 488 and 594). Cryosections were tested for autofluorescence in the absence of any antibodies, simply applying PBS to the section following the fixtation and staining steps required.

3.5.3 Cross-binding control

In co-staining experiments, the primary antibodies were validated by cross-reaction negative controls. For example, when mTOR and Lamp2 were co-stained, secondary antibody targeting Lamp2 antibody was used to stain the mTOR primary antibody. In contrast, Lamp2 primary antibody was also incubated with secondary antibody recognizing mTOR primary antibody. This cross-binding test identifies unspecific cross- binding between primary antibodies and secondary antibodies.

Multiple antibodies costaining	Primary Antibodies costained	Secondary Antibodies costained
3.8.1 Costaining of mTOR with Lamp2	Mouse monoclonal antibody anti-mTOR,isotype IgG γ1 kappa	Goat anti- mouse IgG γ1 Alexa®594
	Rabbit polyclonal antibody anti-Lamp2,isotype IgG	Goat anti- rabbit IgG Alexa®488
3.8.2 Costaining of mTOR with Rheb	Mouse monoclonal antibody anti-mTOR,isotype IgG γ1 kappa	Goat anti- mouse IgG γ1 Alexa®594
	Rabbit monoclonal antibody anti-Rheb,isotype IgG	Goat anti- rabbit IgG Alexa®488
3.8.3 Costaining of mTOR with Rab7	Mouse monoclonal antibody anti-mTOR,isotype IgG γ1 kappa	Goat anti- mouse IgG γ1 Alexa®594
	Mouse monoclonal antibody anti-Rab7,isotype IgG 2 β	Goat anti- mouse IgG 2 β Alexa®488
3.8.4 Costaining of mTOR with EIF3F	Mouse monoclonal antibody anti-mTOR,isotype IgG γ1 kappa	Goat anti- mouse IgG γ1 Alexa®594
	Rabbit polyclonal antibody anti-EIF3F, isotype IgG	Goat anti- rabbit IgG Alexa®488
3.8.5 Costaining of Tuberin with Rheb	Mouse monoclonal antibody anti-Tuberin, isotype IgGγ1	Goat anti- mouse IgG γ1 Alexa®594
	Rabbit monoclonal antibody anti-Rheb,isotype IgG	Goat anti- rabbit IgG Alexa®488
3.8.6 Costaining of Lamp2 with Rab7	Rabbit polyclonal antibody anti-Lamp2,isotype IgG	Goat anti- rabbit IgG Alexa®594
	Mouse monoclonal antibody anti-Rab7,isotype IgG 2 β	Goat anti- mouse IgG 2 β Alexa®488
3.8.7 Costaining of mTOR with UEA-I	Mouse monoclonal antibody anti-mTOR,isotype IgG γ1 kappa	Goat anti- mouse IgG γ1 Alexa®594
	Lectin from *Ulex europaeus* Agglutinin conjugated with FITC fluorescences (UEA-I)	Alexa Fluor® 488 Conjugated
3.8.8 Costaining of mTOR with MHCI	Mouse monoclonal antibody anti-mTOR,isotype IgG γ1 kappa	Goat anti- mouse IgG γ1 Alexa®594
	Mouse monoclonal antibody anti-myosin heavy chain I , isotype IgG M	Goat anti- mouse IgG M Alexa®488
3.8.9 Costaining of mTOR with MHCIIx	Mouse monoclonal antibody anti-mTOR,isotype IgG γ1 kappa	Goat anti- mouse IgG γ1 Alexa®594
	Mouse monoclonal antibody anti-myosin heavy chain IIx , isotype IgG M	Goat anti- mouse IgG M Alexa®488

Table 3.2 List of validated primary antibodies combined with secondary antibodies for costaining study.

3.5.4 Antibody Reproducibility

Antibody reproducibility was verified by three repeats of staining from the same human skeletal muscle sample. For each trial, measurement of protein colocalisation or content was performed in duplicates and the average value of one trial was achieved from the duplicates results. Data from three experiments was analysised by the coefficient of variance (CV) to represent the reproducibility of antibodies on immunofluorescences histological staining.

3.5.5 Blocking peptide competition assay

To confirm the targeting specificity of primary antibodies, a designed blocking peptide competitively targeting the specific antigen- antibody interaction domain was produced, which was fully mixed with primary antibody for 24h at 4° C. Following which, the primary antibody solution pre- incubated with blocking peptide was applied to skeletal muscle sections following the same incubation protocol stated in 2.4.3. Blockade of antibody recognition site by blocking peptide resulted in diminishing or disappearance of fluorescence signals observed in antibody-only staining.

3.6 Statistics analysis

All immunofluorescence image analysis was performed in duplicate (mean of duplicate sections on one slide). Reproducibility validation for individual primary antibody was performed on the same sample from one participant. Data was obtained from repeated colocalisation or protein quantification analysis of three slides from successive experiments. The reproducibility performance was assessed by coefficient of variation (CV) among repeats.

Results

3.7 Single antibody staining validation

3.7.1 mTOR immunofluorescence method development

3.7.1.1 mTOR antibody staining concentration

For mTOR primary antibody dilution optimisation, mTOR primary antibody was serially diluted by 1:100, 1:200 and 1:400 (Figure 3.7.1.1). The 1: 200 antibody dilution was selected because of its higher staining recognition than 1:400, while comparatively lower background noise than 1:100 dilution.

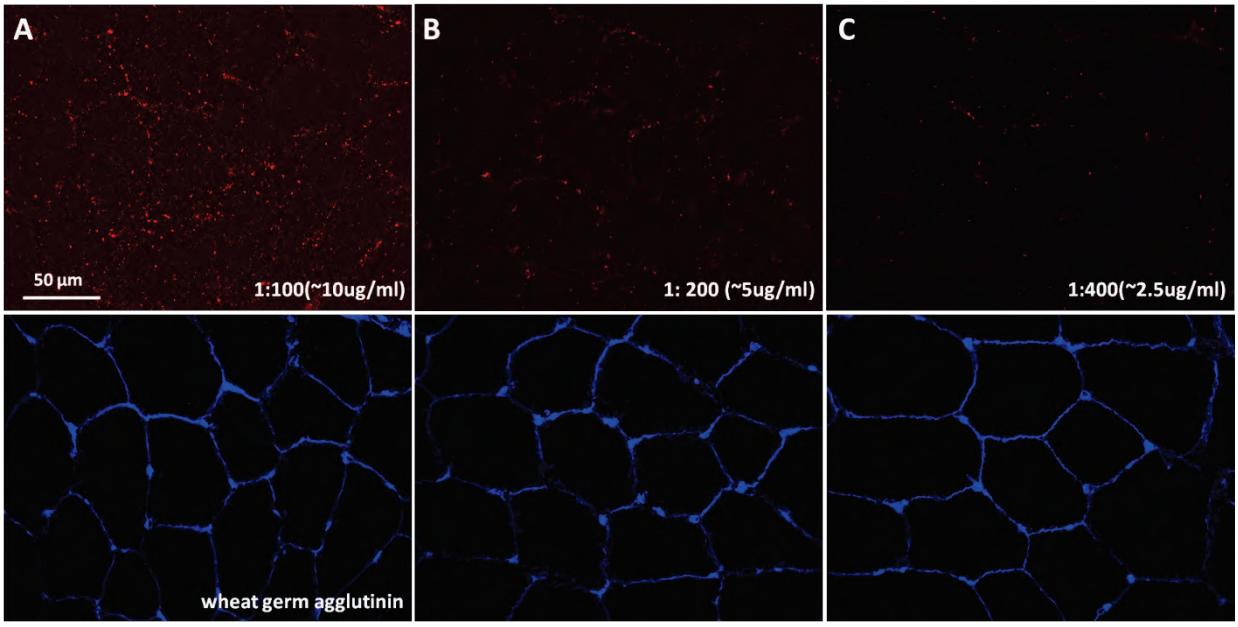

Figure 3.7.1.1 Optimization of mTOR primary antibody dilution. mTOR primary antibody was serially diluted to 1:100, 1:200 and 1:400. The secondary antibody dilution was 1:200, and was generally applied into the other primary antibodies concentration optimisaton. The same staining procedure was followed in each different dilution. Samples come from the same young volunteer. Scale bars 50 µm.

3.7.1.2 mTOR antibody double negative control

mTOR antibody was validated for its specific binding capability to the target proteins. As seen in Figure 3.7.1.2, mTOR stains can be visualized when samples were incubated with the primary antibody as well as corresponding secondary antibody conjugated with fluorescence (A, Figure 3.7.1.2). In contrast, whenever sections were incubated with primary antibody alone, or the secondary antibody only, mTOR signals were not found in negative control images. This indicates that the antibody can specifically recognize mTOR in human skeletal muscle *in vivo*. The weak fluorescence found in negative control was possibly from the auto- fluorescence from muscle samples.

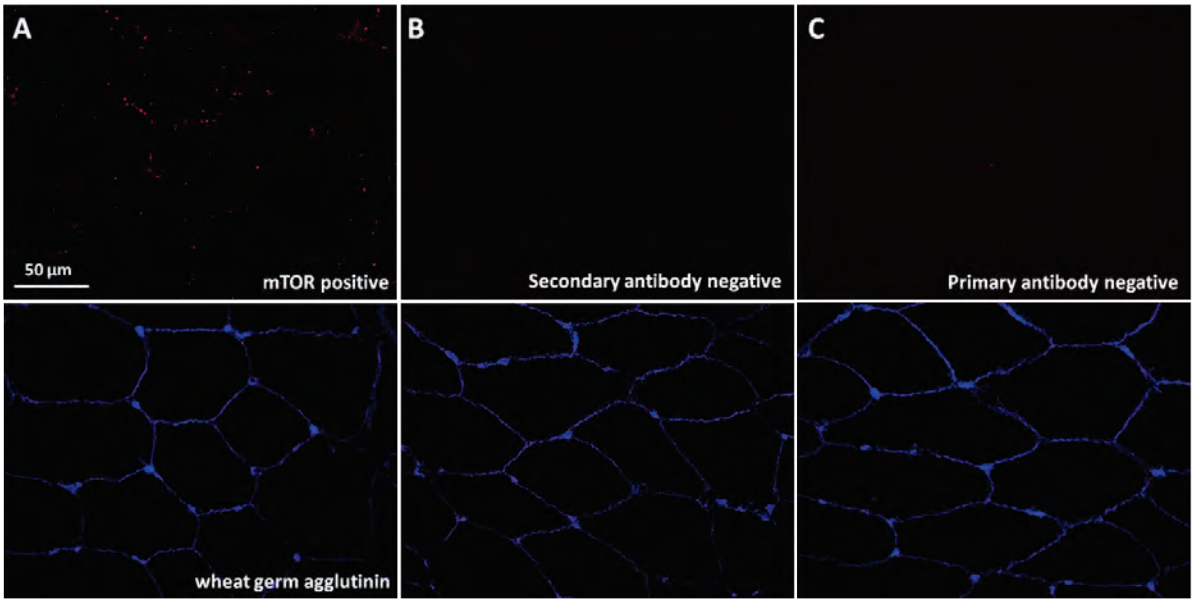

Figure 3.7.1.2 mTOR antibody validation. A) Positive control of mTOR antibody staining. mTOR antibody concentration was 1:200; B) Only primary antibody staining negative contorl and C) only secondary antibody staining negative control. Cell membrane was stained by the wheat germ agglutinin conjugated with Alexa 350 fluorescence. Scale bars 50 µm.

3.7.1.3 mTOR signal channel specificity controls

In Figure 3.7.1.2, we validated that mTOR antibody staining was specific. We next further tested the specificity of fluorescences signals under different excitation wavelength, which is necessary for multiple antibodies co-staining approaches. As seen in Figure 3.7.1.3, mTOR signals stained with

Alexa 594nm secondary antibody were only visualised under Texas red filter rather than the other two filters. This result indicated that the fluorescence excited from secondary antibody was restricted within the specific wavelength ranges.

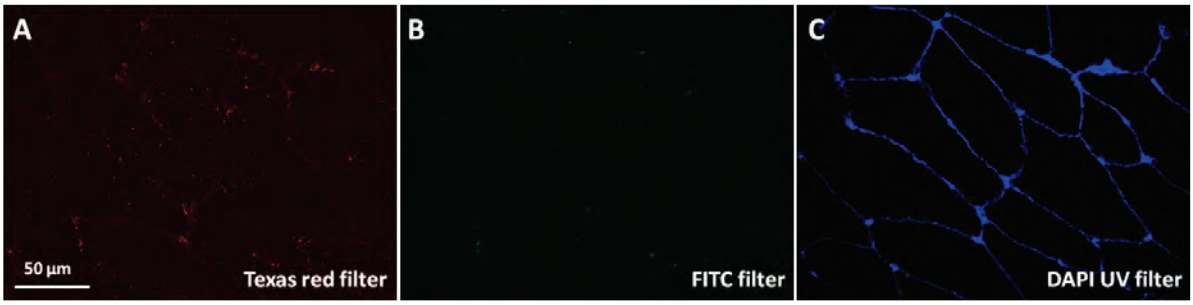

Figure 3.7.1.3 mTOR signal channel specificity under widefield microscope. A) mTOR stains was imaged under Texas red filter. The mTOR antibody concentration was 1:200; B) mTOR signal was observed under FITC filter. C) Cell membrane was stained by the wheat germ agglutinin conjugated with Alexa 350 fluorescence. Scale bars 50 µm.

3.7.1.4 mTOR localisation in basal human skeletal muscle

As shown in Figure 3.7.1.4, mTOR protein was visualized both inside the sarcoplasm and the sarcolemma membrane in skeletal muscle cells, in agreement with the previous images from rodent studies [14]. When images were magnified, it was found that the localization of mTOR on sarcolemma membrane was uneven, with parts of fluorescence stacking in specific plasma membrane area. When images were further amplified, it was found that some mTOR stains were located near the inner plasma membrane. And mTOR stains in sarcoplasm were not universal in protein size, which was possibly due to composition differences among mTOR complex, or the cutting angle of the cryostated muscle section.

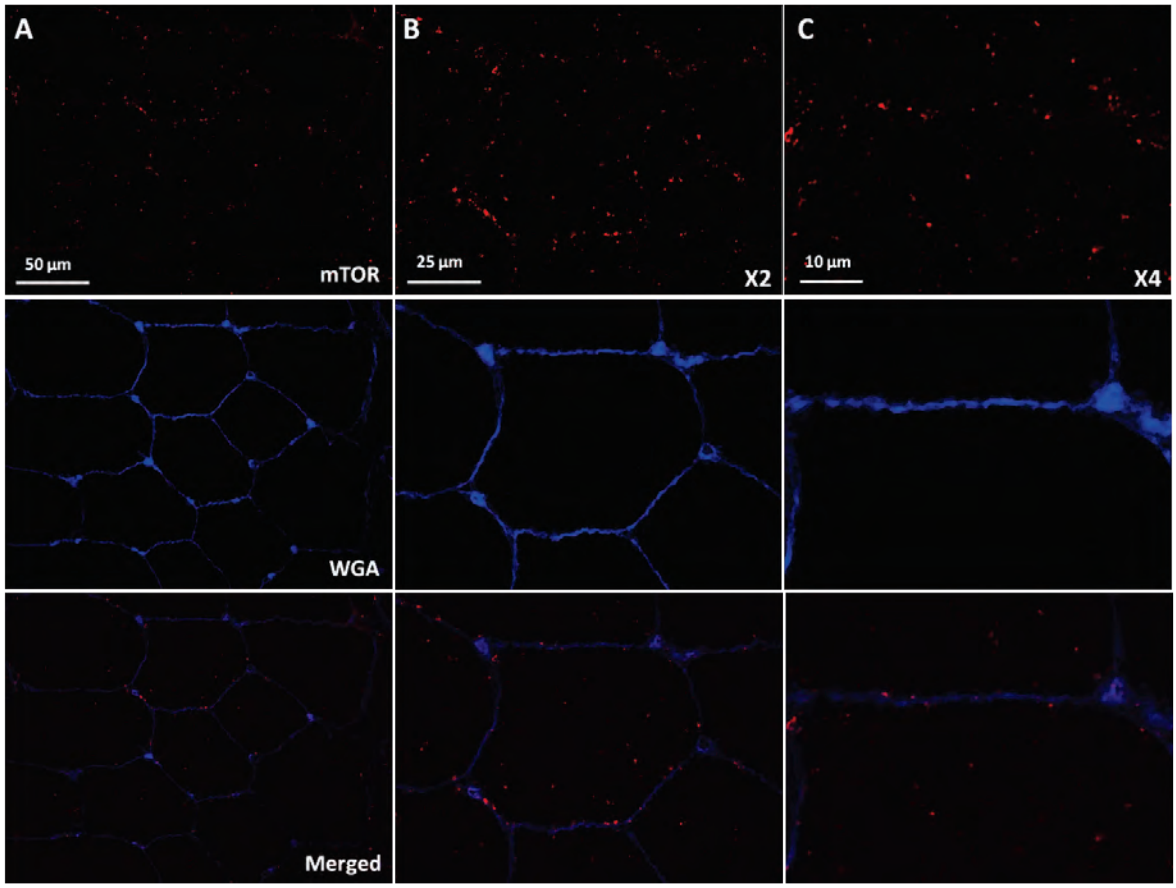

Figure 3.7.1.4 The basal localization of mTOR in young human skeletal muscle at rest level. A) The imaged were taken under widefield microscope with x40 objective len. B, C) Images were partially zoomed in by x2 and x4 times to show the mTOR localization details in skeletal muscle cells. Cell membrane was stained by the wheat germ agglutinin conjugated with Alexa 350 fluorescence. Scale bars 50 µm, 25µm and 10µm.

3.7.1.5 Reproducibility of colocalisation between mTOR and cell membrane

Reproducibility testing was applied on the immunofluorescences histological experiment studying association of mTOR with cell membrane (marked with WGA). Serial sections from the same sample were stained three times and imaged at the similar areas under microscope. Data for each repeat was the mean value from duplicates section on one slide. The reproducibility was quantified as the coefficient of variance (CV). CV value for colocalisation between mTOR and WGA was 5%.

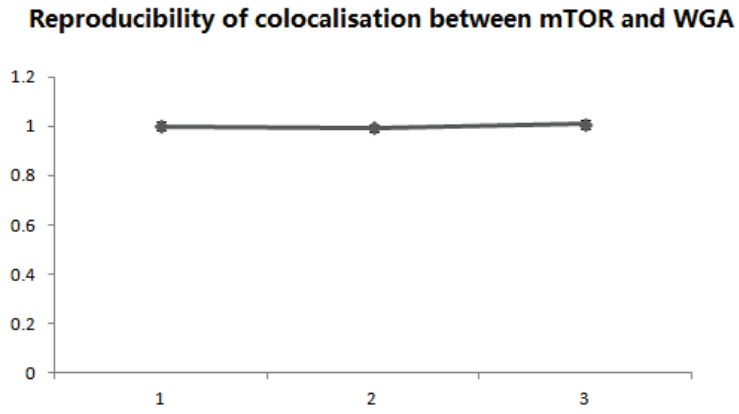

Figure 3.7.1.5 Reproducibility testing on colocalisation between mTOR and WGA. mTOR antibody was stained with WGA conjugated with Alexa@ 350 on the sections from the same sample. Colocalisation was measured and shown as Pearson's Correlation coefficient under Image- Pro software.

3.7.2 Lamp2 immunofluorescence method development

3.7.2.1 Lamp2 antibody staining concentration optimisation

Lamp2 primary antibody was serially diluted by 1:50, 1:100 and 1:200. The staining effect was evaluated by the signal strength and the background noise. Of the different dilutions, the 1: 100 dilution (B, Figure 3.7.2.1) was selected because of its higher staining strength than 1:200 (C, Figure 3.7.2.1), while comparatively lower background noise than 1:50 dilution (A, Figure 3.7.2.1).

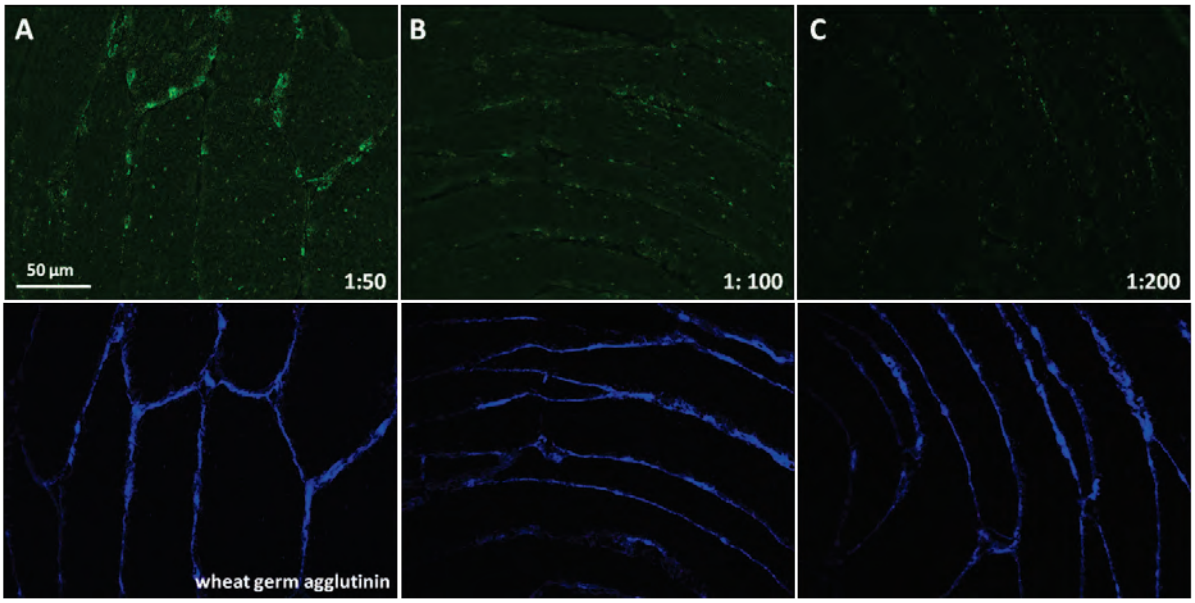

Figure 3.7.2.1 Optimization of Lamp2 primary antibody dilution. Lamp2 primary antibody was serially diluted to 1:50, 1:100 and 1:200. The same staining procedure was followed in each different dilution concentration. Samples come from the same young volunteer. Secondary antibody dilution was 1:200. Scale bars 50 µm.

3.7.2.2 Lamp2 antibody double negative control

As seen in Figure.3.7.2.2, Lamp2 stains were only visualized when samples were incubated with the primary antibody as well as corresponding secondary antibody conjugated with fluorescence (A, Figure 3.7.2.2). In contrast, whenever sections were incubated with the primary antibody alone, or with the secondary antibody only, signals were not found in images (B/C, Figure 3.7.2.2). This indicated that the Lamp2 antibody could specifically recognize Lamp2 protein content in human skeletal muscle *in vivo*.

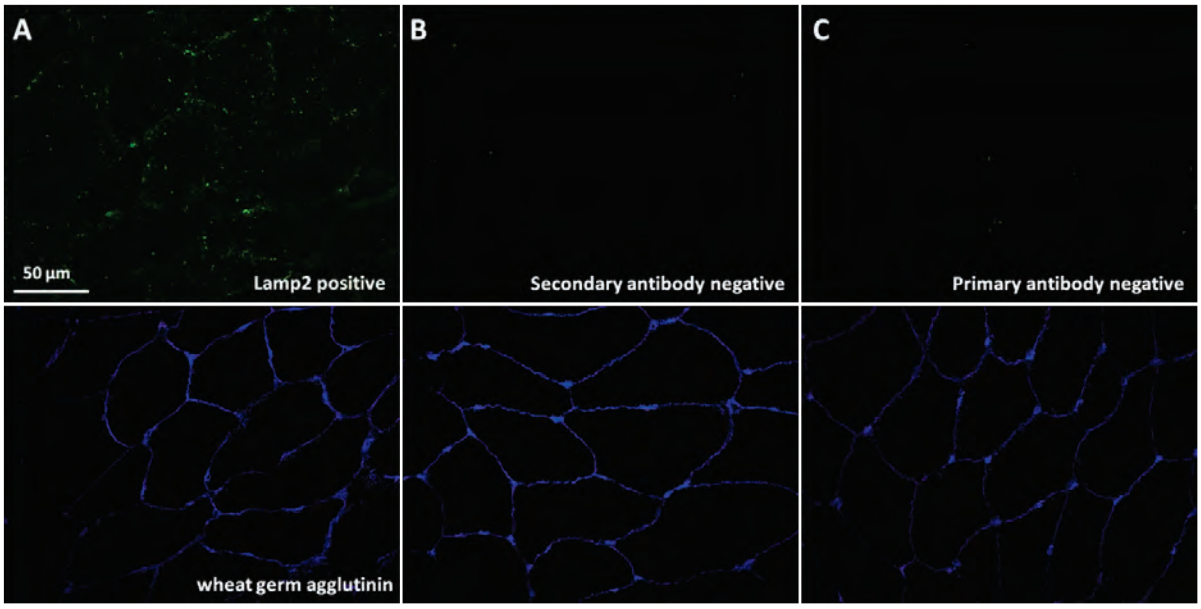

Figure 3.7.2.2 Negative control of Lamp2 antibody immunofluorescences staining. A) Lamp2 was stained with Alexa 488nm secondary antibody (green). The negative control was only stained by primary (B) and secondary antibody (C), respectively. Cell membrane was stained by the wheat germ agglutinin conjugated with Alexa 350 fluorescence (blue). Scale bars 50 µm.

3.7.2.3 Lamp2 signal channel specificity

As seen in Figure 3.7.2.3, Lamp2 signals associated with Alexa 488nm secondary antibody were only observed under FITC filter rather than under the other filters. This result suggests that the fluorescence signal excited from Lamp2 antibodies was wavelength specific, and can be used for multiple antibodies costaining.

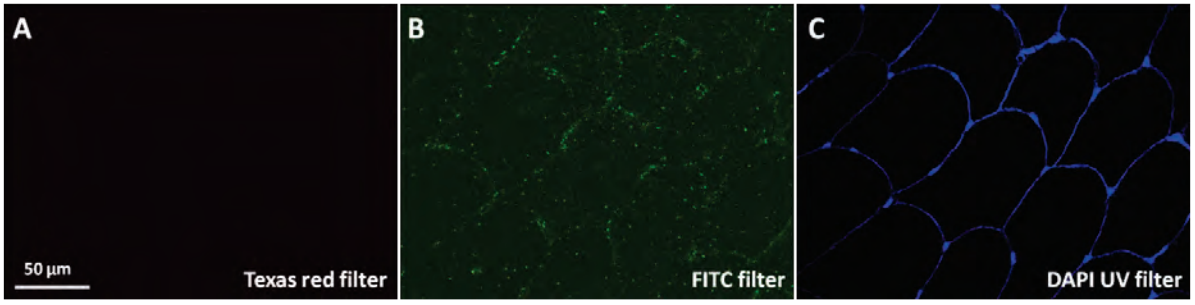

Figure 3.7.2.3 Lamp2 signal channel specificity under widefield microscope. A) Lamp2 stains were imaged under Texas red filter. B) Lamp2 signal was observed under FITC filter. Lamp2

antibody concentration was diluted to 1:100; C) Cell membrane was stained by the wheat germ agglutinin conjugated with Alexa 350 fluorescence. Scale bars 50 µm.

3.7.2.4 Lamp2 localisation in basal human skeletal muscle

In a similar manner with mTOR distribution, Lamp2 was distributed both in the sarcoplasm and on the sarcolemma membrane seen from Figure 3.7.2.4. Some Lamp2 staining was found to stack in specific areas of plasma membrane, rather than distribute evenly along the membrane. When images were further magnified, Lamp2 stains formed a 'semicircle' or 'palm' under widefield microscope (C, Figure 3.7.2.4). Lamp2 was reported to localise on the cytoplasm organnells like late lysosomes [14, 15].

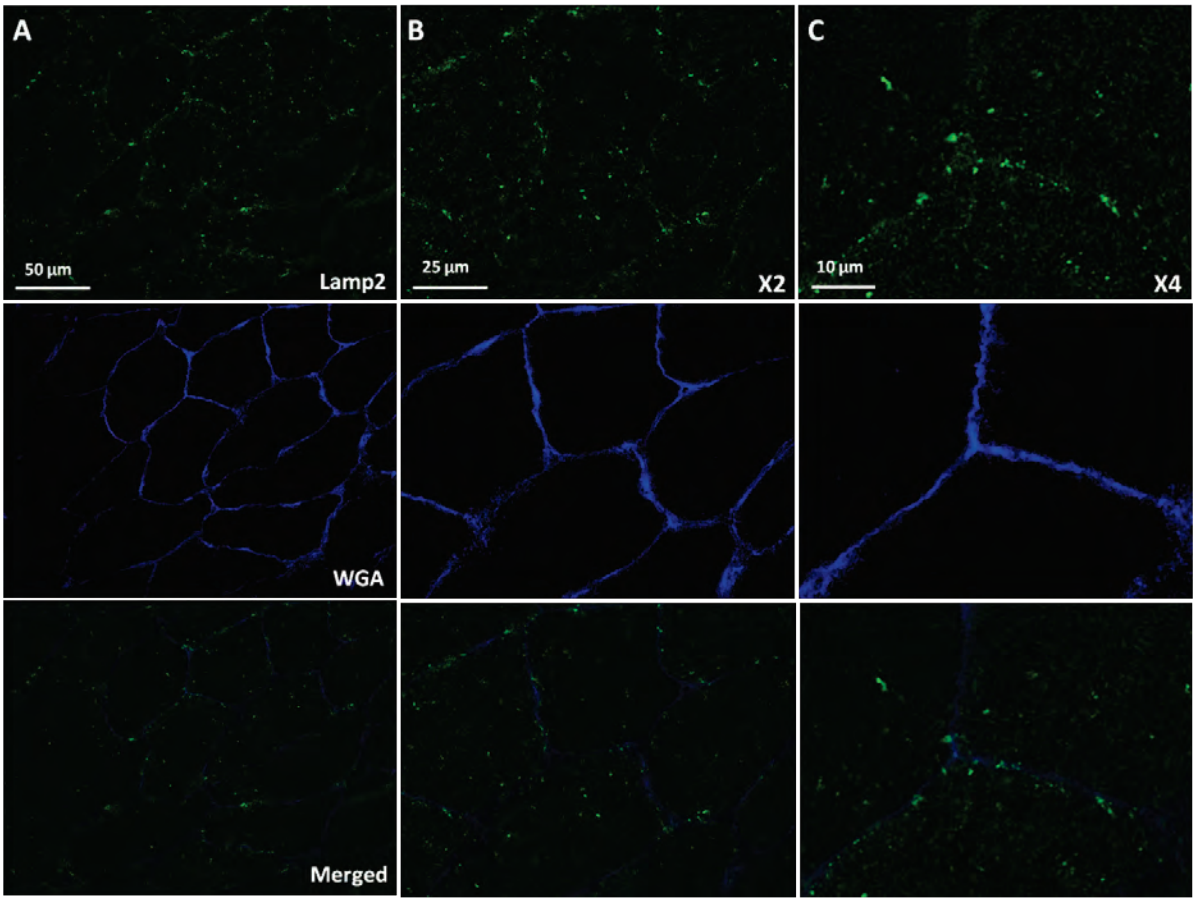

Figure 3.7.2.4 The basal localization of Lamp2 in young human skeletal muscle at rest level. A) The images were taken under widefield microscope with x40 objective. B, C) Images were partially magnified x2 and x4 times to show the details of mTOR localization in skeletal muscle

cells. Cell membrane was stained by the wheat germ agglutinin conjugated with Alexa 350 fluorescence. Scale bars 50 µm, 25µm and 10µm.

3.7.3 Rheb immunofluorescence method development

3.7.3.1 Rheb antibody staining concentration optimisation

Rheb primary antibody was serially diluted by 1:25, 1:50 and 1:100. The staining effect was evaluated by the signal strength and the background noise. As shown in Figure 3.7.3.1, the 1: 50 dilution of Rheb primary antibody was used because of its higher staining recognition than 1:100, while comparatively lower background noise than 1:25 dilution.

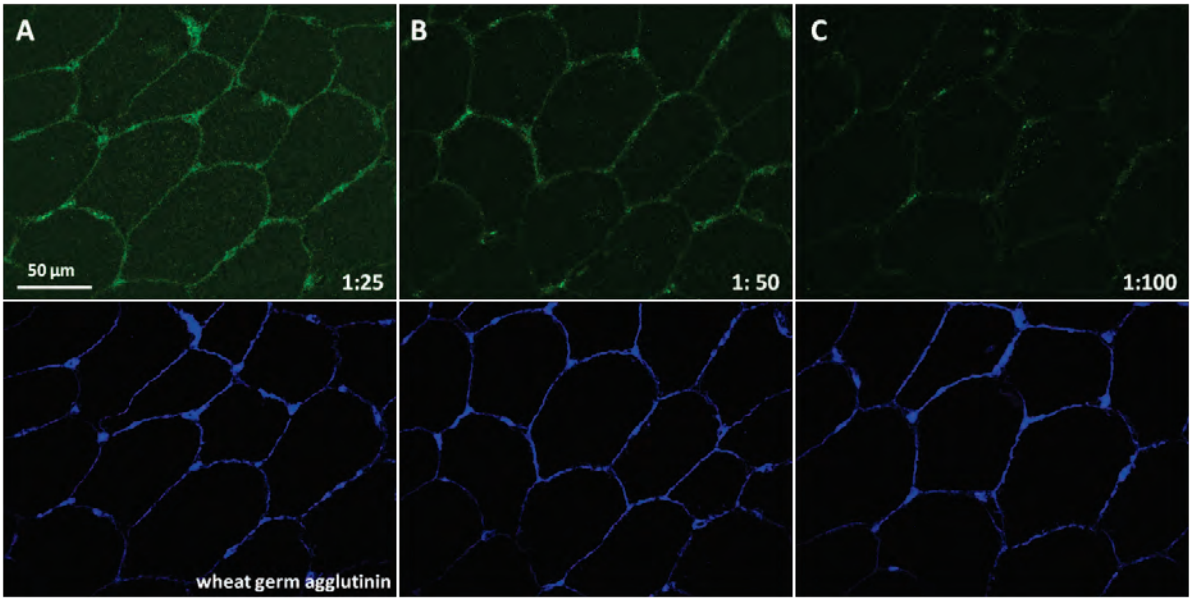

Figure 3.7.3.1 Optimization of Rheb primary antibody dilution. Rheb primary antibody was serially diluted to 1:25, 1:50 and 1:100. The same staining procedure was followed in each different dilutions. Samples come from the same young volunteer. Secondary antibody dilution was 1:200. Scale bars 50 µm.

3.7.3.2 Rheb antibody double negative control

Similar with mTOR and Lamp2, Rheb fluorescences stains were validated for the double negative control (Figure 3.7.3.2). As exhibited in Figure 3.7.3.2, Rheb signals were not found either in primary antibody staining alone control or secondary antibody incubation alone control. This proved the stains were from the specific incubation between primary antibody and secondary antibody.

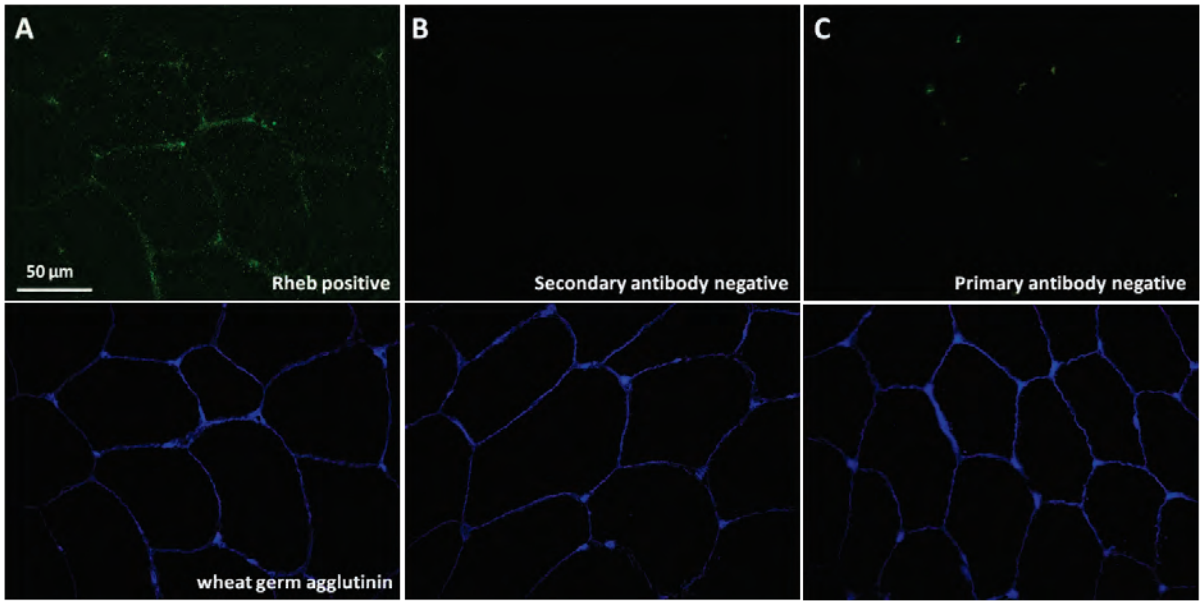

Figure 3.7.3.2 Negative control of Rheb antibody immunofluorescences staining. A) Rheb was stained with Alexa 488nm secondary antibody (green). B, C) The negative control was only stained by primary and secondary antibodies, respectively. Cell membrane was stained by the wheat germ agglutinin conjugated with Alexa 350 fluorescence (blue). Scale bars 50 µm.

3.7.3.3 Rheb signal channel specificity controls

As shown in Figure 3.7.3.3, Rheb signals stained with Alexa 488nm secondary antibody were only observed under FITC filter rather than under the other filters. This indicated that the fluorescence excited from Rheb antibodies was wavelength specific.

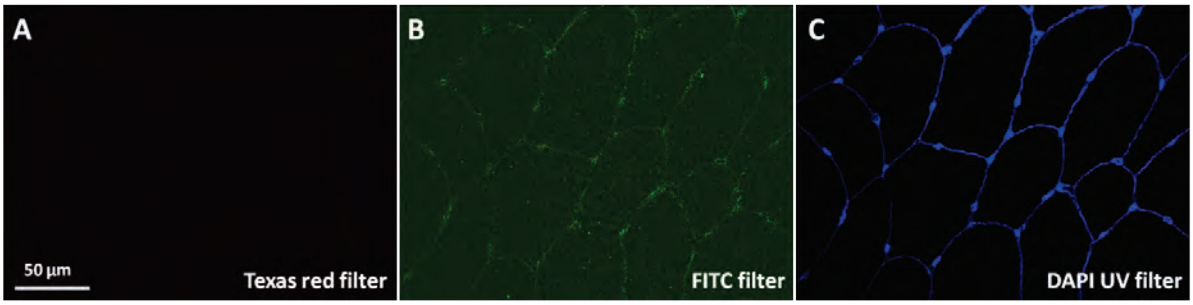

Figure 3.7.3.3 Rheb signal channel specificity under widefield microscope. A) Rheb stains were imaged under Texas red filter. B) Rheb signal was observed under FITC filter. The Rheb antibody concentration was 1:50; C) Cell membrane was stained by the wheat germ agglutinin conjugated with Alexa 350 fluorescence. Scale bars 50 µm.

3.7.3.4 Rheb localisation in basal human skeletal muscle

As seen in Figure 3.7.3.4, the content of Rheb proteins in basal human skeletal muscle cells was at high level. Rheb stains were visualized both in the sarcoplasm and on the sarcoplasm membrane. When images magnification was increased, Rheb was found to stack on the specific sarcolemma membrane areas rather than evenly distribute along the plasma membrane. In the skeletal muscle of this subject, large amounts of Rheb proteins were observed to localize near the inner sarcolemma membrane (C, Figure 3.7.3.4), suggesting their tight association with the plasma membrane.

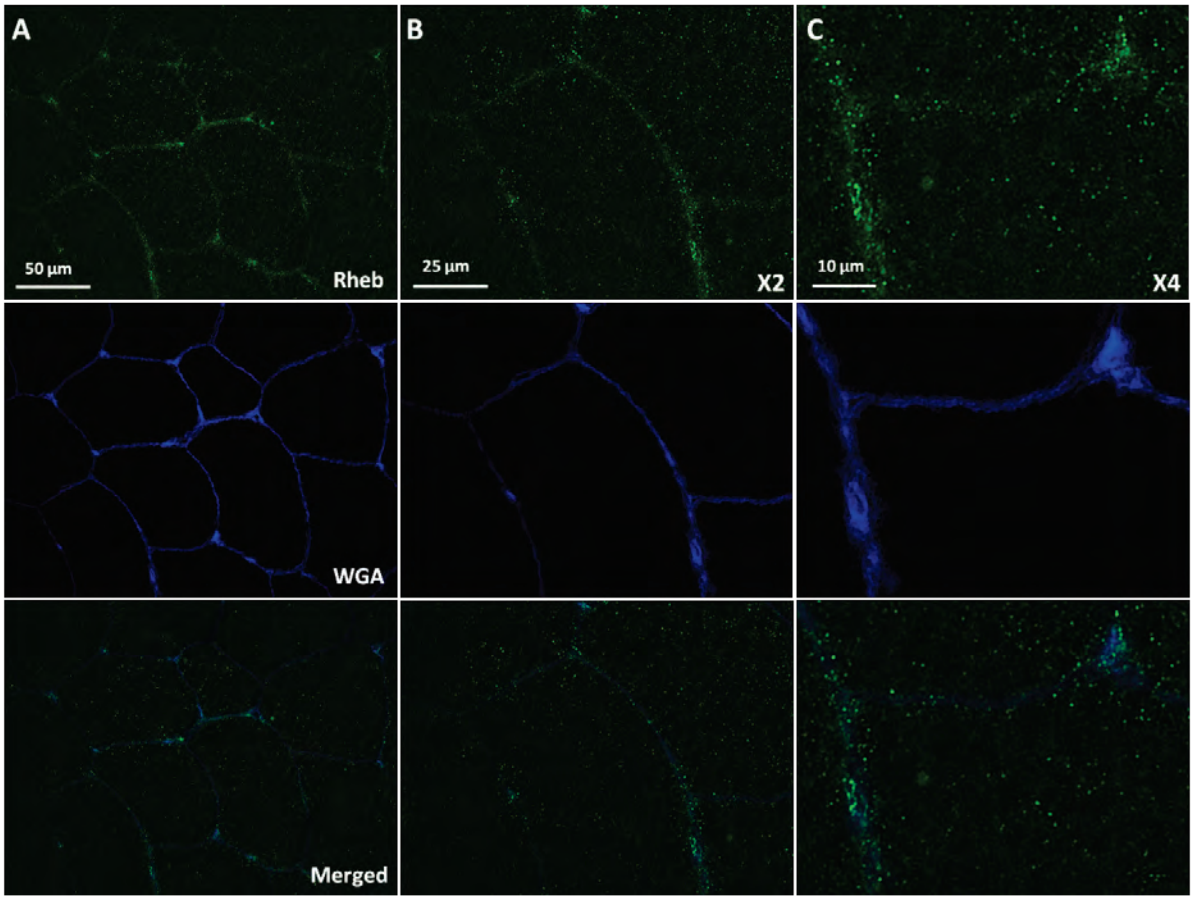

Figure 3.7.3.4 The basal localization of Rheb in untrained young human skeletal muscle. A) Images were taken under widefield microscope with x40 objective. B, C) Images were partially zoomed in by x2 and x4 times to show the details of Rheb localization in skeletal muscle cells. Cell membrane was stained by the wheat germ agglutinin conjugated with Alexa 350 fluorescence. Scale bars 50 µm, 25µm and 10µm.

3.7.4 Rab7 immunofluorescence method development

3.7.4.1 Rab7 antibody staining concentration optimisation

Rab7 primary antibody was serially diluted by 1:100, 1:200 and 1:400. The staining effect was evaluated by the signal strength and the background noise. As viewed from Figure 3.7.4.1, the 1: 200 antibody dilution was the best of three dilutions because of its higher staining recognition than 1:400, while comparatively lower background noise than 1:100 dilution.

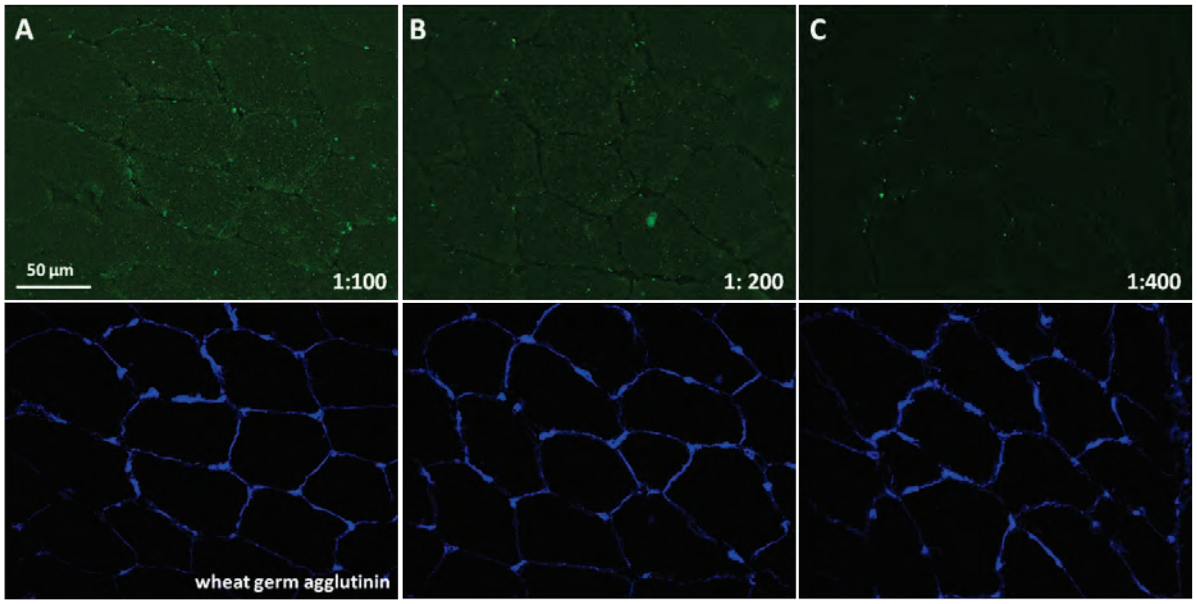

Figure 3.7.4.1 Optimization of Rab7 primary antibody dilution. Rab7 primary antibody was serially diluted to 1:100, 1:200 and 1:400. The same staining procedure was followed in each different dilutions. Samples come from the same young volunteer. Secondary antibody dilution was 1:200. Scale bars 50 µm.

3.7.4.2 Rab7 antibody double negative control

Rab7 antibody was validated for the double negative specificity (Figure.3.7.4.2) to exclude unspecific fluorescences from primary antibody or secondary antibody. The result suggested that that both the Rab7 primary antibody and secondary antibody were specific to their targets.

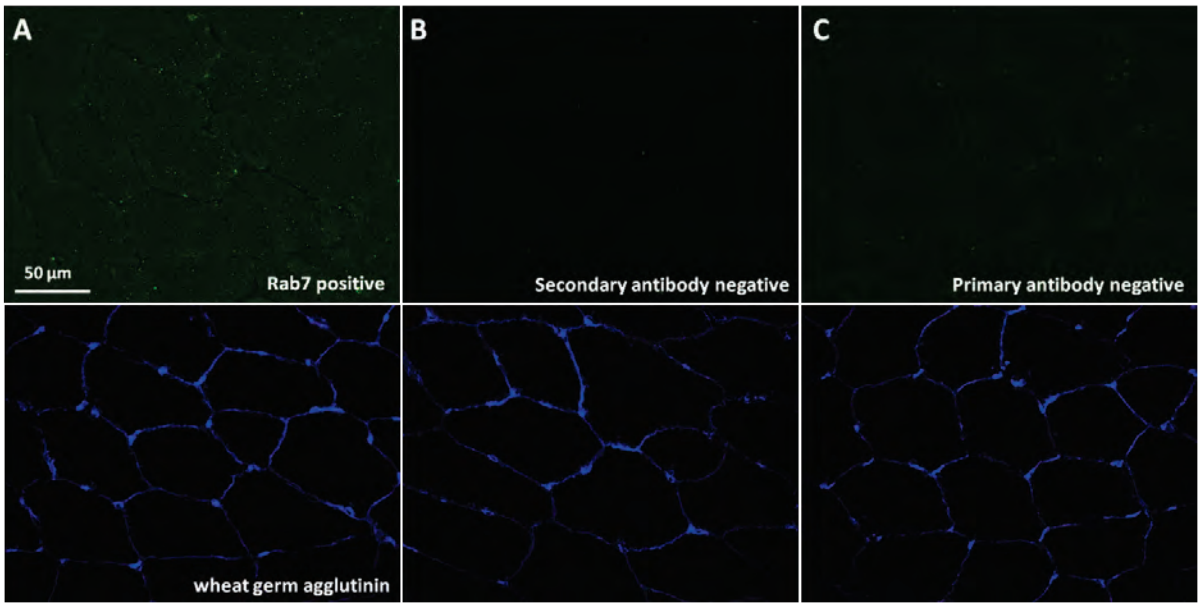

Figure 3.7.4.2 Negative control of Rab7 antibody immunofluorescences staining. A) Rab7 was stained with Alexa 488nm secondary antibody (green). B, C) The negative control was only stained by primary and secondary antibodies, respectively. Cell membrane was stained by the wheat germ agglutinin conjugated with Alexa 350 fluorescence (blue). Scale bars 50 µm.

3.7.4.3 Rab7 signal channel specificity controls

As seen in Figure 3.7.4.3, Rab7 signals stained with Alexa 488nm secondary antibody were only observed under FITC filter rather than the other filters. This result indicated that the fluorescences excited from Rab7 signals were wavelength specific for multiple antibodies costaining.

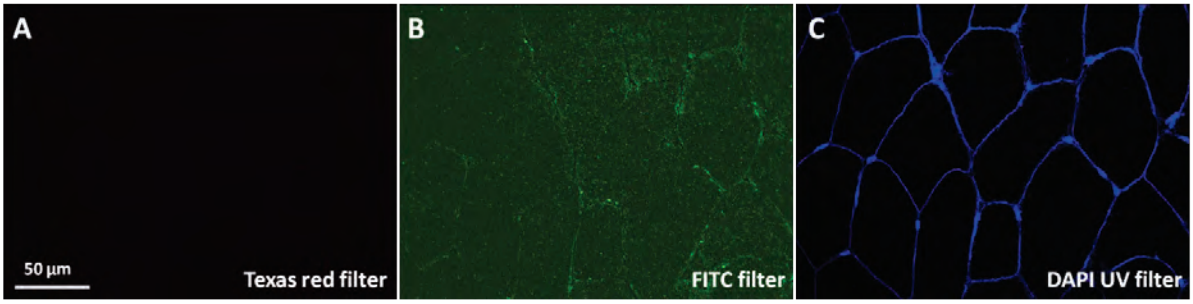

Figure 3.7.4.3 Rab7 signal channel specificity under widefield microscope. A) Rab7 stains was not found in image under Texas red filter. B) Rab7 signal was observed under FITC filter. The

Rheb antibody concentration was 1:50; C) Cell membrane was stained by the wheat germ agglutinin conjugated with Alexa 350 fluorescence. Scale bars 50 µm.

3.7.4.4 Rab7 localisation in basal human skeletal muscle

In Figure 3.7.4.4, it was observed that Rab7 stains were much smaller than mTOR, generally because its molecular weight is 23kDa as a small GTPase. Rab7 proteins were mostly visualized inside the sarcoplasm of muscloskeletal cells. Some Rab7 signals were found near the sarcolemma membrane in basal human skeletal muscle(C, Figure 3.7.4.4).

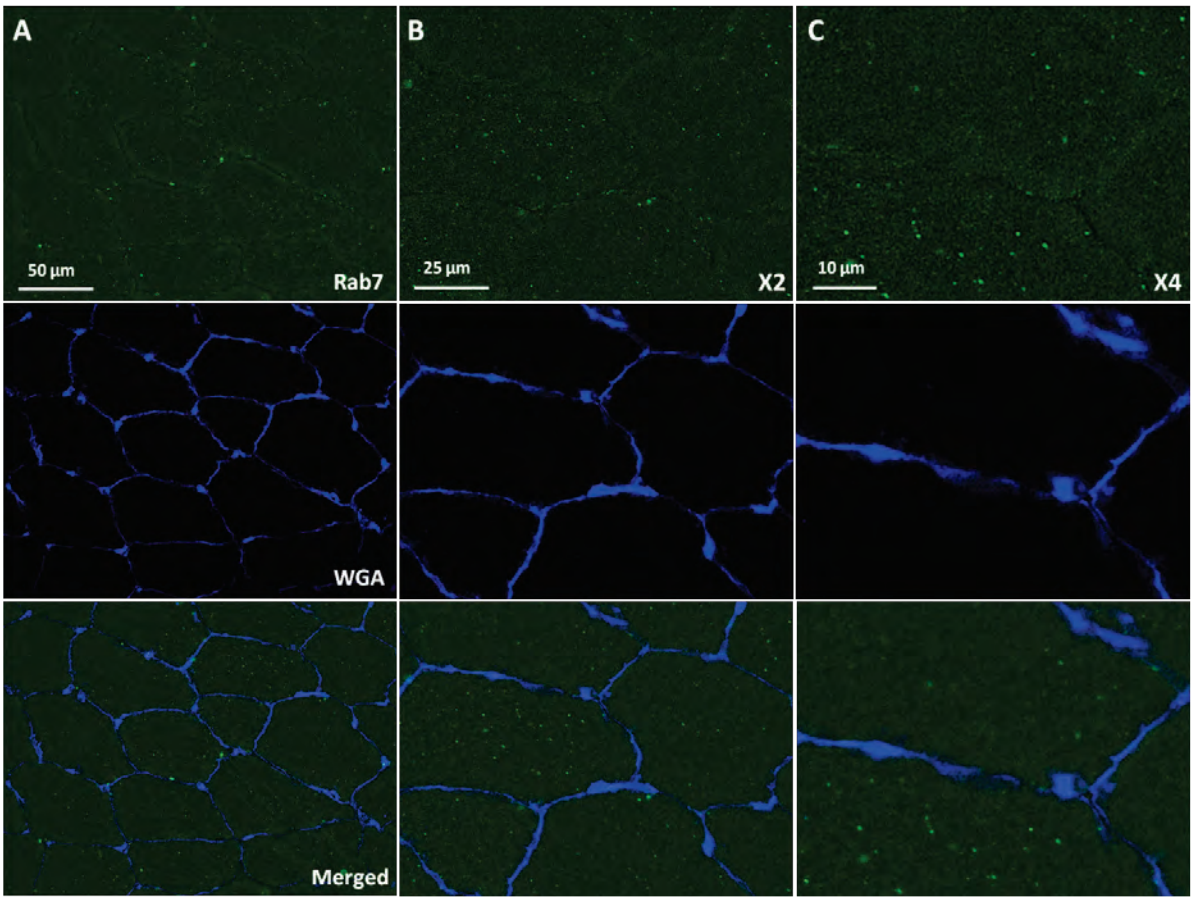

Figure 3.7.4.4 The basal localization of Rab7 in basal young human skeletal muscle. A) The imaged were taken under widefield microscope with x40 objective len. B, C) Images were partially zoomed in by x2 and x4 times to show the details of Rab7 localization in skeletal muscle cells. Cell membrane was stained by the wheat germ agglutinin conjugated with Alexa 350 fluorescence. Scale bars 50 µm, 25µm and 10µm.

3.7.5 EIF3F immunofluorescence method development

3.7.5.1 EIF3F antibody staining concentration optimisation

EIF3F primary antibody was serially diluted by 1:75, 1:150 and 1:300. As shown in Figure 3.7.5.1, of the three dilutions the 1: 150 antibody concentration exhibited better staining effect than 1:300, while comparatively lower background noise than 1:75 dilution.

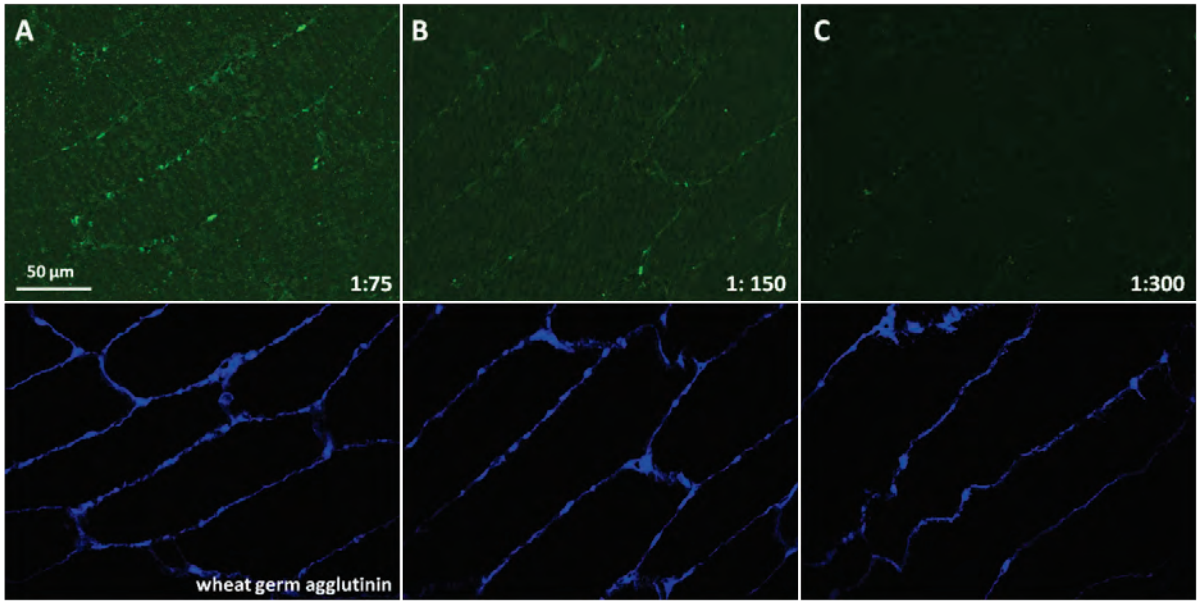

Figure 3.7.5.1 Optimization of EIF3F primary antibody dilution. EIF3F primary antibody was serially diluted to 1:75, 1:150 and 1:300. The same staining procedure was followed in each different dilution. Samples come from the same young volunteer. Secondary antibody dilution was 1:200. Scale bars 50 µm.

3.7.5.2 EIF3F antibody double negative control

EIF3F antibodies were validated for their specificity on antigens. As seen in Figure.3.7.5.2, EIF3F stains can be visualized when samples were incubated with the primary antibody as well as specific secondary antibody conjugated with Alexa fluorphores. In contrast, whenever staining with the primary antibody itself, or with the secondary antibody alone, signals could not be found inside the

skeletal muscle cells (B/ C, Figure 3.7.5.2). The background fluorescence in negative control was probably from the auto- fluorescence of muscle samples.

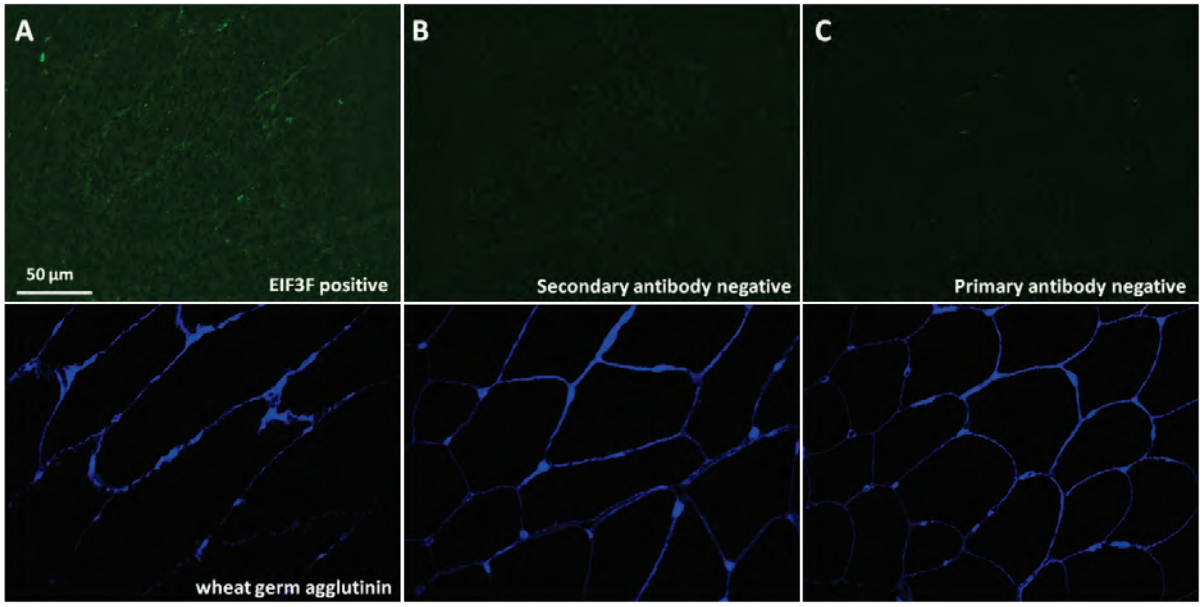

Figure 3.7.5.2 Double negative validation on EIF3F antibodies. A) Positive control EIF3F antibody staining, EIF3F antibody concentration was 1:150; B) primary antibody staining alone negative contorl and C) secondary antibody staining alone negative control. Cell membrane was outlined by the wheat germ agglutinin conjugated with Alexa 350 fluorescence. Scale bars 50 µm.

3.7.5.3 EIF3F signal channel specificity controls

As seen in Figure 3.7.5.3, EIF3F signals stained with Alexa 488nm secondary antibody were only observed under FITC filter rather than the other two filters. This indicated that the fluorescences excited from EIF3F secondary antibody was wavelength specific.

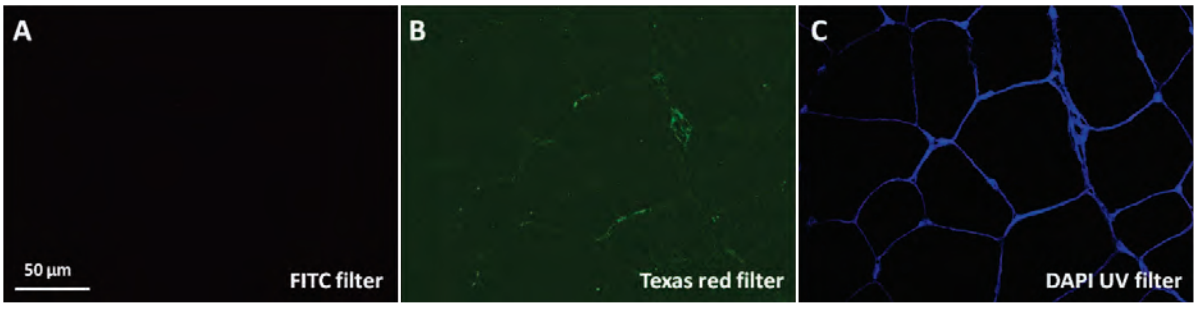

Figure 3.7.5.3 EIF3F signal channel specificity under widefield microscope. A) EIF3F stains were not found in image under Texas red filter. B) EIF3F signal was observed under FITC filter. The EIF3F antibody concentration was 1:150; C) Cell membrane was stained by the wheat germ agglutinin conjugated with Alexa 350 fluorescence. Scale bars 50 µm.

3.7.5.4 EIF3F localisation in human skeletal muscle

EIF3F stains were visualized on the sarcolemma membrane of the human skeletal muscle cells (A, Figure 3.7.5.4). Being similar with mTOR, EIF3F signals were unevenly localizated on the sarcolemma membrane, with fluorphores stacking at specific membrane area (B/ C, Figure 3.7.5.4).

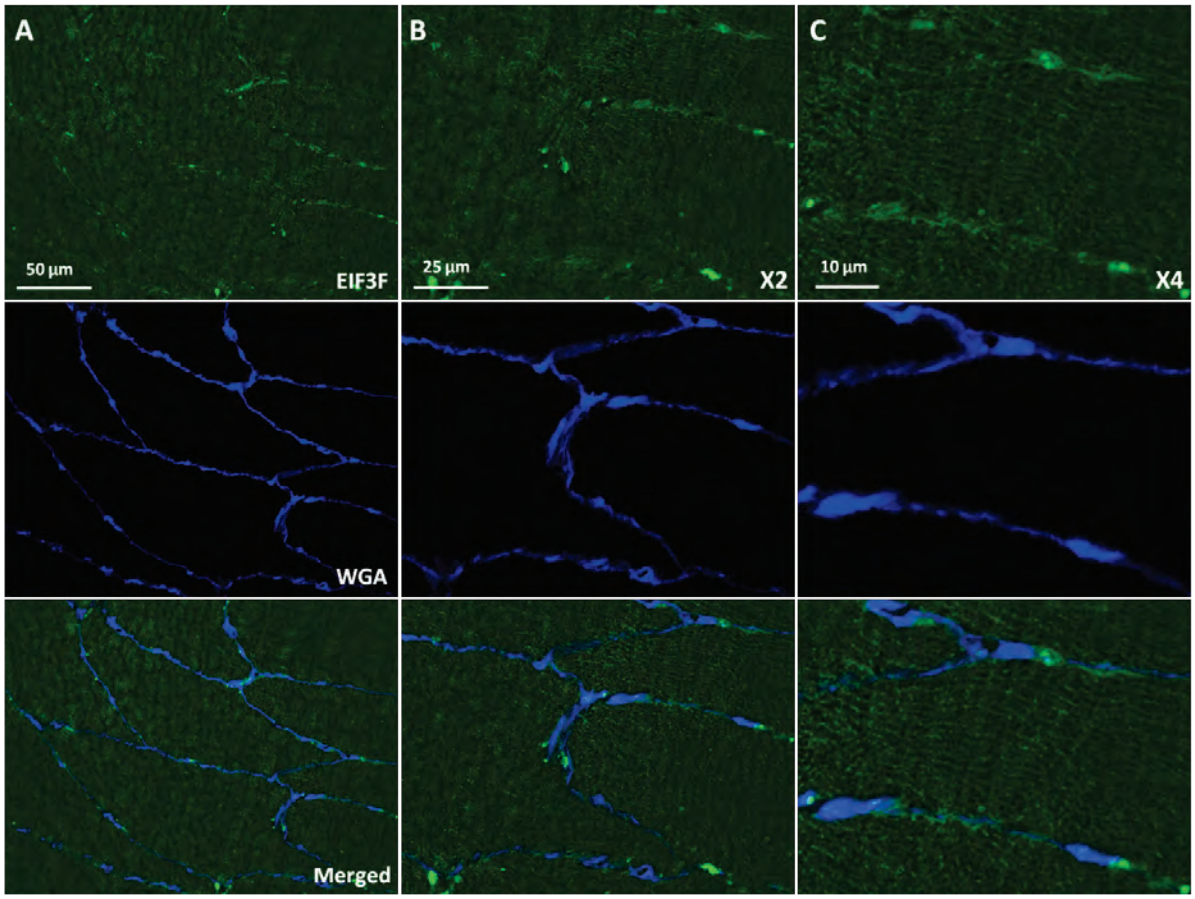

Figure 3.7.5.4 The localization of EIF3F in young human skeletal muscle. A) Signals were taken under widefield microscope (Nikon), x40 objective. B, C) Images were partially amplified by ImagePro software to show the EIF3F subcellular localization. Cell membrane was outlined by

the wheat germ agglutinin conjugated with Alexa 350 fluorescence. Sections for staining were from the same human muscle sample. Scale bars 50 µm, 25µm and 10µm.

3.7.6 Tuberin (TSC2) immunofluorescence method development

3.7.6.1 Tuberin antibody staining concentration optimisation

Tuberin signals were stained and excited under Texas red wavelength. The Tuberin primary antibody was serially diluted by 1:25, 1:50 and 1:100. Signal strength was shown in positive relationship with the antibody concentration. However, high background noise was observed if the antibody concentration was too high to influence the measurement accuracy of protein signals. For Tuberin primary antibody, the 1: 50 antibody concentration was used for its brighter staining effect than the dim signals under 1:100 dilution (C, Figure.3.7.6.1), while comparatively lower background noise than 1:25 dilution (A, Figure.3.7.6.1).

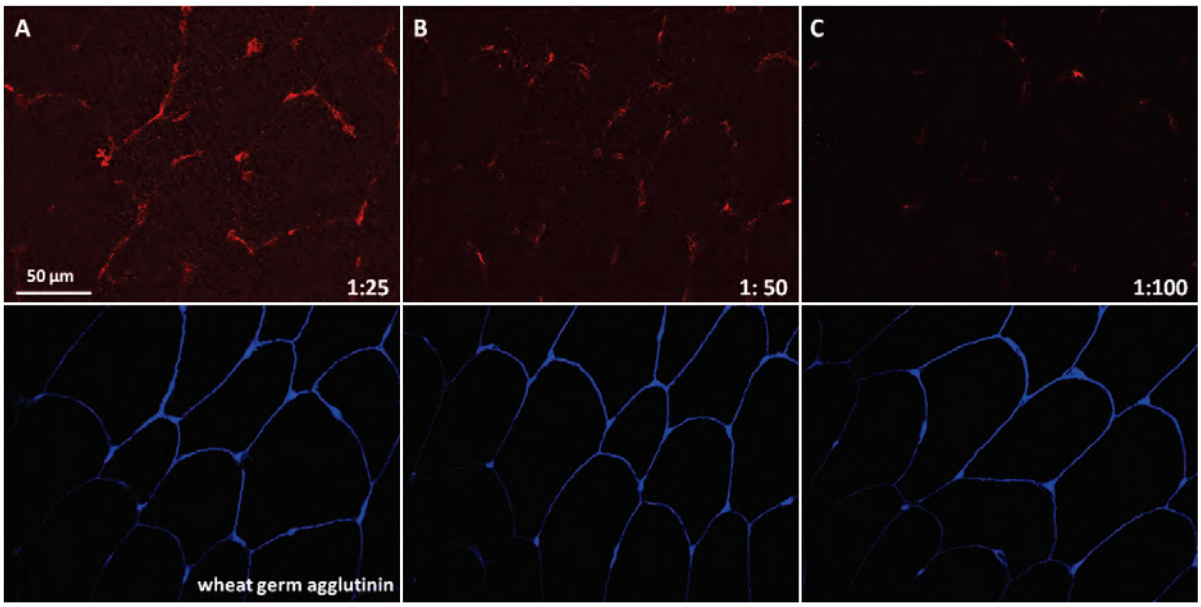

Figure 3.7.6.1 Optimization of Tuberin primary antibody dilution. Tuberin primary antibody was serially diluted to 1:25, 1:50 and 1:100. The same staining procedure was used in each dilution trial. Secondary antibody dilution was 1:200, conjugated with Alexa 594nm fluorescences. Scale bars 50 µm.

3.7.6.2 Tuberin antibody double negative control

As seen in Figure 3.7.6.2, Tuberin stains can only be visualized when samples were incubated with primary antibody and corresponding secondary antibody conjugated with fluorescence (A, Figure 3.7.6.2). In contrast, whenever incubating with the primary antibody alone (B, Figure 3.7.6.2), or with the secondary antibody alone (C, Figure 3.7.6.2), signals can not be observed inside the sections. This experiment therefore indicates that Tuberin antibody can specifically recognize the targeted proteins in human skeletal muscle *in vivo*.

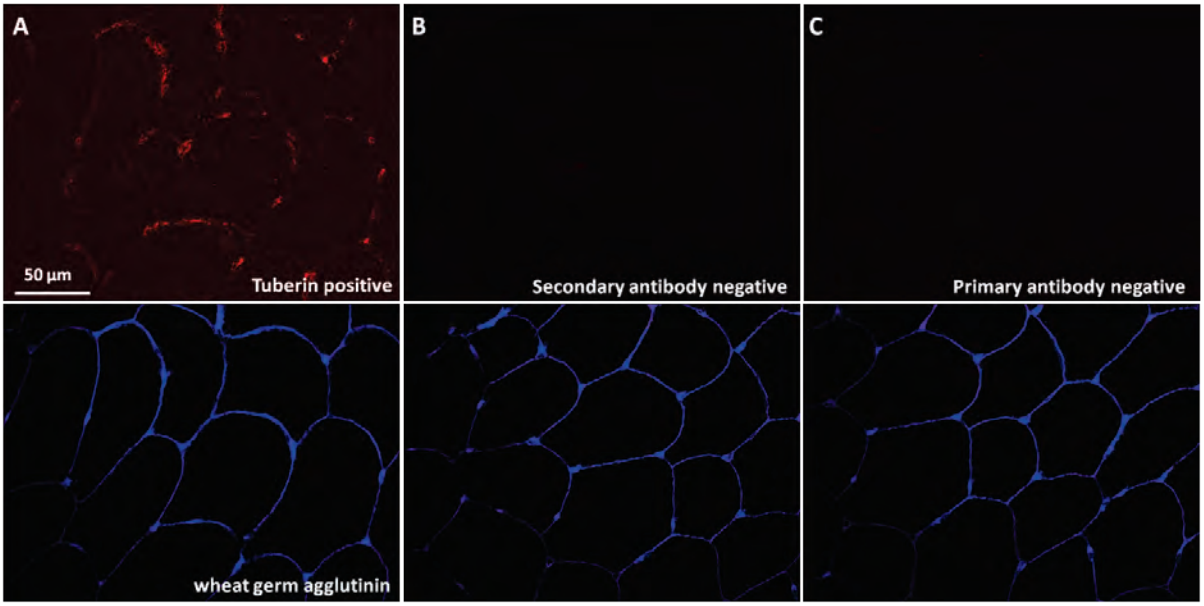

Figure 3.7.6.2 Tuberin antibody validation. A) Positive control Tuberin antibody staining, Tuberin primary antibody was incubated with its secondary antibody. Tuberin antibody concentration was 1:50; B) primary antibody staining alone negative contorl and C) secondary antibody staining alone negative control. Cell membrane was stained with the wheat germ agglutinin conjugated with Alexa 350 fluorescence. Scale bars 50 µm.

3.7.6.3 Tuberin signal channel specificity controls

As seen in Figure 3.7.6.3, Tuberin signals stained with Alexa 594nm secondary antibody were only observed under Texas red filter, indicating that the fluorescences excited from Tuberin secondary antibody was wavelength specific.

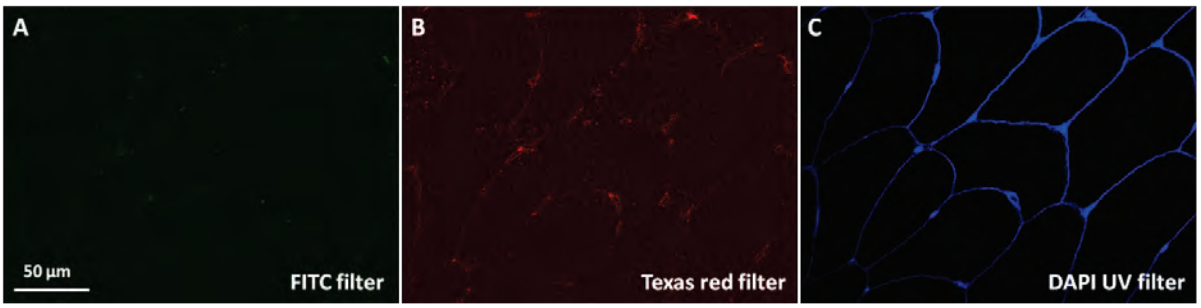

Figure 3.7.6.3 Tuberin signal channel specificity under widefield microscope. A) Tuberin stains were not observed in image taken under FITC filter. B) Tuberin signal was observed under Texas red filter. The Tuberin antibody concentration was 1:50; C) Cell membrane was stained by the wheat germ agglutinin conjugated with Alexa 350 fluorescence. Secondary antibody dilution was 1:200. Scale bars 50 µm.

3.7.6.4 Tuberin localisation in basal human skeletal muscle

As shown in Figure 3.7.6.4, the majority of Tuberin signals were found to localize along the sarcolemma membrane of basal human skeletal muscle cells. When images were magnified, some Tuberin stains were found to localize near the the sarcolemma membrane. Also, it was observed that the distribution of Tuberin fluorescences was uneven along the plasma membrane.

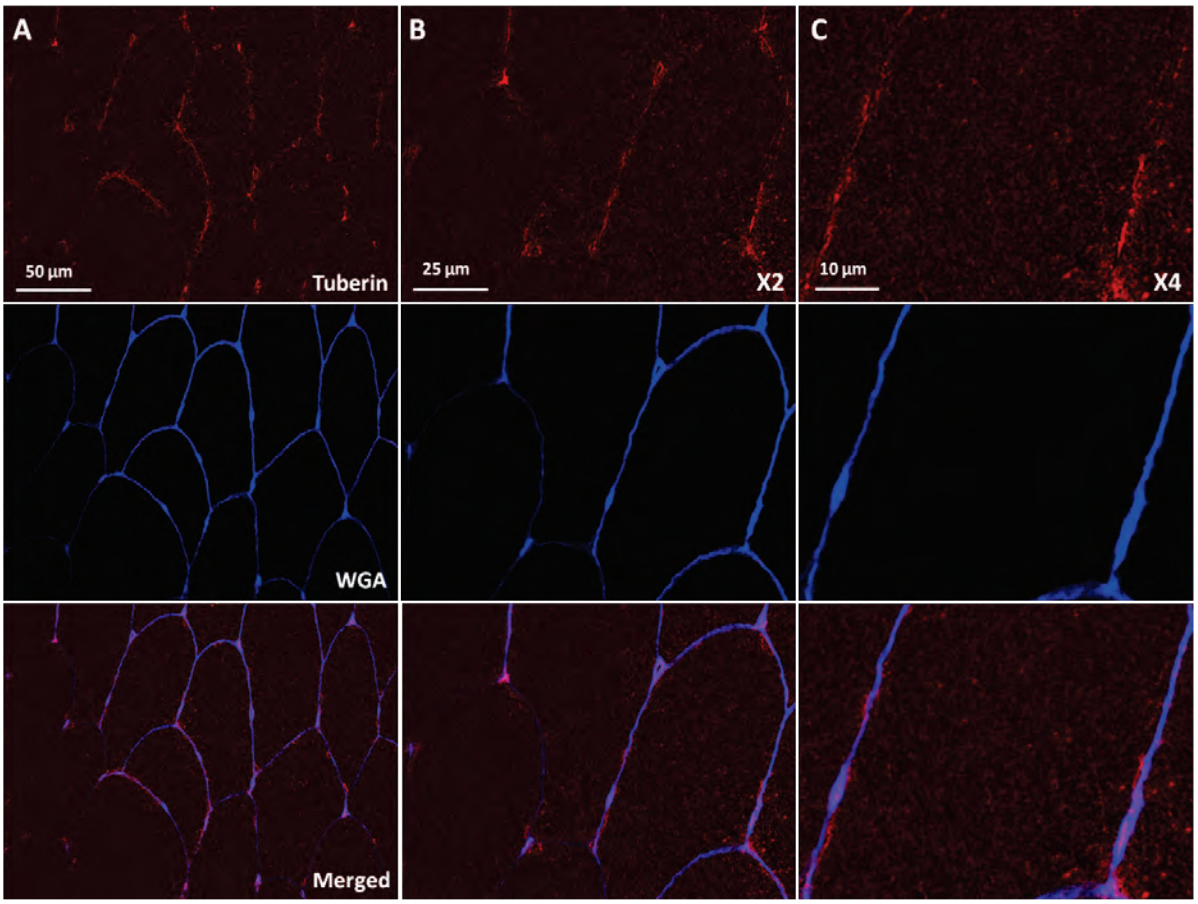

Figure 3.7.6.4 The basal localization of Tuberin in untrained young human skeletal muscle. A) Imaged were taken under Nikon widefield microscope, x40 objective. B, C) Images were partially amplified by 2 times and 4 times to show the details of Tuberin subcellular localization. Cell membrane was outlined by the wheat germ agglutinin conjugated with Alexa 350 fluorescence. Scale bars 50 µm, 25µm and 10µm.

3.8 Multiple antibodies co-staining validation

3.8.1 Costaining of mTOR with Lamp2

3.8.1.1 Cross-binding negative control

Two approaches were used to validate the accuracy of specific binding among antibodies when pairs of antibodies were co-stained. Firstly we examined the cross reaction between two primary antibodies

(PA negative, Figure 3.8.1.1), or from the unspecific binding between two secondary antibodies (SA negative, Figure 3.8.1.1). Secondly, as it is also possible to generate the unspecific signals that with the secondary antibody binding to the primary antibody, antibody validation control experiments in which the secondary antibodies were incubated with the primary antibody with different isotype were performed.

As shown in Figure 3.8.1.1, there were no signals observed in controls when mTOR and Lamp2 primary antibodies were costained, or their secondary antibodies were incubated. Results were also negative when mTOR primary antibody was stained with secondary antibody targeting Lamp2 primary antibody, and *vice versa*. These tests confirmed that the antibodies used in immunofluorescence histology costaining experiment were specific to their antigens. The co-staining of other protein antibodies were also tested following this method to gurantee the specificity of proteins stains achieved in 3.8.

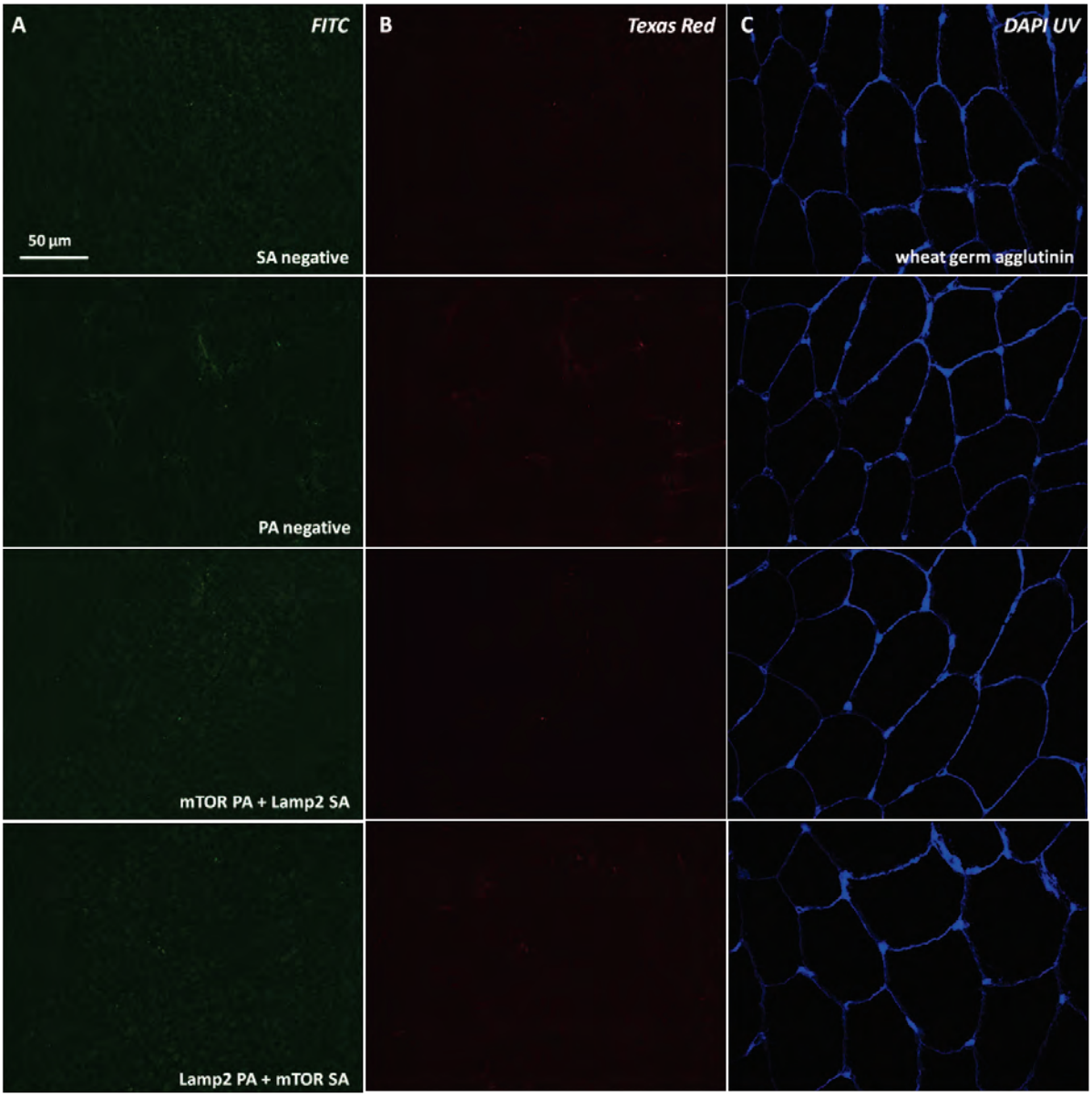

Figure 3.8.1.1 Cross binding negative controls on costaining of mTOR and Lamp2 antibodies under widefield microscope. The antibodies used for co-staining were tested with double negative control. Only primary antibodies (PA negative) or only secondary antibodies (SA negaive) were incubated with muscle samples, respectively. mTOR primary antibody was stained with secondary antibody targeting Lamp2 primary antibody (mTOR PA+ Lamp2 SA), while Lamp2 primary antibody was stained with secondary antibody specific to mTOR primary antibody (Lamp2 PA + mTOR SA). Signals were captured under two excitation wavelength channels, FITC (A) and Texas red (B). Cell membrane was outlined by the wheat germ

agglutinin conjugated with Alexa 350 fluorescence under DAPI UV channel (C). PA is short for primary antibody, and SA is short for secondary antibody. Scale bars 50 µm.

3.8.1.2 mTOR with Lamp2 co-localisation in basal human skeletal muscle

mTOR and Lamp2 antibodies have been validated as shown in 3.8.1.1. Figure 3.8.1.2 demonstrates that mTOR colocalises with Lamp2 positive areas in human skeletal muscle at rest level. Lamp2 fluorescence areas were much larger in size than that of mTOR, possibly because of Lamp2 proteins accumulating on the lysosome/endosome membranes. This can be visualized more clearly for details under the advanced confocal microscope images (Figure 3.8.1.3). Some mTOR stains localize on the Lamp2-positive 'palm-like' area. However, compared wih mTOR signals Lamp2 stains were more abundant than mTOR expression *in vivo*, in keeping with Lamp2's use as a lysosomal marker. Colocalised mTOR/ Lamp2 stains were observed to distribute near the sarcolemma membrane and in the sarcoplasm in basal human skeletal muscle.

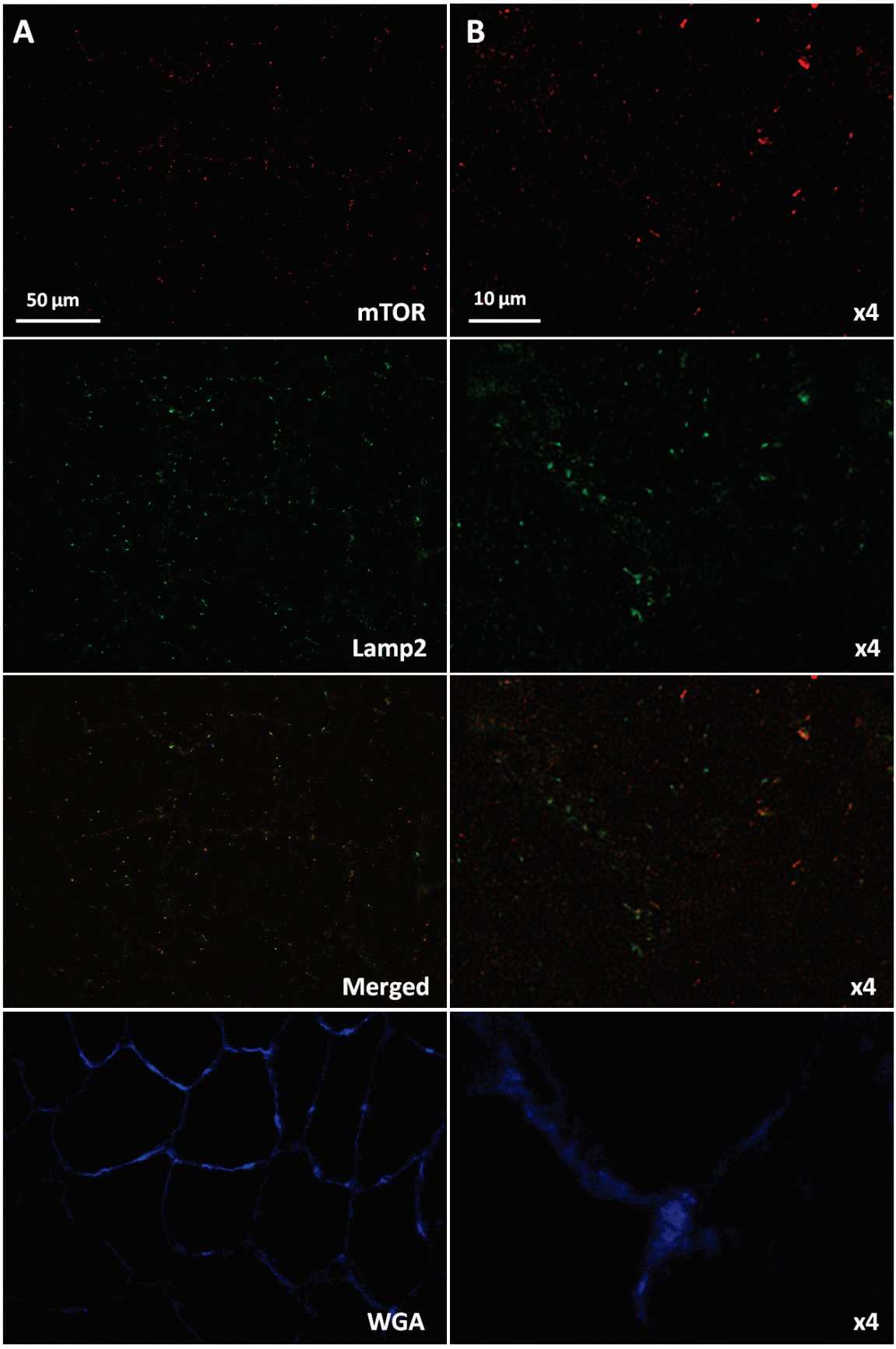
A
B
50 µm
mTOR
10 µm
x4
Lamp2
x4
Merged
x4
WGA
x4

Figure 3.8.1.2 immunofluorescences costaining of mTOR and Lamp2 under widefield microscope. mTOR was stained with Alexa 594nm secondary antibody (red), while Lamp2 was marked with Alexa 488nm secondary antibody (green). Cell membrane was marked by the wheat germ agglutinin conjugated with Alexa 350 fluorescence (blue). Scale bars 50 µm and 10µm.

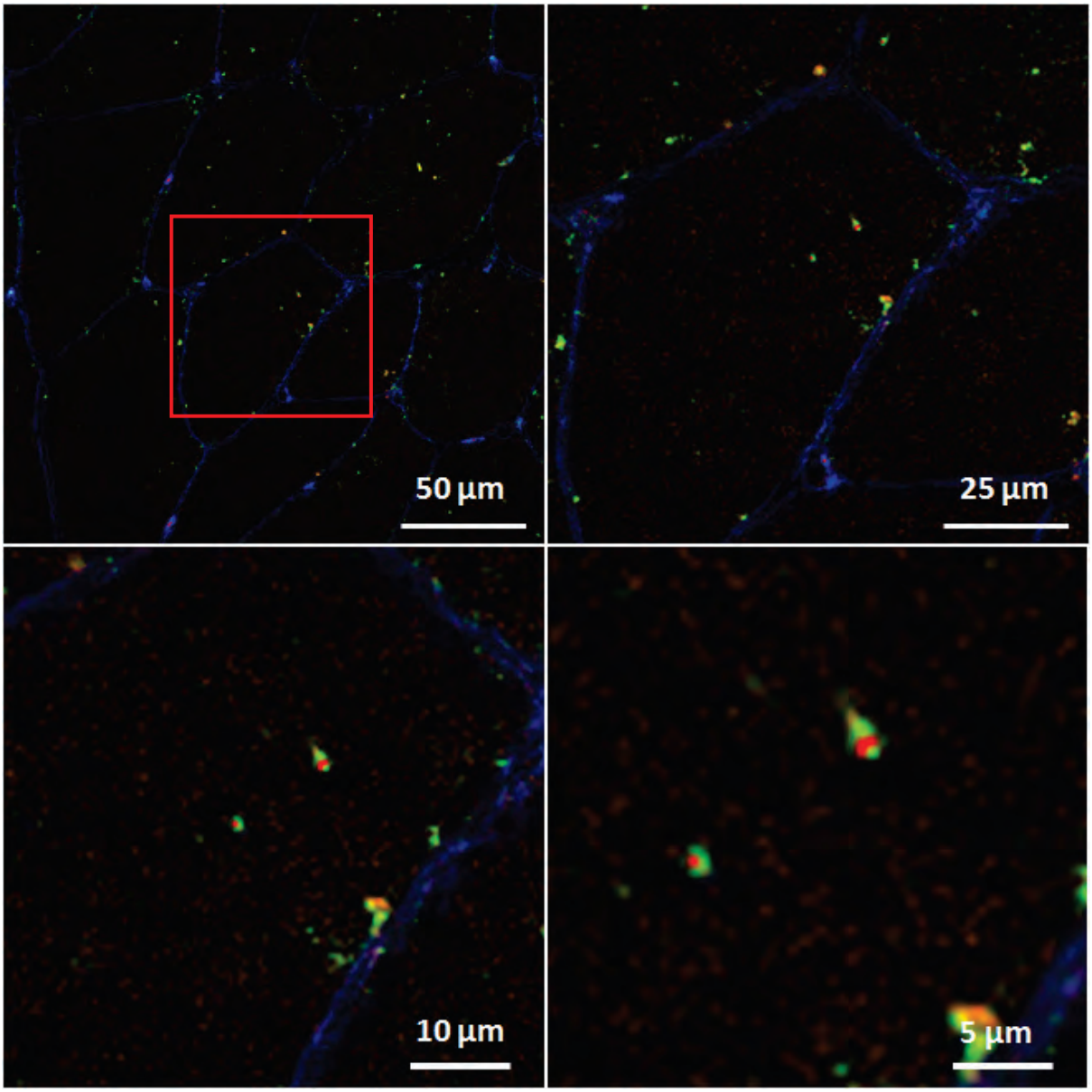

Figure 3.8.1.3 Colocalisation image between mTOR and Lamp2 under super resolution confocal microscope. mTOR was stained with Alexa 594nm secondary antibody (red) and observed under 561nm wavelength, while Lamp2 was marked with Alexa 488nm secondary antibody

(green)and visualized under 488nm wavelength. Cell membrane was marked with the wheat germ agglutinin conjugated with Alexa 350 fluorescence (blue) and observed under 405nm wavelength. Scale bars 50 µm,25 µm, 10 µm and 5µm.

3.8.1.3 Reproducibility of costaining between mTOR and Lamp2

Reproducibility testing was applied on the immunofluorescences samples examining association between mTOR and Lamp2. Sections from the same sample were repeatedly stained three times and images captured at the similar areas under microscope. And the coefficient of variance value for colocalisation analysis between mTOR and Lamp2 was 4.8%.

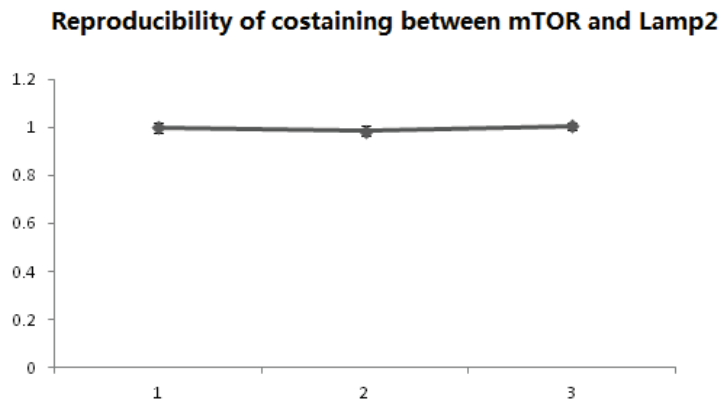

Figure 3.8.1.4 Reproducibility testing on colocalisation between mTOR and Lamp2. mTOR antibody was costained with Lamp2 antibody on the serial sections from the same sample. Data for each trial was the mean value from duplicates on one slide. Colocalisation value was measured as Pearson's Correlation coefficient under Image- Pro software. Images were taken under widefield microscope (x 40).

3.8.2 Costaining of mTOR with Rheb

3.8.2.1 Cross-binding negative control

All the four negative control experiments on mTOR and Rheb antibodies, as previously described in 3.8.1 were applied to mTOR and Rheb costaining.

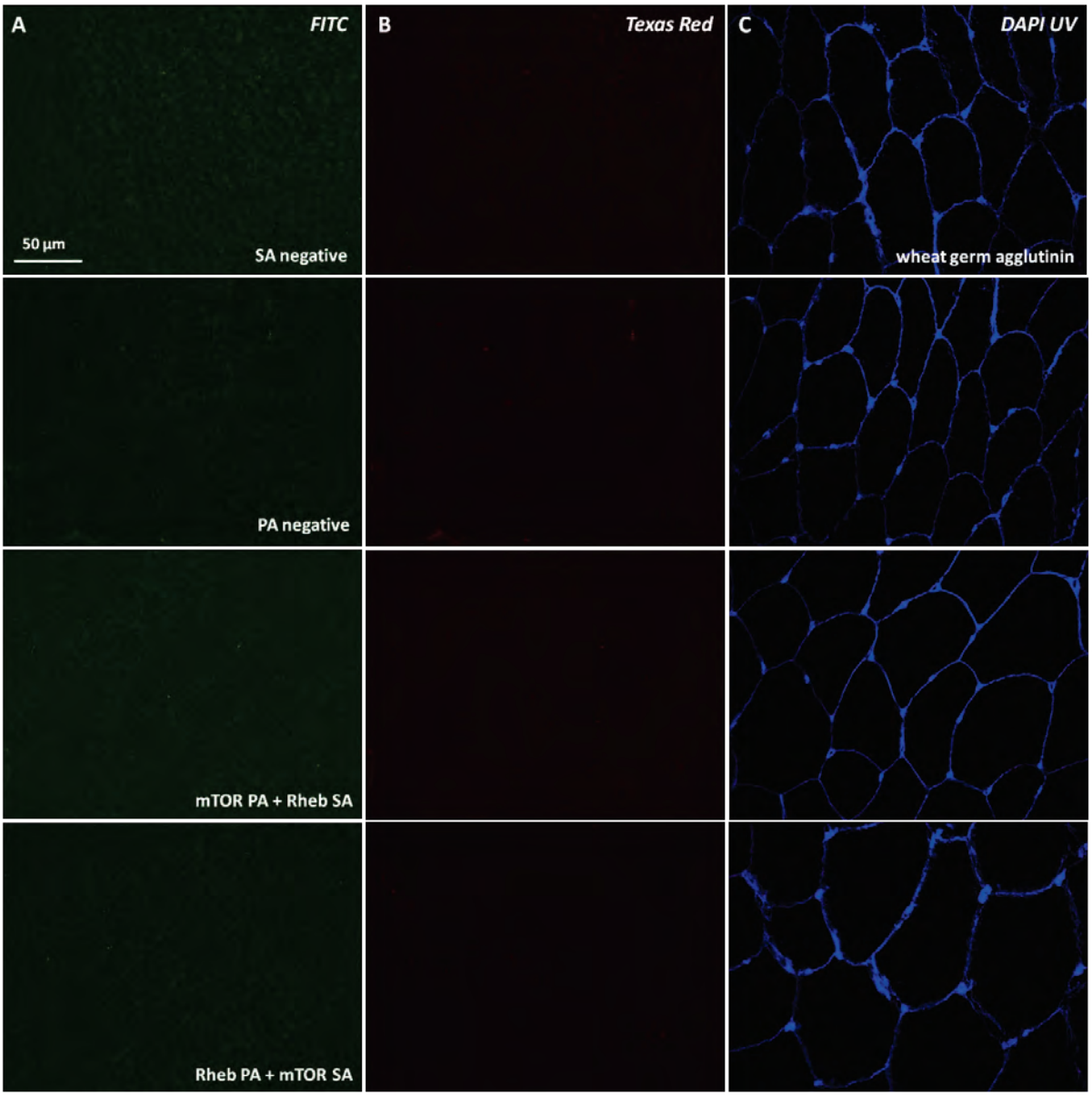

Figure 3.8.2.1 Negative control of mTOR and Rheb antibodies immunofluorescences costaining. Co-stained primary antibodies and secondary antibodies were incubated with muscle sections from the same sample, respectively. mTOR primary antibody (mouse IgG γ1) was incubated with the goat-anti rabbit IgG secondary antibodiy targeting the Rheb primary antibody. Reversely, Rheb primary antibody (rabbit IgG) was incubated with the goat-anti mouse IgG γ1 secondary antibodiy binding to the mTOR primary antibody. Protein stains were validated under two excitation wavelength, FITC (A) and Texas red (B). Cell membrane was marked by the wheat germ agglutinin conjugated with Alexa 350 fluorescence under DAPI UV channel (C). PA is short for primary antibody, and SA is short for secondary antibody. Scale bars 50 µm.

3.8.2.2 Colocalisation between mTOR and Rheb in basal human skeletal muscle

Figure 3.8.2.2 demonstrates the colocalisation between mTOR and Rheb in human skeletal muscle at basal status, with the distribution of two proteins in musculoskeletal cells quite disparate. Large amounts of Rheb positive stains were found to associate with the sarcolemma membrane at basal level, while only a few mTOR stains were visualized to localize near the plasma membrane (B, Figure 3.8.2.2). Also, the distribution of two proteins in sarcoplasm was also not in correspondence with each other.

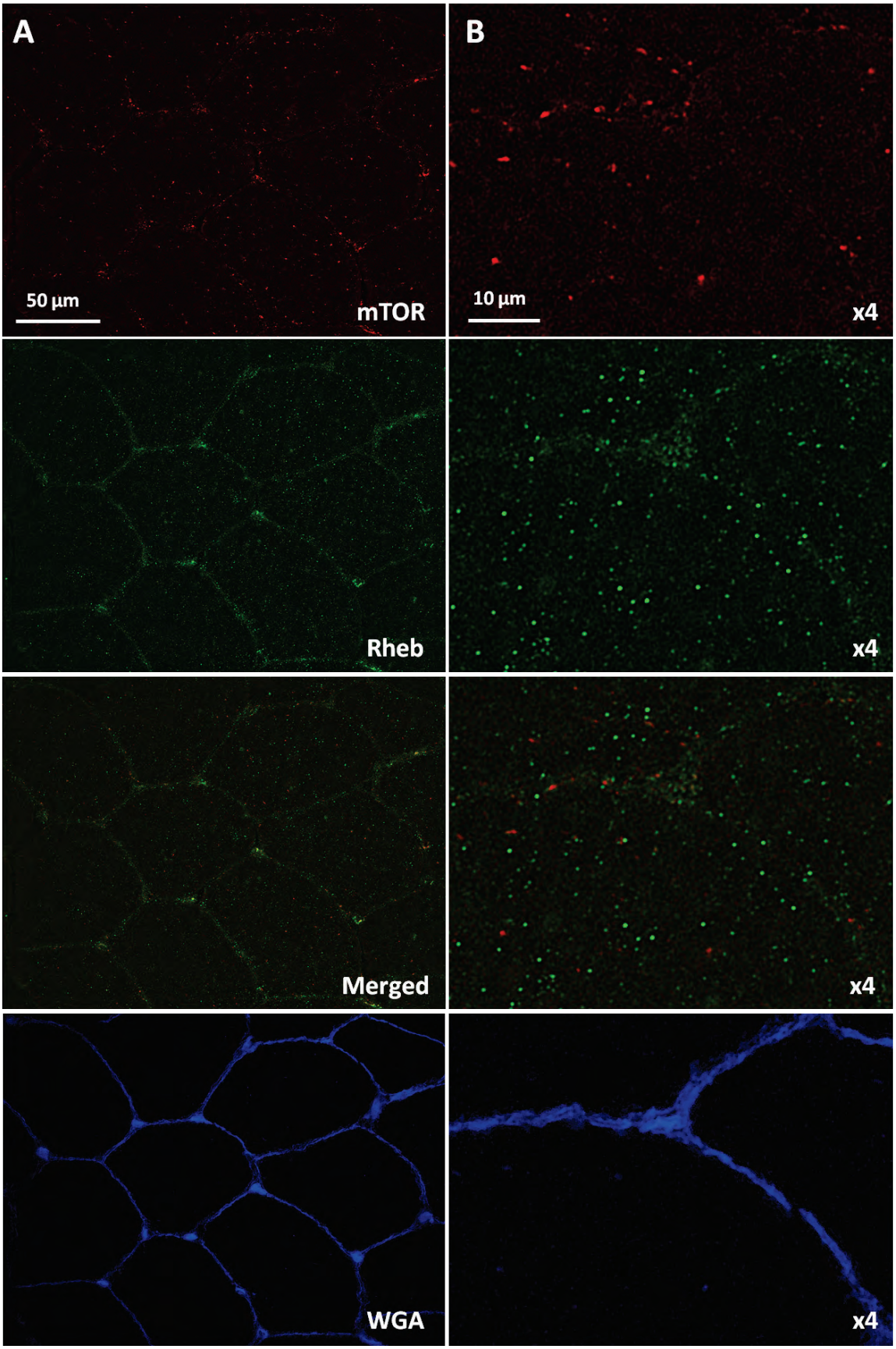
A
50 µm
mTOR
B
10 µm
x4
Rheb
x4
Merged
x4
WGA
x4

Figure 3.8.2.2 Immunofluorescences costaining of mTOR and Rheb under widefield microscope. mTOR was stained with Alexa 594nm secondary antibody (red), while Rheb protein was marked with Alexa 488nm secondary antibody (green). Cell membrane was outlined by the wheat germ agglutinin conjugated with Alexa 350 fluorescence (blue). Scale bars 50 µm and 10µm.

3.8.2.3 Reproducibility of costaining between mTOR and Rheb

The reproducibility test was applied on the immunofluorescences samples examining association between mTOR and Rheb. Serially cryostated sections from the same sample were stained with images captured at the similar areas under microscope. The CV value for colocalisation analysis between mTOR and Rheb was 6.3%.

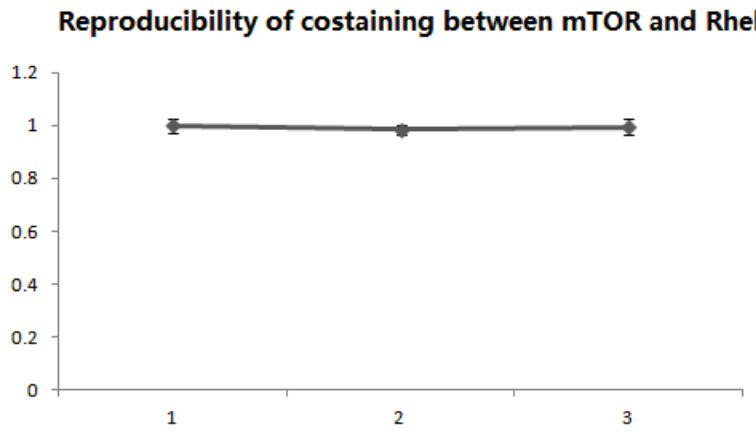

Figure 3.8.2.3 Reproducibility testing on colocalisation between mTOR and Rheb. mTOR antibody was costained with Rheb antibody on the sections from the same sample. Data of each trial was the mean value from duplicates on one slide. Colocalisation was measured and shown as Pearson's Correlation coefficient under Image- Pro software. Images were taken under widefield microscope (x40).

3.8.3 Costaining of mTOR with Rab7

3.8.3.1 Cross-binding negative control

As shown in Figure 3.8.3.1, possible cross binding among antibodies was validated by the negative control approaches. No cross reactivity was observed between primary antibodies (PA negative), or beween secondary antibodies (SA negative). Also, negative controls indicate there was no cross reaction between the mTOR primary antibody and Rab7 secondary antibody, and *vice versa*. These validation methods supported that signals stained by these antibodies were therefore specific to their antigens.

To confirm the fluorescence sensitivity to excitation, different excitation channels were used to visualize the specific protein fluorescence. For example, Rab7 stained by Alexa 488nm (green) was confirmed under both the FITC channel (green) and the Texa red channel (red).

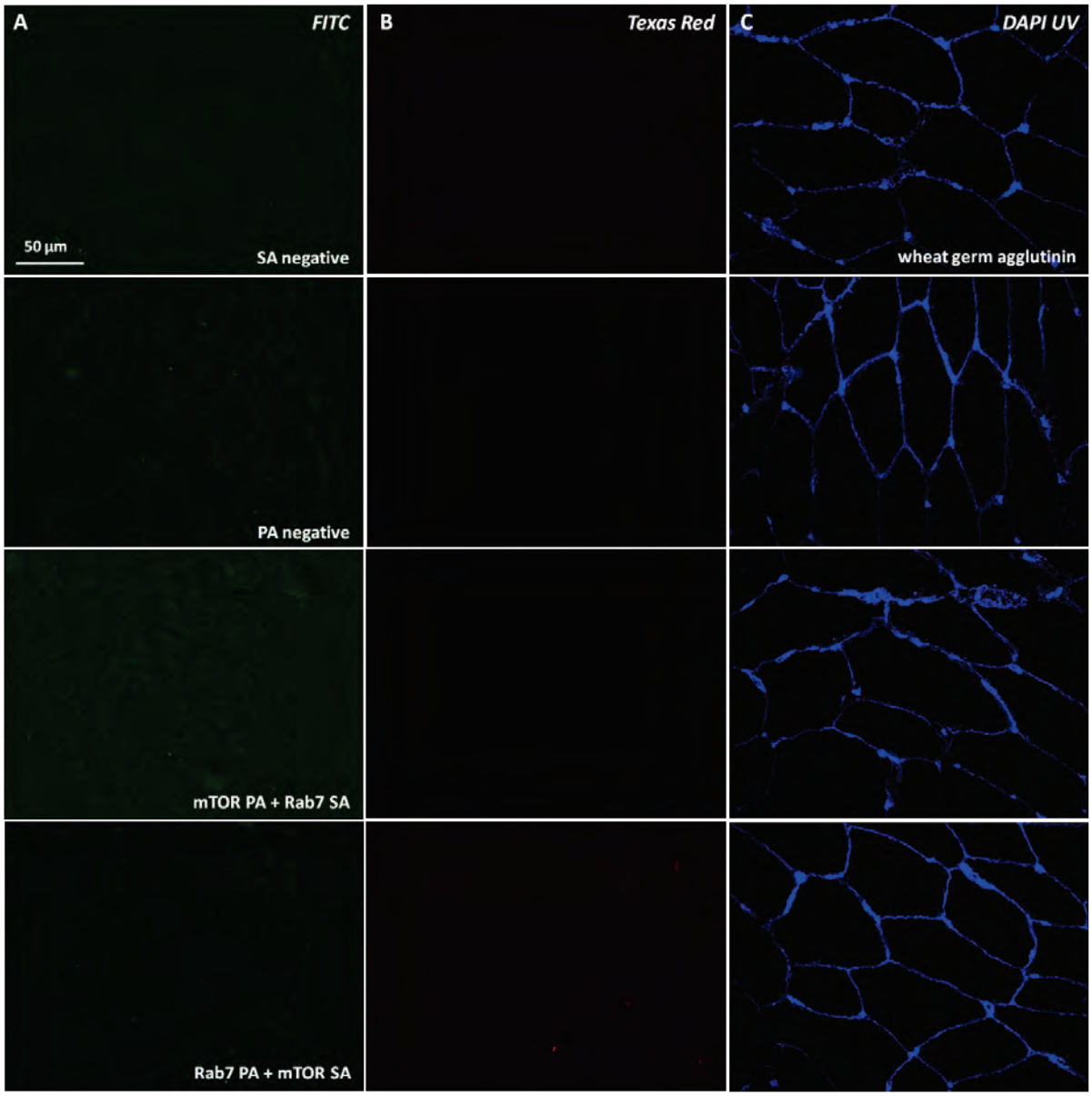

Figure 3.8.3.1 Negative control of mTOR and Rab7 antibodies immunofluorescences costaining. The co-stained primary antibodies and secondary antibodies were incubated with samples, respectively. mTOR primary antibody (mouse IgG γ1) was incubated with the goat-anti mouse IgG 2β secondary antibodiy. Reversely, Rab7 primary antibody (mouse IgG 2β isotype) was incubated with the goat-anti mouse IgG γ1 secondary antibodiy targeting the mTOR primary antibody. Stains were checked under two-excitation wavelength, FITC (A) and Texas red (B). Cell membrane was outlined by the wheat germ agglutinin conjugated with Alexa 350 fluorescence under DAPI UV channel (C). PA is short for primary antibody, and SA is short for secondary antibody. Scale bars 50 µm.

3.8.3.2 Colocalisation between mTOR and Rab7 in basal human skeletal muscle

Figure 3.8.3.2 displays clear colocalisation between mTOR and Rab7. It was observed that partially mTOR and Rab7 stains were associated with each other near the sarcolemma membrane and in sarcoplasm at basal level, which can be visualized more clearly following magnification.

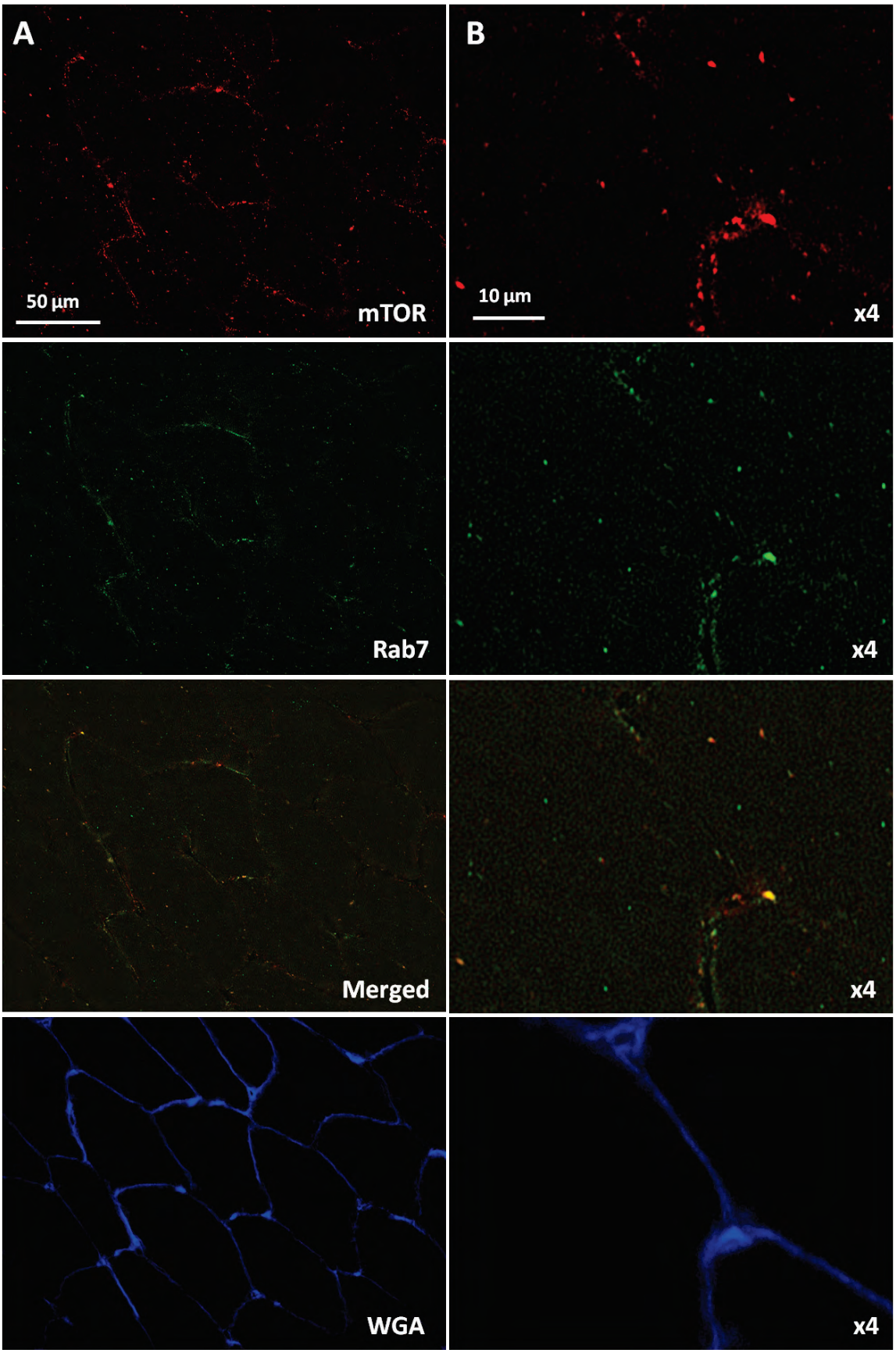
A
50 µm
mTOR
B
10 µm
x4
Rab7
x4
Merged
x4
WGA
x4

Figure 3.8.3.2 Immunofluorescences histological costaining of mTOR and Rab7 antibodies. mTOR was marked with Alexa 594nm secondary antibody (red), while Rab7 primary antibody was incubated with Alexa 488nm secondary antibody (green). Cell membrane was outlined by WGA conjugated with Alexa 350 fluorescence (blue). WGA was not merged into composite image to allow for observing mTOR/ Rab7 signals on cell membrane. B) Images were zoomed in x4 to show the details of subcellular colocalisation between mTOR and Rab7. Scale bars 50 µm and 10µm.

3.8.3.3 Reproducibility of costaining between mTOR and Rab7

Reproducibility testing was applied on the immunofluorescences samples examining association between mTOR with Rab7. Sections from the same sample were repeatedly stained three times and imaged at similar areas under microscope. The coefficient of variance value for colocalisation analysis between mTOR and Rab7 was 4.5%.

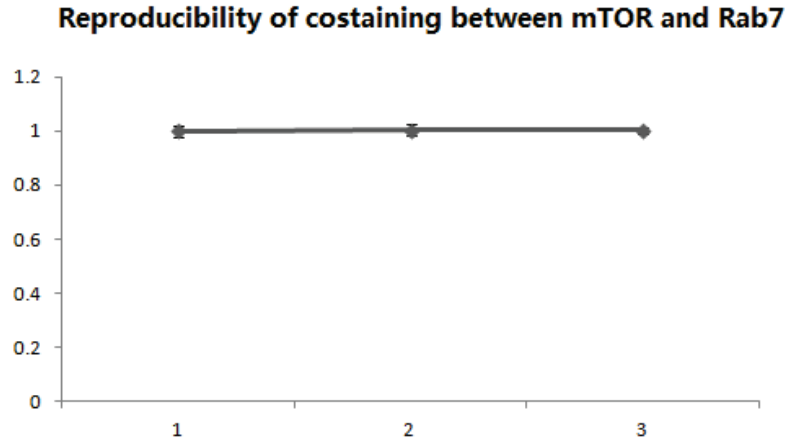

Figure 3.8.3.3 Reproducibility testing on colocalisation between mTOR and Rab7. mTOR antibody was costained with Rab7 antibody on the sections from the same sample. Data for each trial was the mean value from duplicates on one slide. Colocalisation was measured as Pearson's Correlation coefficient under Image- Pro software. Images were taken under widefield microscope.

3.8.4 Costaining of mTOR with EIF3F

3.8.4.1 Cross-binding negative control

As seen in Figure 3.8.4.1, all negative control experiments on mTOR and EIF3F antibodies indicate that antibodies applied to the mTOR and EIF3F costaining were specific to their antigens.

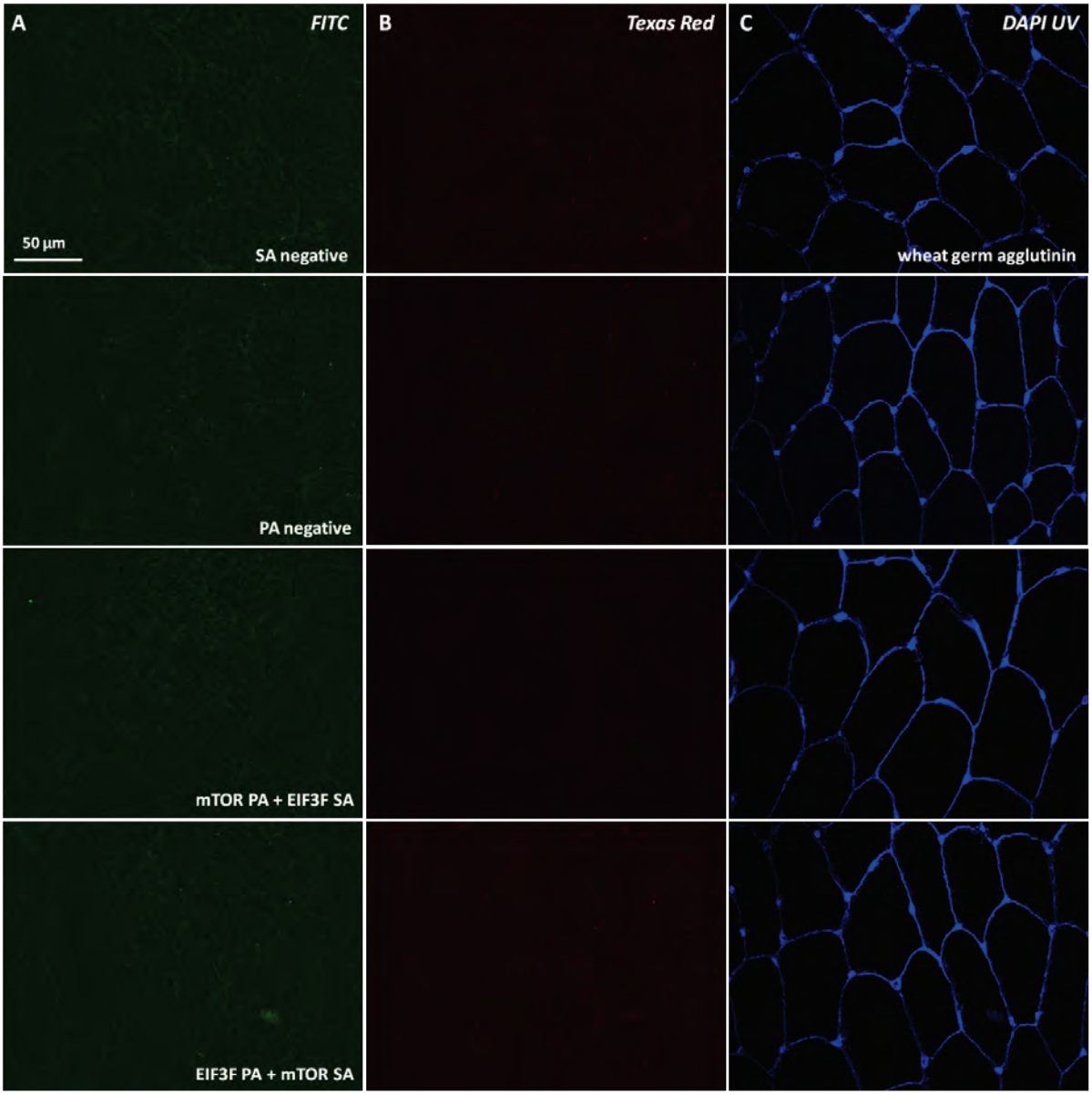

Figure 3.8.4.1 Cross binding negative controls on costaining of mTOR and EIF3F antibodies under widefield microscope. Co-staining was tested with double negative control. Only primary antibodies (PA negative) or only secondary antibodies (SA negative) were incubated with muscle samples, respectively. mTOR primary antibody was stained with secondary antibody

recognizing EIF3F primary antibody, while EIF3F primary antibody was stained with secondary antibody to stain mTOR primary antibody. Signals were captured under two excitation wavelength channels, FITC (A) and Texas red (B). Cell membrane was outlined by the wheat germ agglutinin conjugated with Alexa 350 fluorescence under DAPI UV channel (C). PA is short for primary antibody, and SA is short for secondary antibody. Scale bars 50 μm.

3.8.4.2 Colocalisation between mTOR with EIF3F in human skeletal muscle

EIF3F is an important regulator mediating mTORC signal transduction in eukaryotic cells [16, 17]. As shown in Figure 3.8.4.2, EIF3F fluorescences were visualized to localize on the plasma membrane, stains of which were associated with mTOR localisation on the plasma membrane in skeletal muscle cells (B, Figure 3.8.4.2).

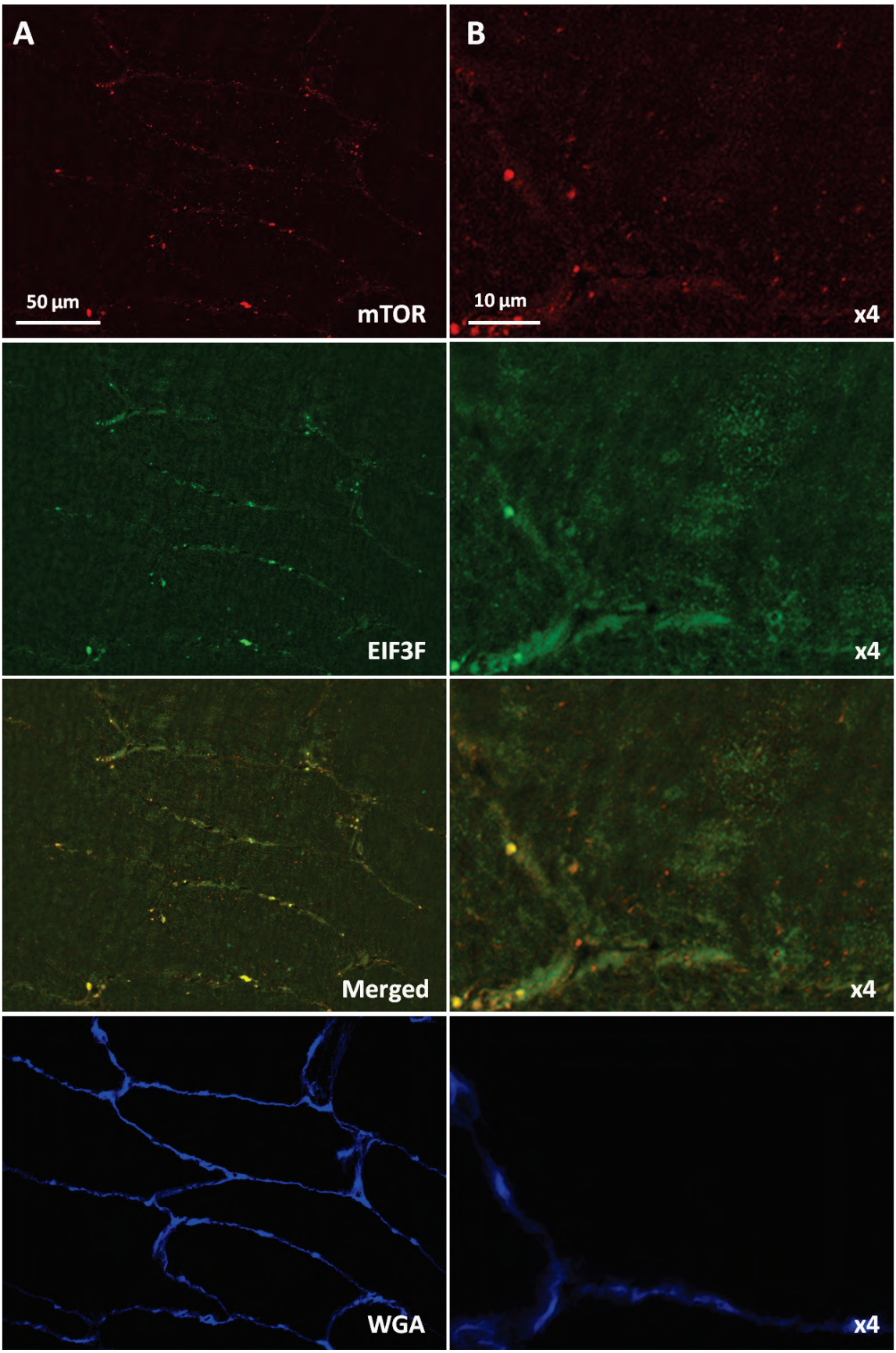
A
50 µm
mTOR
B
10 µm
x4
EIF3F
x4
Merged
x4
WGA
x4

Figure 3.8.4.2 Immunofluorescences histological costaining of mTOR and EIF3F antibodies. mTOR was stained with Alexa 594nm secondary antibody (red), while EIF3F primary antibody was incubated with Alexa 488nm secondary antibody (green). Cell membrane was outlined by WGA conjugated with Alexa 350 fluorescence (blue). B) Images were magnified x 4 to show the subcellular colocalisation between mTOR and EIF3F. Scale bars 50 µm and 10µm.

3.8.4.3 Reproducibility of costaining between mTOR and EIF3F

Reproducibility testing was applied on the immunofluorescences samples to examine association between mTOR and EIF3F. Serially cryostated sections from the same sample were stained and images captured at similar areas under microscope. The reproducibility was shown as the coefficient of variance (CV), which was 8.1% for colocalisation analysis between mTOR and EIF3F.

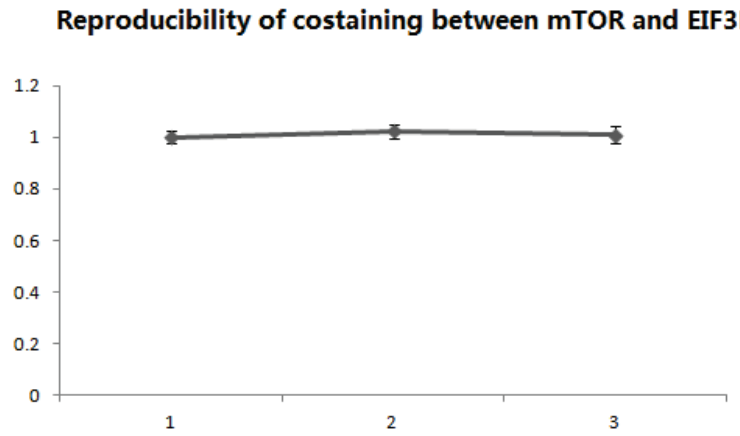

Figure 3.8.4.3 Reproducibility testing on colocalisation between mTOR and EIF3F. mTOR antibody was costained with EIF3F antibody on sections from the same sample. Data for each trial was the mean value from duplicates on one slide. Colocalisation was measured and shown as Pearson's Correlation coefficient under Image- Pro software. Images were taken under widefield microscope.

3.8.5 Costaining of Tuberin with Rheb

3.8.5.1 Cross-binding negative control

Figure 3.8.5.1 reports that all negative control experiments on Tuberin and Rheb indicated that antibodies applied into the Tuberin and Rheb costaining were specific to their antigens.

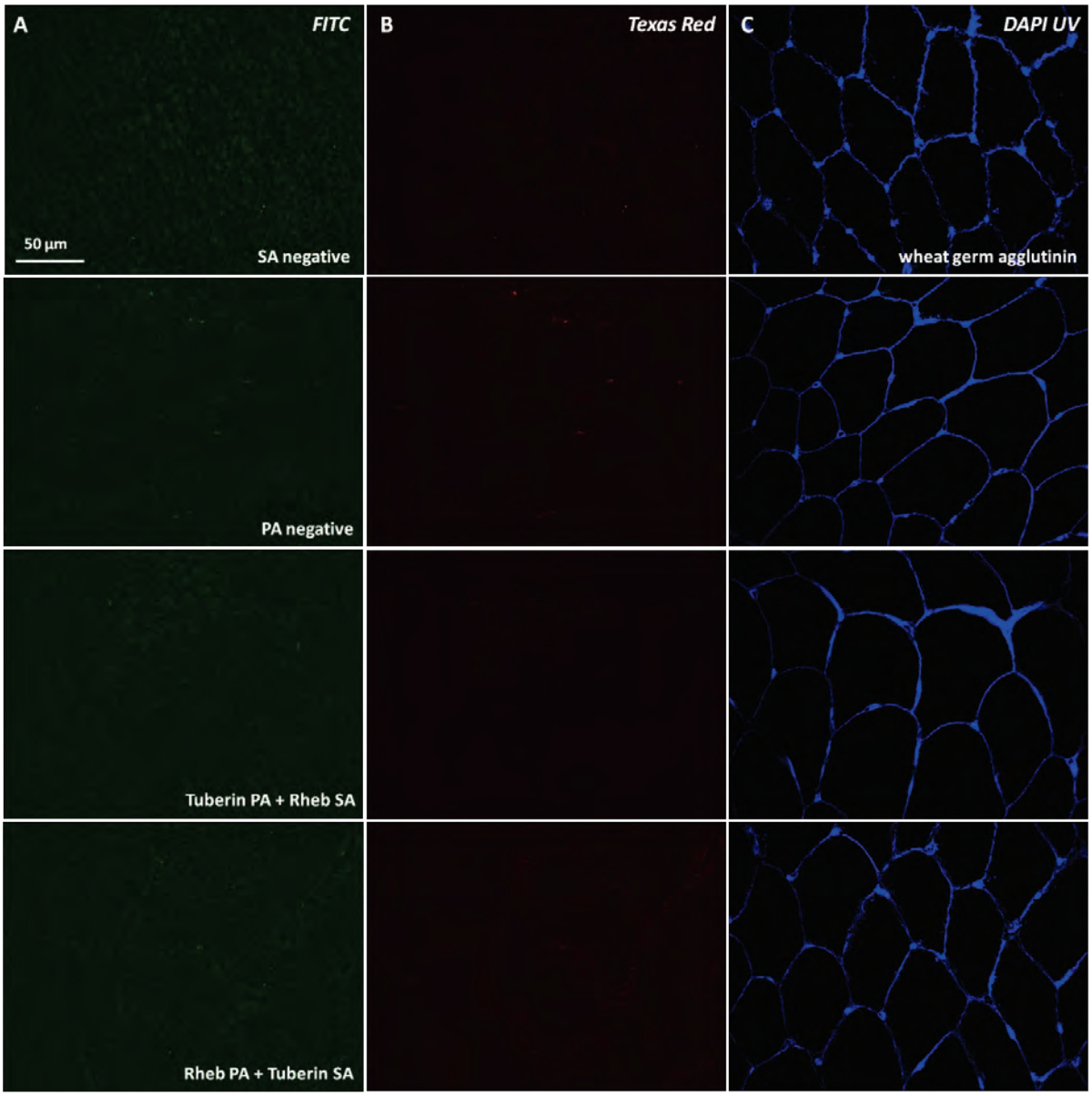

Figure 3.8.5.1 Cross binding negative controls on costaining of Tuberin and Rheb antibodies under widefield microscope. The co-staining was tested with double negative control. Only primary antibodies (PA negative) or only secondary antibodies (SA negative) were incubated with muscle samples, respectively. Tuberin primary antibody was stained with secondary

antibody recognizing Rheb primary antibody, while Rheb primary antibody was stained with secondary antibody to stain Tuberin primary antibody. Signals were captured under two excitation wavelength channels, FITC (A) and Texas red (B). Cell membrane was outlined by the wheat germ agglutinin conjugated with Alexa 350 fluorescence under DAPI UV channel (blue). PA is short for primary antibody, and SA is short for secondary antibody. Scale bars 50 µm.

3.8.5.2 Rheb and Tuberin colocalisation in basal human skeletal muscle

As seen in Figure 3.8.5.2, the Tuberin and Rheb signals were tightly associated with each other on the plasma membrane at rest level. Some Tuberin stains were also found inside the sarcoplasm, but they were not associated with the Rheb stains. These findings indicate the cell membrane as a main site for the colocalisation between Tuberin and Rheb.

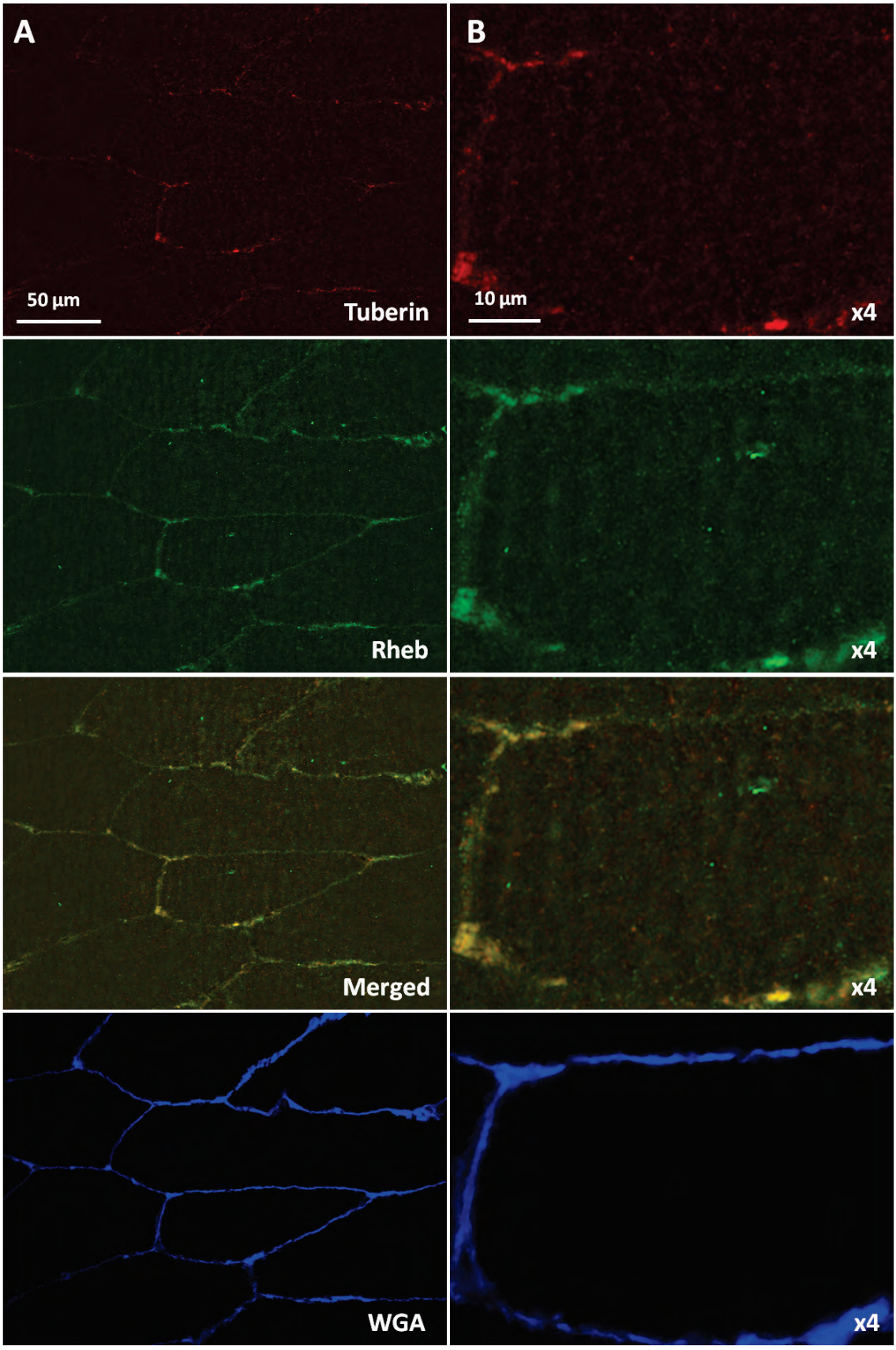
A
50 µm
Tuberin
B
10 µm
x4
Rheb
x4
Merged
x4
WGA
x4

Figure 3.8.5.2 Immunofluorescences costaining of Tuberin and Rheb antibodies. Tuberin primary antibody was stained with Alexa 594nm secondary antibody (red), while Rheb primary antibody was incubated with Alexa 488nm secondary antibody (green). Cell membrane was outlined by WGA conjugated with Alexa 350 fluorescence (blue). B) Images were magnified x 4 to show the subcellular colocalisation between Tuberin and Rheb. Scale bars 50 µm and 10µm.

3.8.5.3 Reproducibility of costaining between Tuberin and Rheb

Reproducibility testing was applied on the immunofluorescences samples to examine association between Tuberin and Rheb. Sections serially cut from the same sample were stained for three repeats and microscope images captured under the similar area of each section. The reproducibility was shown as coefficient of variance (CV), which was 7.5% for colocalisation analysis between Tuberin and Rheb.

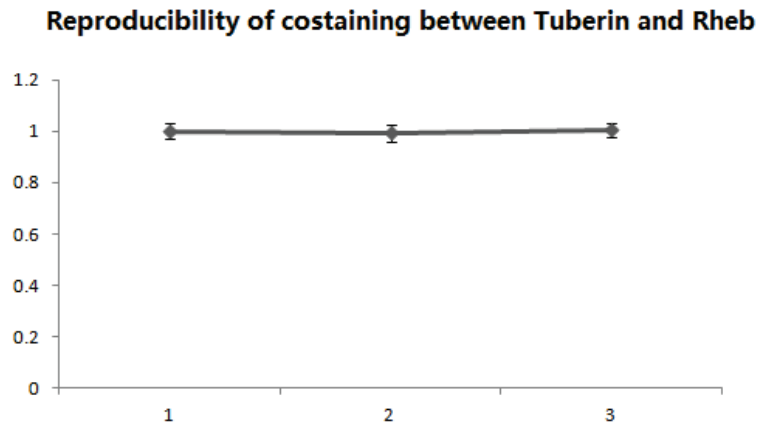

Figure 3.8.5.3 Reproducibility testing on colocalisation between Tuberin and Rheb. Tuberin antibody was costained with Rheb antibody on the sections from the same sample. Data for each trial was the mean value from duplicates on one slide. Colocalisation was measured shown as Pearson's Correlation coefficient under Image- Pro software. Images were taken under widefield microscope.

3.8.6 Costaining of Lamp2 with Rab7

3.8.6.1 Cross-binding negative control

As seen in Figure 3.8.6.1, all negative control experiments on Lamp2 and Rab7 antibodies indicate that antibodies applied into the Lamp2 and Rab7 costaining were specific to their antigens.

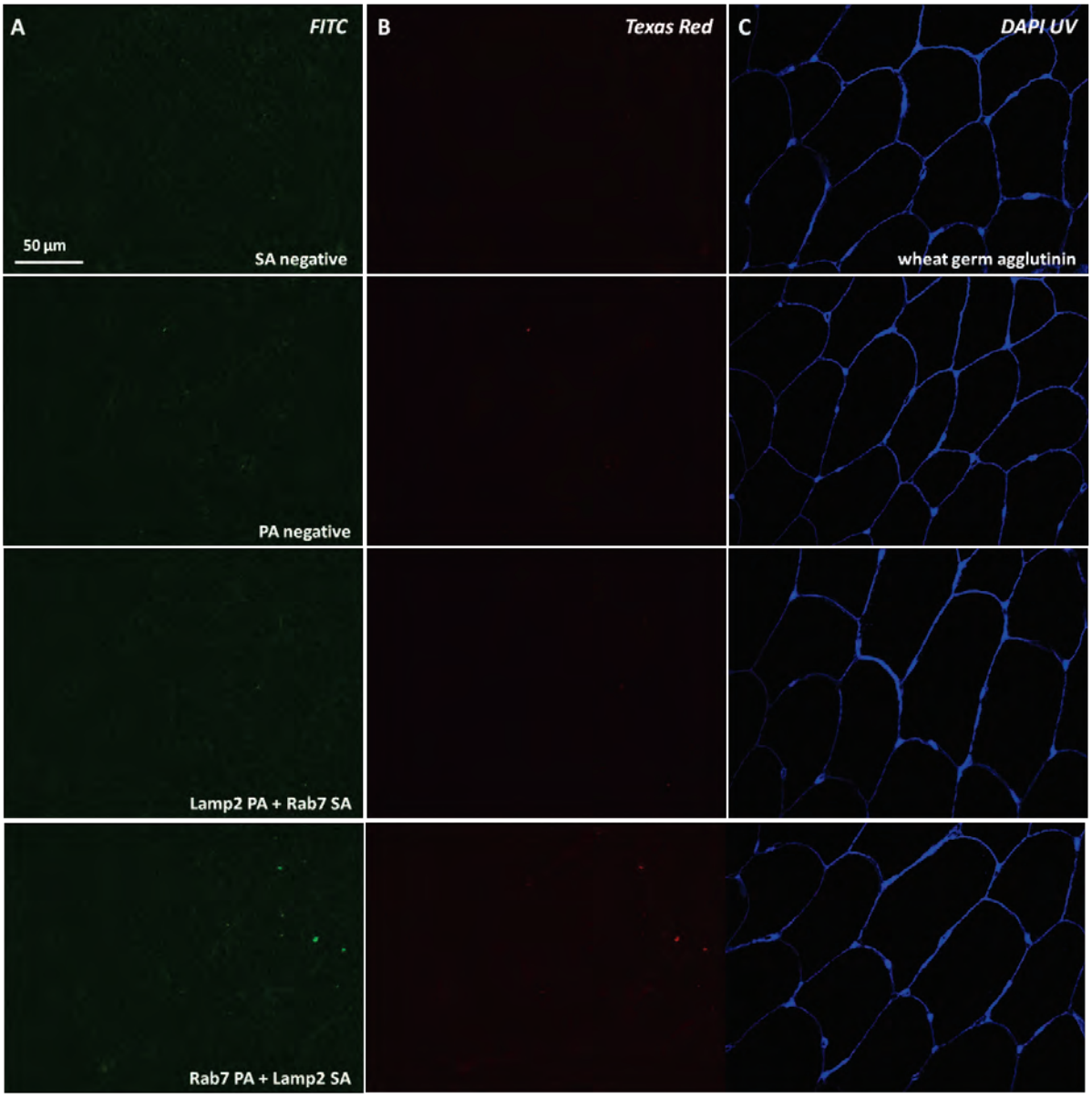

Figure 3.8.6.1 Cross binding negative controls on costaining of Lamp2 and Rab7 antibodies under widefield microscope. The co-staining was tested with double negative control. Only primary antibodies (PA negative) or only secondary antibodies (SA negative) were incubated with muscle samples, respectively. Lamp2 primary antibody was stained with secondary

antibody recognizing Rab7 primary antibody, while Rab7 primary antibody was stained with secondary antibody to stain Lamp2 primary antibody. Signals were captured under two excitation wavelength channels, FITC (A) and Texas red (B). Cell membrane was outlined by the wheat germ agglutinin conjugated with Alexa 350 fluorescence under DAPI UV channel (blue). PA is short for primary antibody, and SA is short for secondary antibody. Scale bars 50 µm.

3.8.6.2 Lamp2 and Rab7 co-localisation in basal human skeletal muscle

As shown in Figure 3.8.6.2, Some Lamp2 and Rab7 stains were visualised to associate near the plasma membrane and in sarcoplasm in basal human skeletal muscle, although additional Rab7 stains were not observed to colocalise with Lamp2 in the sarcoplasm.

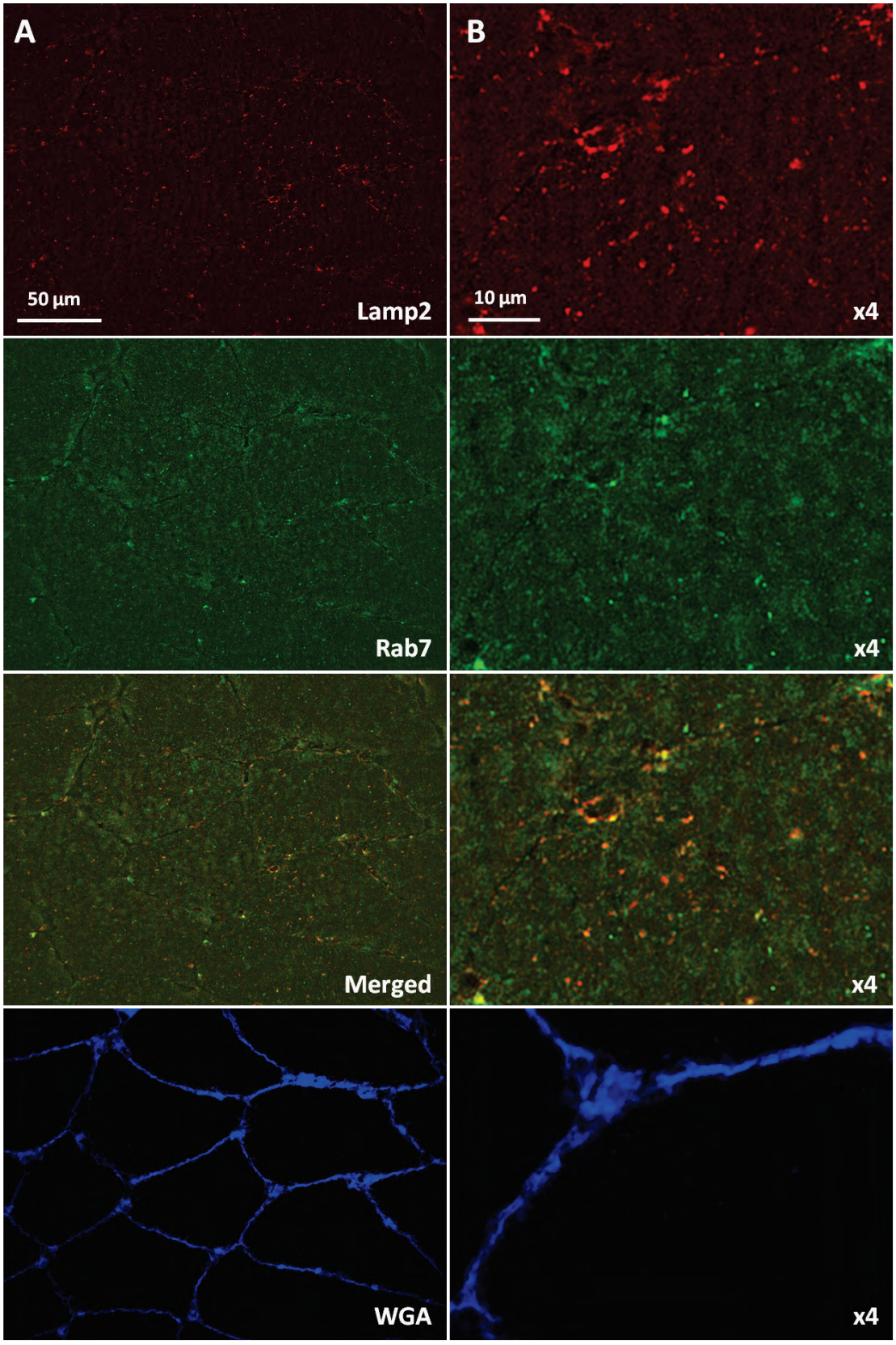

Figure 3.8.6.2 Immunofluorescences costaining of Lamp2 and Rab7 antibodies. Lamp2 primary antibody was stained with Alexa 594nm secondary antibody (red), while Rab7 primary

antibody was incubated with Alexa 488nm secondary antibody (green). Cell membrane was marked by WGA conjugated with Alexa 350 fluorescence (blue). B) Images were magnified x 4 to demonstrate the subcellular colocalisation between Lamp2 and Rab7. Scale bars 50 µm and 10µm.

3.8.6.3 Reproducibility of costaining between Lamp2 and Rab7

Reproducibility testing was applied on the immunofluorescences histological experiment investgating the association between Lamp2 and Rab7. Sections serially cut from the same sample were stained for three repeats and imaged at the similar areas under microscope. The reproducibility was represented as coefficient of variance (CV), value of which was 5.0% for the colocalisation analysis between Lamp2 and Rab7.

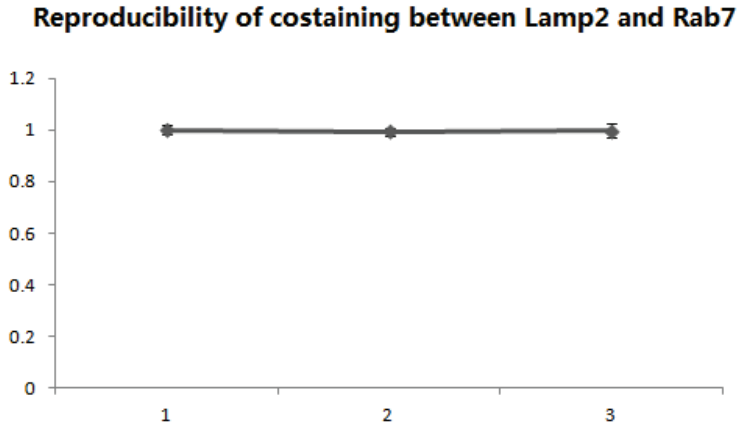

Figure 3.8.6.3 Reproducibility testing on colocalisation between Lamp2 and Rab7. Lamp2 antibody was costained with Rab7 antibody on the sections from the same sample. Data for each trial was the mean value from duplicates on one slide.Colocalisation was measured and shown as Pearson's Correlation coefficient under Image- Pro software. Images were taken under widefield microscope.

3.8.7 Costaining of mTOR with UEA-I in basal human skeletal muscle

As the UEA-I antibody used in the study was conjugated with the Alexa dye, and the mTOR antibody has been validated to be specific, cross binding negative control experiments were not applied to the costaining between mTOR and UEA-I antibodies.

3.8.7.1 mTOR and UEA-I co-localisation in basal human skeletal muscle

Ulex Europaeus Agglutinin (UEA-I) is a biomarker used to indicate the capillaries' position. As seen from Figure 3.8.7.1, skeletal muscle capillaries were localized on the membrane borders between adjacent musculoskeletal cells. Only a few mTOR stains were observed to localize on or near the blood vessel areas at basal human skeletal muscle.

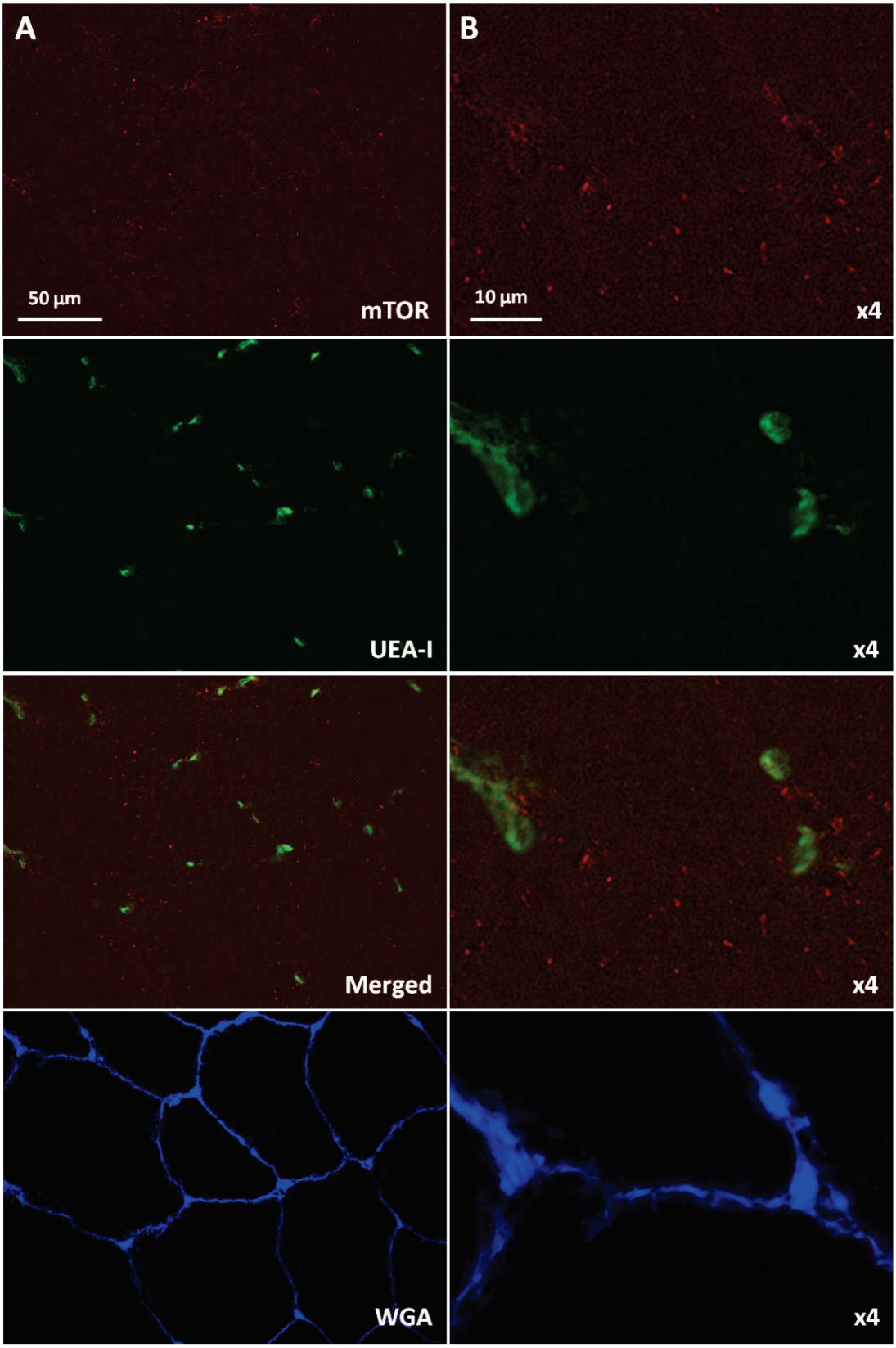

Figure 3.8.7.1 Immunofluorescences co-staining of mTOR and blood vessels staind by UEA-I under widefield microscope. A) mTOR was stained with Alexa 594nm secondary antibody (red),

while Ulex Europaeus Agglutinin (UEA-I) was conjugated with Alexa 488nm secondary antibody (green). Cell membrane was outlined by the wheat germ agglutinin conjugated with Alexa 350 fluorescences (blue). B) Images were magnified x 4 to exhibit the subcellular colocalisation between mTOR and blood vessels. Scale bars 50 µm and 10µm.

3.8.7.2 Reproducibility of costaining between mTOR and UEA-I

Reproducibility validation was applied on the immunofluorescences samples examining association between mTOR and UEA-I. Sections from the same sample were serially cut and stained for three repeats. Microscope images were captured from the similar areas of each section. The reproducibility was quantified as coefficient of variance (CV), which was 8.8% for the colocalisation analysis between mTOR and UEA-I.

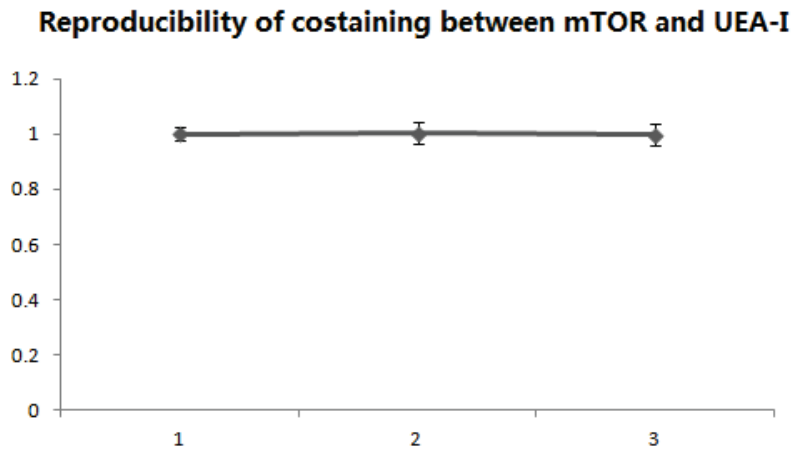

Figure 3.8.7.2 Reproducibility testing on colocalisation between mTOR and UEA-I. mTOR primary antibody incubated with secondary antibody was costained with UEA-I conjugated with FITC dye on the sections from the same sample. Data for each trial was the mean value from duplicates on one slide. Colocalisation was measured and shown as Pearson's Correlation coefficient under Image- Pro software. Images were taken under widefield microscope.

3.8.8 Costaining of mTOR with MHCI

3.8.8.1 Cross-binding negative control

As seen in Figure 3.8.8.1, all negative control experiments on mTOR and MHCI antibodies indicated that antibodies applied into the mTOR with MHCI costaining were specific to their antigens.

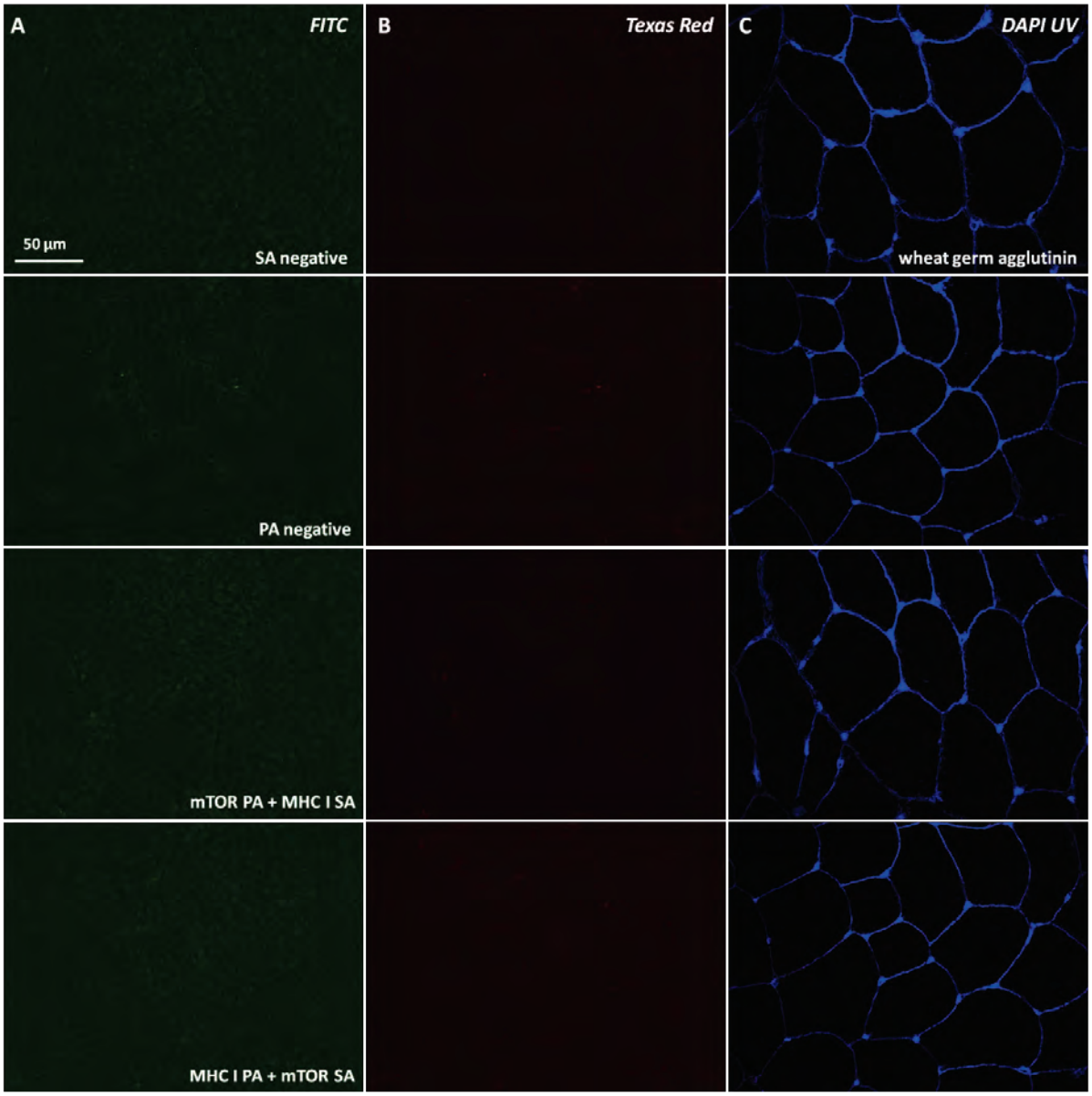

Figure 3.8.8.1 Cross binding negative controls on costaining of mTOR and myosin heavy chain I antibodies under widefield microscope. The co-staining was tested with double negative control. Only primary antibodies (PA negative) or only secondary antibodies (SA negative) were incubated with muscle samples, respectively. mTOR primary antibody was stained with

secondary antibody recognizing MHC I primary antibody, while MHC I primary antibody was stained with secondary antibody to stain mTOR primary antibody. Signals were captured under two excitation wavelength channels, FITC (A) and Texas red (B). Cell membrane was outlined by wheat germ agglutinin conjugated Alexa 350 fluorescence under DAPI UV channel (blue). Scale bars 50 μm.

3.8.8.2 mTOR distribution in type I muscle fibers in basal human skeletal muscle

Myosin heavy chain I antibody is the biomarker used to indicate human type I muscle fibers in skeletal muscle. As seen from Figure 3.8.8.2, mTOR signals were observed both on the sarcolemma membrane and sarcoplasm in type I muscle fibres. There was no visiable distribution difference of mTOR stains between type I muscle fibers and other muscle fibers in basal human skeletal muscle.

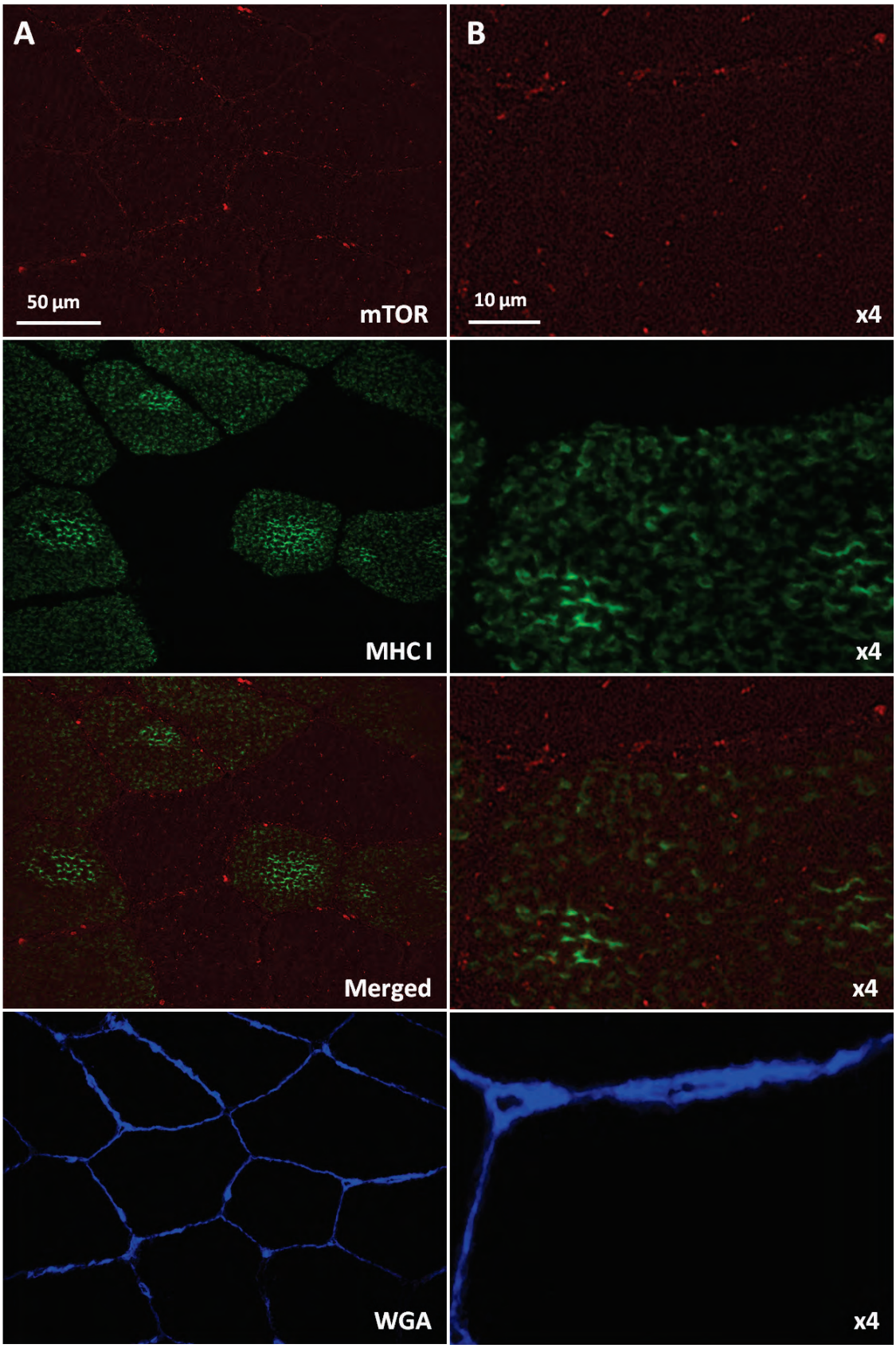
A
B
50 µm
mTOR
10 µm
x4
MHC I
x4
Merged
x4
WGA
x4

Figure 3.8.8.2 Immunofluorescences costaining of mTOR antibody with Myosin heavy chain I antibody. mTOR primary antibody was stained with Alexa 594nm secondary antibody (red), while myosin heavy chain I primary antibody was incubated with Alexa 488nm secondary antibody (green). Cell membrane was outlined by WGA conjugated with Alexa 350 fluorescence (blue). B) Images were magnified x 4 to exhibit the subcellular localisation of mTOR in type I muscle fibres. Scale bars 50 µm and 10µm.

3.8.8.3 Reproducibility of mTOR fluorescence content quantification

Reproducibility validation was applied on immunofluorescences samples examining mTOR content in different muscle fiber types. Sections serially cut from the same sample were stained for three repeats and microscope images captured from the similar areas of each section. The reproducibility was quantified coefficient of variance (CV). The CV value for mTOR fluorescence content analysis was 6.6%.

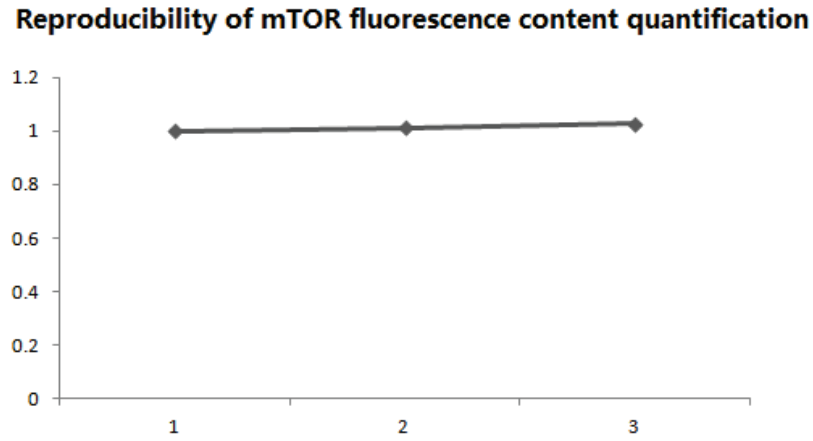

Figure 3.8.8.3 Reproducibility testing on mTOR fluorescence content measurement. mTOR antibody and WGA antibody were stained on the sections from the same sample. mTOR content was measured and shown as averaged density of pixel units per fiber under Image- Pro software. Data for each trial was the mean value from duplicates on one slide. Images were taken under widefield microscope.

3.8.9 Costaining of mTOR with MHCIIx in basal human skeletal muscle

3.8.9.1 Cross-binding negative control

As seen in Figure 3.8.9.1, all negative control experiments on mTOR and MHCIIx antibodies indicated that antibodies applied to the mTOR and MHCIIx costaining were specific to their antigens.

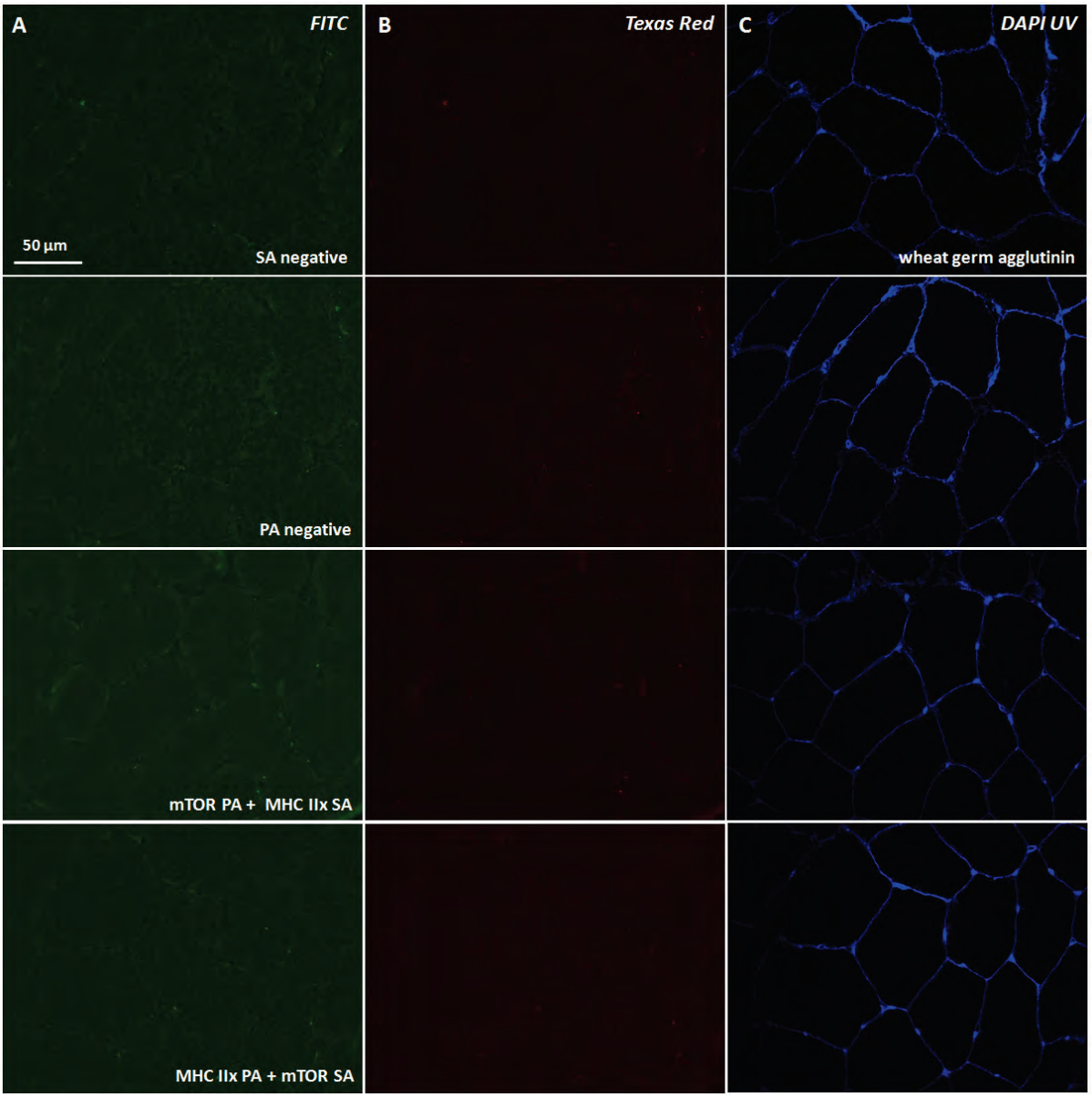

Figure 3.8.9.1 Cross binding negative controls on costaining of mTOR with myosin heavy chain IIx antibody under widefield microscope. The co-staining was tested with double negative control. Only primary antibodies (PA negative) or only secondary antibodies (SA negative) were incubated with muscle samples, respectively. mTOR primary antibody was stained with

secondary antibody targeting MHC IIx primary antibody, while MHC IIx primary antibody was stained with secondary antibody binding to mTOR primary antibody. Signals were captured under two excitation wavelength channels, FITC (A) and Texas red (B). Cell membrane was marked by the wheat germ agglutinin conjugated with Alexa 350 fluorescence under DAPI UV channel (blue). Scale bars 50 µm.

3.8.9.2 mTOR distribution in type IIx muscle fibers in basal human skeletal muscle

Co-staining method of mTOR with myosin heavy chain IIx (MHC IIx) was developed to investigate the expression of mTOR in different muscle fibers. As seen in Figure 3.8.9.2, there were no visuable distribution differences of mTOR fluorescences between type IIx muscle fibers and the other muscle fibers in basal human skeletal muscle.

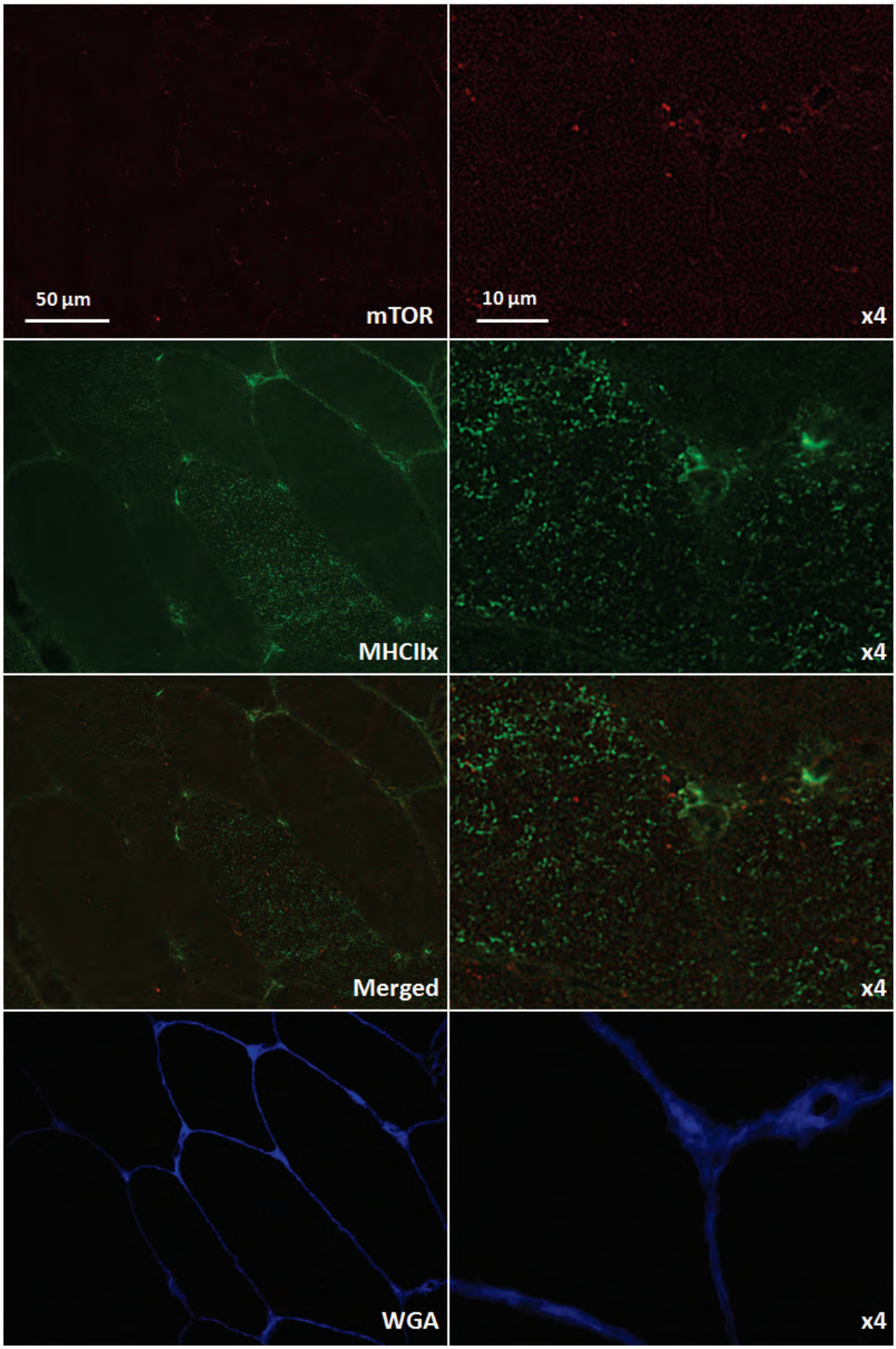
50 µm
mTOR
10 µm
x4
MHCIIx
x4
Merged
x4
WGA
x4

Figure 3.8.9.2 Immunofluorescences costaining of mTOR antibody with Myosin heavy chain IIx antibody. mTOR primary antibody was stained with Alexa 594nm secondary antibody (red), while myosin heavy chain IIx primary antibody was incubated with Alexa 488nm secondary antibody (green). Cell membrane was outlined by WGA conjugated with Alexa 350 fluorescence (blue). B) Images were magnified x 4 to exhibit the subcellular localisation of mTOR in type IIx muscle fibres. Scale bars 50 µm and 10µm.

3.8.10 Costaining of mTOR with DAPI in basal human skeletal muscle

DAPI was used to costain the nucleus with mTOR antibody. There was no cross binding negative control experments applied into the staining of mTOR antibodies and DAPI.

3.8.10.1 mTOR with DAPI colocalisation in basal human skeletal muscle

Nuclei stained by DAPI were observed to locate along the sarcolemma membrane. As seen in Figure 3.8.10.1, mTOR stains were hardly visualised in the nucleus area. Some mTOR stains localize peri nuclear region in magnified microscope images. The other mTOR stains were distributed in the sarcoplasm.

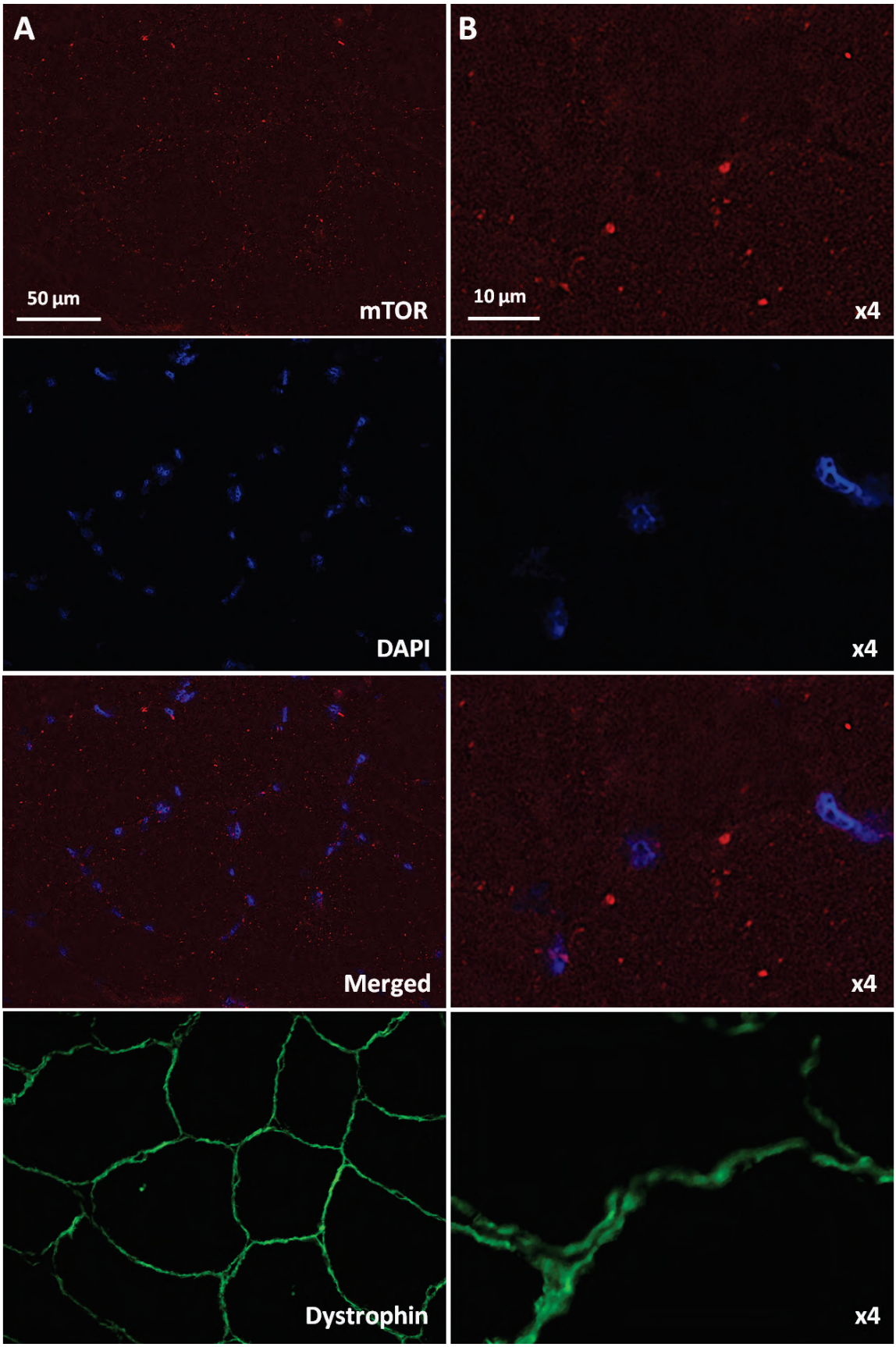
A
B
50 µm
mTOR
10 µm
x4
DAPI
x4
Merged
x4
Dystrophin
x4

Figure 3.8.10.1 Immunofluorescences staining of mTOR antibody with nucleus dye DAPI. A) mTOR primary antibody was stained with Alexa 594nm secondary antibody (red), while cell membrane was outlined with dystrophin primary antibody conjugated with Alexa 488nm secondary antibody (green). DAPI (1:1000) solution was incubated with section to stain nucleus area (blue). B) Images were magnified x 4 to exhibit the subcellular localisation of mTOR around nuclei. Scale bars 50 µm and 10µm.

3.9 Antibodies validated by blocking peptides competition assay

As shown in Figure 3.9.1, following pre-incubation with blocking peptides, signals generated by Rheb, TSC2 and eIF3F antibodies staining were not observed in COMP images, which showed similar signal strength as that in no antibody incubation control. These data support that the positive staining of Rheb, TSC2 and eIF3F antibodies generated specific fluorescence signals in human skeletal muscle *invivo*.

Figure 3.9.1 Blocking competition assay was applied to validate the recogition specificity of primary antibodies used in the study. Images were achived under the similar regions from the same sample. COMP is short for competition assay, and No Ab is short for no primary antibody

incubation. Cell membrane was outlined by WGA conjugated with Alexa 350 fluorescence (blue). Images were taken under x40 objective.

mTOR specific knock-out mouse sample were obtained from Dr Yann-Gaël Gangloff (Université de Lyon) and used to validate mTOR specific staining. As shown in Figure 3.9.2, mTOR signals were observed in skeletal muscle of wild type mouse, whist mTOR fluoresecence stained were remarkably diminished in mTOR knock- out mouse, similar with no primary antibody incubation control. This experiment further proved that mTOR signals from immunofluorescence staining stand for expression of mTOR proteins.

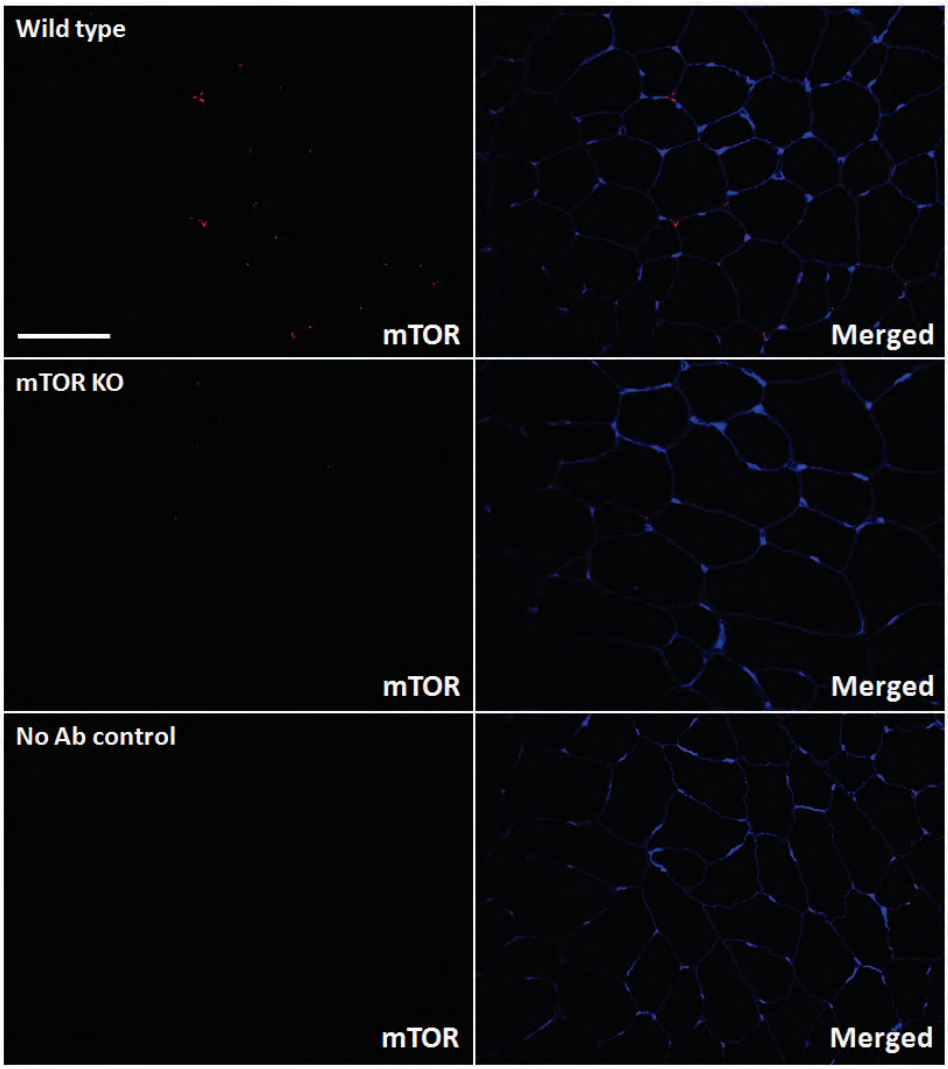

Figure 3.9.2 mTOR signals were diminished in mTOR knock- out mouse. Mouse skeletal muscle was stained with mTOR primary antibody and secondary antbody conjugated with Alexa@ 594

fluorphore. Cell membrane was outlined by WGA conjugated with Alexa 350 fluorescence (blue). Imaged were taken under x40 objective lens. Scale bars 50 µm.

3.10 Discussion

This chapter described validation methods for immunofluorescence experiment studying mTOR content and distribution in human skeletal muscle *in vivo*. Through a series of antibody validation methods, we have proved that both primary and secondary antibodies applied into immunofluorescences experiment specifically target proteins in human skeletal muscle *in vivo*. Signal sensitivity of each antibody was optimized and signal/ background noise ratio was maintained to avoid either high background noise or too weak signals.

A multiple antibodies 'cocktail' costaining method was developed to observe association between mTOR and associating proteins. All antibodies used in costaining were validated by cross binding negative control to exclude potential unspecific staining. It is possible that protein signals may change along with the depth of muscle samples sectioned, resulting in data variance. So we introduced reproducibility testing on antibodies to guarantee staining experiments repeatability.

Total mTOR stains were firstly observed as in human skeletal muscle, showing a similar distribution with phosphorylated mTOR reported in human [18]. mTOR was observd to disassociate from Rab7 and Lamp2 in cultured cells following nutrient starvation [15, 19], whist partial mTOR stains were found colocalise with Rab7 and Lamp2 in human at basal level in this study. Reasons resulting in difference between cell model and human model are unclear but possibly because of necessity to maintain basal mTOR activity under physiological conditions. Korolchuk *et al* reported mild nutrition condition retained mTOR on Lamp2- positive areas in cells *in vitro* [20]. Taking advantage of super resolution microscope, details on mTOR/Lamp2 association were revealed with Lamp2 proteins observed to surround mTOR protein for mTOR docking.

Rheb and TSC2 are reported as mTOR activator [19] and inhibitor [14], respectively. Here microscope images demonstrated that these two proteins were primarily colocalised on the cell membrane in basal human skeletal muscle, which have never been reported in cell and rodent before. Physiological meaning of TSC2 and Rheb localisation on cell membrane is unclear. Colocalisation between Rheb and TSC2 indicated Rheb inhibition by TSC2 directly [14], suggesting mTOR docking to lysosome

membrane *per se* did not mean mTOR activation, as mTOR is directly activated by Rheb [21]. In consistence, mTOR and Rheb colocalisation images showed disassociation between two proteins in basal human skeletal muscle, supporting the deduction.

In conclusion, we have deleveloped an immunofluorescence-based approach to study mTOR localisation and protein complex interaction in human skeletal muscle. Utilizins this technique, the data presented herein demonstrates interesting relationships between mTOR and its associating proteins in basal human skeletal muscle. This methodological approach will be used in subsequent chapters to assess temporal mTOR signalling in response to acute and chronic anabolic stimuli.

3.11 Acknowledgement

I appreciate for the help and suggestion from Dr Helen Bradley and Dr Oliver Wilson on developing the immunofluorescences staining methods and quantification technology. Dr Matthew Cocks give valuable advice on the UEA-I staining method.

3.12 Reference

[1] Coons, Albert H., Hugh J. Creech, R. Norman Jones, and Ernst Berliner. The demonstration of pneumococcal antigen in tissues by the use of fluorescent antibody. J. Immunol 45, no. 3 (1942): 159-70.

[2] Burry, Richard W. Controls for Immunocytochemistry An Update. Journal of Histochemistry & Cytochemistry 59, no. 1 (2011): 6-12.

[3] Bancroft, John D., and Marilyn Gamble, eds. Theory and practice of histological techniques. Elsevier Health Sciences, 2008.

[4] Larsson, Lars-Inge. Immunocytochemistry: theory and practice. CRC press, 1988.

[5] Schur, Peter H. IgG subclasses--a review. Annals of allergy 58, no. 2 (1987): 89-96.

[6] Roux, Kenneth H., Lioudmila Strelets, and Terje E. Michaelsen. Flexibility of human IgG subclasses. The Journal of Immunology 159, no. 7 (1997): 3372-3382.

[7] Putnam, Frank W., Koiti Titani, Maurice Wikler, and Tomotaka Shinoda. Structure and evolution of kappa and lambda light chains. In Cold Spring Harbor Symposia on Quantitative Biology, vol. 32, pp. 9-29. Cold Spring Harbor Laboratory Press, 1967.

[8] Bradley, Helen Elizabeth. Glucose transporter 4 and localisation in skeletal muscle: the effect of glucose and insulin administration, acute exercise and exercise training. PhD diss., University of Birmingham, 2014.

[9] Van der Loos, C. M. User Protocol: Practical Guide to Multiple Staining. (2008).

[10] Wilson, Oliver. Visualisation of focal adhesion-associated proteins in the skeletal muscle of young and elderly individuals: effect of exercise training. PhD diss., University of Birmingham, 2014.

[11] Kim DH, Sarbassov DD, Ali SM, Latek RR, Guntur KV, et al. 2003. GbetaL, a positive regulator of the rapamycin-sensitive pathway required for the nutrient-sensitive interaction between raptor and mTOR. Mol. Cell 11:895–904

[12] Wang, Wei, Satish Singh, David L. Zeng, Kevin King, and Sandeep Nema. Antibody structure, instability, and formulation. Journal of pharmaceutical sciences 96, no. 1 (2007): 1-26.

[13] Edelman, Gerald M. Antibody structure and molecular immunology. Science 180, no. 88 (1973): 830-840.

[14] Jacobs, Brittany L., Craig A. Goodman, and Troy A. Hornberger. The mechanical activation of mTOR signaling: an emerging role for late endosome/lysosomal targeting. Journal of muscle research and cell motility 35, no. 1 (2014): 11-21.

[15] Sancak, Yasemin, Liron Bar-Peled, Roberto Zoncu, Andrew L. Markhard, Shigeyuki Nada, and David M. Sabatini. Ragulator-Rag complex targets mTORC1 to the lysosomal surface and is necessary for its activation by amino acids. Cell 141, no. 2 (2010): 290-303.

[16] Holz, Marina K., Bryan A. Ballif, Steven P. Gygi, and John Blenis. mTOR and S6K1 mediate assembly of the translation preinitiation complex through dynamic protein interchange and ordered phosphorylation events. Cell 123, no. 4 (2005): 569-580.

[17] Harris, Thurl E., An Chi, Jeffrey Shabanowitz, Donald F. Hunt, Robert E. Rhoads, and John C. Lawrence. mTOR‐dependent stimulation of the association of eIF4G and eIF3 by insulin. The EMBO journal 25, no. 8 (2006): 1659-1668.

[18] Parkington, Jascha D., Adam P. Siebert, Nathan K. LeBrasseur, and Roger A. Fielding. Differential activation of mTOR signaling by contractile activity in skeletal muscle. American Journal of Physiology-Regulatory, Integrative and Comparative Physiology 285, no. 5 (2003): R1086-R1090.

[19] Sancak, Yasemin, Timothy R. Peterson, Yoav D. Shaul, Robert A. Lindquist, Carson C. Thoreen, Liron Bar-Peled, and David M. Sabatini. The Rag GTPases bind raptor and mediate amino acid signaling to mTORC1. Science 320, no. 5882 (2008): 1496-1501.

[20] Korolchuk, Viktor I., Shinji Saiki, Maike Lichtenberg, Farah H. Siddiqi, Esteban A. Roberts, Sara Imarisio, Luca Jahreiss et al. Lysosomal positioning coordinates cellular nutrient responses. Nature cell biology 13, no. 4 (2011): 453-460.

[21] Long, Xiaomeng, Yenshou Lin, Sara Ortiz-Vega, Kazuyoshi Yonezawa, and Joseph Avruch. Rheb binds and regulates the mTOR kinase. Current Biology 15, no. 8 (2005): 702-713.

Chapter 4

Fiber- specific determination of mTOR protein content in skeletal muscle of trained individuals following 10- weeks resistance training

---

4.1 Abstract

Muscle protein synthesis is stimulated by resistance exercise, accompanied by an increase in skeletal muscle mass. This study was designed to examine the effects of 10 weeks resistance exercise training on mTOR protein content in different muscle fibers in trained human skeletal muscle. 7 healthy male strength- trained participants were recruited to take a 10-week long resistance training study. Muscle biopsies were taken pre- and post- training and immunofluorescence histological staining applied to observe and quantify mTOR protein content. In addition, muscle cross sectional area (CSA) and muscle strength were measured to determine muscle hypertrophy.

Compared with basal status, total fibre mTOR content, CSA and lean muscle mass did not increases following the resistance training. In consistence, muscle mass was not increase following training, suggesting no muscle hypertrophy found. We then examined mTOR protein content in specific muscle fiber types. No significant mTOR protein content increase were found post training in either type I or type IIx fibres. Despite no change in mTOR protein content, we did observe an increase of the proportion of type IIa fibres from 50% to 62% following resistance training ($p=0.002$), whist proportion of type I fibres was reduced from 41% to 33% post training ($p=0.02$). In parallel, strength as assessed following 1RM was also observed to increase from 764.43±78.92 newtons to 937.29±91.16 newtons (Mean ± SEM, $P<0.05$) post training.

Based on these findings, it would appear that increases in total or fibre-type specific mTOR content are not a prerequisite for improvements in strength or fibre-type alterations following a 10-week long resistance training in trained group. However, due to the lack of noticeable differences in skeletal muscle CSA or mass following the training period, the relationship between fibre-specific gains in mass and mTOR protein content are currently unclear.

4.2 Introduction

It is documented that high intensity resistance training results in muscle adaption and muscle hypertrophy in human skeletal muscle [1, 2, 3, 4, 35]. Ingestion of PRO/EAA in combination of resistance training is shown to further augment gains in muscle size [5]. Many factors, however, mediate the hypertrophic response to training such as age, gender, training modes, nutrition and genetic background [6]. Mechanistically, muscle hypertrophy originates from the addition of new sarcomeres in parallel force- producing arrangement, which requires the synthesis of new myofibrillar proteins [6, 10]. And resistance exercise training is usually manifested histologically by increased size of Type II fibers [55].

At the molecular level, training stimulates a series of myogenic events leading to increases in muscle fiber size reflected by increase in cross- sectional area (CSA) [11, 12]. The mTOR signalling pathway is thought to be one of the key mechanisms regulating muscle protein synthesis in exercise- induced muscle hypertrophy [6, 13]. mTOR is mechanically activated by PI3K-Akt dependent- or independent- pathways in mammalian cells [13, 14]. Substrates of mTOR (*e.g.* S6K1, 4E-BP1) are subsequently phosphorylated to initiate protein translation events [15]. Following a 8- week resistance training leading to muscle hypertrophy in untrained individuals, the expression of phosphorylated mTOR ^{Ser2448} was found to be significantly increased via immunoblotting, which was maintained at least 8 weeks after the training [16]. However, no studies to date have examined the relationship between mTOR and muscle CSA, or examined the potential change in mTOR content post training in human skeletal muscle.

Muscle fibers are categored as type I fiber, type IIa fiber and type IIx fiber based on the myosin heavy chain protein (MHC) difference, with limited intermediate subtypes found as type I/IIa, type IIax in human skeletal muscle [18- 22]. MHC Type I fiber is a slow- twitch fiber characterized by slow contractile rate [21, 22], while type IIa and type IIx fibers are fast- twitch fibers [17, 22]. Compared with type I fibers, type II fibers experiences muscle fatigue more easily because of quick depletion of ATPs generated from glycolysis [18- 22]. Constitution of three muscle fiber types varies depending on skeletal muscle subgroups [17, 21]. For example, type I fibers are predominently found in the soleus, while

triceps muscle is mainly composed of type IIa fibers [36]. Vastus lateralis muscle is a mixture of both type I and type II fibers in human [36].

Skeletal muscle is characterized by plasticity with muscle fibers types in adaptation to exercise training [23, 25]. Over-representation of Type I fibers were found in individuals following long-term endurance training [23]. Currently no literature concerns skeletal muscle fiber composition in trained individuals in response to resistance training. Effects of resistance training on skeletal muscle remodeling in untrained individuals were not consistent. Whilst some studies found no increase or decrease in type IIa fibers proportion [43, 44], significant increase of type IIa fibers percentage was reported in other human studies [45, 46, 47, 53].

Based on these reports, the aim of the study was to investigate the effects of resistance exercise training on mTOR protein content in healthy young people. Based on the microscopy technique and image quantification method developed in chapter 3, mTOR fluorescence signals will be analysed in total muscle fibers and in a muscle fiber type manner. We hypothesised that resistance training would enhance mTOR content in type II fibers post training in parallel to an increase in fibre CSA and strength post-training. In addition, it was hypothesised that muscle fibers adaptation (shifting towards a glycolytic phenotype) would occur following resistance training.

4.3 Methods

4.3.1 Ethical approval

Ethical approval for this study was granted from the west midlands NHS ethics committee (NHS REC Solihul West Midlands, 14/WM/0088).

4.3.2 Experiment design

Young healthy male participants who had experienced at least 3 months leg-based resistance exercise (n=7, age=23±2y, BMI = 25.2±1.7 kg/m^2; means ± SD) were recruited to attend a 10-week resistance training programme, two sessions per week including leg press, knee extension, hamstring curl and calf extension. For each session, 4 sets were performed until volitional fatigue, with either 1 min or 4 min rest between sets. Individuals were given a serving of 25g whey protein supplement (Optimum Nutrition 100% Whey Gold Standard) following the training.

Muscle biopsies were taken from the *vastus lateralis* at pre- training and post- training, respectively. Muscle biopsies were collected, frozen and prepared for staining following the procedures mentioned in Chapter 2. Briefly, samples were blotted to remove excess blood and dissected free of fat and collagen were then embedded in Tissue-Tek OCT compound (Sakura, 4583) and frozen in liquid nitrogen cooled isopentane solution (Sigma Aldrich, 270342). After immediate freeznig, samples were stored at -80^{o}C until experimental analysis was performed. Muscle samples from pre- and post-training were sectioned under -20^{o}C and collected on the same loading slide for immunofluorescence histological staining.

4.3.3 Muscle strength and muscle hypertrophy measurement

Exercise performance was measured by maximal muscle strength/ 1RM pre- and post- training. Muscle strength/ 1RM followed protocols as below: (1) a warm-up period, easy 10 reps minimum with 1 minute rest; (2) load that will allow 4-5 reps maximum by adding around 15 kg with 2 minute rest; (3) heavier load that will allow 3-4 reps maximum with 2 minute rest; (4) near maximal load that

will allow 2-3 reps maximum with 2 minute rest; (5) weight further increase that allow 1 rep maximum. If successful, new load performed after 3 minute rest until load failure. If unsuccessful, decreased load performed after 3 minute rest until success.

A Kin-Com dynamometer (Shelton Technical Ltd., Milton Keynes, UK) was used to determine maximal voluntary contraction (MVC) of the knee extensors in the dominant leg. The testing protocol was described as below: Participants sat on the dynamometer with their hips and torso securely strapped down to prevent any hip-extension or upper-body movements during contraction. And the fulcrum of the dynamometer lever arm was aligned with the lateral condyle of the participant's knee. Force measurement was taken at a knee angle of 75º as the isometric torque reached peak value in the knee extensors of isometric contraction reported in previous study [56]. Each individual performed one familiarization effort, and completed at least 3 trials divided by 2min. The maximum force generated was taken and used in statistical analysis. Verbal encouragement was given to participants during strength testing.

DEXA scanning was used to automatically measure muscle lean mass (LM) from both legs, as well as lean body mass (LBM) and fat mass (FM) pre- and post- resistance training.

4.3.4 CSA measurement

Immunofluorescence staining method was used to determine CSA (see 4.3.6). Sarcoplasm membrane area was outlined by WGA conjugated with Alexa@350 and imaged by Image- pro software (see 4.3.7). Averaged CSA was calculated between pre- and post- training for statistic analysis (see 4.3.8).

4.3.5 Antibodies and other reagents

All primary and secondary antibodies applied in this study were validated following the procedures developed in Chapter 3. WGA conjugated with Alexa@350 is used as the biomarker indicating cell membrane and mTOR antibody was applied for mTOR staining and costaining with antibodies binding to myosin heavy chain I and IIx, respectively.

4.3.6 Immunofluorescence Staining

The method for multiple antibodies co-staining is described in Chapter 2. For each study, muscle sections from both pre- training and post- training were stained in one trial to standardize staining conditions and minimize variability.

4.3.7 Image Capturing

Images achieved in one trial were taken under the same image capture settings through all the muscle sections (see chapter 2). Specifically, 5- 7 images per section were captured for quantification analysis. Image quantification was performed under the same measurement settings using Image-Pro software.

4.3.8 Statistic analysis

The mean value of two repeats for each time point was calculated, and values of two time points (pre - training and post- training) achieved from each person. SPSS software was used to analyse group data. Paired student T- test was used to compare total mTOR content and CSA between pre- training and post- training, and one- way ANOVA was used to study mTOR content, CSA and cell number in specific muscle fibers. Data was reported as Mean± SEM. Significance was set as $P<0.05$.

4.4 Results

4.4.1 Total mTOR protein content was not altered in trained individuals following 10 weeks resistance training

As seen in Figure 4.4.1 A, mTOR stains (red) were visualized dispersed both on plasma membrane and the cytoplasm in both pre training and post training samples. Total mTOR fluorescence in muscle fibres was measured (Figure. 4.1 B) and quantification result showed that mTOR content was increased by 3% following resistance training compared with that at basal level (15.86±0.83 for post training *vs.* 15.41±0.63 for pre training, P= 0.45). In addition, as shown in Figure 4.4.1 C CSA was not different between pre-training and post-training muscle samples (6566±439 μm^2 for post training *vs.* 6642±299 μm^2 for pre training, P=0.86).

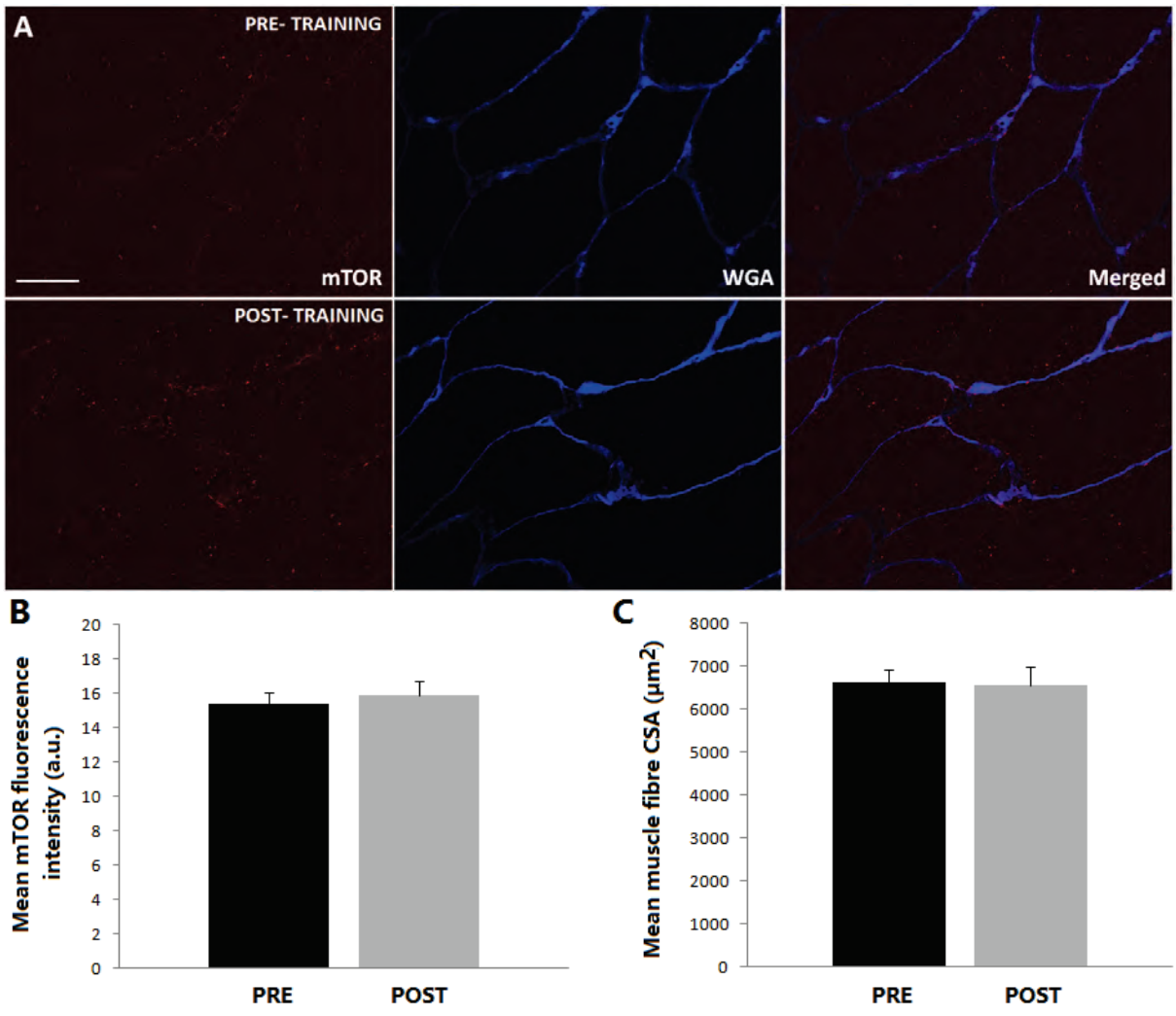

Figure 4.4.1 Total mTOR protein was not increased following 10- week resistance training. (A) Widefield images of mTOR stained with Alexa @594 fluophore and WGA conjugated with Alexa @350 fluophore. (B) mTOR fluorescence and muscle CSA (C) were both measured to quantify mTOR content and muscle hypertrophy in pre- training and post- training human skeletal muscle samples. Data presented as mean± SEM (n=7).

4.4.2 mTOR protein content in type I fibers was not significantly increased in trained invididuals following 10 weeks resistance training

To observe mTOR protein content and distribution in type I muscle fibers, mTOR antibody was co-stained with myosin heavy chain I antibody, and WGA was used to outline the cell membrane (Figure.4.4.2 A). There was no significant difference observed in muscle fiber dependent mTOR content between type I fibers and other muscle types at basal level (15.46±0.45 for type I fiber *vs.* 15.28±0.51 for rest muscle fibers, p=0.82). mTOR fluorescence in type I muscle fibers increased by 4% after resistance training (16.09±0.62 for post training *vs.* 15.46±0.45 for pre taining, P=0.43). When testing mTOR content in other muscle fibers, no increase was found following the training (15.76±0.58 for post training *vs.* 15.28±0.51 for pre training, P=0.54). Measurement of CSA in type I fibers showed that there was 12% increase after training, though the increase was not significant compared with pre training status (7298±390 μm^2 for post training *vs.* 6537±393 μm^2 for pre training, P=0.16). Also, no significant change in CSA was shown in all other muscle fibers (6336±413 μm^2 for post training *vs.* 6557±291 μm^2 for pre training, P=0.68).

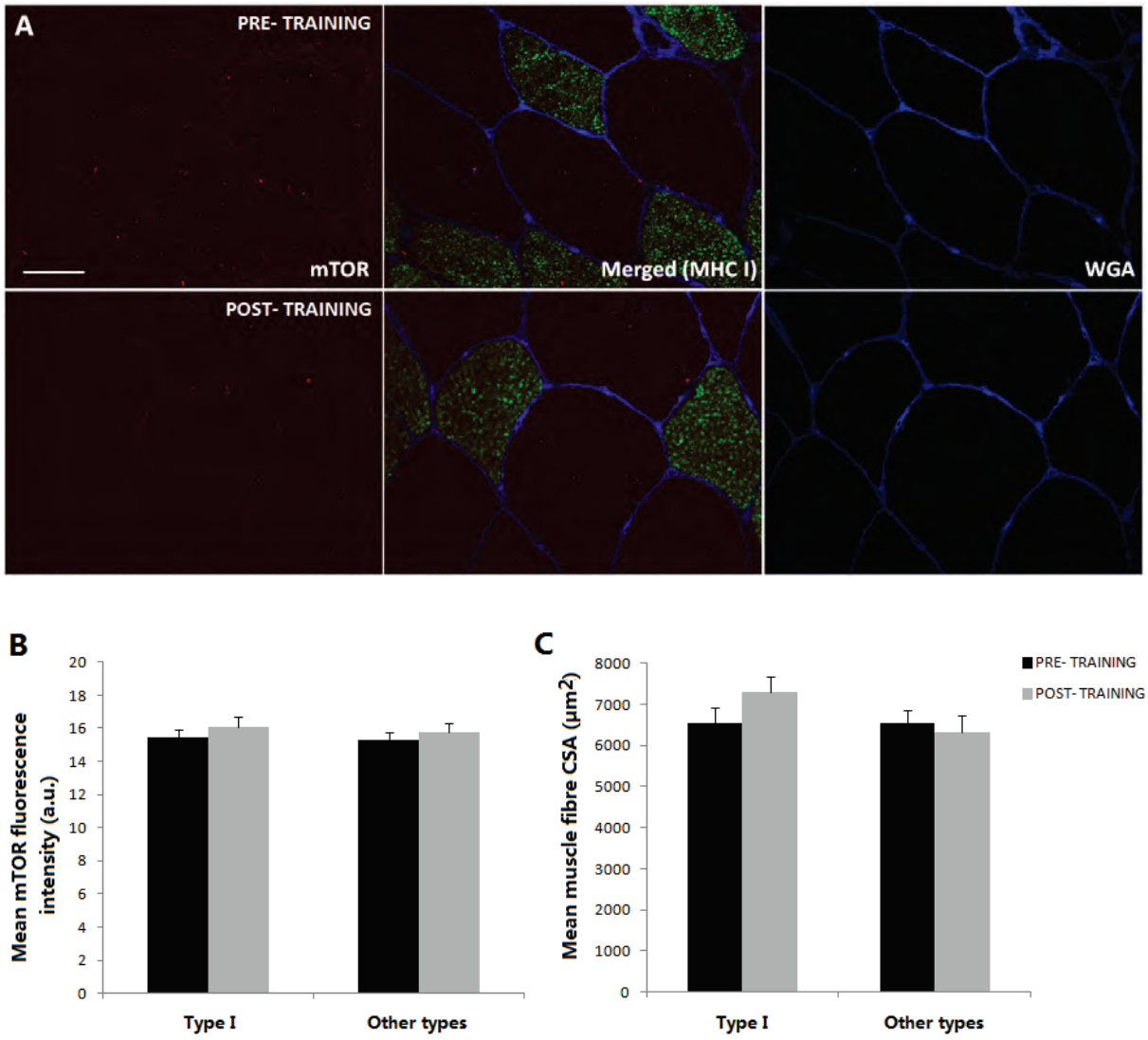

Figure 4.4.2 mTOR protein content in type I muscle fibers was not significantly increased following 10- week resistance training. (A) Widefield images of mTOR stained with Alexa $^{@}$594 fluophore, myosin heavy chain I combined with Alexa $^{@}$488 fluophore and WGA conjugated with Alexa $^{@}$350 fluophore. (B) mTOR fluorescence and muscle CSA (C) were measured to quantify mTOR content and muscle hypertrophy in type I muscle fibers in both pre- training and post- training human skeletal muscle samples. Data presented as mean± SEM (n=7).

4.4.3 mTOR protein content in type IIx fibers was not significantly increased after 10 weeks resistance training in trained indivduals

As shown in Figure.4.4.3 B, there was no significant increase in mTOR content in type IIx fibers following resistance training (13.08±0.34 for post training *vs.* 13.38±0.35 for pre training, P=0.54). mTOR content in resting muscle fibers was also not increased post training (12.34±0.28 for post training *vs.* 12.56±0.30 for pre training, P=0.61). When it came to CSA (Figure.4.4.3 C), there was a ~7% increase of CSA in type IIx fibers post training (6567±367 μm^2 for post training *vs.* 5919±286 μm^2 for pre training, P=0.21), but there was no increase of CSA in other muscle fibers following training (6051±312 μm^2 for post training *vs.* 6165±349 μm^2 for pre training, P=0.81).

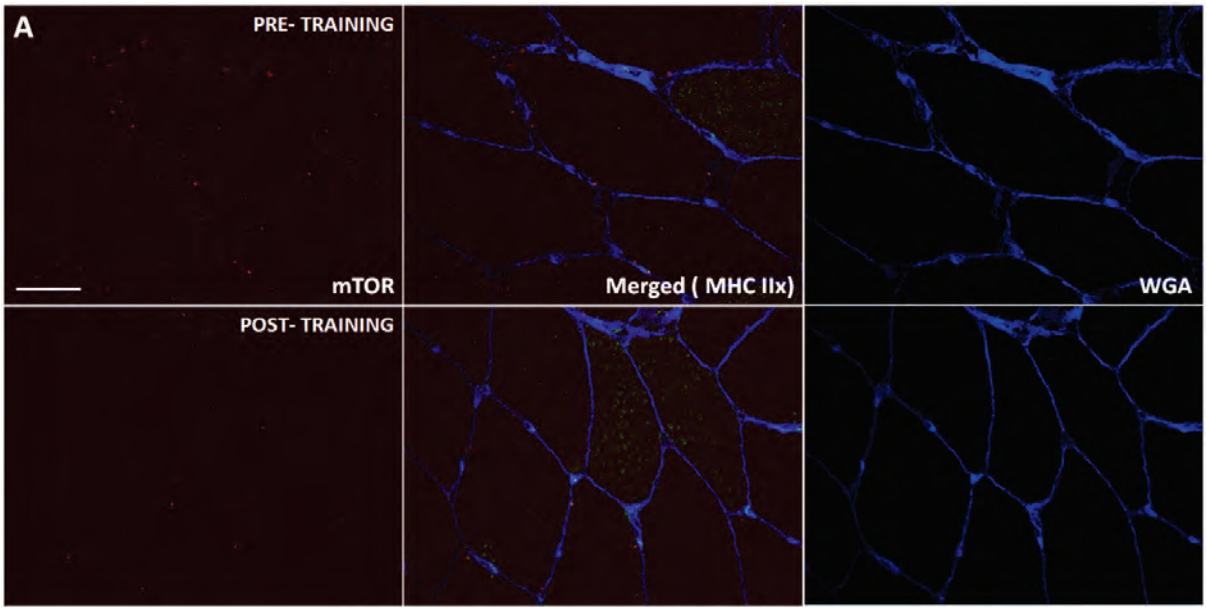

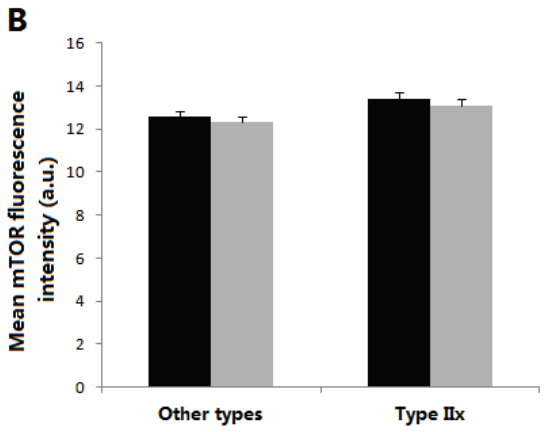

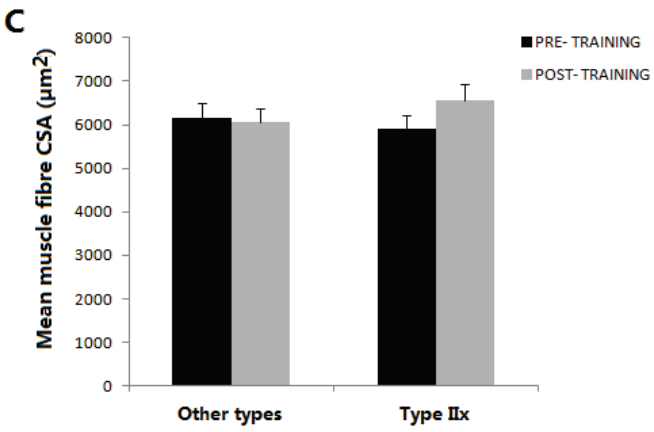

Figure 4.4.3 mTOR protein content in type IIx muscle fibers was increased following 10- week resistance training. (A) Widefield images of mTOR stained with Alexa @594 fluophore, myosin heavy chain IIx combined with Alexa @488 fluophore and WGA conjugated with Alexa @350 fluophore. (B) mTOR fluorescence and muscle CSA (C) were measured to quantify mTOR and muscle hypertrophy in type IIx muscle fibers in both pre- training and post- training human skeletal muscle samples. Data presented as mean± SEM (n=7).

4.4.4 Type IIa muscle fibers proportion is increased in trained individuals following 10 weeks resistance exercise training

Taking advantage of immunofluorescence histology technique, we also investigated MHC composition in both pre- training and post- training human skeletal muscle samples. We identified that the proportion of myosin heavy chain type IIa muscle fibers was increased from 50% pre-training to 62% post- training (P=0.002), meanwhile the proportion of type I muscle fibers decreased from 41% to 33% after training (P=0.02). The proportion of other muscle fiber types dropped from 9% to 5%, which was not significantly different.

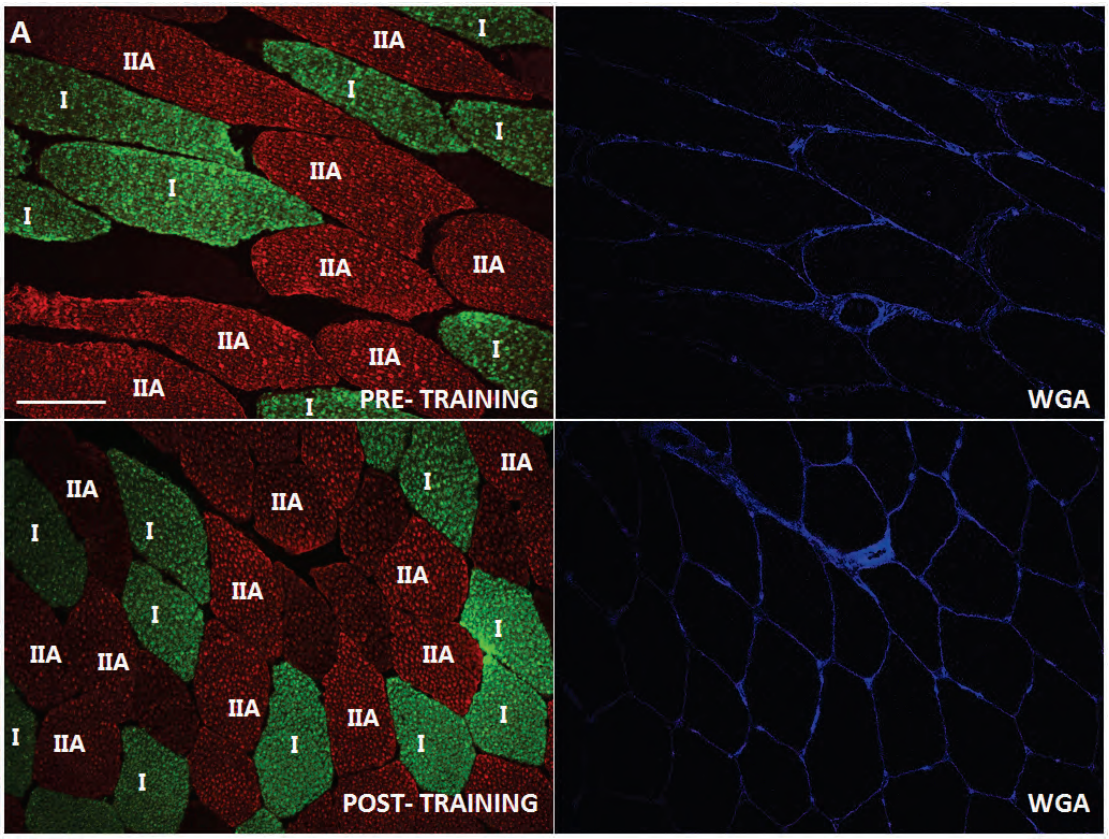

B Composition of muscle fiber types under per- training and post- training status in human skeletal muscle

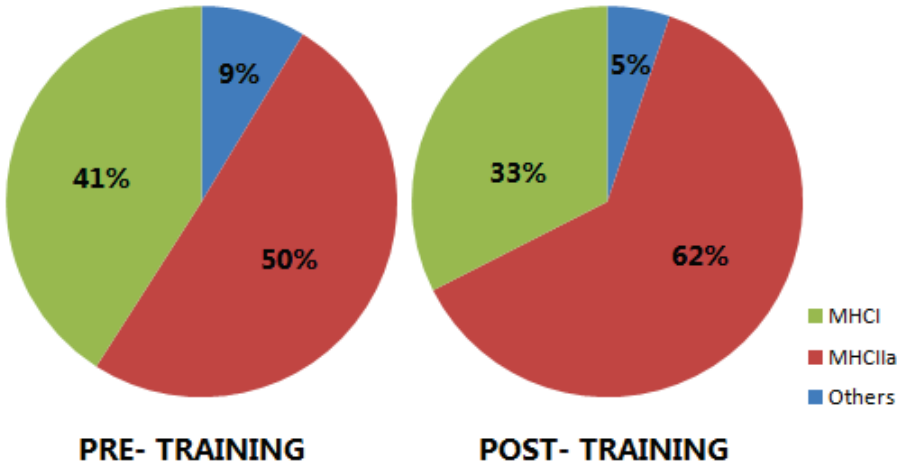

Table. Cell number accounted in different muscle fiber types

	PRE- TRAINING	POST- TRAINING	P VALUE
MHC I	511	433	0.02 *
MHC IIA	629	831	0.002 *
Others	108	69	0.11
TOTAL	1248	1333	0.33

Figure 4.4.4 Proportion of type IIa muscle fibers is increased following 10- week resistance training. (A) Widefield images of type I fibers stained with Alexa @488 fluophore, type IIa fiber stained with Alexa @594 fluophore and cell membrane marked by WGA conjugated with Alexa @350 fluophore. (B) Numbers of type I fibers and type IIa fibers were quantified to calculate the proportion of two muscle fibers accounting for the whole muscle fibers under both pre- training and post- training in human skeletal muscle. Proportion calculation was shown in Pie figure and cell number counted is listed in table below. Data presented as mean± SEM (n=7). *Significant difference to PRE- TRAINING (P<0.05).

4.4.5 No significant increases of muscle mass in trained individuals following 10- week resistance training

As shown in Table 4.1, muscle mass of participants were analysed by DXEA scanning. Results showed that there was no significant increase of muscle mass in both legs of participants, as well as no changes on fat mass post training. However, muscle strength was increased after training exhibited by Kin- com study (from 764.43±78.92 N pre- training to 937.29±91.16 N post- training, P = 0.04) and 1RM testing (from 1666±75.58 lbs pre- training to 2157±77.19 lbs post- training, P = 0.0002), respectively.

	PRE- TRAINING	POST- TRAINING
LBM (g)	61914±1843	62736±2326
FM (g)	17307±1608	16601±1666
L Leg LM (g)	10076±381	10320±479
R Leg LM (g)	10109±442	10353±468
L Leg FM (g)	3193±295	3007±286
R Leg FM (g)	3161±299	3154±330
%BF (Total)	21±1.7	20±1.7

Data is shown as Mean±SEM.

Table 4.1 DEXA scanning data showed no increase of muscle mass following 10 weeks resistacne training in trained individuals. LBM= lean body mass; FM= fat mass; LM= lean mass; BF= body fat

4.5 Discussion

There is a well-documented increase in mTOR activation in response to acute resistance exercise [13, 14, 15]. Leger *et al* reported that mTOR ^{ser2448} phosphorylation was increased following 8- weeks resistance training in untrained individuals [16]. However, little is known regarding fiber specific changes in mTOR content in response to resistance training. Six weeks cycle training increased phosphoryalted mTOR content in a fiber type II specific manner in sedentary individuals [54]. In this study, we measured mTOR protein content using an immunofluorescence histology methodology. Taking this approach, we report no changes in mTOR protein content following a 10- week resistance training, along with unaltered CSA or increases in lean muscle mass in trained individuals.

The lack of improvements in CSA and muscle mass were unexpected and the precise explanation unclear at this time. Age and exercise training mode may influence the muscle hypertrophy post training. For example, participants in study carried by Leger *et al* [16] or Stuart *et al* [54] are generally 10 years older than volunteers we recruited. The other difference between two studies is the training background of volunteers. Subjects participating in our study had recreationally training experience before taking the training, while volunteers in studies reporting mTOR content increase either had not taken resistance training for more than 12 months before the study [16] or sedentary individuals [54]. As such, the basal level of mTOR content and skeletal muscle CSA of participants in our study may be higher than theirs compromising effects of adaptive response to resistance training., Also, sample numbers in this study were much smaller than those in the study by Leger *et al* [16].

Muscle protein synthesis rates are different between muscle fibers in rodent, possibly due to different muscle fiber- type composition [37]. Basal protein synthesis rates were correlated with the content of slow- twitch type II fibers in rat muscle [38]. In addition, rodent studies revealed that protein synthesis in slow- and fast- twitch muscle fibers exhibited different sensitivity to anabolic stimuli (*e.g.* exercise and feeding) [31, 39, 40], and mTOR activation was detected predominantly in fibers expressing type IIa but not type I in response to contractile activity in Rat hindlimb muscle [41]. Compared with animal studies, little information is available regarding the effect of resistance training on muscle protein synthesis in different fiber types in human. Protein synthesis rates was not determined by fiber- type

composition in response to feeding in human skeletal muscle [37] , which might be because genes encoding transcriptional regulators are not expressed in fiber type specific manner [36]. In agreement with this, our data suggest that mTOR protein content does not alter between fibres of differing MHC content and so by extension does not seem to influence difference in fibre-specific contractile or metabolic properties.

Though we did not find significant muscle hypertrophy as assessed by CSA or muscle mass gains, a clear training effect was observed through an increase in peak force of strength/ 1RM following training. This may indicate that anatomical CSA *per se* might not reflect changes in the physiological CSA or maximal contractile force [51], since a simultaneous change in muscle fibre pennation angle could also occur [51], which also might influence sectioning angle leading to inaccurate CSA quantified. Moreover, our immunofluorescence data showed that proportion of type IIa fibers was significantly increased following training contributing to increased concentric force. Simultaneously, a reduction of type I fibers was reported, suggesting remodeling of muscle fiber composition in response to resistance training. A consensus as to the effects of resistance training on skeletal muscle remodeling in trained people is not currently apparent. In untrained people, Aagard *et al* reported there was a decrease in type II fibre content following resistance training [51], which might be because the study did not analyze type IIa and type IIx fibers, respectively. As in many reports proportion of type IIx fibers was reported to decrease following training [32, 43, 45, 47, 53], mixture analysis of two fast-twitch myofiber subtypes would compromise the significant increase of type IIa fibers. However, some other studies reported a decrease in type IIa fibers following training [43, 44]. In our study, in agreement with other reports [32, 45, 46, 47, 53], we observed a significant increase in type IIa fibers following resistance training, with a slight reduction in type IIx fibers.

The molecular mechanisms regulating skeletal muscle phenotypic remodeling are still not fully understood. Motor neurons are thought to exert influence on muscle fibers they innervate, as cross-connection of neurones in slow- twitch fibers with fast- twitch fibers reduce the contraction speed, whist linkage of neurones in fast- twitch fibers with slow- twitch fibers increase the contractile speed [49]. Neuronal transduction is believed to influence myofiber gene expression relying calcium as

second messenger. Input signals from motor neurons are received by voltage- operated calcium channel in the T- tubeles, which interacts with skeletal muscle specific sarcoplasmic reticulum calcium- release channel [48, 52]. The latter one releases calcium from sarcoplasmic reticulum in response to stimulation, determining contractile pattern, regulating signaling pathways and mediating expression of a myriad of genes involving in skeletal muscle remodelling [48]. It will be interesting to see whether future investigation can determine the precise control of fibre-type regulation following resistance exercise in human skeletal muscle, and determine the contribution of mTOR to this process.

In conclusion, this study reports a novel immunofluorescence approach to study mTOR content in different muscle fiber types in response to a physiological stimulus. Our first hypothesis was that mTOR content would be enhanced following resistance training in type II fibers post training along with an increase in fibre CSA and strength post-training. Whilst resistance training lead to an increase in type IIA fibres and a paralleled increase in skeletal muscle strength, we did not observe increases in total or fibre-specific protein content of mTOR post-training. As such, it might be that the temporal changes in mTOR activity/signaling following each training bout, as opposed to chronic changes in mTOR content/localization are the key determining factors relating to adaptation to resistance training. Coupling our immunofluorescence approach with measurements of long-term protein synthesis (i.e. D2O incorporation) may help to link acute signaling to chronic adaptation in human skeletal muscle. These findings lead us to further discuss the temporal changes of mTOR signaling in response to one bout of resistance exercise in the next chapter.

4.6 Acknowledgements

I would like to thank Dr. Leigh Breen, Baubak Shamim and Daniel Craig for their help during this study and for useful discussion relating to the results presented herein. In addition, I would like to thank Dr. Helen Bradley for her suggestion on the quantification methodology.

4.7 Reference

[1] Hortobagyi, Tibor, Jeff P. Hill, Joseph A. Houmard, David D. Fraser, Nancy J. Lambert, and Richard G. Israel. Adaptive responses to muscle lengthening and shortening in humans. Journal of Applied Physiology 80, no. 3 (1996): 765-772.

[2] McCall, G. E., W. C. Byrnes, A. Dickinson, P. M. Pattany, and S. J. Fleck. Muscle fiber hypertrophy, hyperplasia, and capillary density in college men after resistance training. Journal of applied physiology 81, no. 5 (1996): 2004-2012.

[3] Gonyea, WJ. Adaptations in the elbow flexors of elderly males after heavy-resistance training. (1993).

[4] Staron, R. S., D. L. Karapondo, W. J. Kraemer, A. C. Fry, S. E. Gordon, J. E. Falkel, F. C. Hagerman, and R. S. Hikida. Skeletal muscle adaptations during early phase of heavy-resistance training in men and women. Journal of Applied Physiology 76 (1994): 1247-1247.

[5] Hulmi, Juha J., Christopher M. Lockwood, and Jeffrey R. Stout. Review Effect of protein/essential amino acid and resistance training on skeletal muscle hypertrophy: A case for whey protein. (2010).

[6] Schoenfeld, Brad J. The mechanisms of muscle hypertrophy and their application to resistance training. The Journal of Strength & Conditioning Research 24, no. 10 (2010): 2857-2872.

[7] Welle, Stephen, Saara Totterman, and Charles Thornton. Effect of age on muscle hypertrophy induced by resistance training. The Journals of Gerontology Series A: Biological Sciences and Medical Sciences 51, no. 6 (1996): M270-M275.

[8] Mulligan, Susan E., Steven J. Fleck, Scott E. Gordon, L. Perry Koziris, N. Travis Triplett-McBride, and William J. Kraemer. Influence of resistance exercise volume on serum growth hormone and cortisol concentrations in women. The Journal of Strength & Conditioning Research 10, no. 4 (1996): 256-262

[9] Tesch, PA. Skeletal muscle adaptations consequent to long-term heavy resistance exercise. Medicine and Science in Sports and Exercise 20, no. 5 Suppl (1988): S132-4.

[10] Phillips, Stuart M., K. D. Tipton, Arny A. Ferrando, and Robert R. Wolfe. Resistance training reduces the acute exercise-induced increase in muscle protein turnover. American Journal of Physiology-Endocrinology And Metabolism 276, no. 1 (1999): E118-E124.

[11] Paul, Angelika C., and Nadia Rosenthal. Different modes of hypertrophy in skeletal muscle fibers. The Journal of cell biology 156, no. 4 (2002): 751-760.

[12] Tesch, Per A., and Lars Larsson. Muscle hypertrophy in bodybuilders. European journal of applied physiology and occupational physiology 49, no. 3 (1982): 301-306.

[13] Bodine, Sue C., Trevor N. Stitt, Michael Gonzalez, William O. Kline, Gretchen L. Stover, Roy Bauerlein, Elizabeth Zlotchenko et al. Akt/mTOR pathway is a crucial regulator of skeletal muscle hypertrophy and can prevent muscle atrophy in vivo. Nature Cell Biology 3, no. 11 (2001): 1014-1019.

[14] Frost, Robert A., and Charles H. Lang. Protein kinase B/Akt: a nexus of growth factor and cytokine signaling in determining muscle mass. Journal of Applied Physiology 103, no. 1 (2007): 378-387.

[15] Fingar, Diane C., Sofie Salama, Christina Tsou, E. D. Harlow, and John Blenis. Mammalian cell size is controlled by mTOR and its downstream targets S6K1 and 4EBP1/eIF4E. Genes & development 16, no. 12 (2002): 1472-1487.

[16] Léger, Bertrand, Romain Cartoni, Manu Praz, Séverine Lamon, Olivier Dériaz, Antoinette Crettenand, Charles Gobelet et al. Akt signalling through GSK-3β, mTOR and Foxo1 is involved in human skeletal muscle hypertrophy and atrophy. The Journal of Physiology 576, no. 3 (2006): 923-933.

[17] Bloemberg, Darin, and Joe Quadrilatero. Rapid determination of myosin heavy chain expression in rat, mouse, and human skeletal muscle using multicolor immunofluorescence analysis. PLoS One 7, no. 4 (2012): e35273.

[18] Spangenburg, E. E., and F. W. Booth. Molecular regulation of individual skeletal muscle fibre types. Acta Physiologica Scandinavica 178, no. 4 (2003): 413-424.

[19] Schiaffino, Stefano and Carlo Reggiani. Myosin isoforms in mammalian skeletal muscle. Journal of Applied Physiology 77, no. 2 (1994): 493-501.

[20] Smerdu, V. I. K. A., I. L. E. N. E. Karsch-Mizrachi, M. A. R. I. N. A. Campione, L. E. S. L. I. E. Leinwand, and Stefano Schiaffino. Type IIx myosin heavy chain transcripts are expressed in type IIb fibers of human skeletal muscle. Am. J. Physiol 267 (1994): C1723-C1728.

[21] Schiaffino, S. Fibre types in skeletal muscle: a personal account. Acta Physiologica 199, no. 4 (2010): 451-463.

[22] Scott, Wayne, Jennifer Stevens, and Stuart A. Binder–Macleod. Human skeletal muscle fiber type classifications. Physical Therapy 81, no. 11 (2001): 1810-1816.

[23] Zierath, Juleen R., and John A. Hawley. Skeletal muscle fiber type: influence on contractile and metabolic properties. PLoS Biology 2, no. 10 (2004): e348.

[24] Tesch, P. A., and J. Karlsson. Muscle fiber types and size in trained and untrained muscles of elite athletes. Journal of applied physiology 59, no. 6 (1985): 1716-20.

[25] Holloszy, John O., and Edward F. Coyle. Adaptations of skeletal muscle to endurance exercise and their metabolic consequences. Journal of applied physiology 56, no. 4 (1984): 831-838.

[26] Costill, D. L., E. F. Coyle, W. F. Fink, G. R. Lesmes, and F. A. Witzmann. Adaptations in skeletal muscle following strength training. J Appl Physiol 46, no. 1 (1979): 96-9.

[27] Alderton, P., J. Babraj, K. Smith, J. Singh, M. Rennie, and H. Wakerhage. Selective activation of AMPK-PGC-1 or PKB-TSC2-mTOR signaling can explain specific adaptive responses to endurance or resistance training-like electrical muscle stimulation. The FASEB Journal 19 (2005): 786-788.

[28] Winder, W. W. Energy-sensing and signaling by AMP-activated protein kinase in skeletal muscle. Journal of Applied Physiology 91, no. 3 (2001): 1017-1028.

[29] Dreyer, Hans C., Satoshi Fujita, Jerson G. Cadenas, David L. Chinkes, Elena Volpi, and Blake B. Rasmussen. Resistance exercise increases AMPK activity and reduces 4E-BP1 phosphorylation and protein synthesis in human skeletal muscle. The Journal of Physiology 576, no. 2 (2006): 613-624.

[30] Wang, Xuemin, and Christopher G. Proud. The mTOR pathway in the control of protein synthesis. Physiology 21, no. 5 (2006): 362-369.

[31] Goodman, Craig A., Jack A. Kotecki, Brittany L. Jacobs, and Troy A. Hornberger. Muscle fiber type-dependent differences in the regulation of protein synthesis. PLoS One 7, no. 5 (2012): e37890.

[32] Adams, GREGORY R., BRUCE M. Hather, KENNETH M. Baldwin, and Gary A. Dudley. Skeletal muscle myosin heavy chain composition and resistance training. Journal of Applied Physiology 74 (1993): 911-911.

[33] Fry, A. C., C. A. Allemeier, and R. S. Staron. Correlation between percentage fiber type area and myosin heavy chain content in human skeletal muscle. European Journal of Applied Physiology and Occupational Physiology 68, no. 3 (1994): 246-251.

[34] Mackey, Abigail L., L. Holm, S. Reitelseder, T. G. Pedersen, S. Doessing, Fawzi Kadi, and Michael Kjær. Myogenic response of human skeletal muscle to 12 weeks of resistance training at light loading intensity. Scandinavian Journal of Medicine & Science in Sports 21, no. 6 (2011): 773-782.

[35] Abe, Takashi, Diego V. DeHoyos, Michael L. Pollock, and Linda Garzarella. Time course for strength and muscle thickness changes following upper and lower body resistance training in men and women. European Journal of Applied Physiology 81, no. 3 (2000): 174-180.

[36] Plomgaard, Peter, Milena Penkowa, Lotte Leick, Bente K. Pedersen, Bengt Saltin, and Henriette Pilegaard. The mRNA expression profile of metabolic genes relative to MHC isoform pattern in human skeletal muscles. Journal of Applied Physiology 101, no. 3 (2006): 817-825.

[37] Mittendorfer, B., J. L. Andersen, P. Plomgaard, B. Saltin, J. A. Babraj, K. Smith, and M. J. Rennie. Protein synthesis rates in human muscles: neither anatomical location nor fibre ‐ type composition are major determinants. The Journal of Physiology 563, no. 1 (2005): 203-211.

[38] Garlick, Peter J., Charlotte A. Maltin, A. G. Baillie, Margaret I. Delday, and David A. Grubb. Fiber-type composition of nine rat muscles. II. Relationship to protein turnover. American Journal of Physiology-Endocrinology And Metabolism 257, no. 6 (1989): E828-E832.

[39] Bates, Peter C., and David J. Millward. Myofibrillar protein turnover. Synthesis rates of myofibrillar and sarcoplasmic protein fractions in different muscles and the changes observed during postnatal development and in response to feeding and starvation. Biochem. J 214 (1983): 587-592.

[40] Fluckey, James D., Thomas C. Vary, Leonard S. Jefferson, and Peter A. Farrell. Augmented insulin action on rates of protein synthesis after resistance exercise in rats. American Journal of Physiology-Endocrinology And Metabolism 270, no. 2 (1996): E313-E319.

[41] Parkington, Jascha D., Adam P. Siebert, Nathan K. LeBrasseur, and Roger A. Fielding. Differential activation of mTOR signaling by contractile activity in skeletal muscle. American Journal of Physiology-Regulatory, Integrative and Comparative Physiology 285, no. 5 (2003): R1086-R1090.

[42] Carroll, Chad C., James D. Fluckey, Rick H. Williams, Dennis H. Sullivan, and Todd A. Trappe. Human soleus and vastus lateralis muscle protein metabolism with an amino acid infusion. American Journal of Physiology-Endocrinology and Metabolism 288, no. 3 (2005): E479-E485.

[43] Campos, Gerson E., Thomas J. Luecke, Heather K. Wendeln, Kumika Toma, Fredrick C. Hagerman, Thomas F. Murray, Kerry E. Ragg, Nicholas A. Ratamess, William J. Kraemer, and Robert S. Staron. Muscular adaptations in response to three different resistance-training regimens: specificity of repetition maximum training zones. European Journal of Applied Physiology 88, no. 1-2 (2002): 50-60.

[44] Coyle, Edward F., D. C. Feiring, T. C. Rotkis, R. W. Cote, F. B. Roby, W. Lee, and J. H. Wilmore. Specificity of power improvements through slow and fast isokinetic training. Journal of Applied Physiology 51, no. 6 (1981): 1437-1442.

[45] Hather, B. M., P. A. Tesch, P. Buchanan, and G. A. Dudley. Influence of eccentric actions on skeletal muscle adaptations to resistance training. Acta Physiologica Scandinavica 143, no. 2 (1991): 177-185.

[46] Karavirta, L., A. Häkkinen, E. Sillanpää, D. García -López, A. K
Alen et al. Effects of combined endurance and strength training on muscle strength, power and hypertrophy in 40–67 year old men. Scandinavian Journal of Medicine & Science in Sports 21, no. 3 (2011): 402-411.

[47] Kraemer, William J., John F. Patton, Scott E. Gordon, Everett A. Harman, Michael R. Deschenes, Katy Reynolds, Robert U. Newton, N. Travis Triplett, and Joseph E. Dziados. Compatibility of high-intensity strength and endurance training on hormonal and skeletal muscle adaptations. Journal of Applied Physiology 78, no. 3 (1995): 976-989.

[48] Bassel-Duby, Rhonda, and Eric N. Olson. Signaling pathways in skeletal muscle remodeling. Annu. Rev. Biochem. 75 (2006): 19-37.

[49] Buller, A. J., J. C. Eccles, and Rosamond M. Eccles. Interactions between motoneurones and muscles in respect of the characteristic speeds of their responses. The Journal of Physiology 150, no. 2 (1960): 417-439.

[50] Lin, Jiandie, Hai Wu, Paul T. Tarr, Chen-Yu Zhang, Zhidan Wu, Olivier Boss, Laura F. Michael et al. Transcriptional co-activator PGC-1α drives the formation of slow-twitch muscle fibres. Nature 418, no. 6899 (2002): 797-801.

[51] Aagaard, Per, Jesper L. Andersen, Poul Dyhre‐Poulsen, Anne‐Mette Leffers, Aase Wagner, S. Peter Magnusson, Jens Halkjær‐Kristensen, and Erik B. Simonsen. A mechanism for increased contractile strength of human pennate muscle in response to strength training: changes in muscle architecture. The Journal of Physiology 534, no. 2 (2001): 613-623.

[52] Berchtold, Martin W., Heinrich Brinkmeier, and Markus Müntener. Calcium ion in skeletal muscle: its crucial role for muscle function, plasticity, and disease. Physiological Reviews 80, no. 3 (2000): 1215-1265.

[53] Carroll, Timothy J., Peter J. Abernethy, Peter A. Logan, Margaret Barber, and Michael T. McEniery. Resistance training frequency: strength and myosin heavy chain responses to two and three bouts per week. European Journal of Applied Physiology and Occupational Physiology 78, no. 3 (1998): 270-275.

[54] Stuart, Charles A., Mary EA Howell, Jonathan D. Baker, Rhesa J. Dykes, Michelle M. Duffourc, Michael W. Ramsey, and Michael H. Stone. Cycle training increased GLUT4 and activation of mTOR in fast twitch muscle fibers. Medicine and science in sports and exercise 42, no. 1 (2010): 96.

[55] Bodine, Sue C. mTOR signaling and the molecular adaptation to resistance exercise. Medicine and Science in Sports and Exercise 38, no. 11 (2006): 1950-1957.

[56] Thorstensson, Alf, Gunnar Grimby, and J. Karlsson. Force-velocity relations and fiber composition in human knee extensor muscles. Journal of Applied Physiology 40, no. 1 (1976): 12-16.

Chapter 5

Resistance exercise initiates mechanistic target of rapamycin (mTOR) translocation and protein complex co-localisation in human skeletal muscle

---

5.1 Abstract

The mechanistic target of rapamycin (mTOR) is a central mediator of protein synthesis in skeletal muscle in response to resistance exercise and nutrition. We utilized immunofluorescence approaches to study mTOR localisation and protein-protein interaction in human skeletal muscle in the basal state as well as immediately, 1 and 3h after an acute bout of resistance exercise in a fed (FED; 20g Protein/40g carbohydrate/1g fat) or energy-free control (CON) state. mTOR and the lysosomal protein LAMP2 were highly co-localised in basal samples. Resistance exercise resulted in rapid translocation of mTOR/LAMP2 towards the cell membrane. Concurrently, Tuberin (TSC2) and Ras-homolog enriched in brain (Rheb) were found to co-localise at the cell membrane at rest level. Resistance exercise led to the dissociation of TSC2 from Rheb and subsequent reduction of TSC2 at the cell membrane in both FED and CON. Further, there was an increase in the interaction of mTOR and Rheb after exercise that was sustained for up to 3h in both FED and CON. In addition, mTOR co-localised with EIF3F at the cell membrane post-exercise in both groups, with the response significantly greater at 1h of recovery in the FED compared to CON. Collectively our data demonstrate that cellular trafficking of mTOR occurs in human muscle in response to an anabolic stimulus, events that appear to be primarily influenced by muscle contraction. The translocation and association of mTOR with positive regulators (*i.e.* Rheb and eIF3F) is consistent with an enhanced mRNA translational capacity after resistance exercise.

5.2 Introduction

Resistance training is an effective strategy to increase muscle strength and muscle hypertrophy, with the latter ultimately mediated by an exercise-induced increase in muscle protein synthesis and net protein balance [1]. Skeletal muscle protein balance is generally dependent on the activity of the serine/threonine protein kinase mechanistic target of rapamycin (mTOR), which when active stimulates protein synthesis and attenuates protein degradation [2].

mTOR exists as 1 of 2 complexes (mTORC1 and mTORC2) and with their respective substrate preference and, ultimately, biological activity related to the specific associated subunits [2]. For example, mTORC1 contains mTOR, GβL, raptor, DEPTOR and PRAS40 and is inhibited by the bacterial macrolide rapamycin [2]. In contrast, mTORC2 consists of mTOR, rictor, GβL, Sin1, DEPTOR and Protor/PRR5 and is insensitive to acute rapamycin administration [2].

Although each mTOR complex responds to unique subsets of biological stimuli and generally localize to different subcellular compartments [3], mTORC1 is the most widely studied of the two complexes and responds to anabolic stimuli such as insulin, amino acids, and/or resistance exercise [2]. For example, acute administration of rapamycin blocks the independent anabolic effects of resistance exercise and amino acid ingestion on mTOR signaling molecule phosphorylation and subsequently protein synthesis in human skeletal muscle [4, 5]. Collectively, these data highlight a pivotal role for mTORC1 activity in the regulation of muscle protein synthesis in response to resistance exercise and amino acid ingestion.

Current understanding regarding the physiological regulation of mTOR in human skeletal muscle has come in large part from phosphorylation-specific profiling of the mTOR pathway in response to anabolic stimuli [6]. Consistent with the ability of resistance exercise to increase muscle protein synthesis in the fasted state [7, 8], phosphorylation of mTOR substrates (as a proxy for mTOR activity) has indicated that mTOR is activated following resistance exercise [9] with this response maintained for at least 24h post-exercise [10]. Moreover, the provision of exogenous amino acids (either orally or intravenously) augments post-exercise rates of muscle protein synthesis [11, 12], which is generally

coincident with changes in phosphorylation status of proteins within the mTOR signaling cascade that are consistent with an enhanced translational activity [13, 14].

Beyond immunoblotting approaches, in vitro studies have indicated that cellular localization and protein-protein interaction may be fundamentally important in the regulation of mTOR activity in response to physiological stimuli [3]. Following mitogen or amino acid stimulation, mTOR has been observed to translocate to the lysosome where it associates with GTP bound ras-homolog enriched in brain (Rheb) to achieve full activation [15]. In contrast, amino acid removal results in mTOR dissociation from the lysosome and cytosolic degradation [15]. mTOR interaction with Rheb is restricted in basal conditions due to the enzymatic activity of the tuberous sclerosis complex proteins TSC1 and TSC2, which maintain Rheb in a GDP-bound state [16]. However, phosphorylation of TSC2 by AKT leads to TSC2 inactivation [17], Rheb-TSC2 dissociation, GTP-loading of Rheb and interaction with mTOR [18]. Jacobs and coworkers [19] recently reported that mTOR and TSC2 associate at the lysosome in mouse tibialis-anterior skeletal muscle, with eccentric contractions stimulating an increase in mTOR-lysosomal interaction and subsequent dissociation of TSC2 from the lysosome. Collectively these studies would suggest that targeting of mTOR to the lysosome is a fundamentally important event to initiate cellular protein synthesis [20].

The aim of the present study was to examine cellular distribution and co-localization of proteins involved in mTOR assembly/activity in human skeletal muscle in response to resistance exercise. Immunofluorescences staining techniques, as well as quantitative methods developed in Chapter 3 were applied to observe and quantatively identify translocation of mTOR and its regulatory proteins in response to one bout of resistance exercise in human skeletal muscle. In addition, we also evaluated the effect of post-exercise protein/carbohydrate ingestion on mTOR complex assembly and localisation. We hypothesized that resistance exercise would increase mTOR abundance at the lysosomal surface to facilitate interaction with Rheb and that post-exercise nutrients would augment these responses.

5.3 Methods

5.3.1 Subjects

Fourteen healthy, recreationally active males volunteered to participate in the study. Participants were informed about the experimental procedure to be used as well as the purpose of the study and all potential risks prior to obtaining written consent. All participants were deemed healthy based on their response to a routine medical screening questionnaire. The study carried approval by the local Research Ethics Board of McMaster University and Hamilton Health Sciences and the University of Guelph Research Ethics Board and conformed to all standards for the use of human subjects in research as outlined in the Declaration of Helsinki.

5.3.2 Experimental Design

Participants were randomly assigned into groups that received either a protein-carbohydrate beverage (FED; n=7, age=25±2y, BMI = 26.1±2.3 kg/m2; means±SD) or an energy-free control (CON; n=7, age=24±3y, BMI=26.3±2.6 kg/m2) after exercise. Participants reported to the laboratory after an overnight fast having refrained from strenuous exercise for at least 48h. A single biopsy was taken from the vastus lateralis of a randomly selected thigh under local anesthesia (2% xylocaine), as previously described [21]. Participants performed an intense bout of bilateral leg resistance exercise consisting of 5 sets each of leg press and knee extension (with an inter-set rest period of 2-min) using a predetermined weight that elicited voluntary failure in 8-10 repetitions. Similar exercise protocols have been shown to elicit a robust increase in muscle protein synthesis over 3h of recovery in both the fasted [22] and fed states [23]. A second muscle biopsy was taken 10 min after completion of the exercise bout from the same thigh as the first biopsy to determine mTOR co-localization early in recovery. Participants were then randomly assigned to consume a commercially available beverage (Gatorade Recover®, Gatorade, IL, USA) providing 20/44/1g of protein/carbohydrate/fat (FED) or an energy-free control (CON). As such, the 20g of high quality milk-based protein consumed by FED would be expected to maximize muscle protein synthesis [24] and the 44g of carbohydrate would elicit a marked insulin response [25] to enhance mTOR signalling [26]. Subsequently, muscle biopsies were

taken 1 and 3h after the beverage ingestion from separate incisions on the contralateral thigh from the initial biopsies to determine the time-dependent changes in mTOR co-localization during recovery in CON and FED.

5.3.3 Skeletal muscle immunohistochemistry

Biopsy samples (~25mg) were blotted and freed from any visible fat and connective tissue prior to being mounted in Optimal Cutting Temperature Compound (Tissue-Tek®, VWR) and frozen in isopentane cooled by liquid nitrogen prior to storage at -80°C for subsequent immunofluorescence analysis. Embedded muscle samples were fixed on the position in front of the blade of the microtome (Bright 5040, Bright Instrument Company limited, Huntingdon, England) and serial sections (5μm) collected onto room temperature uncoated glass slides (VWR international, UK). Sections were left to air dry at room temperature for 10min to remove excess crystallized water inside sections under storage.

Sections (5 μm) were fixed in acetone and ethanol (3:1) solution (Fisher technology) for 5 min and then washed for 3 x 5min in phosphate buffered saline (PBS) to remove fixation reagent. Sections were subsequently pre-incubated with 5% normal goat serum for 30min, the PBS wash step repeated, prior to incubation (2h) in primary antibody solution diluted 1:200 with 5% normal goat serum (Invitrogen, UK). Following incubation, sections were washed for 3 x 5min in PBS and incubated in the appropriate secondary antibody for 30min at room temperature. Sections were finally incubated with wheat Germ Agglutinin (WGA-350) for 20min at room temperature to mark the sarcolemmal membrane. Slides were left to air dry until the visual water stains evaporated for 1-2 min at room temperature. Then sections were mounted with 20μL Mowiol® 4-88 (Sigma-Aldrich, UK) and sealed by glass coverslips to protect the muscle sections and to preserve fluorescence signals. Slides were left overnight before observation. All primary antibodies used and their corresponding secondary antibodies are listed in Table 2.1.

5.3.4 Image capture

Prepared slides were observed under a Nikon E600 microscope using a 40×0.75 numerical aperture objective. Images per area were captured under three colour filters achieved by a SPOT RT KE colour three shot CCD camera (Diagnostic Instruments Inc., MI, USA), illuminated by a 170 W Xenon light source. For images capture, DAPI UV (340–380 nm) filter was used to view WGA-350 (blue) signals and mTOR stains tagged with Alexa 594 fluorophore (red) was visualised under the Texas red (540–580 nm) excitation filter. FITC (465–495nm) excitation filter was left to capture signals of mTOR-associated proteins, which were conjugated with Alexa Fluor 488 fluorophore unless stated otherwise (Table 3.1). DAPI UV (340-380 nm) was also used to observe the DAPI stained nucleus. All widefield images were obtained using a 40x objective (0.75 NA). Co-localisation experiments between mTOR and associated proteins were performed on an upright confocal microscope (Zeiss LSM 510 Meta, Carl Zeiss), using a 40× 1.4 NA water immersion objective. Fluorophores were visualised under three laser filters simultaneously. Alexa Fluor 488 fluorophore was excited by an argon laser and 498-571 nm emission, while a 594nm line of the helium–neon laser with 601-713 nm emission was used to excite Alexa Fluor 594 fluorophore. WGA conjugated with Alexa 350 and DAPI could be visualised under the excitation of the 405nm line from a Diode 405-30 filter.

For total protein quantification, 3 slide replicates for each individual were stained, imaged and quantified. At least 7 images were captured per section. All image processing and quantitation was carried out in ImagePro Plus 5.1 and kept constant between images. Total protein fluorescence intensity was quantified by measuring the signal intensity within the intracellular regions of a mask created by a specific membrane marker (dystrophin, WGA). For colocalisation analysis, five to seven areas per section were randomly selected and imaged under the same capture settings. Images were processed and analysed under the Image-Pro Plus 5.1 software (Media Cybernetics, MD, USA). Prior to colocalisation analysis, all images underwent a no neighbour deconvolution algorithm as a filter. Image signals generated by WGA or dystrophin were used to estimate cell membrane borders, which were merged with the corresponding target protein images to identify the association between the protein of interest and the plasma membrane. Pearson's correlation coefficient (Image-Pro software) was used to quantify localization with the plasma membrane and mTOR associated proteins.

5.3.5 Statistical Analysis

Immunofluorescence image analysis was performed in duplicate, with 5- 7 regions per cross section used for analysis. Pearson's correlation coefficient values at each group/time point were analyzed using a two-way ANOVA (SPSS) with Tukeys post-hoc analysis where appropriate. Significance was set at $P<0.05$. Data are presented as fold change (Mean ± SEM) in relative to the baseline biopsy (i.e. -40min timepoint) in CON and FED group, respectively (PRE-EX CON).

5.4 Results

5.4.1 Translocation of mTOR protein to cell membrane in response to one bout of resistance exercise in young healthy human skeletal muscle

As shown in Figure 5.4.1 a/b/c, mTOR was observed to randomly distribute in basal human skeletal muscle skeletal. Some mTOR signals were also associated with the plasma membrane areas (0.30±0.03 for CON; 0.29±0.02 for FED, shown as Pearson's correlation coefficient). More mTOR fluorescences translocated to cell membrane immediately post resistance exercise (0.31±0.01 for CON, 0.33±0.03 for FED, $p<0.05$), maintaining localisation on membrane 1h post exercise (0.34±0.02 for CON, 0.33±0.02 for FED group, $p<0.05$) and 3h post exercise (0.32±0.03 for CON and 0.32±0.01 for FED, $p<0.05$).

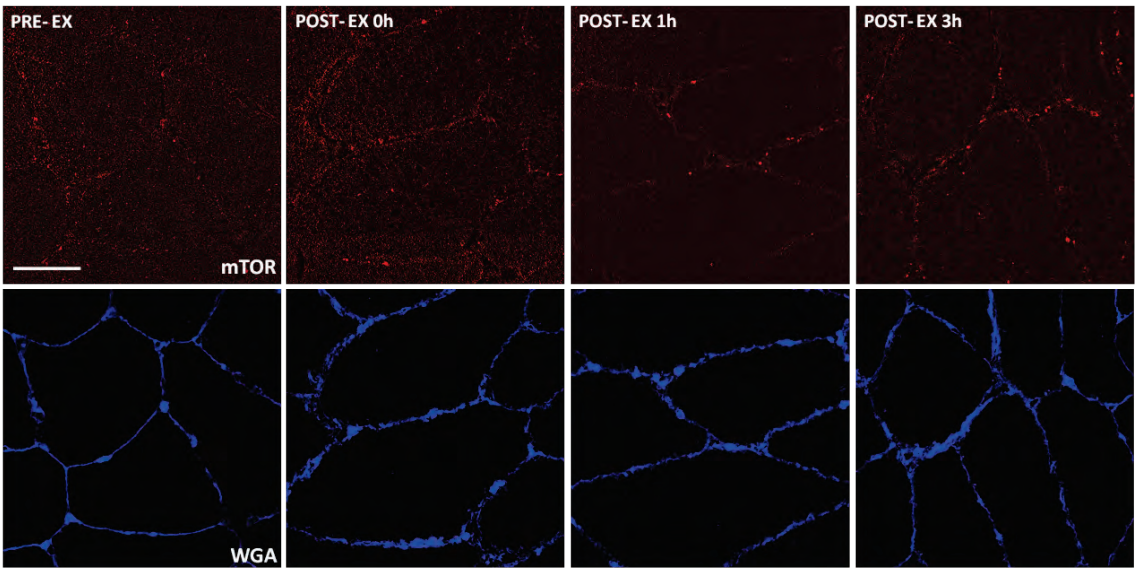

Figure 5.4.1a mTOR translocates to the plasma membrane in response to one bout of resistance exercise in human skeletal muscle. A) mTOR primary antibody was stained with secondary antibody conjugated with Alex fluor® 594nm fluorophore. Images were taken under HeNe 594nm laser, Zeiss LSM510 confocal microscope, x40 /1.2 NA (water) objective. B) Plasma membrane was stained with WGA conjugated with Alexa Fluor® 350nm fluorescences. Images were captured under 405nm Diode laser, Zeiss LSM510 confocal microscope, x40 /1.2 NA

(water) objective len. PRE-EX stands for the pre exercise, and POST- EX 0h, 1h, 3h stand for 0 hour, 1 hour and 3 hours post exercise, respectively. Scale bar 50µm.

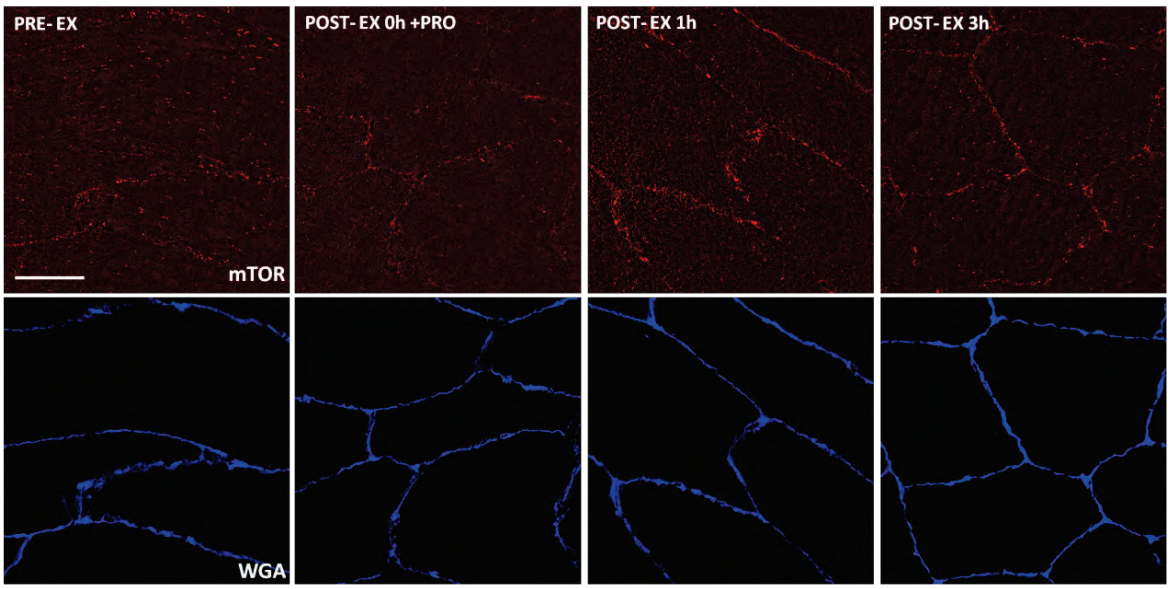

Figure 5.4.1b mTOR translocates to the plasma membrane in response to one bout of resistance exercise combined with nutrition supplementation in human skeletal muscle. A) mTOR primary antibody was stained with secondary antibody conjugated with Alex fluor® 594nm fluorophore. Images were taken under HeNe 594nm laser, Zeiss LSM510 confocal microscope, x40 /1.2 NA (water) objective len. B) Plasma membrane was stained with WGA conjugated with Alexa Fluor® 350nm fluorescences. Images were captured under 405nm Diode laser, Zeiss LSM510 confocal microscope, x40 /1.2 NA (water) objective lense. PRE-EX is short for pre exercise, and POST- EX 0h,1h,3h stand for 0 hour, 1 hour and 3 hours post exercise, respectively. Scale bar 50µm.

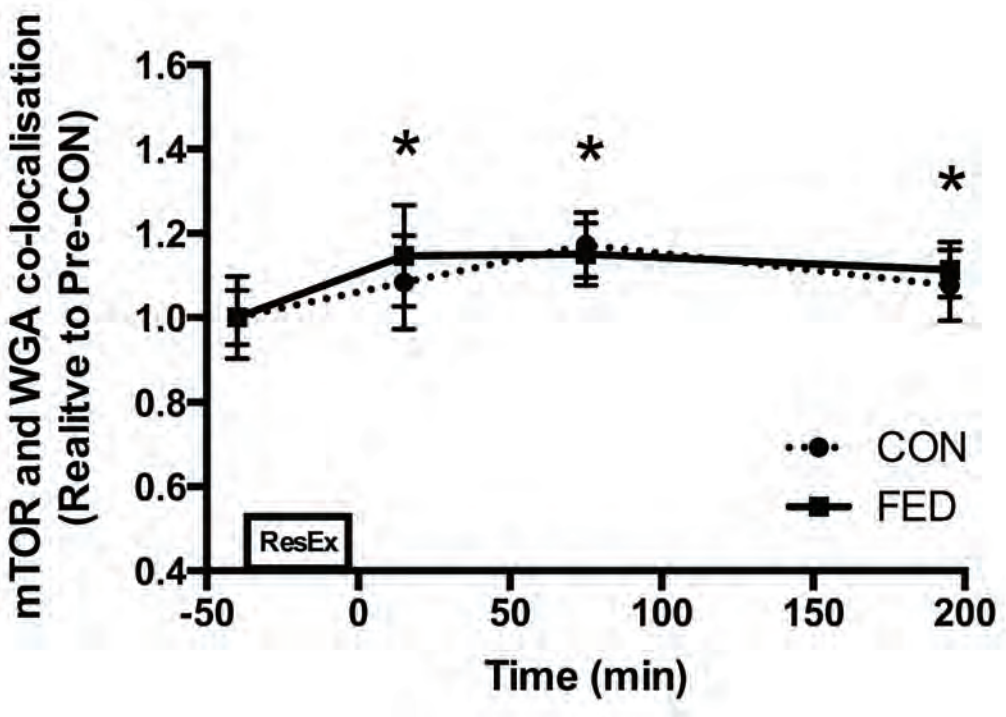

Figure 5.4.1c Quantification of mTOR association with cell membrane marker WGA following resistance exercise. Circles represent CON (energy- free group), squares represent FED (nutrition group). All data presented relative to the Pre exercise CON.Data presented as mean ± SEM (n=7/group). * Significantly different to PRE-CON (P<0.05).

5.4.2 mTOR does not translocate to the nucleus in response to one bout of resistance exercise in young healthy male skeletal muscle

As shown in Figure 5.4.2 a/b/c, part of mTOR stains distributed at the nucleus area in basal human skeletal muscle (39.93±4.59 for CON; 40.58 ±3.95 for FED). During 3h post exercise, it was not observed significant translocation of mTOR to nucleus area, either at immediately post exercise (35.02±4.89 for CON; 37.72±3.91 for FED), 1h post exercise (37.70±5.40 for CON; 41.23±3.35 for FED) or 3h post exercise (37.54±5.70 for CON; 41.84±4.75 for FED).

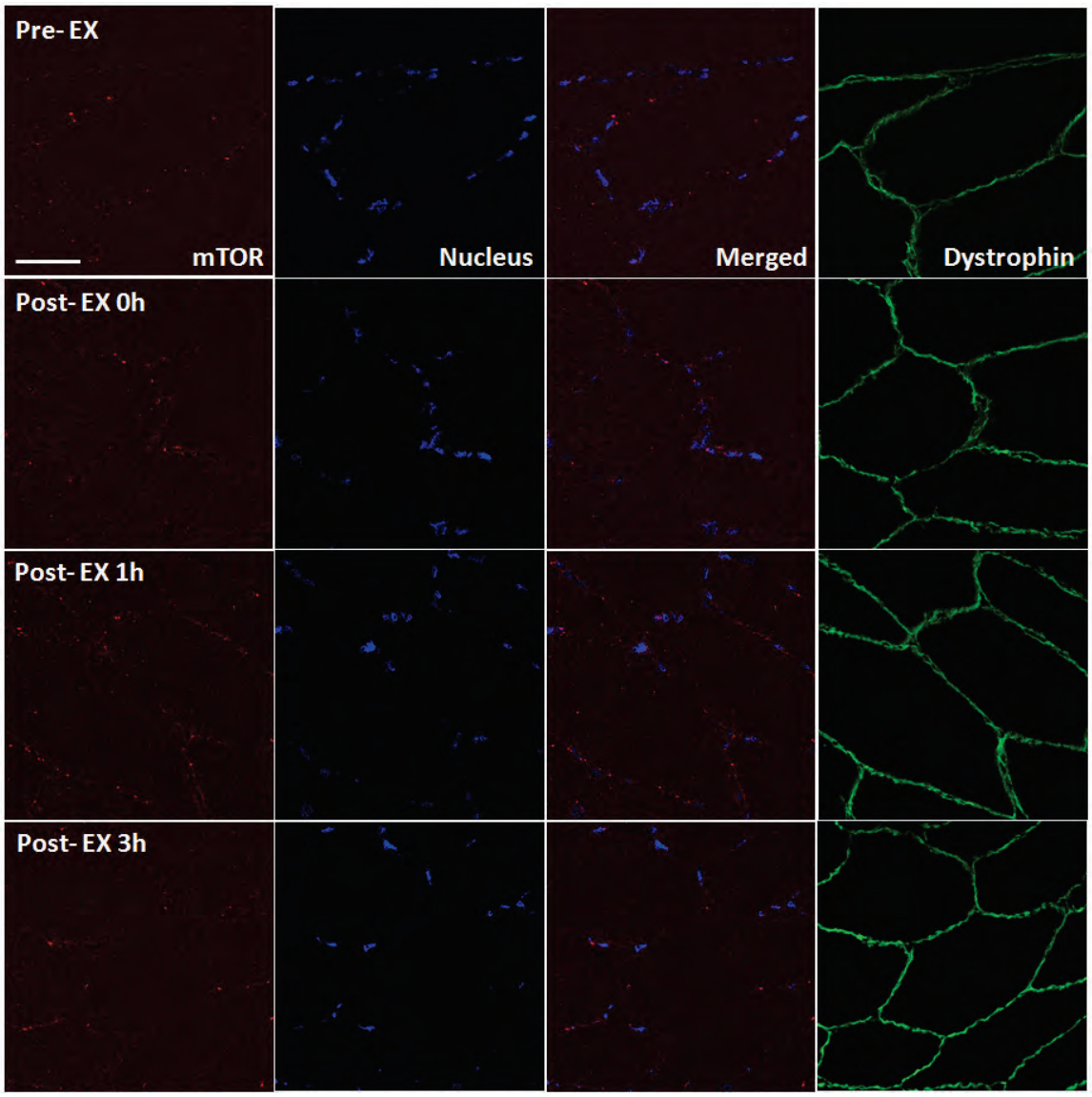

Figure 5.4.2a mTOR is not found translocate to nucleus area in response to one bout of resistance exercise in human skeletal muscle. A) mTOR primary antibody was stained with secondary antibody conjugated with Alex fluor® 594nm fluorophore. Images were taken under HeNe 594nm laser, x40/1.2 NA (water) objective len, Zeiss LSM510 confocal microscope. B) Nucleus was stained by Dapi dye dilution. Images were taken under 405nm Diode laser, x40 /1.2 NA (water) objective len. C) Composite images were merged between mTOR signal and Dapi fluorescence. D) Plasma membrane was stained by dystrophin primary antibody combined with corresponding secondary antibody conjugated with Alex fluor® 488nm fluorophore. Images were taken under 488nm Argon laser, x40/1.2 NA (water) objective len. PRE-EX means pre

exercise, and POST- EX 0h, 1h, 3h stand for 0 hour, 1 hour and 3 hours after resistance exercise, respectively. Scale bar 50µm.

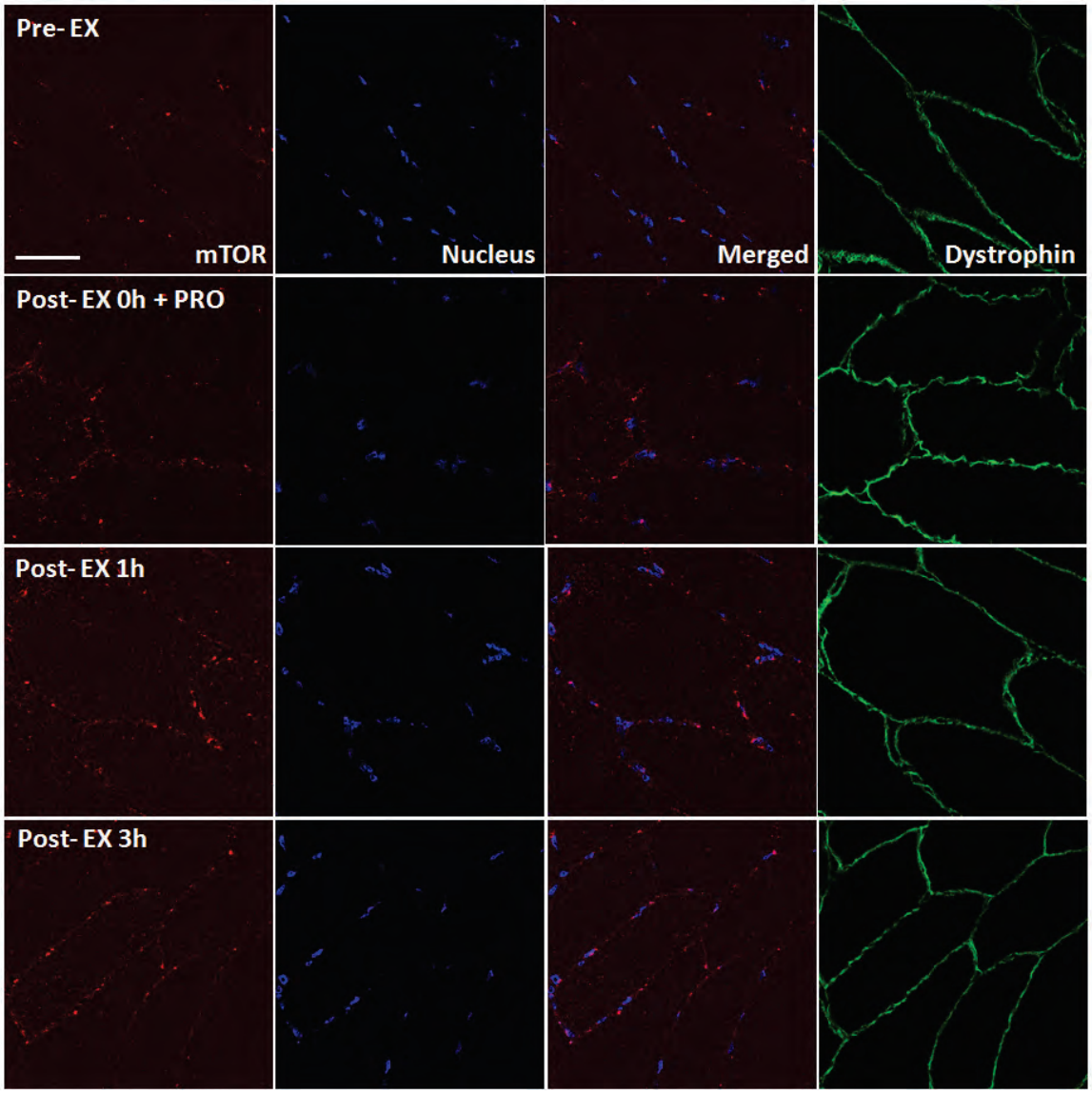

Figure 5.4.2b mTOR is not found translocate to nucleus area in response to one bout of resistance exercise combined with nutrition supplementation in human skeletal muscle. A) mTOR primary antibody was stained with secondary antibody conjugated with Alex fluor® 594nm fluorophore. Images were taken under HeNe 594nm laser, x40/1.2 NA (water) objective len, Zeiss LSM510 confocal microscope. B) Nucleus was stained by Dapi dye dilution. Images were taken under 405nm Diode laser, x40 /1.2 NA (water) objective len. C) Composite images

were merged between mTOR signal and Dapi fluorescence. D) Plasma membrane was stained by dystrophin primary antibody combined with corresponding secondary antibody conjugated with Alex fluor® 488nm fluorophore. Images were taken under 488nm Argon laser, x40/1.2 NA (water) objective len. PRE-EX means pre exercise, and POST- EX 0h, 1h, 3h stand for 0 hour, 1 hour and 3 hours after resistance exercise, respectively. Scale bar 50μm.

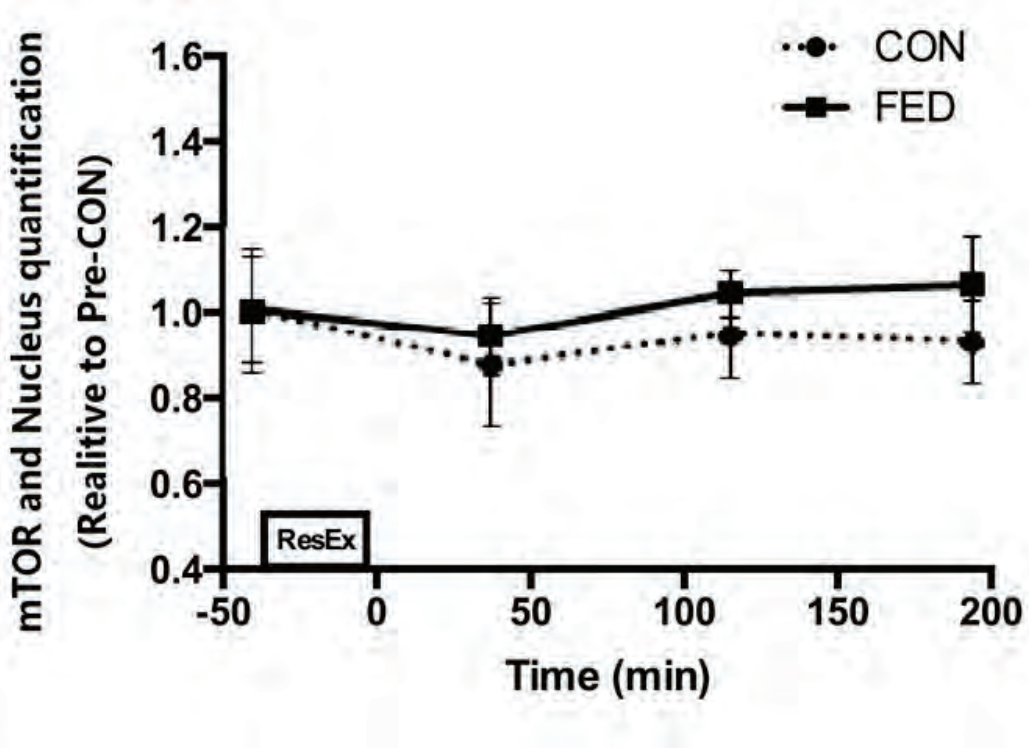

Figure 5.4.2c Quantification of mTOR in nucleus area following resistance exercise. Circles represent CON (energy- free group), squares represent FED (nutrition group). All data presented relative to the Pre exercise CON. Data presented as mean ± SEM (n=7/group). * Significantly different to PRE-CON (P<0.05).

5.4.3 mTOR translocates to blood vessel in response to one bout of resistance exercise in young healthy male

As shown in Figure 5.4.3 a/b/c, mechanistic contraction resulted in immediate translocation of mTOR to associate with blood vessels (0.32±0.03 for CON; 0.30±0.03 for FED, $p<0.05$) compared with basal

level (0.27±0.02 for CON; 0.27±0.03 for FED) in human skeletal muscle. And the association between mTOR and blood vessels lasted for 1h post exercise (0.35±0.03 for CON; 0.37±0.03 for FED, P<0.05) and 3h post exercise (0.34±0.04 for CON; 0.30±0.03 for FED, p<0.05).

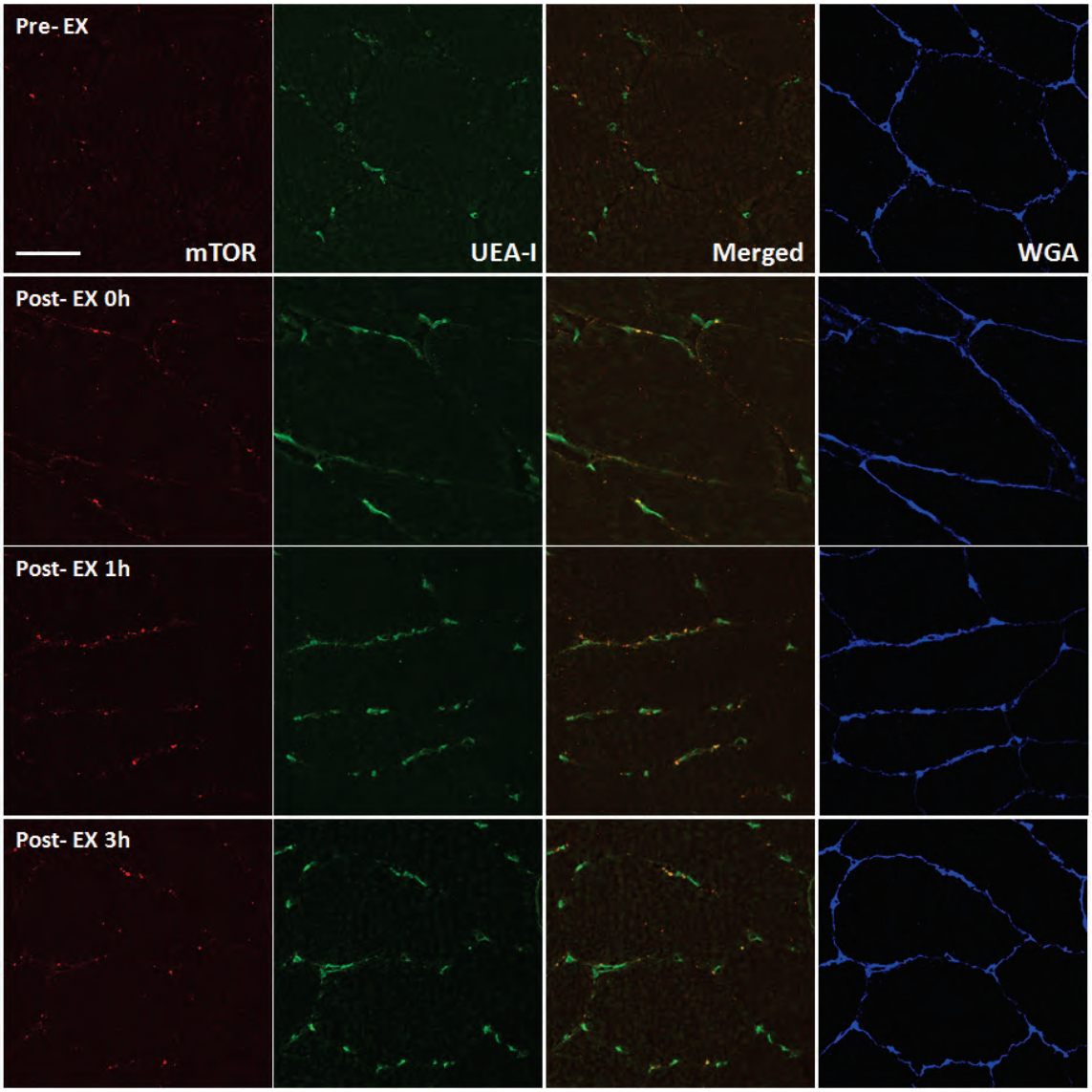

Figure 5.4.3a mTOR translocates to blood vessel area in response to one bout of resistance exercise in human skeletal muscle. A) mTOR primary antibody was stained with secondary antibody conjugated with Alex fluor® 594nm fluorophore. Images were taken under HeNe 594nm laser, x40/1.2 NA (water) objective len, Zeiss LSM510 confocal microscope. B) Capillaries were stained by Ulex Europeus Agglutinin (UEA-I) lectin conjugated with Alex fluor® 488nm fluorophore. Images were taken under 488nm Argon laser, x40/1.2 NA (water)

objective len. C) Composite images were merged between mTOR signal and UEA-I fluorescence. D) Plasma membrane was stained with WGA conjugated with Alexa Fluor® 350 fluorescences. Images were taken under 405nm Diode laser, Zeiss LSM510 confocal microscope, x40 /1.2 NA (water) objective len. PRE-EX means before resistance exercise, and POST- EX 0h, 1h, 3h stand for 0 hour, 1 hour and 3 hours post exercise, respectively. Scale bar 50µm.

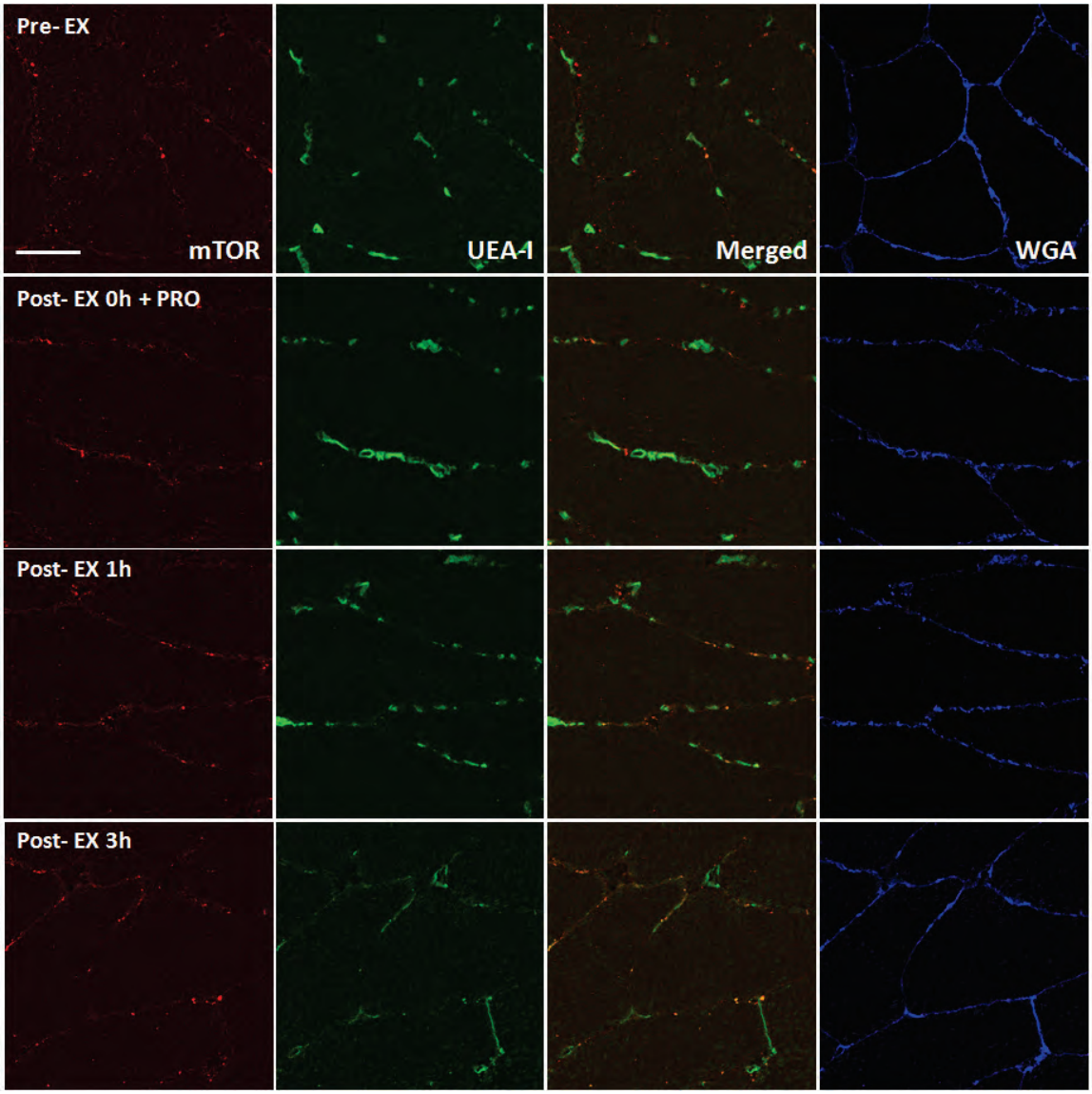

Figure 5.4.3b mTOR translocates to blood vessel area in response to one bout of resistance exercise combined with nutrition supplementation in human skeletal muscle. A) mTOR primary antibody was stained with secondary antibody conjugated with Alex fluor® 594nm fluorophore. Images were taken under HeNe 594nm laser, x40/1.2 NA (water) objective len, Zeiss LSM510

confocal microscope. B) Capillaries were stained by Ulex Europeus Agglutinin (UEA-I) lectin conjugated with Alex fluor® 488nm fluorophore. Images were taken under 488nm Argon laser, x40/1.2 NA (water) objective len. C) Composite images were merged between mTOR signal and UEA-I fluorescence. D) Plasma membrane was stained with WGA conjugated with Alexa Fluor® 350 fluorescences. Images were taken under 405nm Diode laser, Zeiss LSM510 confocal microscope, x40 /1.2 NA (water) objective len. PRE-EX means before resistance exercise, and POST- EX 0h, 1h, 3h stand for 0 hour, 1 hour and 3 hours post exercise, respectively. Scale bar 50μm.

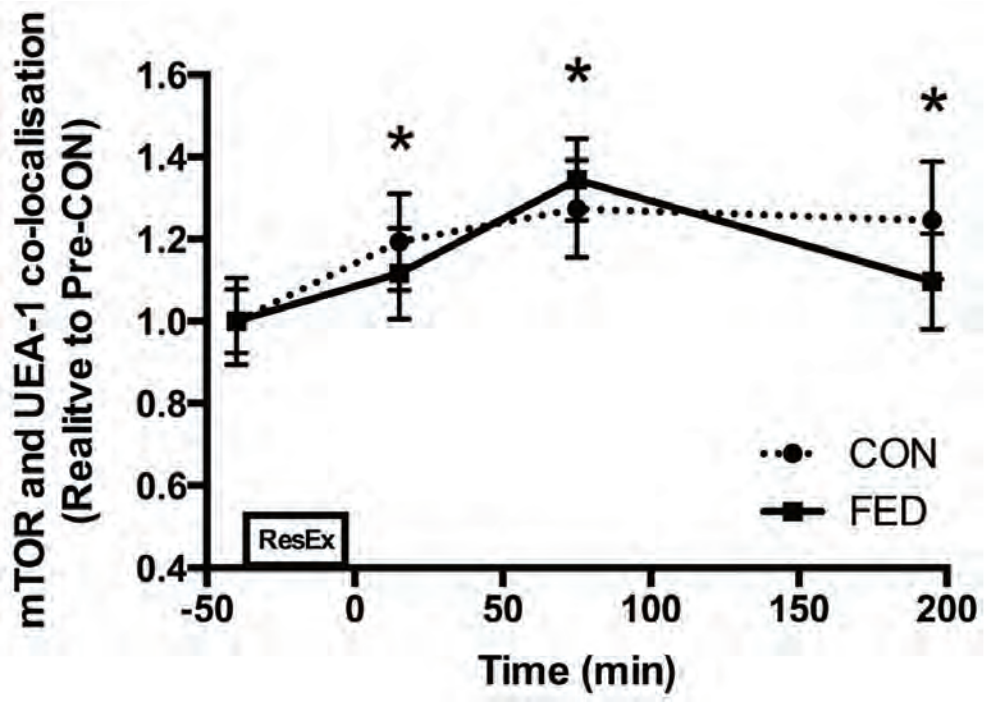

Figure 5.4.3c Quantification of mTOR translocation to the microvasculature following resistance exercise. Circles represent CON, squares represent FED. All data presented relative to the Pre exercise CON. Data presented as mean ± SEM (n=7/group). * Significantly different to PRE-CON (P<0.05).

5.4.4 Association between mTOR and Lamp2 was not changed following one bout of resistance exercise in young healthy skeletal muscle

As seen in Figure 5.4.4 a/b/c, mTOR colocalised with Lamp2 stains in basal human skeletal muscle (0.46±0.02 for CON; 0.46±0.01 for FED). In response to exercise stimulation, both mTOR and Lamp2 translocated to plasma membrane. However, colocalisation between mTOR and Lamp2was not changed during the 3h post exercise (immediately post exercise, 0.47±0.03 for CON and 0.49±0.01 for FED; 1h post exercise, 0.46±0.02 for CON and 0.46±0.02 for FED; 3h post exercise, 0.47±0.02 for CON and 0.47±0.01 for FED).

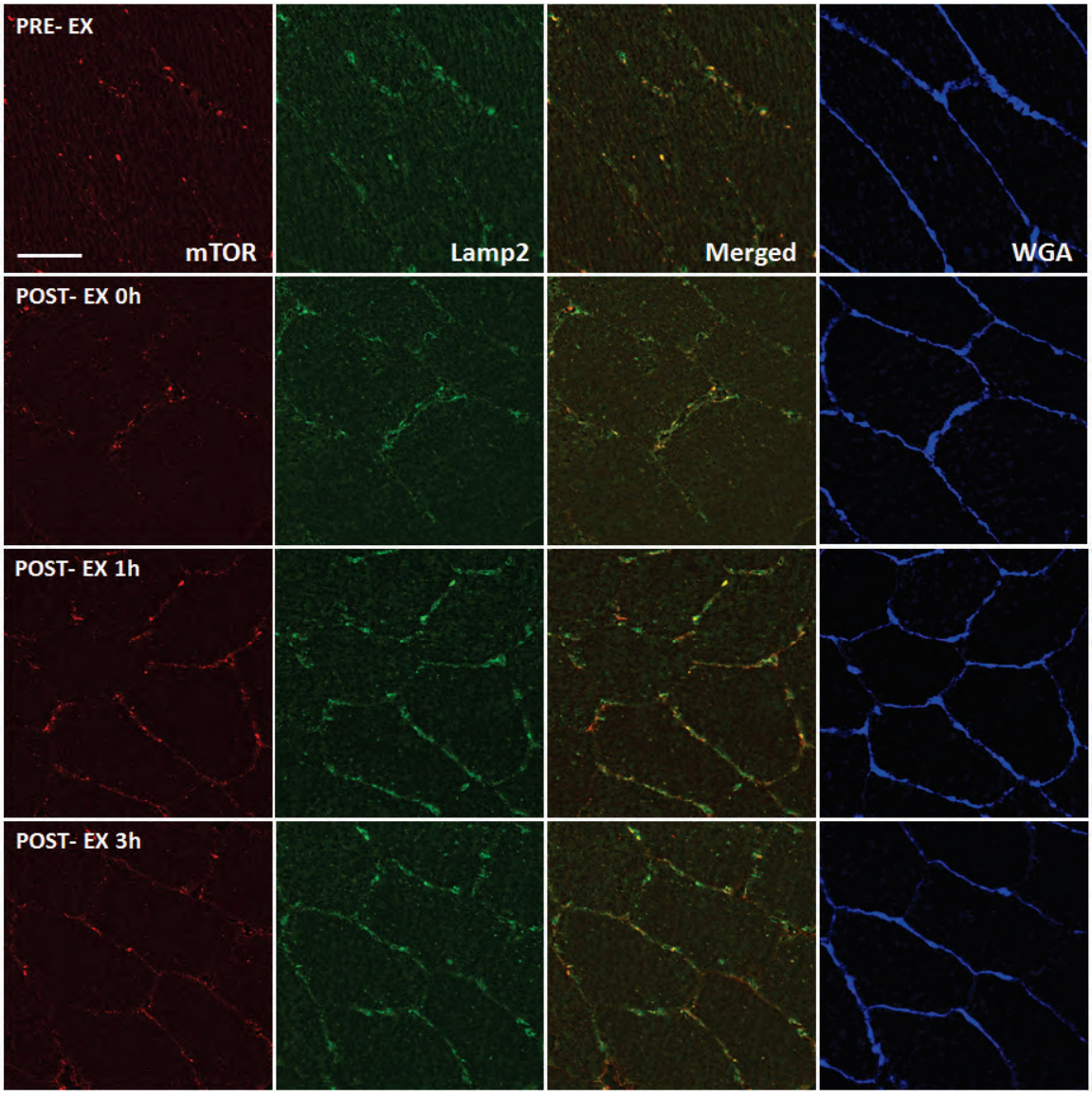

Figure 5.4.4a mTOR colocalises with Lamp2-positive stains consistently from pre exercise to 3h post exercise in human skeletal muscle. A) mTOR primary antibody was stained with secondary antibody conjugated with Alex fluor® 594nm fluorophore. Images were taken under HeNe 594nm laser, x40/1.2 NA (water) objective len, Zeiss LSM510 confocal microscope. B) Lamp2 proteins were stained by primary antibody combined with secondary antibody conjugated with Alex fluor® 488nm fluorophore. Images were taken under 488nm Argon laser, x40/1.2 NA (water) objective len. C) Composite images were merged between mTOR signal and Lamp2 fluorescence. D) Plasma membrane was stained with WGA conjugated with Alexa Fluor® 350 fluorescences. Images were taken under 405nm Diode laser, x40 /1.2 NA (water) objective len. PRE-EX means before resistance exercise, and POST- EX 0h, 1h, 3h stand for 0 hour, 1 hour and 3 hours post exercise, respectively. Scale bar 50µm.

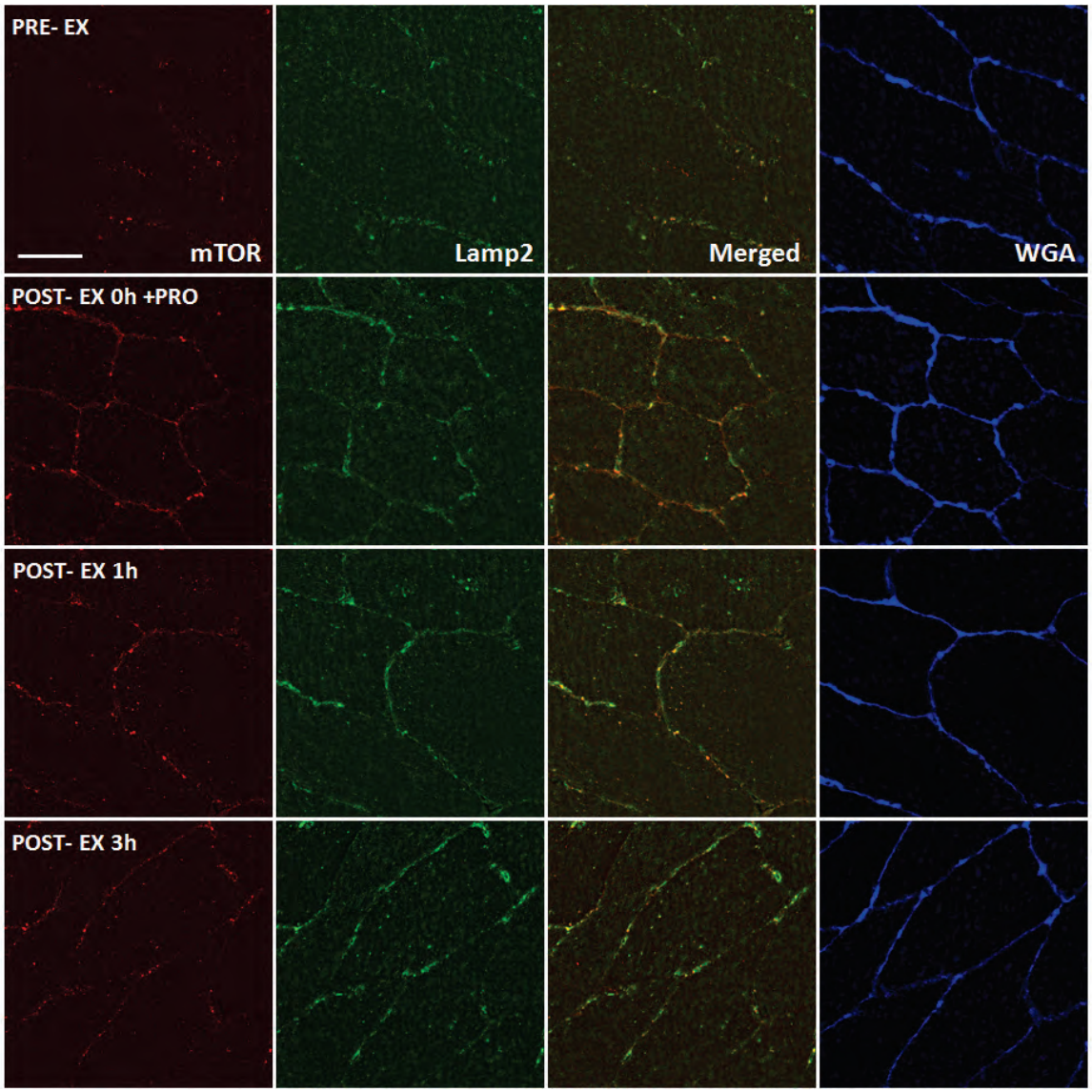

Figure 5.4.4b mTOR colocalises with Lamp2-positive stains consistently from pre exercise to 3h post exercise combined with nutrition supplementation in human skeletal muscle. A) mTOR primary antibody was stained with secondary antibody conjugated with Alex fluor® 594nm fluorophore. Images were taken under HeNe 594nm laser, x40/1.2 NA (water) objective len, Zeiss LSM510 confocal microscope. B) Lamp2 proteins were stained by primary antibody combined with secondary antibody conjugated with Alex fluor® 488nm fluorophore. Images were taken under 488nm Argon laser, x40/1.2 NA (water) objective len. C) Composite images were merged between mTOR signal and Lamp2 fluorescence. D) Plasma membrane was stained with WGA conjugated with Alexa Fluor® 350 fluorescences. Images were taken under 405nm Diode laser, x40 /1.2 NA (water) objective len. PRE-EX means before resistance exercise, and

POST- EX 0h, 1h, 3h stand for 0 hour, 1 hour and 3 hours post exercise, respectively. Scale bar 50μm.

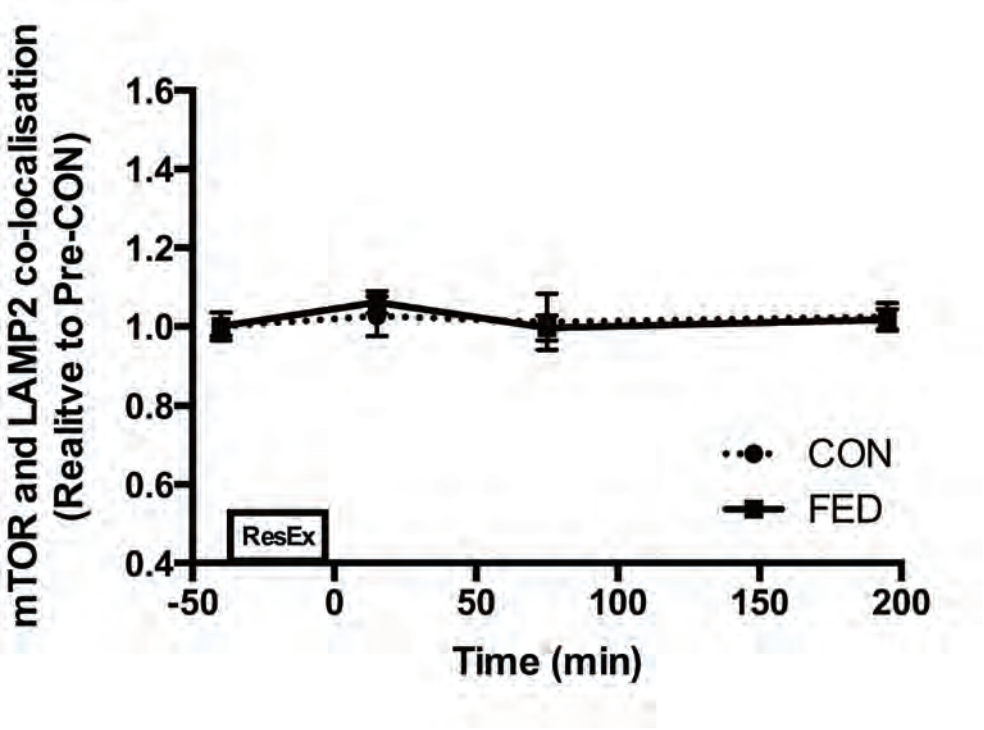

Figure 5.4.4c Quantification of mTOR colocalisation with LAMP2 following resistance exercise. Circles represent CON, squares represent FED. All data presented relative to the Pre exercise CON. Data presented as mean ± SEM (n=7/group). * Significantly different to PRE-CON (P<0.05).

5.4.5 Association between mTOR and Rab7 in response to one bout of resistance exercise

As shown in 5.4.5 a/b/c, mTOR and Rab7 were obsersed partially colocalised in basal human skeletal muscle (0.31±0.01 for CON; 0.31±0.02 for FED, shown as Pearson's correlation coefficient). In response to exercise, both mTOR and Rab7 translocated to plasma membrane immediately post exercise (0.36±0.02 for CON; 0.38±0.02 for FED, $p<0.05$) and maintained colocalisation with each other 1 h post exercise (0.35±0.02 for CON; 0.40±0.02 for FED, $p<0.05$) and 3h post exercise

(0.36±0.03 for CON; 0.38±0.02 for FED, $p<0.05$). It is noticed that significance difference between group was found at 1h post exercise ($p<0.05$).

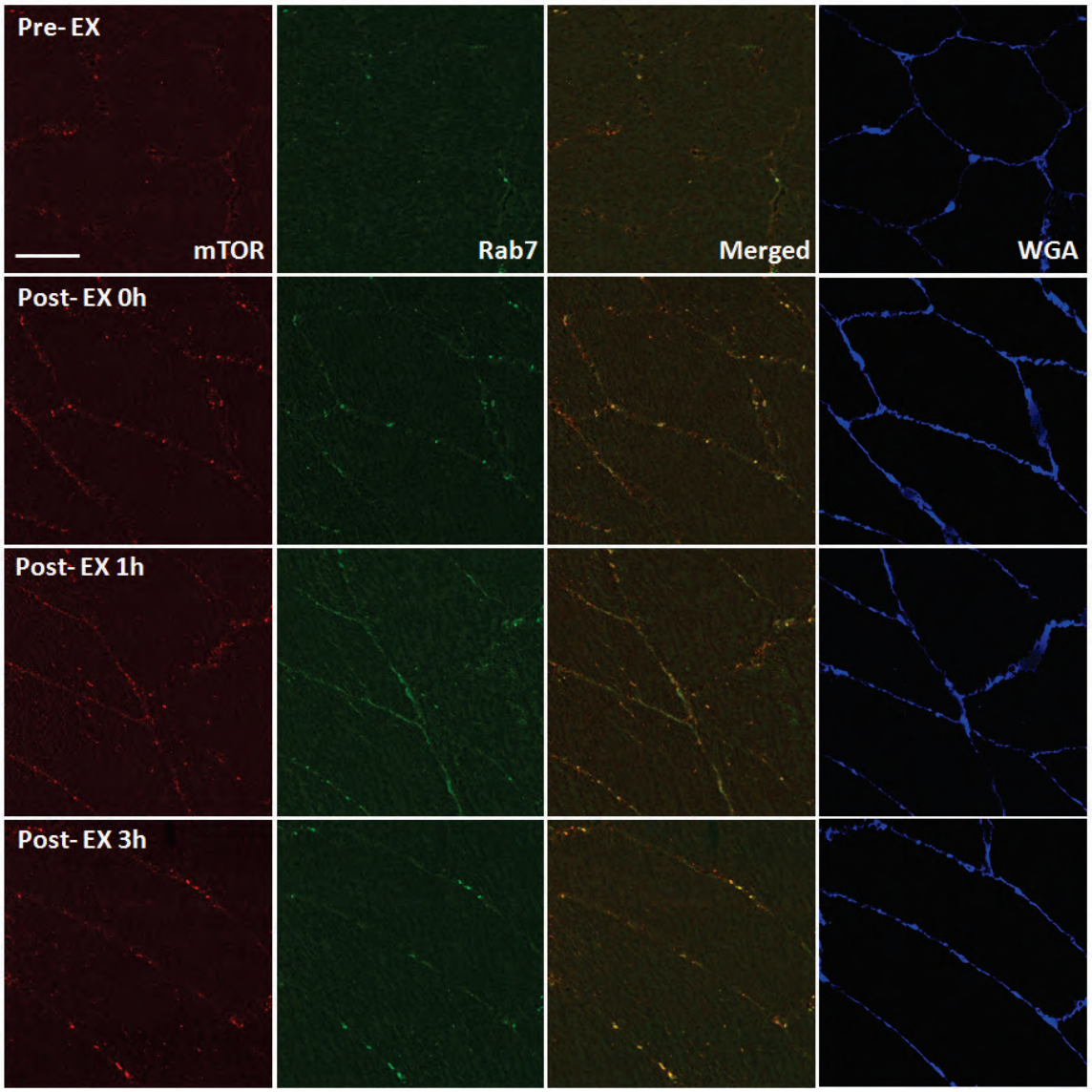

Figure 5.4.5a mTOR translocates to Rab7-positive area in response to one bout of resistance exercise in human skeletal muscle. A) mTOR primary antibody was stained with secondary antibody conjugated with Alex fluor® 594nm fluorophore. Images were taken under HeNe 594nm laser, x40/1.2 NA (water) objective len, Zeiss LSM510 confocal microscope. B) Rab7 proteins were stained by primary antibody combined with secondary antibody conjugated with Alex fluor® 488nm fluorophore. Images were taken under 488nm Argon laser, x40/1.2 NA (water) objective len. C) Composite images were merged between mTOR signal and Rab7

fluorescence. D) Plasma membrane was stained with WGA conjugated with Alexa Fluor® 350 fluorescences. Images were taken under 405nm Diode laser, x40 /1.2 NA (water) objective len. PRE-EX means before resistance exercise, and POST- EX 0h, 1h, 3h stand for 0 hour, 1 hour and 3 hours post exercise, respectively. Scale bar 50µm.

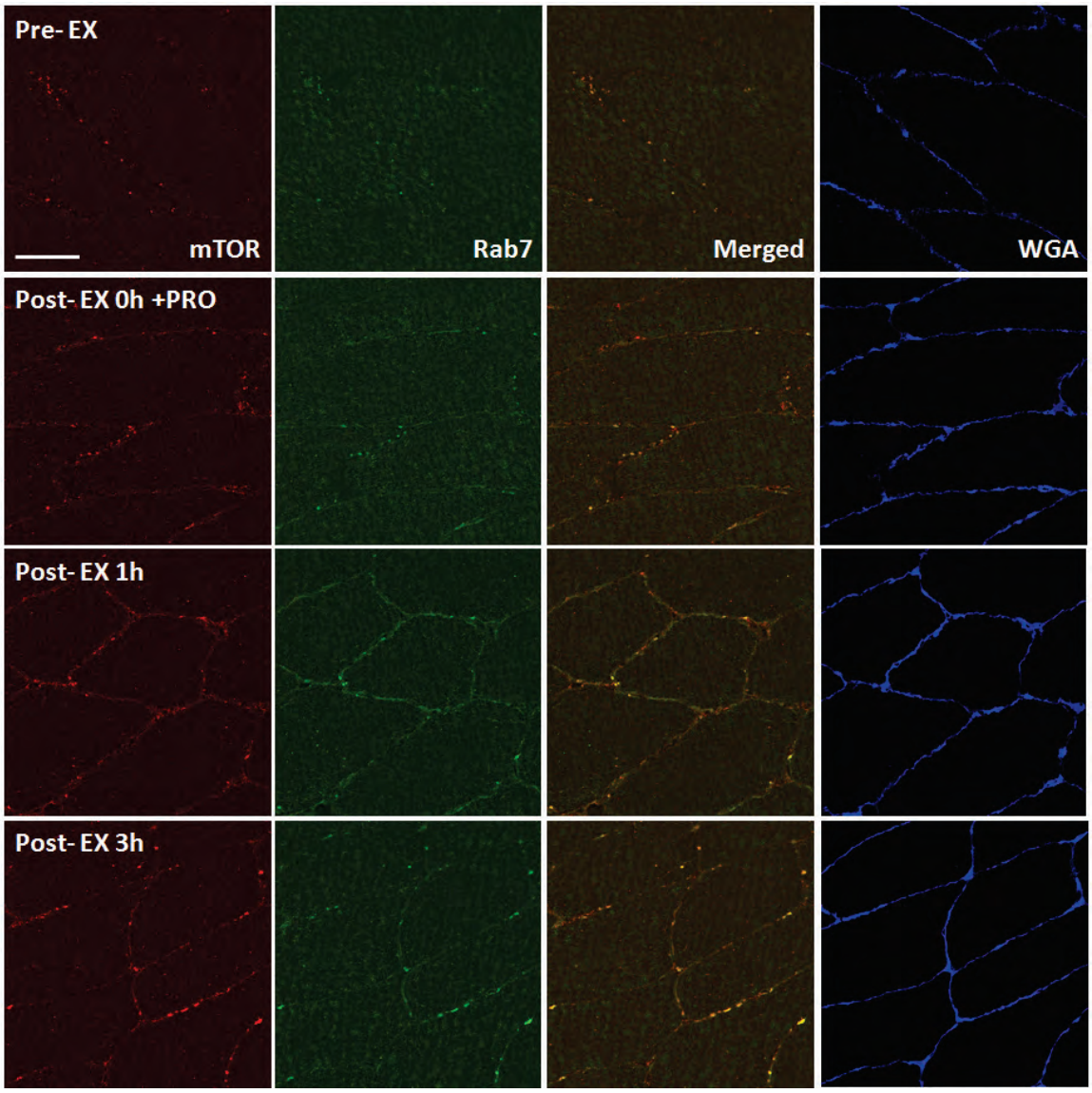

Figure 5.4.5b mTOR translocates to Rab7-positive area in response to one bout of resistance exercise combined with nutrition supplementation in human skeletal muscle. A) mTOR primary antibody was stained with secondary antibody conjugated with Alex fluor® 594nm fluorophore. Images were taken under HeNe 594nm laser, x40/1.2 NA (water) objective len, Zeiss LSM510

confocal microscope. B) Rab7 proteins were stained by primary antibody combined with secondary antibody conjugated with Alex fluor® 488nm fluorophore. Images were taken under 488nm Argon laser, x40/1.2 NA (water) objective len. C) Composite images were merged between mTOR signal and Rab7 fluorescence. D) Plasma membrane was stained with WGA conjugated with Alexa Fluor® 350 fluorescences. Images were taken under 405nm Diode laser, x40 /1.2 NA (water) objective len. PRE-EX means before resistance exercise, and POST- EX 0h, 1h, 3h stand for 0 hour, 1 hour and 3 hours post exercise, respectively. Scale bar 50µm.

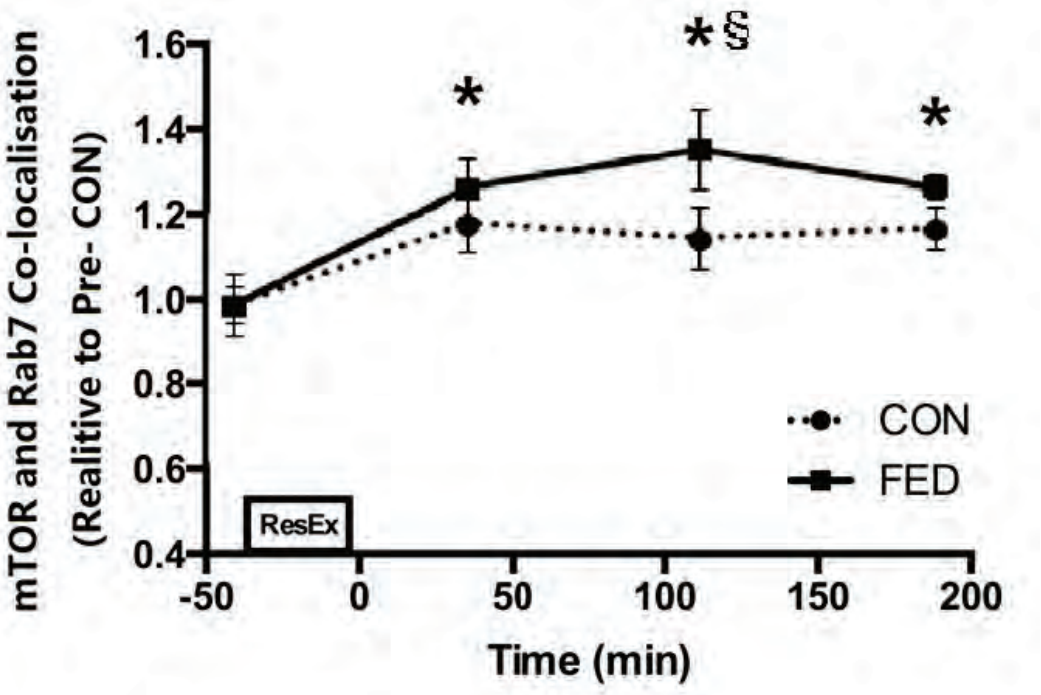

Figure 5.4.5c Quantification of mTOR co- localisation with Rab7 following resistance exercise. Circles represent CON, squares represent FED. All data presented relative to the Pre exercise CON. Data presented as mean ± SEM (n=7/group). * Significantly different to PRE-CON (P<0.05). § Significantly different between groups (P<0.05).

5.4.6 Association between Rab7 and Lamp2 in response to one bout of resistance exercise in young healthy male skeletal muscle

As seen in Figure 5.4.6a/b/c, compared with association between Rab7 and Lamp2 in basal human skeletal muscle (0.38±0.02 for CON; 0.39±0.01 for FED), resistance exercise stimulated Rab7 and Lamp2 translocating to plasma membrane to colocalise with each other immediately post exercise (0.43±0.02 for CON; 0.45±0.01 for FED, $p<0.05$). And their colocalisation lasted 1h post exercise (0.43±0.02 for CON; 0.47±0.01 for FED, $p<0.05$) and 3h post exercise (0.43±0.02 for CON; 0.45±0.01 for FED, $p<0.05$).

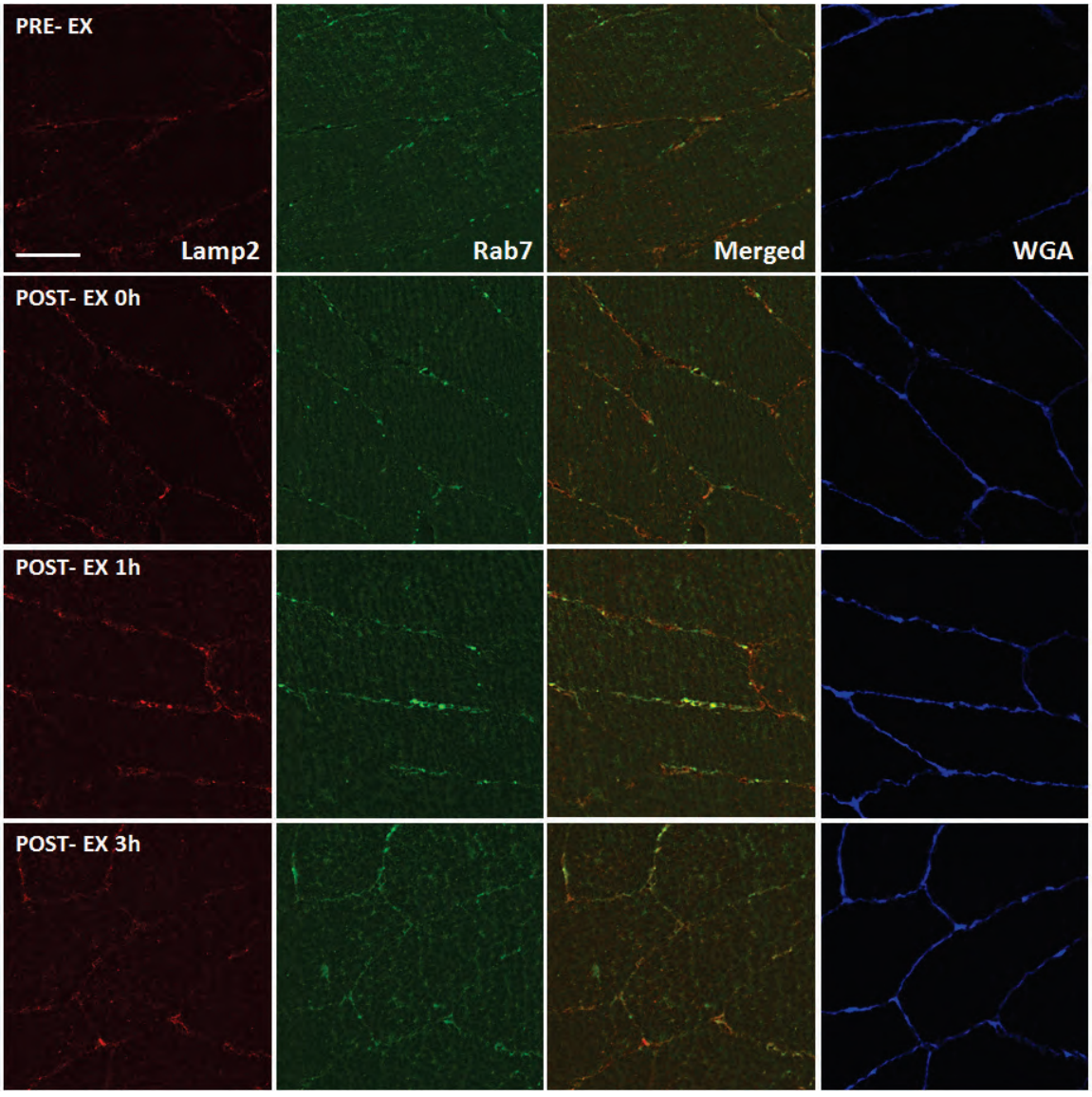

Figure 5.4.6a Lamp2 associates with Rab7-positive in response to one bout of resistance exercise in human skeletal muscle. A) Lamp2 primary antibody was stained with secondary antibody conjugated with Alex fluor® 594nm fluorophore. Images were taken under HeNe 594nm laser, x40/1.2 NA (water) objective len, Zeiss LSM510 confocal microscope. B) Rab7 proteins were stained by primary antibody combined with secondary antibody conjugated with Alex fluor® 488nm fluorophore. Images were taken under 488nm Argon laser, x40/1.2 NA (water) objective len. C) Composite images were merged between Lamp2 signal and Rab7 fluorescence. D) Plasma membrane was stained with WGA conjugated with Alexa Fluor® 350 fluorescences. Images were taken under 405nm Diode laser, x40 /1.2 NA (water) objective len. PRE-EX means before resistance exercise, and POST- EX 0h, 1h, 3h stand for 0 hour, 1 hour and 3 hours post exercise, respectively. Scale bar 50μm.

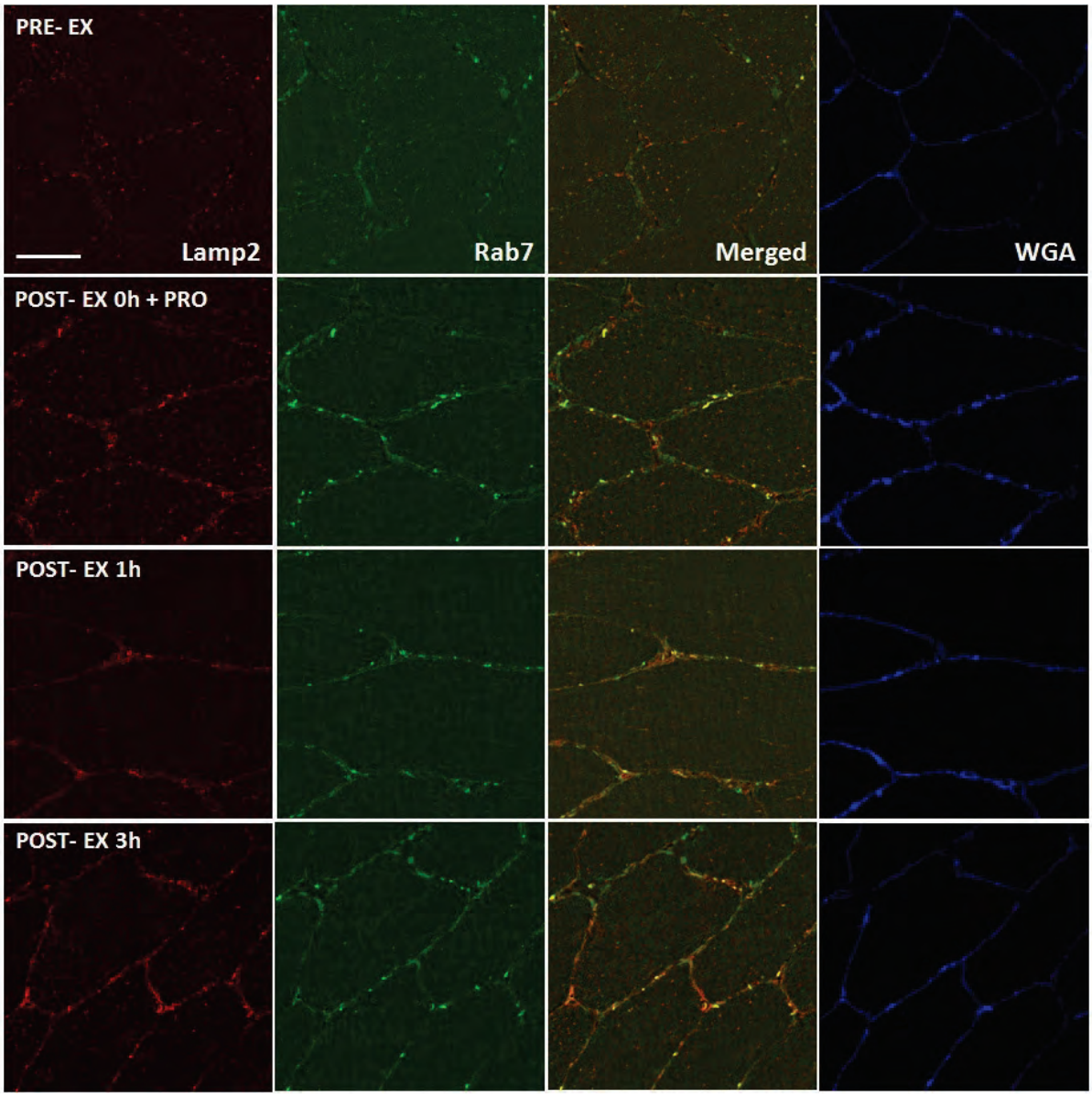

Figure 5.4.6b Lamp2 associates with Rab7-positive in response to one bout of resistance exercise combined with nutrition supplementation in human skeletal muscle. A) Lamp2 primary antibody was stained with secondary antibody conjugated with Alex fluor® 594nm fluorophore. Images were taken under HeNe 594nm laser, x40/1.2 NA (water) objective len, Zeiss LSM510 confocal microscope. B) Rab7 proteins were stained by primary antibody combined with secondary antibody conjugated with Alex fluor® 488nm fluorophore. Images were taken under 488nm Argon laser, x40/1.2 NA (water) objective len. C) Composite images were merged between Lamp2 signal and Rab7 fluorescence. D) Plasma membrane was stained with WGA conjugated with Alexa Fluor® 350 fluorescences. Images were taken under 405nm Diode laser,

x40 /1.2 NA (water) objective len. PRE-EX means before resistance exercise, and POST- EX 0h, 1h, 3h stand for 0 hour, 1 hour and 3 hours post exercise, respectively. Scale bar 50µm.

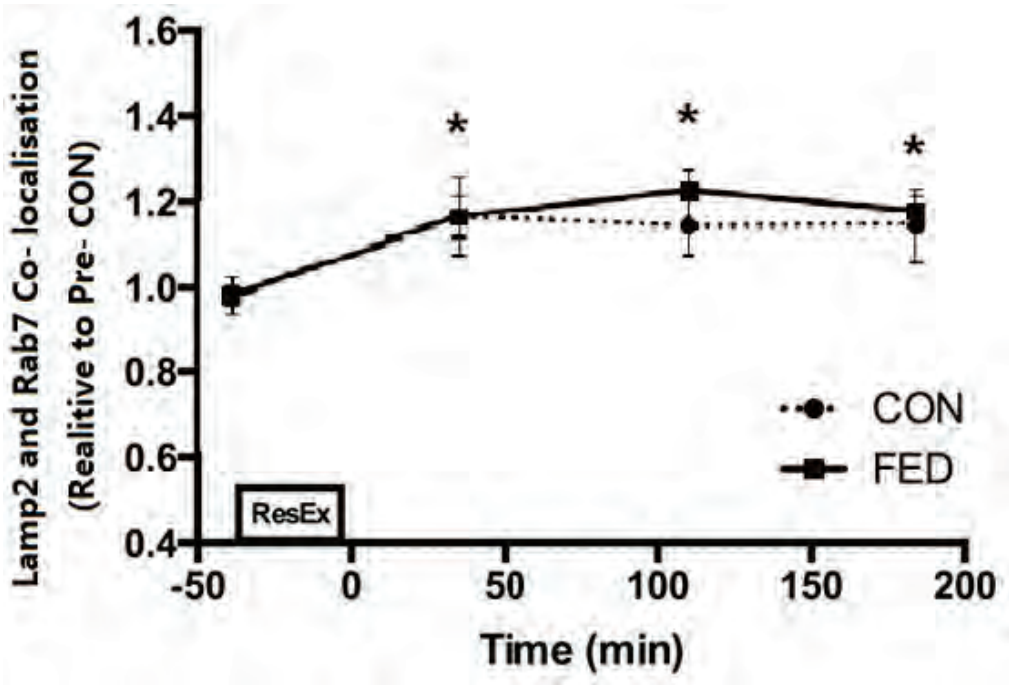

Figure 5.4.6c Quantification of Lamp2 co- localisation with Rab7 following resistance exercise. Circles represent CON, squares represent FED. All data presented relative to the Pre exercise CON. Data presented as mean ± SEM (n=7/group). * Significantly different to PRE-CON (P<0.05). § Significantly different between groups (P<0.05).

5.4.7 Association between mTOR and Rheb in response to one bout of resistance exercise in young healthy male skeletal muscle

As shown in Figure 5.4.7a/b/c, colocalisation between mTOR and Rheb was increased immediately post exercise on the plasma membrane (0.39±0.02 for CON; , 0.43±0.02 for FED, p<0.05) compared with basal level (0.34±0.01 for CON; 0.35±0.01 for FED). And this colocalisation maintained significant 1h post exercise (0.43±0.04 for CON; 0.45±0.02 for FED, P<0.05) and 3h post exercise (0.41±0.04 for CON; 0.42±0.01 for FED, P<0.05).

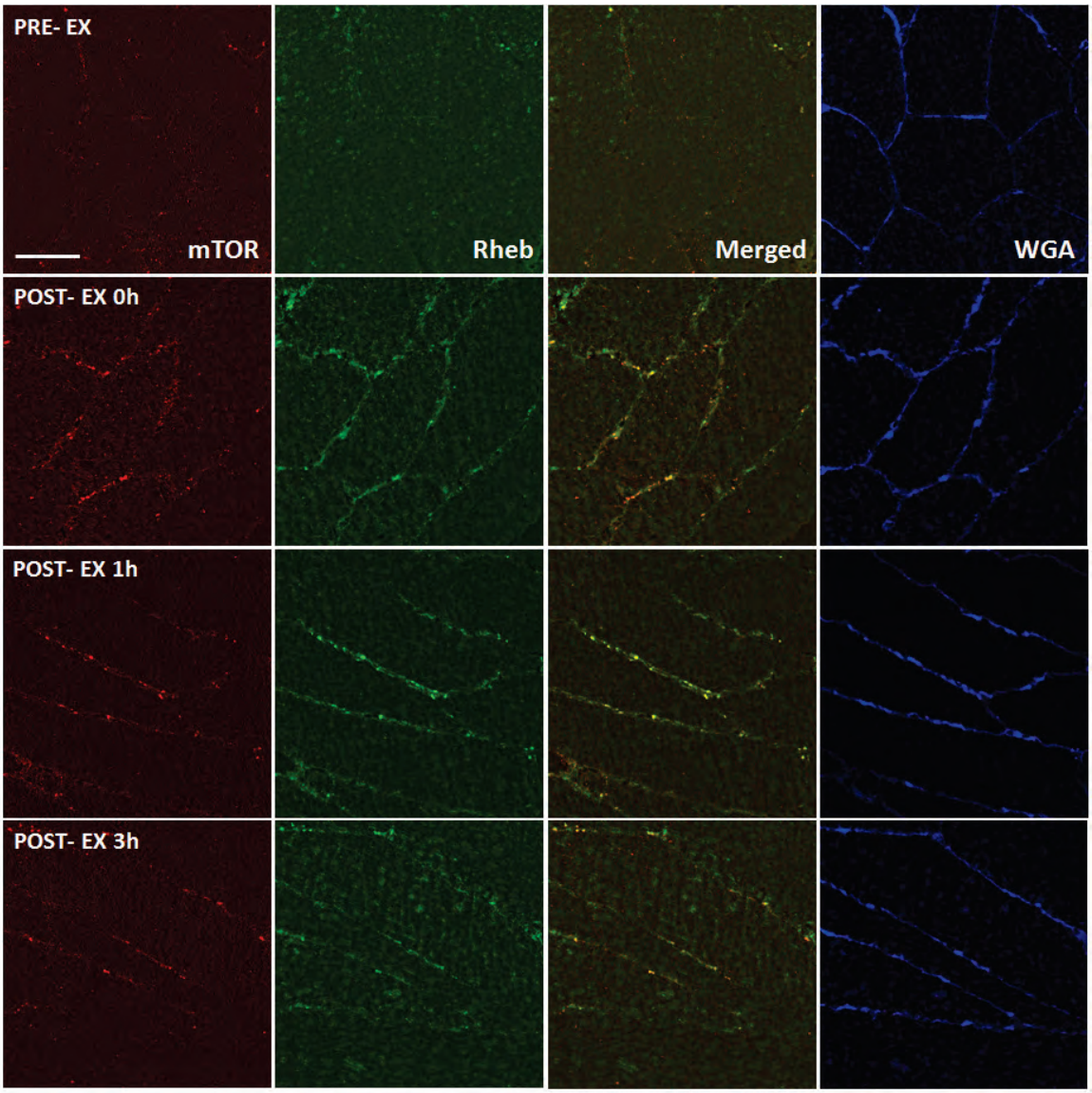

Figure 5.4.7a mTOR translocates to Rheb-positive area in response to one bout of resistance exercise in human skeletal muscle. A) mTOR primary antibody was stained with secondary antibody conjugated with Alex fluor® 594nm fluorophore. Images were taken under HeNe 594nm laser, x40/1.2 NA (water) objective len, Zeiss LSM510 confocal microscope. B) Rheb was stained by primary antibody combined with secondary antibody conjugated with Alex fluor® 488nm fluorophore. Images were taken under 488nm Argon laser, x40/1.2 NA (water) objective len. C) Composite images were merged between mTOR signal and Rheb fluorescence. D) Plasma membrane was stained with WGA conjugated with Alexa Fluor® 350 fluorescences. Images were taken under 405nm Diode laser, x40 /1.2 NA (water) objective len. PRE-EX means

before resistance exercise, and POST- EX 0h, 1h, 3h stand for 0 hour, 1 hour and 3 hours post exercise, respectively. Scale bar 50µm.

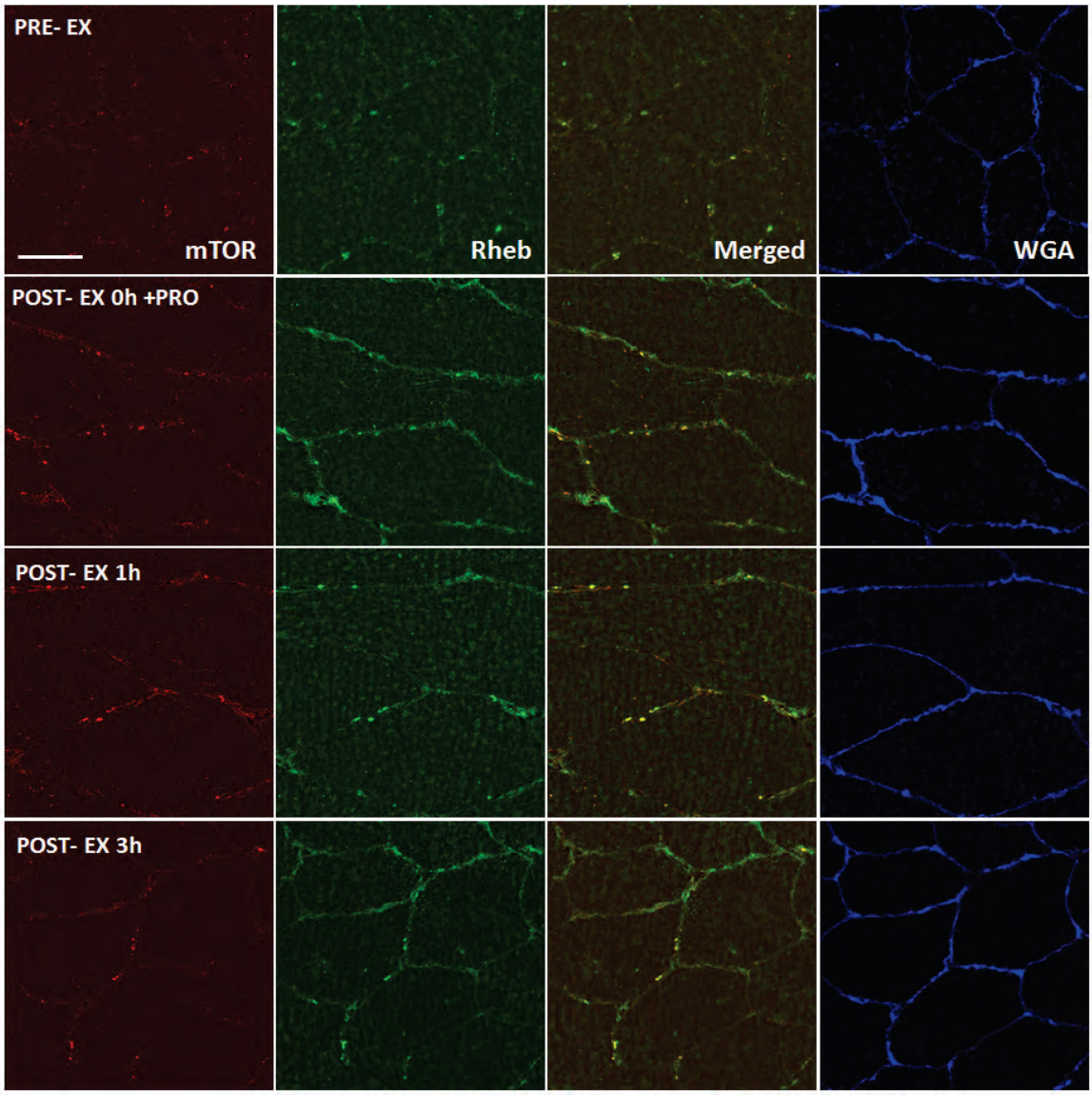

Figure 5.4.7b mTOR translocates to Rheb-positive area in response to one bout of resistance exercise combined with nutrition supplementation in human skeletal muscle. A) mTOR primary antibody was stained with secondary antibody conjugated with Alex fluor® 594nm fluorophore. Images were taken under HeNe 594nm laser, x40/1.2 NA (water) objective len, Zeiss LSM510 confocal microscope. B) Rheb was stained by primary antibody combined with secondary antibody conjugated with Alex fluor® 488nm fluorophore. Images were taken under 488nm

Argon laser, x40/1.2 NA (water) objective len. C) Composite images were merged between mTOR signal and Rheb fluorescence. D) Plasma membrane was stained with WGA conjugated with Alexa Fluor® 350 fluorescences. Images were taken under 405nm Diode laser, x40 /1.2 NA (water) objective len. PRE-EX means before resistance exercise, and POST- EX 0h, 1h, 3h stand for 0 hour, 1 hour and 3 hours post exercise, respectively. Scale bar 50µm.

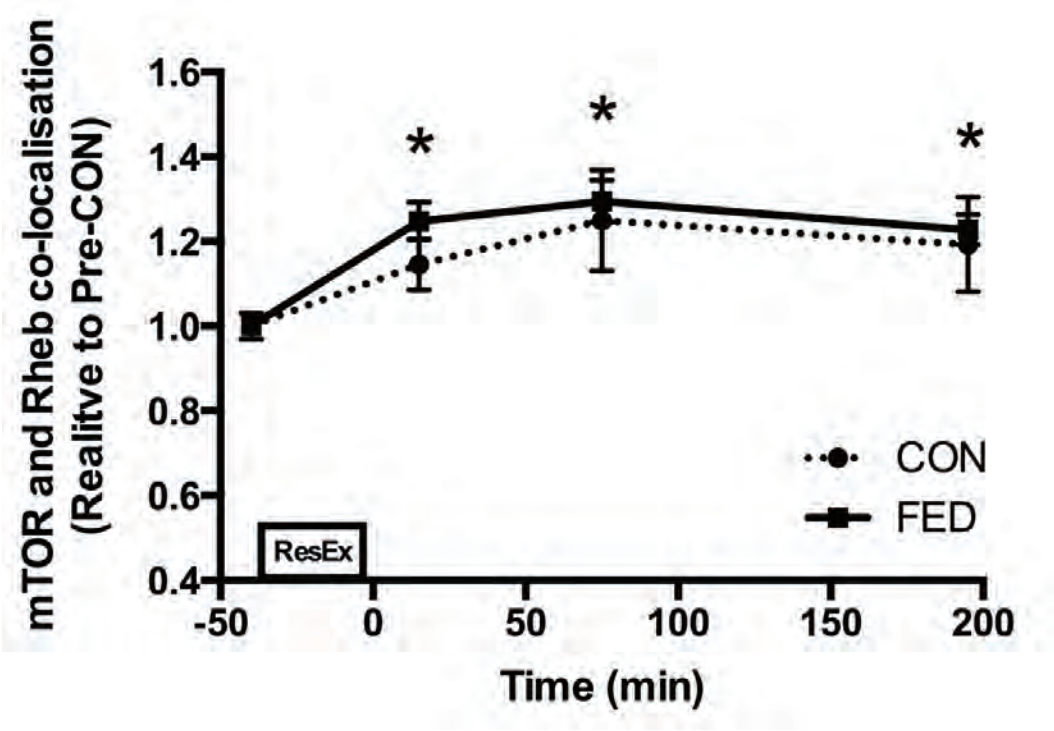

Figure 5.4.7c Quanticication of mTOR and Rheb interaction following resistance exercise. Circles represent CON, squares represent FED. All data presented relative to the Pre exercise CON. Data presented as mean ± SEM (n=7/group). * Significantly different to PRE-CON (P<0.05).

5.4.8 Association between mTOR and EIF3F in response to one bout of resistance exercise in young healthy male skeletal muscle

EIF3F is the component constituting the translation initiation box, which is reported to associate mTORC activating downstream proteins. As shown in Figure 5.4.8a/b/c, EIF3F signals were observed

to associate with mTOR on the plasma membrane immediately post exercise (0.40±0.03 for CON; 0.44±0.01 for FED, $p<0.05$) compared with basal level (0.33±0.01 for CON; 0.35±0.01 for FED). Association between mTOR and EIF3F was further increased 1h (0.41±0.03 for CON; 0.48±0.02 for FED, $p<0.05$). This association lasted to 3h post exercise (0.42±0.03 for CON; 0.45±0.01 for FED, $p<0.05$). It is noticed that association between mTOR and EIF3F was significantly different between two groups at 1h post exercise.

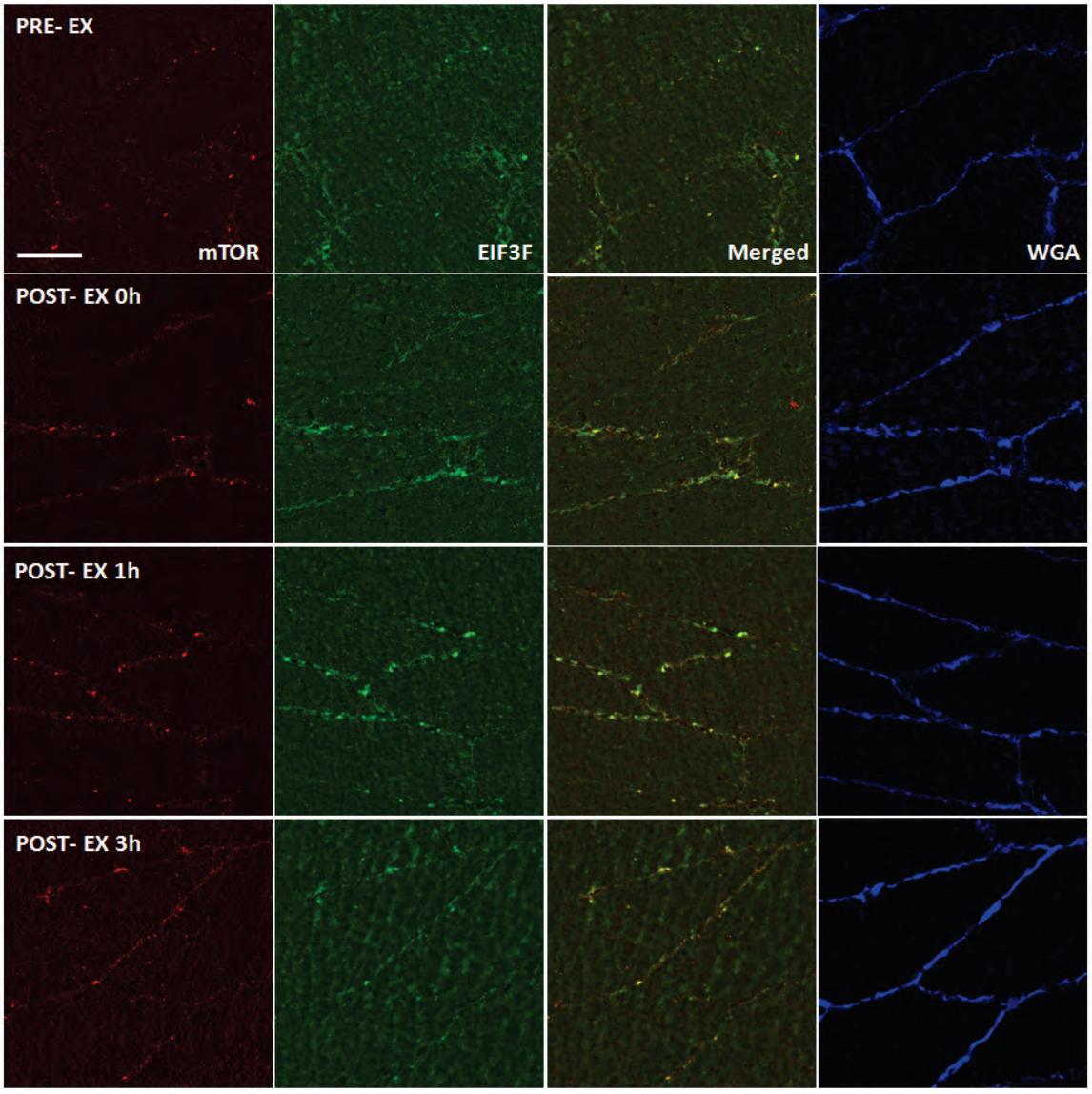

Figure 5.4.8a mTOR associates with EIF3F in response to one bout of resistance exercise in human skeletal muscle. A) mTOR primary antibody was stained with secondary antibody conjugated with Alex fluor® 594nm fluorophore. Images were taken under HeNe 594nm laser,

x40/1.2 NA (water) objective len, Zeiss LSM510 confocal microscope. B) EIF3F was incubated with the primary antibody combined with secondary antibody conjugated with Alex fluor® 488nm fluorophore. Images were taken under 488nm Argon laser, x40/1.2 NA (water) objective len. C) Composite images were merged between mTOR signal and EIF3F fluorescence. D) Plasma membrane was stained with WGA conjugated with Alexa Fluor® 350 fluorescences. Images were taken under 405nm Diode laser, x40 /1.2 NA (water) objective len. PRE-EX means before resistance exercise, and POST- EX 0h, 1h, 3h stand for 0 hour, 1 hour and 3 hours post exercise, respectively. Scale bar 50µm.

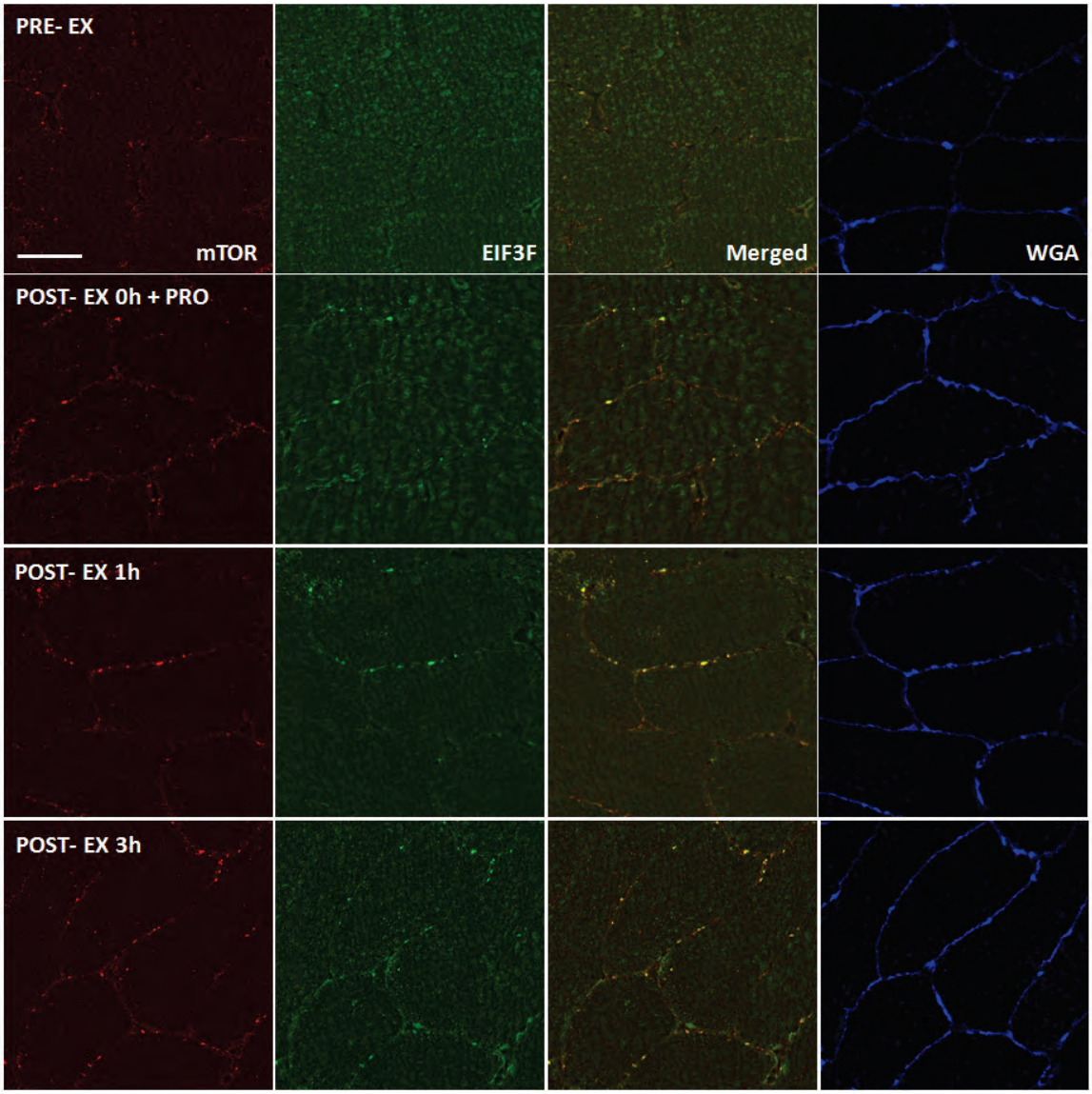

Figure 5.4.8b mTOR associates with EIF3F in response to one bout of resistance exercise combined with nutrition supplementation in human skeletal muscle. A) mTOR primary antibody was stained with secondary antibody conjugated with Alex fluor® 594nm fluorophore. Images were taken under HeNe 594nm laser, x40/1.2 NA (water) objective len, Zeiss LSM510 confocal microscope. B) EIF3F was incubated with the primary antibody combined with secondary antibody conjugated with Alex fluor® 488nm fluorophore. Images were taken under 488nm Argon laser, x40/1.2 NA (water) objective len. C) Composite images were merged between mTOR signal and EIF3F fluorescence. D) Plasma membrane was stained with WGA conjugated with Alexa Fluor® 350 fluorescences. Images were taken under 405nm Diode laser, x40 /1.2 NA (water) objective len. PRE-EX means before resistance exercise, and POST- EX 0h, 1h, 3h stand for 0 hour, 1 hour and 3 hours post exercise, respectively. Scale bar 50µm.

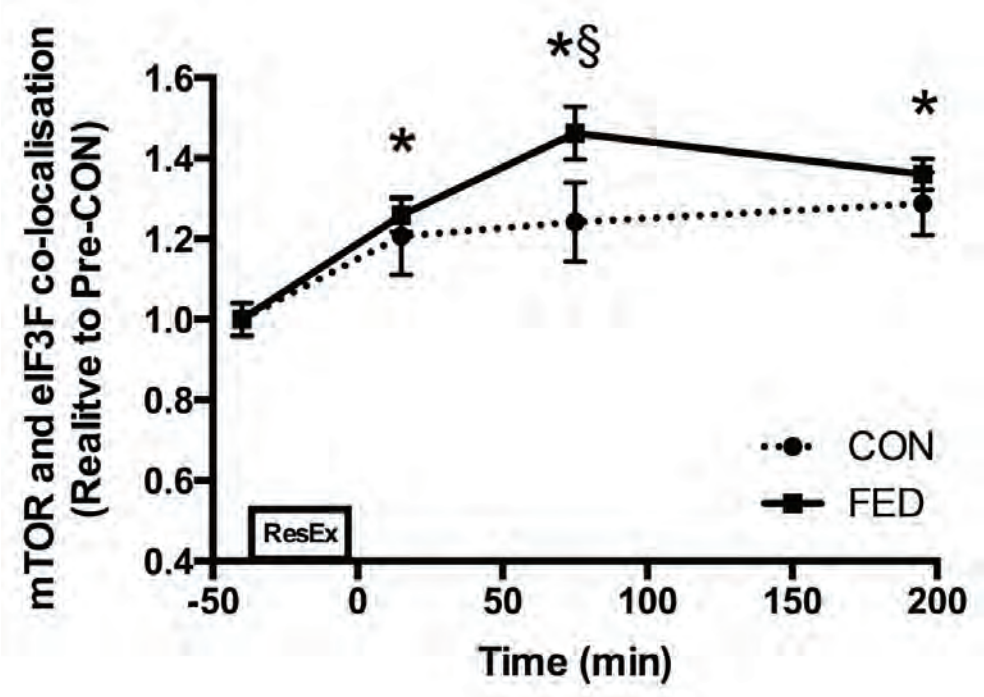

Figure 5.4.8c Quantification of mTOR and eIF3f interaction following resistance exercise. Circles represent CON, squares represent FED. All data presented relative to the Pre exercise CON. Data presented as mean ± SEM (n=7/group). * Significantly different to PRE-CON (P<0.05). § Significantly different between groups (P<0.05).

5.4.9 Disassociation between Rheb and its inhibitor Tuberin in response to one bout of resistance exercise in young healthy male skeletal muscle

As shown in Figure 5.4.9a/b/c, Tuberin is found mainly localized on the plasma membrane, colocalsiing with Rheb in basal human skeletal muscle (0.45±0.02 for CON; 0.46±0.01 for FED). It was observed Tuberin disassociated from Rheb immediately post resistance exercise (0.41±0.02 for CON; 0.41±0.01 for FED, $p<0.05$), and kept on decreasing 1h post exercise (0.39±0.03 for CON; 0.40±0.01 for FED, $p<0.05$). Disassociation between Tuberin and Rheb was also significant 3h post exercise (0.41±0.01 for CON; 0.36±0.01 for FED, $p<0.05$).

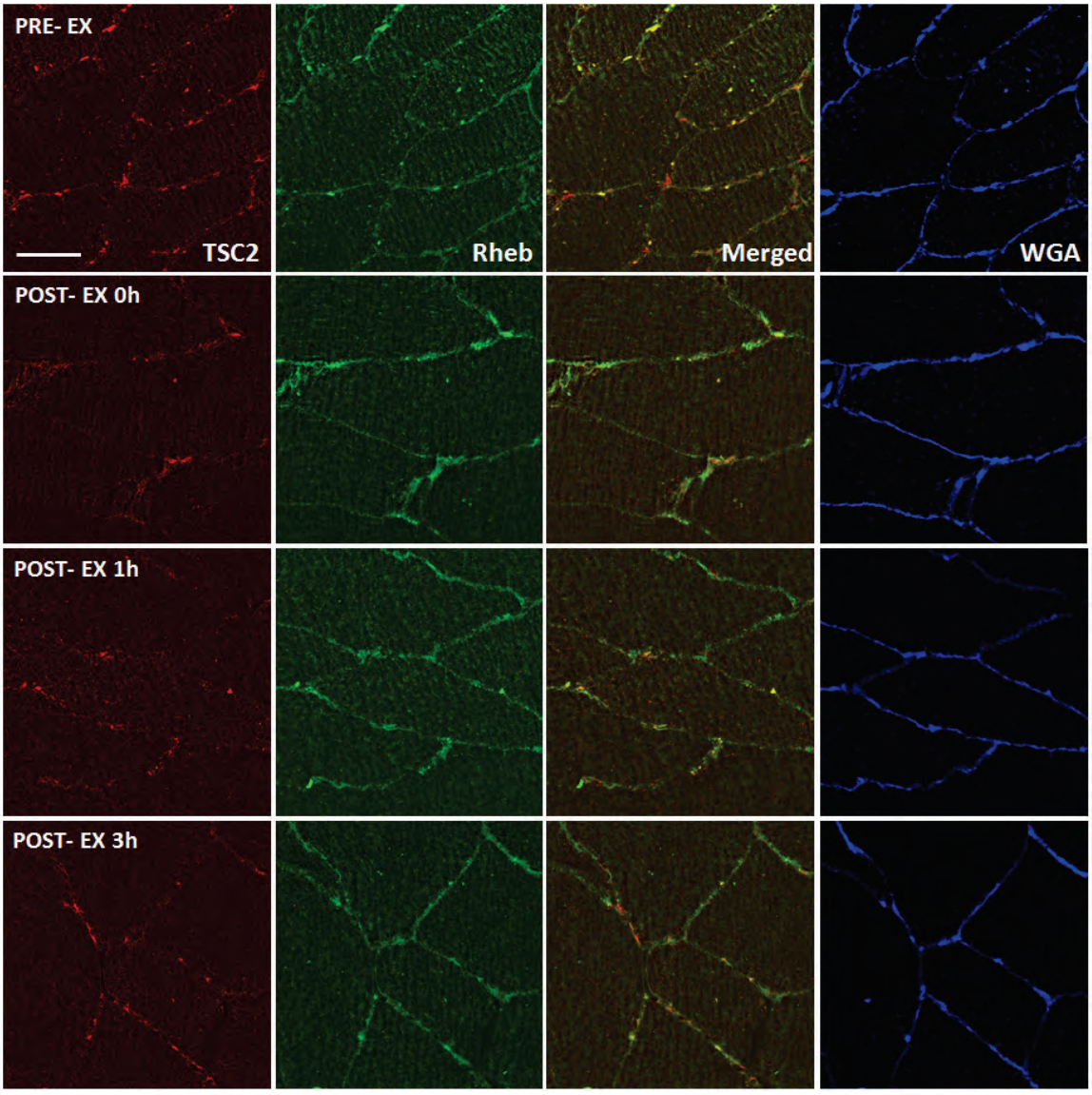

Figure 5.4.9a Tuberin disassociates from Rheb- positive area in response to one bout of resistance exercise in human skeletal muscle. A) Tuberin (TSC1/TSC2) primary antibody was stained with secondary antibody conjugated with Alex fluor® 594nm fluorophore. Images were taken under HeNe 594nm laser, x40/1.2 NA (water) objective len, Zeiss LSM510 confocal microscope. B) Rheb proteins were incubated with the primary antibody combined with secondary antibody conjugated with Alex fluor® 488nm fluorophore. Images were taken under 488nm Argon laser, x40/1.2 NA (water) objective len. C) Composite images were merged between Tuberin signal and Rheb fluorescence. D) Plasma membrane was stained with WGA conjugated with Alexa Fluor® 350 fluorescences. Images were taken under 405nm Diode laser, x40 /1.2 NA (water) objective len. PRE-EX means before resistance exercise, and POST- EX 0h, 1h, 3h stand for 0 hour, 1 hour and 3 hours post exercise, respectively. Scale bar 50µm.

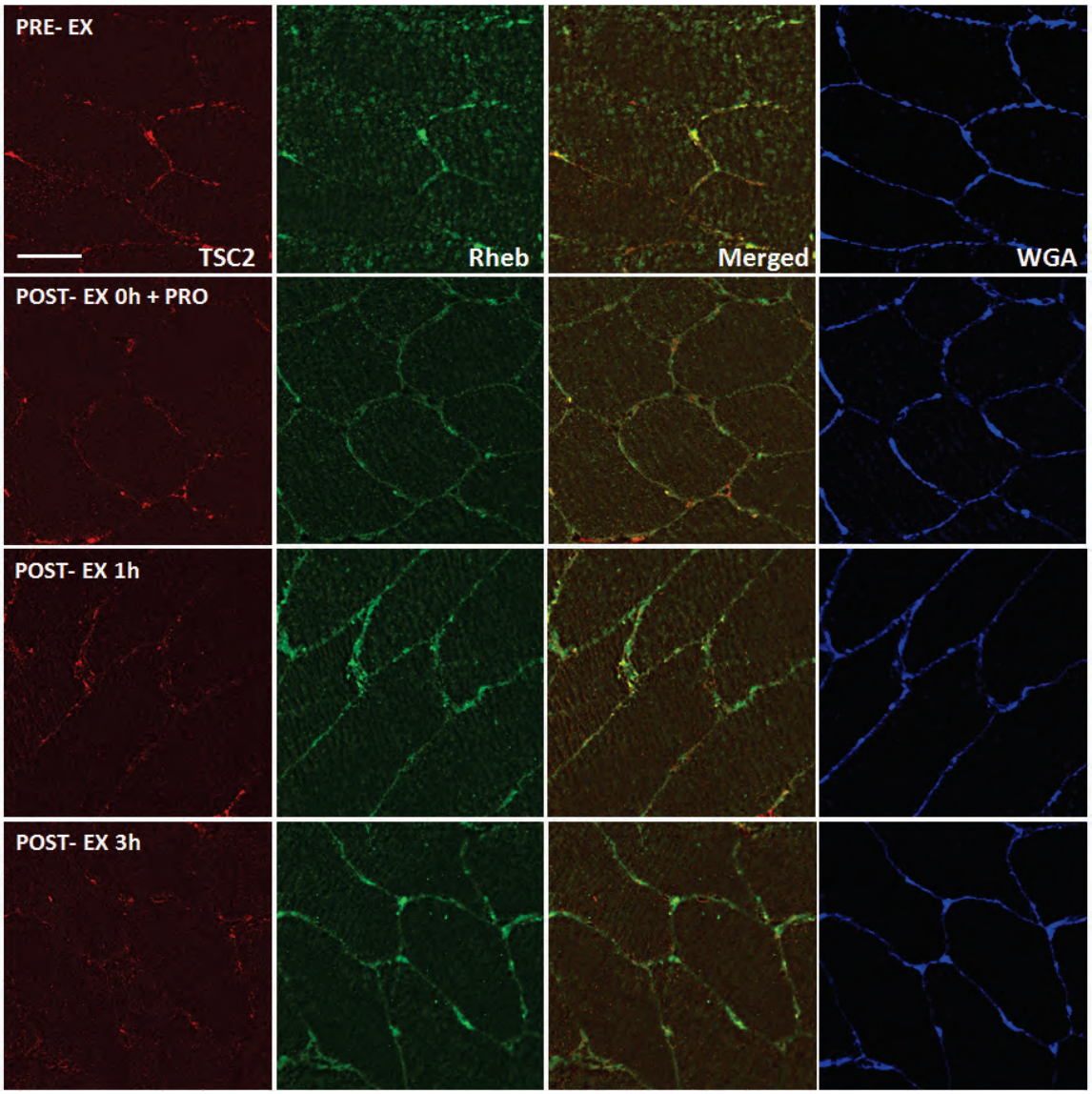

Figure 5.4.9b Tuberin disassociates from Rheb- positive area in response to one bout of resistance exercise combined with nutrition supplementation in human skeletal muscle. A) Tuberin (TSC1/TSC2) primary antibody was stained with secondary antibody conjugated with Alex fluor® 594nm fluorophore. Images were taken under HeNe 594nm laser, x40/1.2 NA (water) objective len, Zeiss LSM510 confocal microscope. B) Rheb proteins were incubated with the primary antibody combined with secondary antibody conjugated with Alex fluor® 488nm fluorophore. Images are taken under 488nm Argon laser, x40/1.2 NA (water) objective len. C) Composite images were merged between Tuberin signal and Rheb fluorescence. D) Plasma membrane was stained with WGA conjugated with Alexa Fluor® 350 fluorescences. Images were taken under 405nm Diode laser, x40 /1.2 NA (water) objective len. PRE-EX means before

resistance exercise, and POST- EX 0h, 1h, 3h stand for 0 hour, 1 hour and 3 hours post exercise, respectively. Scale bar 50μm.

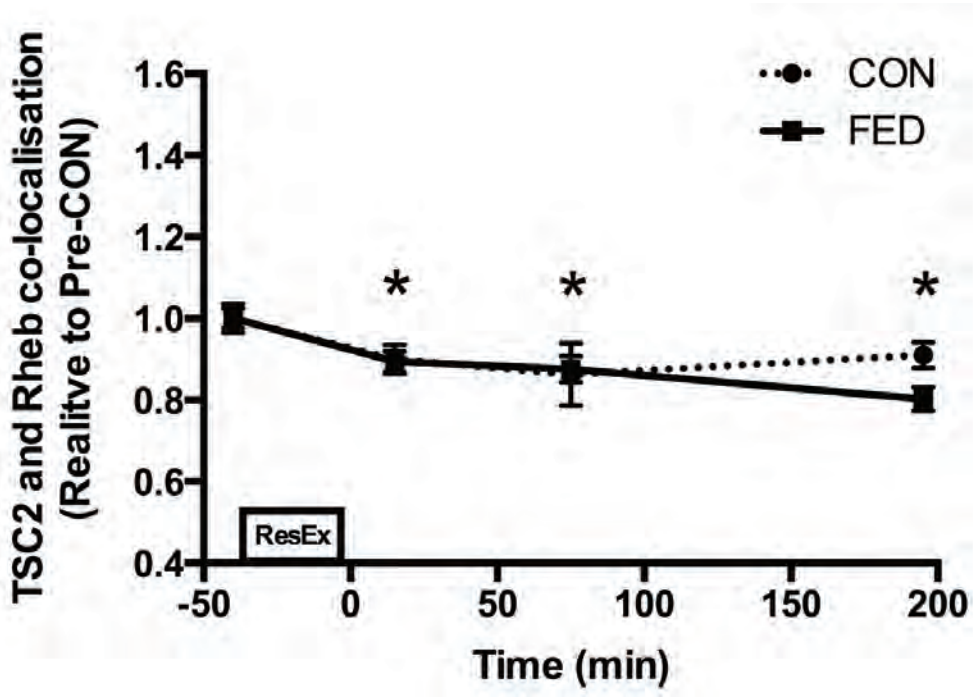

Figure 5.4.9c Quantification of TSC2 and Rheb dissociation following resistance exercise. Circles represent CON, squares represent FED. All data presented relative to the Pre exercise CON. Data presented as mean ± SEM (n=7/group). * Significantly different to PRE-CON (P<0.05).

5.4.10 Disassociation between Tuberin and plasma membrane in response to one bout of resistance exercise in young healthy male skeletal muscle

To verify disassociation of Tuberin from cell membrane, colocalisation between Tuberin and plasma membrane area was further investigated. As shown in Figure 5.4.10a/b, Tuberin disassociateed from plasma membrane immediately post resistance exercise (0.22±0.02 for CON; 0.25±0.01 for FED, $p<0.05$) compared with basal level (0.28±0.02 for CON; 0.30±0.02 for FED). Then the association between Tuberin and cell membrane is partially increased in both groups at 1h and 3h post exercise, though deassociation of Tuberin from cell membrane was also significant compared with pre exercise

(1h post exercise, 0.23±0.02 for CON and 0.29±0.01 for FED, $p<0.05$; 3h post exercise, 0.28±0.02 for CON and 0.26±0.02 for FED, $p<0.05$).

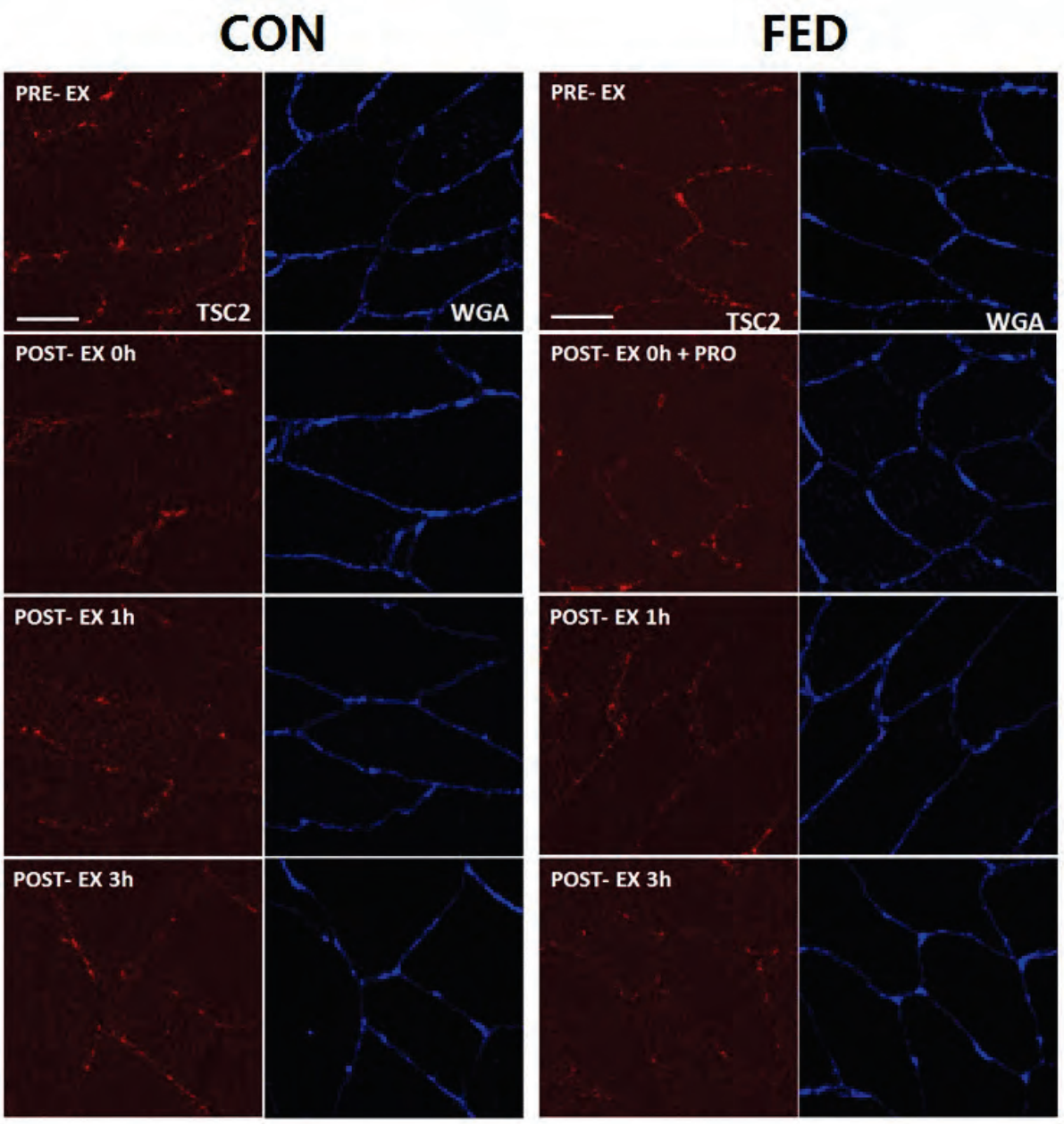

Figure 5.4.10a Tuberin disassociates from cell membrane in response to one bout of resistance exercise in human skeletal muscle at energy- free (CON) and nutritional (FED) conditions. Tuberin (TSC1/TSC2) primary antibody was stained with secondary antibody conjugated with Alex fluor® 594nm fluorophore and cell membrane. Images were taken under HeNe 594nm laser, x40/1.2 NA (water) objective len, Zeiss LSM510 confocal microscope. Plasma membrane

was stained with WGA conjugated with Alexa Fluor® 350 fluorescences. Images were taken under 405nm Diode laser, x40 /1.2 NA (water) objective len. PRE-EX means before resistance exercise, and POST- EX 0h, 1h, 3h stand for 0 hour, 1 hour and 3 hours post exercise, respectively. Scale bar 50μm.

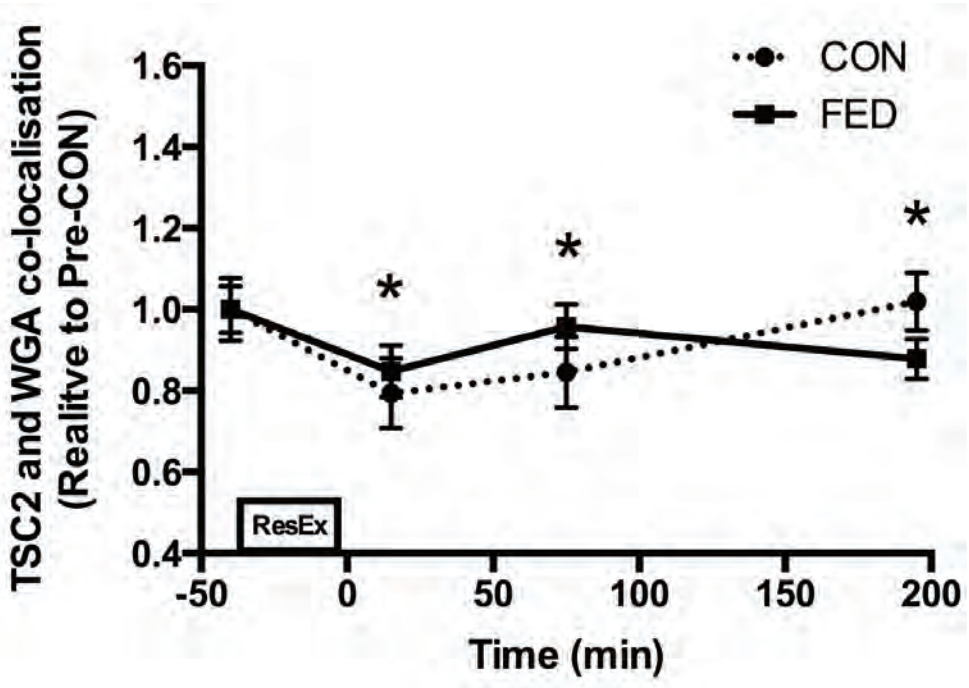

Figure 5.4.10b Quantification of TSC2 dissociation from plasma membrane following resistance exercise. Circles represent CON, squares represent FED. All data presented relative to the Pre exercise CON. Data presented as mean ± SEM (n=7/group). * Significantly different to PRE-CON (P<0.05).

5.5 Discussion

The protein complex mTORC1 is critical for regulating skeletal muscle mass [27]. Numerous studies in humans have demonstrated that mTORC1 activity is increased during the post-exercise period both with and without nutrient (e.g. amino acids) ingestion [1]. Inhibition of mTORC1 activity using the mTORC1 specific inhibitor rapamycin blocks resistance-exercise mediated increases in protein synthesis, indicating that mTORC1 activity is required to activate muscle protein synthesis in humans [4, 5]. Despite this body of work, additional research is warranted to better understand how mTORC1 is activated in skeletal muscle in response to anabolic stimuli such as resistance exercise (both with and without nutrient ingestion) and how mTORC1 activates pathways regulating mRNA translation and, hence, muscle protein synthesis [28]. To this end, utilising immunofluorescence approaches in human skeletal muscle we have detailed, for the first time, intracellular mTOR localisation and protein complex co-localisation in response to an anabolic stimulus. We demonstrate that mTOR co-localises with the lysosome in basal conditions and that these complexes translocate to the cell periphery, in close proximity to capillaries, in response to resistance exercise. In parallel, we also observed that resistance exercise stimulates TSC2 dissociation from Rheb and that this leads a reduction in TSC2 abundance at the cell membrane, which would be consistent with an enhanced mTOR kinase activity. Although post-exercise ingestion of PRO/CHO had little effect on mTOR translocation or TSC2-Rheb-mTOR interaction, nutrient ingestion did increase mTOR and eIF3f association post exercise; this interaction may contribute to the well-documented enhancement of muscle protein synthesis after exercise in the fed state [11, 12].

Recent work from the Hornberger lab [19] in mice has suggested that recruitment of the catalytic component of mTORC1 (mTOR) to the late lysosomal membrane is an important event initiating the protein synthetic response. We therefore sought to utilise immunofluorescence approaches to detail this event in human skeletal muscle in response to resistance exercise during a post-exercise period in which rates of muscle protein synthesis are known to be elevated [7, 8]. Additionally, we investigated whether consumption of a protein/carbohydrate beverage post exercise, which would further enhance the muscle protein synthetic response [13, 23, 25], would augment the mTOR compartmentalisation

during recovery compared to an energy-free control. In contrast to cell and rodent studies, we observed interaction of mTOR with the lysosome in basal conditions, an interaction that is retained during the 3h post-exercise recovery period independently of concomitant protein/carbohydrate ingestion. Thus, recruitment of mTOR to the late-lysosome compartment does not appear to be enhanced relative to basal conditions in response to anabolic stimuli such as amino acids and/or muscle contraction in human skeletal muscle, which is in contrast to reports in cell [15] and rodent [19] models. The explanation for the discrepancy between the present and previous data is not readily apparent; however may be due to different nutrient availability in human skeletal muscle compared to cell-based models. For example, dissociation of mTOR from the lysosome in cell-based models has been observed in amino acid free conditions [15], which is a scenario that would be more reflective of chronic fasting that could initiate an autophagic response [29]. Interestingly, in the same in vitro model, mild amino acid reduction does not result in mTOR dissociation from the lysosome and therefore mTOR activity is unaltered [29]. Similar results could also be expected in human muscle given that muscle protein breakdown (as part of the normal 'turnover' of muscle protein pools) functions to replenish the intracellular amino acid pool to support basal rates of muscle protein synthesis [30]; as such, even in the fasted state there may be sufficient intracellular amino acids to maintain mTOR localization with the lysosomal membrane. Thus, constant mTOR association with the lysosome may reflect amino acid availability and the requirement of mTOR to maintain basal protein synthesis in resting human skeletal muscle.

Our initial hypothesis was that mTOR translocation to the lysosome would be the key activation event for mTOR in response to an exercise stimulus. In contrast, our data clearly demonstrates that mTOR/LAMP2 translocation to the cell periphery is a principal event relocating mTOR following resistance exercise. The direct physiological relevance of this event is currently unclear, however it has previously been suggested that lysosome migration to the cell periphery can act as a stimulus for mTORC1 activation [29]. Nutrition depletion resulted in decreased cells characterised with peripheral lysosome distribution, while nutrition replenishment recovered the lysosome peripheral position [29]. Overexpression of two kinesin superfamily members (KIF1Bβ and KIF2) that target lysosomes to the

cell periphery increased mTORC1 activity. In contrast, siRNA-mediated knockdown of KIF1Bβ and KIF2 targeted lysosomes to peri-nuclear regions, which subsequently reduced mTORC1 activity, and initiated autophagy [29]. As such, lysosomal distribution would appear to be a key initial event in the increased activity of mTOR in response to nutrient stimulation. Our finding of a similar mTOR/LAMP2 translocation event following resistance exercise that is uninfluenced by protein/carbohydrate ingestion would suggest that mTOR/LAMP2 translocation is important for the initial activation of mRNA translation after exercise in human skeletal muscle.

It has been reported that mTOR associates with Rab7 following activation in cultured cells *in vitro* [40]. In consistence, our study in human skeletal muscle also found that mTOR translocated to colocalise with Rab7- positive compartment on the plasma membrane following exercise in both fast and fed status. Although Rab7 and Lamp2 both participate in regulating late lysosome formation, they may involve in disparate activities [20]. Rab7 is a key protein controlling the traffic between early and late endosome [20], while Lamp2 is important for maintaining the integrity of peri- lysosome membrane [20]. Endosome membrane marked with Rab7 is thought to be matured late endosome, which then infuses with lysosome to form the late lysosome [20]. In our investigation around the relationship between Rab7 and Lamp2, it was found that Rab7 translocated to colocalise with Lamp2 in response to muscle contraction, indicating the formation of late lysosome. In combination with result between mTOR and Rab7, these finding suggest that Rab7 is associated with mTOR activation on late lysosome membrane in response to mechanistic contraction in human skeletal muscle. Moreover, association between mTORC with Rab7 was enhanced 1h post exercise in fed status, revealing important roles of nutrition supplementation in stimulating mTOR/ Rab7 interaction.

Previous studies have demonstrated that mTOR interaction with GTP bound Rheb is required to elicit complete mTORC1 activation [31]. Rheb is a small GTPase [31] and is activated by the GTPase activating protein TSC2, which converts GTP-Rheb into GDP-Rheb rendering it unable to activate mTORC1 [32, 18]. Rheb is able to bind to the catalytic domain of mTOR [33, 34] only when associated with GTP [35]. It was recently reported that eccentric contraction in mouse skeletal muscle leads to TSC2 dissociation from the lysosome, which would facilitate the mTOR and GTP-Rheb interaction

[19]. In contrast, we observed TSC2 to be located at the plasma membrane, co-localising with Rheb as opposed to at the lysosome. In our hands, TSC2 dissociated from the membrane following resistance exercise, leaving Rheb and the mTOR/LAMP2 complex to co-localise. It is unclear why the location of this event is different in human as opposed to murine skeletal muscle. It may be reflective of muscle fibre-type differences (predominantly fast-twitch in mouse vs mixed fibres in human), the mode of exercise (eccentric vs concentric), the degree of contraction/recruitment, the nutrient availability in each scenario, and/or interspecies differences. Irrespective, our data are in agreement with Jacobs *et al* [19] reporting that TSC2 dissociation from mTOR positive regions appears to be a key post-exercise event following an anabolic stimulus in human skeletal muscle.

In addition to TSC2-Rheb-mTOR co-localisation, we next sought to examine whether mTOR translocation to the plasma membrane may serve to direct mTOR/LAMP2 to other substrates involved in the initiation of protein synthesis. We report novel data indicating that mTOR associates with the regulatory subunit of the eukaryotic initiation factor 3 complex, eIF3f, post-exercise in both the CON and FED groups. The eIF3 complex is key to the initiation of protein synthesis serving as a scaffold for mTOR and S6K1 interaction, leading to the assembly of the pre-initiation complex [36, 37]. mTOR and eIF3f co-localisation occurred rapidly post-exercise in both the CON and FED groups, which is consistent with the ability of resistance exercise to enhance amino acid uptake and muscle protein synthesis early in recovery [7, 38]. However this interaction was significantly greater in the FED group 1h post exercise, suggesting that feeding may enhance mTOR-eIF3f assembly post-exercise. Given that muscle protein synthesis and the phosphorylation of mTORC1 substrates is amplified post-exercise following protein/carbohydrate ingestion [13, 25], it would appear that the increased mTOR-eIF3f interaction observed in the FED group may be an important mediator of post-exercise nutrition on mTORC1 dependent signaling and potentially muscle protein synthesis.

In addition, we also observed that mTOR/LAMP2 complexes associated with the microvasculature (UEA-I positive regions) at the plasma membrane post exercise. The precise reason for this response is currently unclear, however mTOR association with the microvasculature would in theory position mTOR in close proximity to nutrient provision delivered from the bloodstream. mTOR interaction

with UEA-I positive cells increased equally post-exercise in both the CON and FED groups suggesting that mTOR interaction with the microvasculature is not influenced by protein/carbohydrate ingestion in healthy young men after exercise. Collectively, this adds further support to the hypothesis that mTOR translocation is a mechanically driven event and that protein/carbohydrate facilitating mTOR interaction with protein partners (eIF3f) rather than altering the localisation of mTOR/LAMP2 complexes.

In summary, utilising immunofluorescence approaches in human skeletal muscle, we have detailed for the first time intracellular mTOR localisation and protein complex co-localisation in response to an anabolic stimulus. We demonstrated that mTOR co-localised with the lysosome in basal conditions and that these complexes translocated to the cell periphery in response to resistance exercise. In parallel, resistance exercise stimulates TSC2 dissociation from Rheb and leads a reduction in TSC2 abundance at the cell membrane, which would be consistent with an enhanced mTOR kinase activity. Although post-exercise ingestion of protein/carbohydrate had little effect on mTOR translocation or TSC2-Rheb-mTOR interaction, nutrient ingestion did increase mTOR and eIF3f association post exercise; this effect may contribute to the well-documented enhancement of muscle protein synthesis after exercise in the fed state. Collectively, our data highlight the potential importance of mTOR-lysosomal cellular partitioning for mTORC1 function following a growth stimulus and illustrates another level of complexity to the molecular control of protein synthesis following resistance exercise and nutrition in human skeletal muscle. Future studies could include concurrent measures of muscle protein synthesis and/or effector enzyme activity [39] to further elucidate the physiological significance of mTORC1 complex assembly and intracellular translocation in human skeletal muscle after exercise.

5.6 Acknowledgement

Here we thank Dr. Daniel R. Moore in University of Toronto in Canada, who collected the muscle samples and kindly sent them to us for immunofluorescences histological staining.

5.7 Reference

[1] Burd, Nicholas A., Jason E. Tang, Daniel R. Moore, and Stuart M. Phillips. Exercise training and protein metabolism: influences of contraction, protein intake, and sex-based differences. Journal of Applied Physiology 106, no. 5 (2009): 1692-1701.

[2] Laplante, Mathieu, and David M. Sabatini. mTOR signaling in growth control and disease. Cell 149, no. 2 (2012): 274-293.

[3] Betz, Charles, and Michael N. Hall. Where is mTOR and what is it doing there?. The Journal of cell biology 203, no. 4 (2013): 563-574.

[4] Drummond, Micah J., Christopher S. Fry, Erin L. Glynn, Hans C. Dreyer, Shaheen Dhanani, Kyle L. Timmerman, Elena Volpi, and Blake B. Rasmussen. Rapamycin administration in humans blocks the contraction‐induced increase in skeletal muscle protein synthesis. The Journal of physiology 587, no. 7 (2009): 1535-1546.

[5] Dickinson, Jared M., Christopher S. Fry, Micah J. Drummond, David M. Gundermann, Dillon K. Walker, Erin L. Glynn, Kyle L. Timmerman, Shaheen Dhanani, Elena Volpi, and Blake B. Rasmussen. Mammalian target of rapamycin complex 1 activation is required for the stimulation of human skeletal muscle protein synthesis by essential amino acids. The Journal of nutrition 141, no. 5 (2011): 856-862.

[6] McGlory, Chris, and Stuart M. Phillips. Assessing the regulation of skeletal muscle plasticity in response to protein ingestion and resistance exercise: recent developments. Current Opinion in Clinical Nutrition & Metabolic Care 17, no. 5 (2014): 412-417.

[7] Biolo, Gianni, Sergio P. Maggi, Bradley D. Williams, KEVIN D. Tipton, and Robert R. Wolfe. Increased rates of muscle protein turnover and amino acid transport after resistance exercise in humans. American Journal of Physiology-Endocrinology And Metabolism 268, no. 3 (1995): E514-E520.

[8] Phillips, Stuart M., Kevin D. Tipton, Asle Aarsland, Steven E. Wolf, and Robert R. Wolfe. Mixed muscle protein synthesis and breakdown after resistance exercise in humans. American Journal of Physiology-Endocrinology And Metabolism 273, no. 1 (1997): E99-E107.

[9] Eliasson, Jörgen, Thibault Elfegoun, Johnny Nilsson, Rickard Köhnke, Björn Ekblom, and Eva Blomstrand. Maximal lengthening contractions increase p70 S6 kinase phosphorylation in human skeletal muscle in the absence of nutritional supply. American Journal of Physiology-Endocrinology and Metabolism 291, no. 6 (2006): E1197-E1205.

[10] Burd, Nicholas A., Daniel WD West, Daniel R. Moore, Philip J. Atherton, Aaron W. Staples, Todd Prior, Jason E. Tang, Michael J. Rennie, Steven K. Baker, and Stuart M. Phillips. Enhanced amino acid sensitivity of myofibrillar protein synthesis persists for up to 24 h after resistance exercise in young men. The Journal of Nutrition 141, no. 4 (2011): 568-573.

[11] Biolo, Gianni, Kevin D. Tipton, Samuel Klein, and Robert R. Wolfe. An abundant supply of amino acids enhances the metabolic effect of exercise on muscle protein. American Journal of Physiology-Endocrinology and Metabolism 273, no. 1 (1997): E122-E129.

[12] Børsheim, Elisabet, Kevin D. Tipton, Steven E. Wolf, and Robert R. Wolfe. Essential amino acids and muscle protein recovery from resistance exercise. American Journal of Physiology-Endocrinology And Metabolism 283, no. 4 (2002): E648-E657.

[13] Dreyer, Hans C., Micah J. Drummond, Bart Pennings, Satoshi Fujita, Erin L. Glynn, David L. Chinkes, Shaheen Dhanani, Elena Volpi, and Blake B. Rasmussen. Leucine-enriched essential amino acid and carbohydrate ingestion following resistance exercise enhances mTOR signaling and protein synthesis in human muscle. American Journal of Physiology-Endocrinology and Metabolism 294, no. 2 (2008): E392-E400.

[14] Moore, D. R., P. J. Atherton, M. J. Rennie, M. A. Tarnopolsky, and S. M. Phillips. Resistance exercise enhances mTOR and MAPK signalling in human muscle over that seen at rest after bolus protein ingestion. Acta Physiologica 201, no. 3 (2011): 365-372.

[15] Sancak, Yasemin, Liron Bar-Peled, Roberto Zoncu, Andrew L. Markhard, Shigeyuki Nada, and David M. Sabatini. Ragulator-Rag complex targets mTORC1 to the lysosomal surface and is necessary for its activation by amino acids. Cell 141, no. 2 (2010): 290-303.

[16] Inoki, Ken, Yong Li, Tian Xu, and Kun-Liang Guan. Rheb GTPase is a direct target of TSC2 GAP activity and regulates mTOR signaling. Genes & Development 17, no. 15 (2003): 1829-1834.

[17] Manning, Brendan D., Andrew R. Tee, M. Nicole Logsdon, John Blenis, and Lewis C. Cantley. Identification of the tuberous sclerosis complex-2 tumor suppressor gene product tuberin as a target of the phosphoinositide 3-kinase/akt pathway. Molecular Cell 10, no. 1 (2002): 151-162.

[18] Tee, Andrew R., Brendan D. Manning, Philippe P. Roux, Lewis C. Cantley, and John Blenis. Tuberous sclerosis complex gene products, Tuberin and Hamartin, control mTOR signaling by acting as a GTPase-activating protein complex toward Rheb. Current Biology 13, no. 15 (2003): 1259-1268.

[19] Jacobs, Brittany L., Jae‐Sung You, John W. Frey, Craig A. Goodman, David M. Gundermann, and Troy A. Hornberger. Eccentric contractions increase the phosphorylation of tuberous sclerosis complex‐2 (TSC2) and alter the targeting of TSC2 and the mechanistic target of rapamycin to the lysosome. The Journal of Physiology 591, no. 18 (2013): 4611-4620.

[20] Jacobs, Brittany L., Craig A. Goodman, and Troy A. Hornberger. The mechanical activation of mTOR signaling: an emerging role for late endosome/lysosomal targeting. Journal of Muscle Research and Cell Motility 35, no. 1 (2014): 11-21.

[21] Bergström, Jonas. Percutaneous needle biopsy of skeletal muscle in physiological and clinical research. Scandinavian Journal of Clinical & Laboratory Investigation 35, no. 7 (1975): 609-616.

[22] Burd, Nicholas A., Daniel WD West, Aaron W. Staples, Philip J. Atherton, Jeff M. Baker, Daniel R. Moore, Andrew M. Holwerda et al. Low-load high volume resistance exercise stimulates muscle protein synthesis more than high-load low volume resistance exercise in young men. PLoS One 5, no. 8 (2010): e12033.

[23] Moore, Daniel R., Jason E. Tang, Nicholas A. Burd, Tracy Rerecich, Mark A. Tarnopolsky, and Stuart M. Phillips. Differential stimulation of myofibrillar and sarcoplasmic protein synthesis with protein ingestion at rest and after resistance exercise. The Journal of Physiology 587, no. 4 (2009): 897-904.

[24] Moore, Daniel R., Meghann J. Robinson, Jessica L. Fry, Jason E. Tang, Elisa I. Glover, Sarah B. Wilkinson, Todd Prior, Mark A. Tarnopolsky, and Stuart M. Phillips. Ingested protein dose response of muscle and albumin protein synthesis after resistance exercise in young men. The American Journal of Clinical Nutrition 89, no. 1 (2009): 161-168.

[25] Staples, Aaron W., Nicholas A. Burd, Daniel WD West, Katharine D. Currie, Philip J. Atherton, Daniel R. Moore, Michael J. Rennie, Maureen J. Macdonald, Steven K. Baker, and Stuart M. Phillips. Carbohydrate does not augment exercise-induced protein accretion versus protein alone. Medicine and Science in Sports and Exercise 43 (2010): 1154-61.

[26] Greenhaff, Paul L., L. G. Karagounis, Nicholas Peirce, Elizabeth J. Simpson, Michelle Hazell, Robert Layfield, Henning Wackerhage et al. Disassociation between the effects of amino acids and insulin on signaling, ubiquitin ligases, and protein turnover in human muscle. American Journal of Physiology-Endocrinology and Metabolism 295, no. 3 (2008): E595-E604.

[27] Bodine, Sue C., Trevor N. Stitt, Michael Gonzalez, William O. Kline, Gretchen L. Stover, Roy Bauerlein, Elizabeth Zlotchenko et al. Akt/mTOR pathway is a crucial regulator of skeletal muscle hypertrophy and can prevent muscle atrophy in vivo. Nature Cell Biology 3, no. 11 (2001): 1014-1019.

[28] Philp, Andrew, D. Lee Hamilton, and Keith Baar. Signals mediating skeletal muscle remodeling by resistance exercise: PI3-kinase independent activation of mTORC1. Journal of Applied Physiology 110, no. 2 (2011): 561-568.

[29] Korolchuk, Viktor I., Shinji Saiki, Maike Lichtenberg, Farah H. Siddiqi, Esteban A. Roberts, Sara Imarisio, Luca Jahreiss et al. Lysosomal positioning coordinates cellular nutrient responses. Nature Cell Biology 13, no. 4 (2011): 453-460.

[30] Fujita, Satoshi, Blake B. Rasmussen, Jill A. Bell, Jerson G. Cadenas, and Elena Volpi. Basal muscle intracellular amino acid kinetics in women and men. American Journal of Physiology-Endocrinology and Metabolism 292, no. 1 (2007): E77-E83.

[31] Aspuria, Paul-Joseph, and Fuyuhiko Tamanoi. The Rheb family of GTP-binding proteins. Cellular Signalling 16, no. 10 (2004): 1105-1112.

[32] Tee, Andrew R., Diane C. Fingar, Brendan D. Manning, David J. Kwiatkowski, Lewis C. Cantley, and John Blenis. Tuberous sclerosis complex-1 and-2 gene products function together to inhibit mammalian target of rapamycin (mTOR)-mediated downstream signaling. Proceedings of the National Academy of Sciences 99, no. 21 (2002): 13571-13576.

[33] Long, Xiaomeng, Yenshou Lin, Sara Ortiz-Vega, Kazuyoshi Yonezawa, and Joseph Avruch. Rheb binds and regulates the mTOR kinase. Current Biology 15, no. 8 (2005): 702-713.

[34] Long, Xiaomeng, Sara Ortiz-Vega, Yenshou Lin, and Joseph Avruch. Rheb binding to mammalian target of rapamycin (mTOR) is regulated by amino acid sufficiency. Journal of Biological Chemistry 280, no. 25 (2005): 23433-23436.

[35] Avruch, Joseph, Xiaomeng Long, Yenshou Lin, Sara Ortiz-Vega, Joseph Rapley, Angela Papageorgiou, Noriko Oshiro, and Ushio Kikkawa. Activation of mTORC1 in two steps: Rheb-GTP activation of catalytic function and increased binding of substrates to raptor1. Biochemical Society Transactions 37, no. 1 (2009): 223.

[36] Holz, Marina K., Bryan A. Ballif, Steven P. Gygi, and John Blenis. mTOR and S6K1 mediate assembly of the translation preinitiation complex through dynamic protein interchange and ordered phosphorylation events. Cell 123, no. 4 (2005): 569-580.

[37] Harris, Thurl E., An Chi, Jeffrey Shabanowitz, Donald F. Hunt, Robert E. Rhoads, and John C. Lawrence. mTOR‐dependent stimulation of the association of eIF4G and eIF3 by insulin. The EMBO journal 25, no. 8 (2006): 1659-1668.

[38] Dreyer, Hans C., Satoshi Fujita, Jerson G. Cadenas, David L. Chinkes, Elena Volpi, and Blake B. Rasmussen. Resistance exercise increases AMPK activity and reduces 4E‐BP1 phosphorylation and protein synthesis in human skeletal muscle. The Journal of Physiology 576, no. 2 (2006): 613-624.

[39] McGlory, Chris, Amanda White, Caroline Treins, Barry Drust, Graeme L. Close, Don PM MacLaren, Iain T. Campbell et al. Application of the [γ-32P] ATP kinase assay to study anabolic signaling in human skeletal muscle. Journal of Applied Physiology 116, no. 5 (2014): 504-513.

[40] Sancak, Yasemin, Timothy R. Peterson, Yoav D. Shaul, Robert A. Lindquist, Carson C. Thoreen, Liron Bar-Peled, and David M. Sabatini. The Rag GTPases bind raptor and mediate amino acid signaling to mTORC1. Science 320, no. 5882 (2008): 1496-1501.

Chapter 6

General Discussion

6.1 Introduction

Maintenance of skeletal muscle mass and function are of great importance to human wellbeing and health. Deterioration in skeletal muscle mass and strength lead to muscle atrophy, as well as other associated chronic diseases [1]. Resistance exercise is an efficient strategy to increase muscle strength and muscle hypertrophy in human skeletal muscle, the latter of which is mediated by exercise-induced increase in muscle protein synthesis, which subsequently increases net protein balance [2]. Nutritional supplementation of protein also increases protein synthesis, with the combination of protein ingestion and resistance exercise having an additive stimulatory effect on protein synthesis beyond either in isolation [3].

The molecular regulation of skeletal muscle mass is generally regarded to be mediated by the serine/ threonine protein kinase mTOR, which when active stimulates protein synthesis and attenuates protein degradation [4]. mTOR forms a protein complex (mTORC) which is constituted by two subtypes, mTORC1 and mTORC2. Structural differences between the two subtypes lies in the associated subunits constituting mTORC, which alters the different substrates they bind to, as well as the downstream processes they regulate [4]. mTORC1 contains raptor, GßL, DEPTOR and PRAS40 and is sensitive to rapamycin inhibition [5]. In contrast, mTORC 2 consists of rictor, GßL, Sin1, DEPTOR and Protor/PRR5, and is insensitive to rapamycin [5]. mTORC1 is widely studied and reported to activate protein translation initiation events in response to anabolic stimuli such as insulin and nutrition supplementation [4, 5]. Acute administration of rapamycin blocks the anabolic effects of resistance and AA ingestion in human skeletal muscle [6, 7].

As mTOR plays a pivotal role in activating protein synthesis and muscle hypertrophy, it is relevant to investigate the molecular mechanisms of mTOR activation. Current knowledge regarding the physiological regulation of mTOR activity in human skeletal muscle is mainly from phosphorylation-specific profiling of the mTOR signaling cascade via the immunoblotting technique [8]. The other strategy examining mTOR activity is to measure the downstream substrates mTOR regulates (*e.g.* S6K1, 4E-BP). Consistent with the stimulatory effects of resistance exercise on muscle protein synthesis in the fasted state [9, 10], the phosphorylation of mTOR substrates is also increased, indicating

the activation of mTOR signal pathway following resistance exercise [11] with this response maintained for at least 24h post- exercise in young men [12]. Furthermore, ingestion of nutrients including glucose and AA (either orally or intravenously) augments the rate of the protein synthesis in human skeletal muscle post exercise [13, 14].

Beyond immunoblotting approaches, studies *in vitro* have revealed that subcellular distribution of mTOR and protein- protein association between mTOR and its regulators may be important to mTOR activation in response to physiological stimuli [17]. For example, following AA stimulation, mTOR is visualized to translocate to the lysosome area to associate with the GTP loaded ras- homolog enriched in brain (Rheb) to be fully activated [18]. This phenomenon is reversed by the removal of AA, which results in the dissociation of mTOR from the lysosome and mTOR degradation [18]. The interaction between mTOR and Rheb is maintained at basal levels through restricting Rheb under the GDP-bound status mediated by the activity of tuberous sclerosis complex (TSC) proteins TSC1 and TSC2 [19]. Phosphorylation of TSC2 by Akt causes TSC2 inactivation [20], leading to Rheb disassociated from TSC2 reloading GTP to bind mTOR [21]. From skeletal muscle studies *in vivo*, it was recently reported that mTOR associated with TSC2 on lysosome in basal mouse *tibialis- anterior* skeletal muscle [22]. Eccentric muscle contraction induced disassociation of TSC2 from the lysosome, while association between mTOR and the lysosome was enhanced [22]. These reports emphasize the close relationship between mTOR intracellular distribution/ protein complex assembly and activity.

Resistance training increases the muscle protein turnover in human skeletal muscle [24]. Muscle protein synthesis is increased following resistance training, contributing to the muscle hypertrophy in human skeletal muscle [24, 25]. The mTOR signaling pathway is reported to play a key role in regulating muscle hypertrophy, as well as preventing muscle atrophy [26]. As such, increased content of phosphorylated mTOR has been reported in recovery stage following resistance training suggesting enhancement of mTOR activity is an important factor in response to the training stimulus [44].

It is known that different muscle fiber types contribute to muscle hypertrophy in a different manner [28]. Cross sectional area in type II fibers is increased more in response to resistance training than the

type I muscle fiber in human skeletal muscle, contributing to mean cross sectional area increase in mixed muscle fibers [28]. On the other hand, muscle fiber type composition is adapted to specific exercise training. Endurance exercise promotes the transformation of glycolytic muscle fibers to oxidative muscle fibers [53, 54]. Oxidative type I fibers were detected predominantly existing in skeletal muscle of athletes following long term endurance training [29]. Proportion of type IIa fibers were reported to increase following high intensity resistance training contributing to muscle hypertrophy [28, 55, 56].

Muscle protein synthesis rates were different in a muscle fiber type dependent manner in rodent models [27, 57]. Basal protein synthesis rates were correlated with the content of slow- twitch fibers in rat muscle [57]. Protein synthesis rates were decreased more significantly in type 2X and 2B fibers than other fiber types in the mouse *plantaris* muscle following a 48h food deprivation [27]. However, data on human skeletal muscle protein synthesis in different muscle fibers is limited now. Isotype infusion tracer experiment did not show significant variation of protein synthesis rates between muscles following feeding [58], revealing different metabolic composition of human myofibers from rodents. mTOR is the critical kinase participating in muscle protein synthesis regulation and resistance exercise- induced muscle hypertrophy [4, 5].

6.2 Novel findings in this thesis and relevance to the existing literature

6.2.1 Development of mTOR immunofluorescence staining approaches for human skeletal muscle

mTOR activation is important for regulating muscle protein synthesis in response to contraction and protein ingestion [5, 7]. Immunofluorescence data have been reported in cell and rodent models, highlighting the importance of mTOR cellular distribution as a critical event for its activation [18, 22, 23]. However, to date, no research has examined mTOR localization in human skeletal muscle. To address this gap in knowledge, here we report a novel immunofluorescence method to visualize mTOR and it's associating proteins in human skeletal muscle.

Systematical methods were established to validate mTOR antibodies applied in immunofluorescent staining in human skeletal muscle. We report that the antibodies we identified are specific to their targets and provide reproducible results in isolation, in addition to antibody cocktail approaches. Taking advantage of this technique, for the first time mTOR distribution was reported in human skeletal muscle *in vivo*.

A multiple antibody costaining method was developed in human skeletal muscle to further investigate mTOR translocation and protein interaction. Relying on this costaining method, microscope images about association between mTOR and regulating proteins were firstly reported in human skeletal muscle *in vivo*. Moreover, based on high quality microscopy images, image quantification methodology on mTOR and associated proteins were developed to measure mTOR content and association between mTOR and regulators/organelles in human skeletal muscle *in vivo*. Thus, the immunofluorescence staining method developed herein greatly facilitates the progression of research regarding mTOR regualtion in human skeletal muscle *in vivo*.

6.2.2 Effect of chronic resistance training on mTOR protein content in skeletal muscle

Reports emphasize the effects of resistance training on stimulating muscle protein anabolism in human [24, 25]. Acute resistance exercise activates the mTOR signal pathway for ~ 24h post exercise recovery [12] whilst mTOR protein content has been reported to increase in human skeletal muscle following resistance training [44]. Therefore, we hypothesized that total mTOR content would increase following resistance training and that the magnitude of this increase/activation would parallel gains in muscle mass in skeletal muscle. We were able to address this question as the mTOR immunofluorescence approach developed in chapter 3 allowed us to measure mTOR protein content in total muscle fibres relative to their CSA, in addition to specific muscle fibres depending on their MHC profile.

In contrast to our initial hypothesis, we found no significant increases in total mTOR content in human skeletal muscle following 10 weeks high intensity resistance training, nor any fibre-specific alteration in mTOR content relative to MHC abundance. It should also be noted that the resistance-

training program failed to elicit hypertrophy as quantified by fibre CSA or muscle mass assessed via DEXA. The lack of obvious hypertrophy in our participants was surprising and against what we expected. Importantly we did observe an increase in strength in the training group, indicating that there was training adaptation, however the lack of obvious synergy between mTOR protein content and muscle CSA may be due to the limited hypertrophy we observed in this study.

We next investigated mTOR content in different muscle fiber types. In agreement with data of total mTOR content, we did not observe an increase in mTOR content in either type I fibers or type IIx fibers. However, when we profiled the muscle fiber type composition, our data demonstrated that percentage of type IIa fibers was significantly increased post training, while proportion of type I muscle fibers was decreased following training. Exercise training has well-established effects to change MHC isoform expression by transforming a fiber type switch from type IIb to IIx and IIa and in rare cases also to type I muscle fibers [67, 68]. The mechanisms leading to muscle fiber shifting in response to resistance exercise is not clear. Motor neuron unit is thought to play an important role in regulating metabolism and signals pathway in different muscle fibers via calcium as a second messenger [60]. Myocyte enhancer factor- 2 (MEF-2) transcription factors, a muscle- enriched transcription factor, were reported to be a critical regulator in muscle formation through activating muscle- specific genes [60]. MEF2/ histone deacetylase (HDAC) signaling pathway is thought to play an indispensible role in the transformation of myofibers in response to intracellular calcium signals incurred by external physiological signals [60]. Calcineurin is another reported regulator involving in myofibers transformation, which is a sernser of contractile activity by sensing calcium fluctuations [60].Calcineurin is also found to be the upstream regulator of MEF2 [60]. Our results indicate that in response to resistance training, type IIx fibers might transform to type IIa fibers. However, it is not clear of the reduction in type I fibers proportion, which, though, has also been reported in several resistance training studies [70, 71, 72]. In our data, reduction in type IIx fibers was only 4%, while increase of type IIa fibers was 12%. Provided there were no increase of muscle fibers following training, it is interesting to investigate the increase of type IIa fibers. Considering the decrease of type

I fiber composition, it suggests a potential mechanism resulting in myofibers transformation from oxidative to glycolytic type in adaptation to training mode.

Collectively, we conclude 10 weeks high intensity resistance training in trained individuals remodels muscle fibre composition and gains in strength, rather than increasing mTOR protein content and muscle CSA either in mixed fibers or specific fibre-types after 10 weeks.

6.2.3 Effects of resistance exercise on mTOR distribution and colocalisation in the fed and fasted state.

It is well documented that resistance exercise with or without ingestion of exogenous AA stimulates mTORC1 activity in human skeletal muscle [2]. Inhibition of mTORC1 activity using the mTORC1 specific inhibitor rapamycin blocks increases in protein synthesis mediated by resistance exercise, suggesting the indispensible function of mTORC1 in activating muscle protein anabolism in humans [6, 7]. Despite these findings, little is known of the mechanisms of mTORC1 activation in skeletal muscle in response to the anabolic stimuli, as well as the mechanism of mTORC1 regulates translation and, hence, muscle protein synthesis [31].

Recent rodent studies have suggested that recruitment of the catalytic component of mTORC to the late lysosomal membrane is important to initiate protein synthesis [22]. Therefore utilizing our immunofluorescence methodology to investigate this event in human skeletal muscle in response to resistance exercise, during a post- exercise period in which rates of muscle protein synthesis are known to be elevated [9, 32]. In Addition, consumption of a protein/carbohydrate beverage post exercise has been proved to exaggerate the benefits of muscle protein balance in human [15, 16, 33]. Here we investigated if nutritional beverage ingestion post exercise would augment the mTOR compartmentalization in comparison with the energy- free exercise group.

In contrast to cell and rodents models, we visualized the association of mTOR with the late lysosome (marked by Lamp2) at basal level, and this interaction is retained during the 3h post- exercise recovery period. It suggests that recruitment of mTOR to the late- lysosome compartment is not an exclusive event initiated by the anabolic stimuli in human skeletal muscle as has been reported in cell

and rodent studies [18, 22]. It is not readily apparent on the discrepancy between the present and the previous data. However, the different nutrient availability among human skeletal muscle and rodent/ cell models may be a possible explanation. For example, dissociation of mTOR from the lysosome compartment in cell model has been visualized under AA free conditions [18], a scenario that would be more reflective as the chronic fasting to initiate the autophagic response [34]. Intriguingly, in the same *in vitro* model, reduction on AA availability does not induce the mTOR dissociation from the lysosome and therefore mTOR activity is unaltered [34]. In human muscle, the intracellular AA availability is maintained at basal level through the normal degradation of muscle proteins, which is sufficient to support the basal rates of muscle protein synthesis [35]. Therefore, the constant mTOR association with the lysosome may reflect the basal AA availability and the requirement of mTOR to maintain basal protein anabolism in resting human skeletal muscle.

The initial hypothesis was that translocation of mTOR to the lysosome compartment would be the key event for mTOR activation in response to the anabolic stimuli. However, our findings clearly demonstrate that mTOR/ Lamp2 translocation to the cell membrane is a principle event relocating mTOR following resistance exercise. It is still unclear on the physiological relevance of this event on mTOR activity. However, it has been suggested previously that lysosome translocation to the cell membrane can be considered as a stimulus for mTORC1 activation [34]. Overexpression of two kinesin superfamily members (KIF1Bß and KIF2) that target lysosome to the cell membrane increased mTORC1 activity. In contrast, knockdown of KIF1Bß and KIF2 targeted lysosome to the peri-nuclear regions, which reduced the mTORC1 activity subsequently [34]. Thus, the lysosome distribution would be a key initial event in activating mTOR in response to the nutrient stimulation. Our findings of a similar mTOR/Lamp2 translocation to the plasma membrane following resistance exercise would suggest that this event is important for the initiation of protein translation post exercise in human skeletal muscle.

Previous studies have demonstrated that mTOR interaction with the GTP loaded Rheb is required to elicit the complete mTORC1 activation [36]. Rheb is a small GTPase and is activated by the GTPase activating protein TSC2, which converts GTP- Rheb into GDP- Rheb rendering it unable to activate

mTORC1 [21, 37]. Rheb is able to bind to the catalytic domain of mTORC [38, 39] only when loaded with GTP [40]. It is recently published that eccentric contraction results in TSC2 dissociation from the lysosome, which would facilitate the association between mTOR and GTP- Rheb [22]. However, then, we did not observe the dissociation of TSC2 from lysosome but visualized its localisation on the plasma membrane, colocalising with Rheb as opposed to at the lysosome. Further investigation shows that TSC2 dissociated from the cell membrane following resistance exercise, leaving Rheb and mTOR/ Lamp2 translocated to interact on the cell membrane. It is not clear as to why the location of this event is different in human as opposed to the murine skeletal muscle. It may because of the muscle fiber difference (predominantly fast- twitch in mouse *vs.* mixed fibers in human), the mode of exercise (eccentric *vs.* concentric), the degree of contraction/ recruitment and/ or the nutrient availability. Irrespective, our results are in agreement with the studies from Jacobs *et al* [22] reporting TSC2 dissociation from mTOR positive regions appears to be a key event following an anabolic stimulus in human skeletal muscle.

In addition to TSC2- Rheb- mTOR colocalisation, we further examined whether mTOR translocation to the plasma membrane may serve to direct mTOR/Lamp2 to other substrates involved in the initiation of protein synthesis. We reported the novel data indicating that mTOR associates with the regulatory subunit of the eukaryotic initiation factor 3 complex (EIF3F) post exercise in both the exercise group and nutrition group. The eIF3 complex is critical to initiate protein synthesis serving as a scaffold for mTOR and S6K1 interaction, leading to the assembly of the pre- initiation complex [41, 42]. Our data is the first to demonstrate colocalisation between mTOR and EIF3F in human skeletal muscle. mTOR and EIF3F are observed to colocalise immediately post exercise in both the exercise and nutrition groups, which would be consistent with the effects of resistance exercise on enhancing AA update and muscle protein synthesis early in recovery [9, 43]. It is noticed that this interaction is significantly greater in the nutrition group 1h post exercise, suggesting beneficial effects of beverage ingestion on mTOR- EIF3F assembly post exercise. Given the evidence that muscle protein synthesis and phosphorylation of mTORC1 substrates is amplified post exercise following PRO/CHO ingestion [15, 33], it would appear that the increased mTOR- EIF3F interaction found in nutrition group may be an

important mediator of post- exercise nutrition on mTORC1 conducted signal pathway and potentially muscle protein synthesis.

Furthermore, based on the observation that mTOR fluorscence is not evenly distributed on the plasma membrane, we further investigated this issue and found that mTOR/Lamp2 complex accumulates around the microvasculature (marked by UEA-I) on the cell membrane post exercise. It is unclear of the precise reason for this response to exercise, however the association of mTOR with the microvasculature would theoretically place mTOR in close proximity to nutrients provision from the bloodsteam transportation. In addition, the increased interaction between mTOR and microvasculature are found in both the exercise group and nutrition group, which suggests the spatial association is not influenced by the PRO/CHO ingestion in healthy young men post exercise. Collectively, this further supports the hypothesis that mTOR translocation to cell membrane is a mechanically driven event and that PRO/CHO ingestion facilitates mTOR interaction with the EIF3F rather than altering the localisation of mTOR/ Lamp2.

6.3 Does mTOR association with the cell membrane facilitate mTOR activation

Not only does the plasma membrane maintain integrity of cells, but also serves as a scaffold to facilitate signal transduction from the extracellular environment to intracellular cytoplasm. Crosstalk can be mediated by number of receptors, such as insulin receptor and IGF receptor localise as the transmembrane proteins [45]. Once binding with ligands, conformational change of receptors leads to their activation and interaction with downstream substrates [46]. PI3K- Akt is repoted to be one of the upstream pathways mediating mTOR activation [47]. As demonstrated in Figure 6.3, phosphoinositide 3-kinase (PI3K) activated by growth factor receptor converts membrane lipid phosphatidylinositol-4,5- bisphosphate (PIP2) to phosphatidylinositol- 3, 4, 5- trisphosphate(PIP3) [47]. PIP3 can bind with various signaling proteins including serine-threonie kinases, tyrosine kinases and exchange factors to activate functions of these proteins [47]. In unstimualted cells, these signaling proteins are located in the cytoplasm and accumulate to plasma membrane once phosphatidylinositol lipid is phospharylated

[47]. Akt is recruited from cytosol to plasma membrane to be activated [47]. Mechanism of Akt activating mTOR is not fully understood, yet two regulatory pathways have been proposed. Firstly, Akt phosphorylate Ser2448 on mTOR [48, 49]. Secondly, Akt mediates mTOR activity through inhibiting TSC1/TSC2 and PRAS40, both of which participate in mTOR inhibition [50, 51]. Via these two signal pathways mTOR activity is increased to stimulate protein synthesis [26, 52].

However, recent studies suggest that mTORC1 induced skeletal muscle hypertrophy can be independent of PI3 kinase activation [62, 63]. Specific inhibition of PI3K by wortmannin did not prevent stretch- induced activation in S6K1 in isolated extensor digitorum longus muscles [62]. Moreover, Akt was not required for S6K1 activation by stretch [62]. Mechanism on contractile induced mTOR activation is not clear now, potentially via a stretch- activated calcium channel, integrins, integrin linked kinases and/or amino acids [64].

Our data show that Rheb and TSC2 are colocalized on the plasma membrane in human skeletal muscle at basal level, with TSC2 disassociation from cell membrane in response to exercise, whist Rheb colocalise with mTOR. TSC2 on plasma membrane would be phosphoryalted and inhibited by Akt translocated to cell membrane. TSC2 degradation release Rheb activity, leaving mTOR and Rheb association with each other [21, 22, 37, 38, 39]. The event mTOR translocation to cell membrane would facilitate mTOR spatially access to Rheb to be directly activated. In addition, distribution of mTOR on cell membrane is correlated with microvasculture, suggesting mTOR sensing to nutrients availability carried by blood stream transport. In conclusion, in response to exercise mTOR translocation to cell membrane would enhance its interaction with activator Rheb, the latter one being released by degraded plasma membrane TSC2.

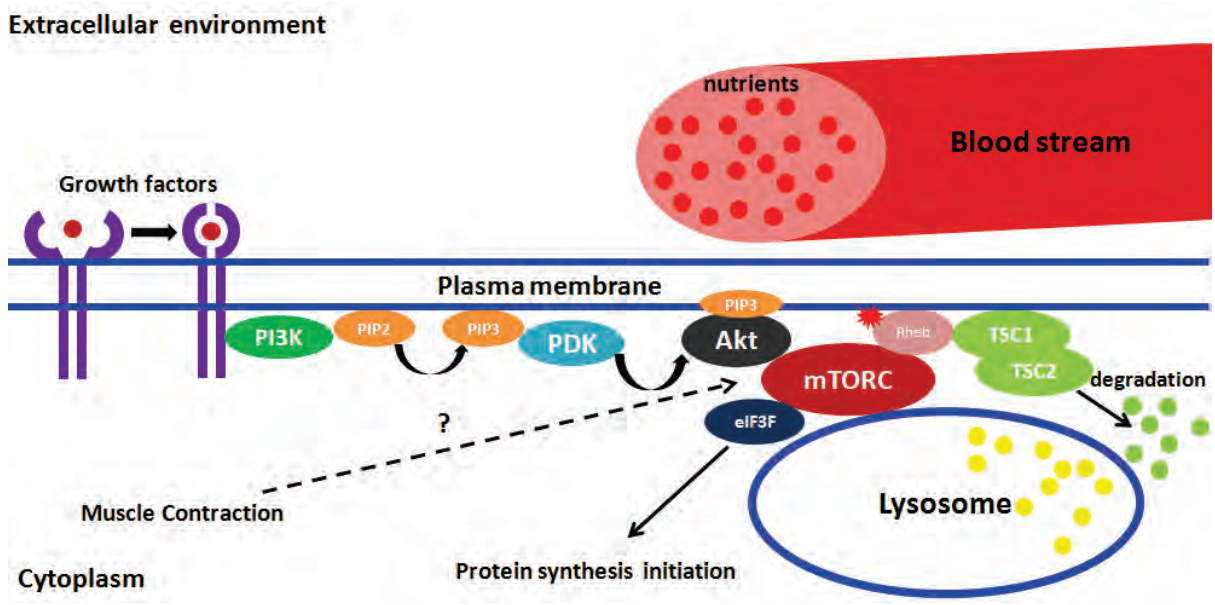

Figure 6.1 Overview of potential mechanisms explaining why mTOR translocation to cell membrane in response to anabolic stimuli. It is illustrated that the event mTOR translocate to membrane would facilitate interaction between mTOR and Rheb, both of which translocates to the plasma membrane in response to stimulatory signals. In this study, TSC2 was observed to distribute near plasma membrane. In response to exercise, TSC2 on cell membrane was degraded, possibly by Akt, to release active Rheb. mTOR translocated to cell membrane was found interacte with Rheb to be activated. Image is drawn by the author.

6.4 Suggestions for future research

Léger *et al* reported increased phosphorylated mTOR $^{\text{Serine } 2448}$ content by immunoblotting post resistance training [44]. Another study in cycle training showed significant increase of phosphorylated mTOR content in fast- twitch fibers in human following a 6 weeks training [59]. It would be interesting to examine mTOR phosphorylation and mTOR substrate activity in muscle samples between pre-training and post- training, as total mTOR fluorescence content *per se* may not be sufficient to reflect mTOR activation level. Training status is another issue which may have influenced mTOR activity in muscle fibers. Individuals in the current study have recreationally training experience which might

compromise the training effect. So it worthy investigating effects of resistance training on mTOR content in skeletal muscle of untrained or sedentary people.

Though mTOR translocation to cell membrane would facilitate its activation, the biological function and regulation of mTOR translocation to plasma membrane need further investigation, given that it is currently unclear as to how this translocation contributes to mTOR signaling transduction, as well as muscle protein synthesis. In our results, mTOR was found always associated with lysosome, which is different from findings in rodent studies [22, 23]. Korolchuk *et al* reported that mild nutrition availability could retain mTOR on lysosome without mTOR activation in cell model [34]. So it is interesting to investigate which factors or mechanisms retain mTOR on lysosome surface in human cells, and what factors result in the different mTOR/ lysosome distribution between human and rodents at basal level, which might help better understand the physiological variance between two models. Reports show that lysosome translocation to cell membrane happens in human skeletal muscle when cell membrane is damaged by mechanistic contraction [65]. mTOR associated with lyososome may be transported to cell membrane via this mechanism or other mechanisms. In addition, studies can be done on mechanism leading to mTOR/ lysosome translocation. Lysosome positioning has been revealed to be important for mTOR activity in autophagy [34], though it is not clear of the physiological functions of lysosome translocation in rodent and human *in vivo*. Hela cell study found that when lysosome localized to nucleus area, mTOR activity was inhibited; conversely, mTOR activity was activated when lysosome translocated to cell membrane [34]. Kinesin kinase belongs to motor protein which is reported to conduct lysosome intracellular transportation [66]. Genetic manipulation of two kinesin protein, KIF1Bß and KIF2, could determine lysosome positioning [34]. As our results show mTOR was tightly associated with lysosome, it is hypothesized that these two kinesin proteins would colocalise with mTOR/ lysosome to facilitate mTOR translocation in response to exercise in human skeletal muscle. We used two biomarkers, Rab7 and Lamp2, to indicate late lysosome positioning. However, immunofluorescence data showed different distribution patterns between two proteins. Lamp2 always associated with mTOR under both basal status and post exercise status, while Rab7 translocated to associate with mTOR in response to exercise stimulation. Reasons are not very clear as late lysosome

formation is a dynamic process which is difficult to be monitored. It is reported that Rab7 appears on the late endosome membrane to conduct vehicles sorting, while Lamp2 primarily locates on lysosome to protect lysosome membrane integrity [23]. Endosomes sorted by Rab7 are then infused with lysosome to form late lysosome [23]. It seems that our results support this theory as Rab7 was observd to translocate to colocalise with Lamp2/ mTOR following exercise, suggesting contraction induced mTOR docking on matured late lysosome. However, this hypothesis needs to be supported by more evidence.

6.5 Final conclusions

In summary, we have developed an immunofluorescence staining technique to examine mTOR and associating proteins in human skeletal muscle *in vivo*. Taking advantage of immunofluorescence histology approaches, for the first time we report the intracellular localisation and protein complex association of mTOR in basal and in response to acute and chronic anabolic stimuli in human skeletal muscle. It is hoped that this experimental approach will unveil numerous process relating to mTOR-mediated regulation of protein synthesis in healthy human skeletal muscle in response to anabolic stimuli, and in skeletal muscle in individuals with chronic disease in which muscle growth is compromised.

6.6 Reference

[1] Wolfe, Robert R. The underappreciated role of muscle in health and disease. The American Journal of Clinical Nutrition 84, no. 3 (2006): 475-482.

[2] Burd, Nicholas A., Jason E. Tang, Daniel R. Moore, and Stuart M. Phillips. Exercise training and protein metabolism: influences of contraction, protein intake, and sex-based differences. Journal of Applied Physiology 106, no. 5 (2009): 1692-1701.

[3] Rasmussen, Blake B., Kevin D. Tipton, Sharon L. Miller, Steven E. Wolf, and Robert R. Wolfe. An oral essential amino acid-carbohydrate supplement enhances muscle protein anabolism after resistance exercise. Journal of Applied Physiology 88, no. 2 (2000): 386-392.

[4] Laplante, Mathieu, and David M. Sabatini. mTOR signaling in growth control and disease. Cell 149, no. 2 (2012): 274-293.

[5] Kim, Joungmok, and Kun-Liang Guan. Amino acid signaling in TOR activation. Annual Review of Biochemistry 80 (2011): 1001-1032.

[6] Drummond, Micah J., Christopher S. Fry, Erin L. Glynn, Hans C. Dreyer, Shaheen Dhanani, Kyle L. Timmerman, Elena Volpi, and Blake B. Rasmussen. Rapamycin administration in humans blocks the contraction-induced increase in skeletal muscle protein synthesis. The Journal of Physiology 587, no. 7 (2009): 1535-1546.

[7] Dickinson, Jared M., Christopher S. Fry, Micah J. Drummond, David M. Gundermann, Dillon K. Walker, Erin L. Glynn, Kyle L. Timmerman, Shaheen Dhanani, Elena Volpi, and Blake B. Rasmussen. Mammalian target of rapamycin complex 1 activation is required for the stimulation of human skeletal muscle protein synthesis by essential amino acid. The Journal of Nutrition 141, no. 5 (2011): 856-862.

[8] McGlory, Chris, and Stuart M. Phillips. Assessing the regulation of skeletal muscle plasticity in response to protein ingestion and resistance exercise: recent developments. Current Opinion in Clinical Nutrition & Metabolic Care 17, no. 5 (2014): 412-417.

[9] Biolo, Gianni, Sergio P. Maggi, Bradley D. Williams, Kevin D. Tipton, and Robert R. Wolfe. Increased rates of muscle protein turnover and amino acid transport after resistance exercise in humans. American Journal of Physiology-Endocrinology and Metabolism 31, no. 3 (1995): E514.

[10] Phillips, Stuart M., Kevin D. Tipton, Asle Aarsland, Steven E. Wolf, and Robert R. Wolfe. Mixed muscle protein synthesis and breakdown after resistance exercise in humans. American Journal of Physiology-Endocrinology and Metabolism 36, no. 1 (1997): E99.

[11] Eliasson, Jörgen, Thibault Elfegoun, Johnny Nilsson, Rickard Köhnke, Björn Ekblom, and Eva Blomstrand. Maximal lengthening contractions increase p70 S6 kinase phosphorylation in human skeletal muscle in the absence of nutritional supply. American Journal of Physiology- Endocrinology and Metabolism 291, no. 6 (2006): E1197-E1205.

[12] Burd, Nicholas A., Daniel WD West, Daniel R. Moore, Philip J. Atherton, Aaron W. Staples, Todd Prior, Jason E. Tang, Michael J. Rennie, Steven K. Baker, and Stuart M. Phillips. Enhanced amino acid sensitivity of myofibrillar protein synthesis persists for up to 24 h after resistance exercise in young men. The Journal of Nutrition 141, no. 4 (2011): 568-573.

[13] Biolo, Gianni, Kevin D. Tipton, Samuel Klein, and Robert R. Wolfe. An abundant supply of amino acid enhances the metabolic effect of exercise on muscle protein. American Journal of Physiology-Endocrinology and Metabolism 36, no. 1 (1997): E122.

[14] Børsheim, Elisabet, Kevin D. Tipton, Steven E. Wolf, and Robert R. Wolfe. Essential amino acid and muscle protein recovery from resistance exercise. American Journal of Physiology-Endocrinology and Metabolism 283, no. 4 (2002): E648-E657.

[15] Dreyer, Hans C., Micah J. Drummond, Bart Pennings, Satoshi Fujita, Erin L. Glynn, David L. Chinkes, Shaheen Dhanani, Elena Volpi, and Blake B. Rasmussen. Leucine-enriched essential amino acid and carbohydrate ingestion following resistance exercise enhances mTOR signaling and protein synthesis in human muscle. American Journal of Physiology-Endocrinology and Metabolism 294, no. 2 (2008): E392-E400.

[16] Moore, Drpj Atherton, M. J. Rennie, M. A. Tarnopolsky, and S. M. Phillips. Resistance exercise enhances mTOR and MAPK signalling in human muscle over that seen at rest after bolus protein ingestion. Acta Physiologica 201, no. 3 (2011): 365-372.

[17] Betz, Charles, and Michael N. Hall. Where is mTOR and what is it doing there? The Journal of Cell Biology 203, no. 4 (2013): 563-574.

[18] Sancak, Yasemin, Liron Bar-Peled, Roberto Zoncu, Andrew L. Markhard, Shigeyuki Nada, and David M. Sabatini. Ragulator-Rag complex targets mTORC1 to the lysosomal surface and is necessary for its activation by amino acid. Cell 141, no. 2 (2010): 290-303.

[19] Inoki, Ken, Yong Li, Tian Xu, and Kun-Liang Guan. Rheb GTPase is a direct target of TSC2 GAP activity and regulates mTOR signaling. Genes & Development 17, no. 15 (2003): 1829-1834.

[20] Manning, Brendan D., Andrew R. Tee, M. Nicole Logsdon, John Blenis, and Lewis C. Cantley. Identification of the tuberous sclerosis complex-2 tumor suppressor gene product tuberin as a target of the phosphoinositide 3-kinase/akt pathway. Molecular Cell 10, no. 1 (2002): 151-162.

[21] Tee, Andrew R., Brendan D. Manning, Philippe P. Roux, Lewis C. Cantley, and John Blenis. Tuberous sclerosis complex gene products, Tuberin and Hamartin, control mTOR signaling by acting as a GTPase-activating protein complex toward Rheb. Current Biology 13, no. 15 (2003): 1259-1268.

[22] Jacobs, Brittany L., Jae-Sung You, John W. Frey, Craig A. Goodman, David M. Gundermann, and Troy A. Hornberger. Eccentric contractions increase the phosphorylation of tuberous sclerosis complex-2 (TSC2) and alter the targeting of TSC2 and the mechanistic target of rapamycin to the lysosome. The Journal of Physiology 591, no. 18 (2013): 4611-4620.

[23] Jacobs, Brittany L., Craig A. Goodman, and Troy A. Hornberger. The mechanical activation of mTOR signaling: an emerging role for late endosome/lysosomal targeting. Journal of Muscle Research and Cell Motility 35, no. 1 (2014): 11-21.

[24] Seynnes, Olivier Roger, Maarten de Boer, and Marco Vincenzo Narici. Early skeletal muscle hypertrophy and architectural changes in response to high-intensity resistance training. Journal of Applied Physiology 102, no. 1 (2007): 368-373.

[25] Willoughby, Darryn S. Effects of heavy resistance training on myostatin mRNA and protein expression. Medicine and Science in Sports and Exercise 36, no. 4 (2004): 574-582.

[26] Bodine, Sue C., Trevor N. Stitt, Michael Gonzalez, William O. Kline, Gretchen L. Stover, Roy Bauerlein, Elizabeth Zlotchenko et al. Akt/mTOR pathway is a crucial regulator of skeletal muscle hypertrophy and can prevent muscle atrophy in vivo. Nature Cell Biology 3, no. 11 (2001): 1014-1019.

[27] Goodman, Craig A., Jack A. Kotecki, Brittany L. Jacobs, and Troy A. Hornberger. Muscle fiber type-dependent differences in the regulation of protein synthesis. PLoS One 7, no. 5 (2012): e37890.

[28] Hather, B. M., P. A. Tesch, P. Buchanan, and G. A. Dudley. Influence of eccentric actions on skeletal muscle adaptations to resistance training. Acta Physiologica Scandinavica 143, no. 2 (1991): 177-185.

[29] Zierath, Juleen R., and John A. Hawley. Skeletal muscle fiber type: influence on contractile and metabolic properties. PLoS Biology 2, no. 10 (2004): e348.

[30] Coyle, Edward F., Labros S. Sidossis, Jeffrey F. Horowitz, and John D. Beltz. Cycling efficiency is related to the percentage of type I muscle fibers. Medicine and science in sports and exercise 24, no. 7 (1992): 782-788.

[31] Philp, Andrew, D. Lee Hamilton, and Keith Baar. Signals mediating skeletal muscle remodeling by resistance exercise: PI3-kinase independent activation of mTORC1. Journal of Applied Physiology 110, no. 2 (2011): 561-568.

[32] Phillips, Stuart M., Kevin D. Tipton, Asle Aarsland, Steven E. Wolf, and Robert R. Wolfe. Mixed muscle protein synthesis and breakdown after resistance exercise in humans. American Journal of Physiology-Endocrinology And Metabolism 36, no. 1 (1997): E99.

[33] Staples, Aaron W., Nicholas A. Burd, D. W. West, Katharine D. Currie, Philip J. Atherton, Daniel R. Moore, Michael J. Rennie, Maureen J. Macdonald, Steven K. Baker, and Stuart M. Phillips. Carbohydrate does not augment exercise-induced protein accretion versus protein alone. Medicine and Science in Sports and Exercise 43, no. 7 (2011): 1154-1161.

[34] Korolchuk, Viktor I., Shinji Saiki, Maike Lichtenberg, Farah H. Siddiqi, Esteban A. Roberts, Sara Imarisio, Luca Jahreiss et al. Lysosomal positioning coordinates cellular nutrient responses. Nature Cell Biology 13, no. 4 (2011): 453-460.

[35] Fujita, Satoshi, Blake B. Rasmussen, Jill A. Bell, Jerson G. Cadenas, and Elena Volpi. Basal muscle intracellular amino acid kinetics in women and men. American Journal of Physiology-Endocrinology and Metabolism 292, no. 1 (2007): E77-E83.

[36] Aspuria, Paul-Joseph, and Fuyuhiko Tamanoi. The Rheb family of GTP-binding proteins. Cellular Signalling 16, no. 10 (2004): 1105-1112.

[37] Tee, Andrew R., Diane C. Fingar, Brendan D. Manning, David J. Kwiatkowski, Lewis C. Cantley, and John Blenis. Tuberous sclerosis complex-1 and-2 gene products function together to inhibit mammalian target of rapamycin (mTOR)-mediated downstream signaling. Proceedings of the National Academy of Sciences 99, no. 21 (2002): 13571-13576.

[38] Long, Xiaomeng, Yenshou Lin, Sara Ortiz-Vega, Kazuyoshi Yonezawa, and Joseph Avruch. Rheb binds and regulates the mTOR kinase. Current Biology 15, no. 8 (2005): 702-713.

[39] Long, Xiaomeng, Sara Ortiz-Vega, Yenshou Lin, and Joseph Avruch. Rheb binding to mammalian target of rapamycin (mTOR) is regulated by amino acid sufficiency. Journal of Biological Chemistry 280, no. 25 (2005): 23433-23436.

[40] Avruch, Joseph, Xiaomeng Long, Yenshou Lin, Sara Ortiz-Vega, Joseph Rapley, Angela Papageorgiou, Noriko Oshiro, and Ushio Kikkawa. Activation of mTORC1 in two steps: Rheb-GTP activation of catalytic function and increased binding of substrates to raptor1. Biochemical Society Transactions 37, no. 1 (2009): 223.

[41] Holz, Marina K., Bryan A. Ballif, Steven P. Gygi, and John Blenis. mTOR and S6K1 mediate assembly of the translation preinitiation complex through dynamic protein interchange and ordered phosphorylation events. Cell 123, no. 4 (2005): 569-580.

[42] Harris, Thurl E., An Chi, Jeffrey Shabanowitz, Donald F. Hunt, Robert E. Rhoads, and John C. Lawrence. mTOR- dependent stimulation of the association of eIF4G and eIF3 by insulin. The EMBO journal 25, no. 8 (2006): 1659-1668.

[43] Dreyer, Hans C., Satoshi Fujita, Jerson G. Cadenas, David L. Chinkes, Elena Volpi, and Blake B. Rasmussen. Resistance exercise increases AMPK activity and reduces 4E-BP1 phosphorylation and protein synthesis in human skeletal muscle. The Journal of Physiology 576, no. 2 (2006): 613-624.

[44] Léger, Bertrand, Romain Cartoni, Manu Praz, Séverine Lamon, Olivier Dériaz, Antoinette Crettenand, Charles Gobelet et al. Akt signalling through GSK-3β, mTOR and Foxo1 is involved in human skeletal muscle hypertrophy and atrophy. The Journal of Physiology 576, no. 3 (2006): 923-933.

[45] Lee, J., and P. F. Pilch. The insulin receptor: structure, function, and signaling. American Journal of Physiology-Cell Physiology 266, no. 2 (1994): C319-C334.

[46] Lee, Jongsoon, Paul F. Pilch, Steven E. Shoelson, and Suzanne F. Scarlata. Conformational changes of the insulin receptor upon insulin binding and activation as monitored by fluorescence spectroscopy. Biochemistry 36, no. 9 (1997): 2701-2708.

[47] Cantley, Lewis C. The phosphoinositide 3-kinase pathway. Science 296, no. 5573 (2002): 1655-1657.

[48] Nave, B., M. Ouwens, D. Withers, D. Alessi, and P. Shepherd. Mammalian target of rapamycin is a direct target for protein kinase B: identification of a convergence point for opposing effects of insulin and amino-acid deficiency on protein translation. Biochem. J 344 (1999): 427-431.

[49] Sekulić, Aleksandar, Christine C. Hudson, James L. Homme, Peng Yin, Diane M. Otterness, Larry M. Karnitz, and Robert T. Abraham. A direct linkage between the phosphoinositide 3-kinase-

AKT signaling pathway and the mammalian target of rapamycin in mitogen-stimulated and transformed cells. Cancer Research 60, no. 13 (2000): 3504-3513.

[50] Avruch, J., K. Hara, Y. Lin, M. Liu, X. Long, S. Ortiz-Vega, and K. Yonezawa. Insulin and amino-acid regulation of mTOR signaling and kinase activity through the Rheb GTPase. Oncogene 25, no. 48 (2006): 6361-6372.

[51] Cai, Sheng-Li, Andrew R. Tee, John D. Short, Judith M. Bergeron, Jinhee Kim, Jianjun Shen, Ruifeng Guo, Charles L. Johnson, Kaoru Kiguchi, and Cheryl Lyn Walker. Activity of TSC2 is inhibited by AKT-mediated phosphorylation and membrane partitioning. The Journal of Cell Biology 173, no. 2 (2006): 279-289.

[52] Kim, Joungmok, and Kun-Liang Guan. Amino acid signaling in TOR activation. Annual Review of Biochemistry 80 (2011): 1001-1032.

[53] Andersen, Per, and Jan Henriksson. Training induced changes in the subgroups of human type II skeletal muscle fibres. Acta Physiologica Scandinavica 99, no. 1 (1977): 123-125.

[54] Green, H. J., J. A. Thomson, W. D. Daub, M. E. Houston, and D. A. Ranney. Fiber composition, fiber size and enzyme activities in vastus lateralis of elite athletes involved in high intensity exercise. European Journal of Applied Physiology and Occupational Physiology 41, no. 2 (1979): 109-117.

[55] Karavirta, L., A. Häkkinen, E. Sillanpää, D. García López, A. Kauhanen, A. Haapasaari, M. Alen et al. Effects of combined endurance and strength training on muscle strength, power and hypertrophy in 40–67 year old men. Scandinavian Journal of Medicine & Science in Sports 21, no. 3 (2011): 402-411.

[56] Kraemer, William J., John F. Patton, Scott E. Gordon, Everett A. Harman, Michael R. Deschenes, Katy Reynolds, Robert U. Newton, N. Travis Triplett, and Joseph E. Dziados. Compatibility of high-intensity strength and endurance training on hormonal and skeletal muscle adaptations. Journal of applied physiology 78, no. 3 (1995): 976-989.

[57] Garlick, Peter J., Charlotte A. Maltin, A. G. Baillie, Margaret I. Delday, and David A. Grubb. Fiber-type composition of nine rat muscles. II. Relationship to protein turnover. American Journal of Physiology-Endocrinology And Metabolism 257, no. 6 (1989): E828-E832.

[58] Mittendorfer, B., J. L. Andersen, P. Plomgaard, B. Saltin, J. A. Babraj, K. Smith, and M. J. Rennie. Protein synthesis rates in human muscles: neither anatomical location nor fibre‐type composition are major determinants. The Journal of Physiology 563, no. 1 (2005): 203-211.

[59] Kumar, Vinod, Anna Selby, Debbie Rankin, Rekha Patel, Philip Atherton, Wulf Hildebrandt, John Williams et al. Age‐related differences in the dose–response relationship of muscle protein synthesis to resistance exercise in young and old men. The Journal of Physiology 587, no. 1 (2009): 211-217.

[60] Bassel-Duby, Rhonda, and Eric N. Olson. Signaling pathways in skeletal muscle remodeling. Annu. Rev. Biochem. 75 (2006): 19-37.

[61] Lin, Jiandie, Hai Wu, Paul T. Tarr, Chen-Yu Zhang, Zhidan Wu, Olivier Boss, Laura F. Michael et al. Transcriptional co-activator PGC-1α drives the formation of slow-twitch muscle fibres. Nature 418, no. 6899 (2002): 797-801.

[62] Hornberger, Troya, Rudy Stuppard, Kevine Conley, Markj Fedele, Martal Fiorotto, Evar Chin, and Karyna Esser. Mechanical stimuli regulate rapamycin-sensitive signalling by a phosphoinositide 3-kinase-, protein kinase B-and growth factor-independent mechanism. Biochem. J 380 (2004): 795-804.

[63] Goodman, Craig A., Man Hing Miu, John W. Frey, Danielle M. Mabrey, Hannah C. Lincoln, Yejing Ge, Jie Chen, and Troy A. Hornberger. A phosphatidylinositol 3-kinase/protein kinase B-independent activation of mammalian target of rapamycin signaling is sufficient to induce skeletal muscle hypertrophy. Molecular Biology of the Cell 21, no. 18 (2010): 3258-3268.

[64] Philp, Andrew, D. Lee Hamilton, and Keith Baar. Signals mediating skeletal muscle remodeling by resistance exercise: PI3-kinase independent activation of mTORC1. Journal of Applied Physiology 110, no. 2 (2011): 561-568.

[65] Appelqvist, Hanna, Petra Wäster, Katarina Kågedal, and Karin Öllinger. The lysosome: from waste bag to potential therapeutic target. Journal of Molecular Cell Biology 5, no. 4 (2013): 214-226.

[66] Soldati, Thierry, and Manfred Schliwa. Powering membrane traffic in endocytosis and recycling. Nature Reviews Molecular Cell Biology 7, no. 12 (2006): 897-908.

[67] Andersen, Per, and Jan Henriksson. Training induced changes in the subgroups of human type II skeletal muscle fibres. Acta Physiologica Scandinavica 99, no. 1 (1977): 123-125.

[68] Fitts, Robert H. Effects of regular exercise training on skeletal muscle contractile function. American Journal of Physical Medicine & Rehabilitation 82, no. 4 (2003): 320-331.

[69] Gollnick, Philip D., R. B. Armstrong, Bengt Saltin, C. W. T. Saubert, Walter L. Sembrowich, and Roy E. Shepherd. Effect of training on enzyme activity and fiber composition of human skeletal muscle. Journal of Applied Physiology 34, no. 1 (1973): 107-111.

[70] Carroll, Timothy J., Peter J. Abernethy, Peter A. Logan, Margaret Barber, and Michael T. McEniery. Resistance training frequency: strength and myosin heavy chain responses to two and three bouts per week. European Journal of Applied Physiology and Occupational Physiology 78, no. 3 (1998): 270-275.

[71] Thorstensson, Alf, Bodil Hultén, Wilhelm von Döbeln, and Jan Karlsson. Effect of strength training on enzyme activities and fibre characteristics in human skeletal muscle. Acta Physiologica Scandinavica 96, no. 3 (1976): 392-398.

[72] Coyle, Edward F., D. C. Feiring, T. C. Rotkis, R. W. Cote, F. B. Roby, W. Lee, and J. H. Wilmore. Specificity of power improvements through slow and fast isokinetic training. Journal of Applied Physiology 51, no. 6 (1981): 1437-1442.